Variations in hypsodonty of ungulates: testing its utility as a climatic proxy in modern and Late Pleistocene mammal communities

David John Arnold

Department of Geography

Royal Holloway, University of London

Thesis submitted for the degree of Doctor of Philosophy

September 2019

Declaration of authorship

I, David John Arnold, hereby declare that this thesis and the work presented within it is entirely my own. Where I have consulted the work of others, this is always clearly stated.

Signed: 

Date: 27 September 2019

Abstract

The quantification of past levels of precipitation is frequently challenging in fossil localities where limited suitable proxies are present. Recent work has suggested that hypsodonty (tooth crown height) in mammals can be used as a predictor of mean annual precipitation in both modern and fossil contexts. However, previous research on modern hypsodonty-climate relationships was largely based on per species mean hypsodonty at spatial scales of ecoregion level mammal communities, a coarse spatial resolution compared to what is seen in regional and local differences in precipitation. In addition, intraspecific variation in hypsodonty had not been previously tested in a thorough and adequate manner to permit the use of per species mean hypsodonty in palaeoenvironmental reconstruction.

This research reassesses the modern relationship between hypsodonty and climate, departing from the use of per species mean hypsodonty, and instead focussing on individual tooth hypsodonty index (using the lower third molar) and locality mean hypsodonty index, with the ultimate goal of applying this method to Quaternary mammalian dental material. A large dataset of 3,788 hypsodonty index measurements was created from well-provenanced museum specimens representing 148 ungulate taxa from 950 unique localities. Correlations of these measurements with modelled climate data were then tested at the resolution of individual localities rather than large ecoregions. Results show that, contrary to previous work, correlations between hypsodonty index and precipitation-related climate variables are weaker than for those with temperature-related variables, although no correlations are particularly strong, including testing the inclusion of both individual left and right teeth and migratory taxa in the dataset. This highlights not only the complex nature of hypsodonty and its possible controls but also indicates that (1) scale and rate of change in individual and community hypsodonty index need to be considered both temporally and spatially, and (2) that current models are not robust enough for further application.

In order to establish whether the method could detect abrupt climatic and environmental change during the Late Pleistocene, hypsodonty index data was collected from seven well-dated Late Pleistocene Mediterranean cave sites. The Mediterranean was selected as the spatial focus as it is largely assumed that precipitation and moisture availability are the dominant factors influencing environmental change. Mean hypsodonty index of fossil mammal communities through these sequences was compared to existing palaeoecological and geochemical proxies to validate its utility in palaeoenvironmental reconstruction. It is clear that the method's validity is highly dependent on presence, availability and condition of the fossil material and that low sample sizes and differential

resolutions between proxies drastically reduce reliability. Environmental and climatic inferences can, however, be made with caution but are site-specific in nature.

Acknowledgments

Firstly, I must thank my supervisors Professor Danielle Schreve and Professor Simon Blockley. Throughout my Ph.D. they have encouraged and supported me academically, professionally and personally through some very challenging periods. I am so grateful to have had a supervisory “dream team” where their respective knowledge complemented each other throughout the development of my research project, both of them opening many doors of collaboration across Europe. I am extremely grateful for Danielle’s personal guidance through the years and to Simon’s unwavering faith in me as a scientist. I would also like to thank my advisor Professor Ian Candy for not only his personal support, advice and guidance, but his genuine scientific interest in my project throughout.

Thank you to the Department of Geography at Royal Holloway University of London and to all in the Centre for Quaternary Research. I would especially like to thank Rachel Devine and Julian Martin for their support on our shared journey on the London NERC Doctoral Training Partnership. I would not have completed this thesis without the personal support of Rachel, who brings a whole new level of meaning to the word ‘friend’. I also give special thanks to Dr Lucy Flower, Dr Angharad Jones and Emily Wiesendanger who provided me with many hours of interesting palaeontological discussions and always were there to listen to my troubles with teeth. To Amy Walsh and Dr Ashley Abrook, thank you for all those chats and coffee breaks when the going got tough! I must also give special thanks to Becca Smith at the University of Oxford for her periodic encouragement and for inviting me on respite visits so many times. I am indebted to Emilie Ancelin, who ensured I was remaining alive and well (and sane) throughout my Ph.D.

There are a number of collaborators at institutions across Europe, without which this thesis would not have been possible. For providing me with access to material, their guidance and support, I give thanks to the following: Roberto Portela Miguez, Roula Pappa (Natural History Museum, London, UK), Mathew Lowe (University Museum of Zoology, Cambridge, UK), Inbal Livne (Powell-Cotton Museum, Quex Park, Birchington-on-Sea, UK), Joséphine Lesur (Muséum national d’Histoire naturelle, Paris, France), Steffen Bock (Museum für Naturkunde, Berlin, Germany), Daniela Kalthoff (Naturhistoriska riksmuseet, Stockholm, Sweden), Olivier Pauwels (Royal Belgian Institute of Natural Sciences, Brussels, Belgium), Emmanuel Gilissen (Royal Museum of Central Africa, Tervuren, Belgium), Palmira Saladié and Florent Rivals (Institut Català de Paleoecologia Humana i Evolució Social, Tarragona, Spain), Anne-Marie Moigne (Centre Européen de Recherches Préhistoriques, Tautavel, France), Fabio Martini and

Domenico Lo Vetro (Museo e Isituto Fiorentino di Preistoria “Paolo Graziosi” and Università degli Studi di Firenze, Florence, Italy), Rivka Rabinovich (Hebew University of Jerusalem, Jerusalem, Israel), Christopher Stimpson (Queens University Belfast, Belfast, UK), Graeme Barker (University of Cambridge, Cambridge, UK) and Imogen Gunn and Annie McKay (Museum of Archaeology and Anthropology, University of Cambridge, Cambridge, UK). I would also like to thank Maura Pellegrini (University of Oxford) for some helpful discussions and advice.

I am extremely grateful to the Natural Environment Research Council for funding me and this research through the London Doctoral Training Partnership. I would also like to thank the Quaternary Research Association for providing me with some additional funding in order to present this research at the International Quaternary Association XX Congress 2019 in Dublin.

Finally, I would like to thank my family, for always encouraging me through my studies and for immeasurable support throughout my life and I would not have reached this point without you.

Contents

List of Figures

List of Tables

CHAPTER 1
Introduction

1.1 Introduction

The Intergovernmental Panel on Climate Change (IPCC) indicates that over the 21st century, in a warming world under "business-as-usual" anthropogenic emission scenarios, important precipitation changes will occur, and these will not be uniform across the globe. The high latitudes and the Pacific are likely to experience increases in mean annual precipitation by 2100, whilst mid-latitudes and sub-tropical dry regions are likely to experience decreases in mean annual precipitation. Accompanying these changes, extreme precipitation events are predicted to increase (Stocker *et al*., 2013). As over 50% of the world's population lives in the mid-latitudes (Moon *et al*., 2017), and this is set to increase, thereby putting pressure on water resources, it is important to be able to predict and model future precipitation change reliably. There is also a need to assess potential impacts of this climate change on the world's ecosystems. For this, it is imperative to be able to model current and past conditions accurately, with estimates for climatic variables needed to parameterise these models. Palaeoclimate models have improved in recent decades in response to technological advances, but there is still a need to validate their outputs with palaeoenvironmental data. Whilst temperature reconstructions are more readily available, precipitation estimates in the past are more difficult to obtain.

Reconstructing past patterns of precipitation can use both abiotic and biotic proxy methods (van Dam and Utescher, 2016). Abiotic proxies include elemental ratios reflecting palaeosol weathering (e.g. Sheldon and Tabor, 2009) and carbon isotope ratios in soil carbonates or fossil plant remains or animal bones (e.g. Kohn, 2010). Whilst these methods may be successful in indicating precipitation trends, the complex pathways of isotopic fractionation hamper their use as quantitative values for precipitation variations. Biotic precipitation proxies may include terrestrial vegetation records (although the controls on vegetation include, amongst others, temperature and nutrient availability in some regions), but also vertebrate communities through herbivory (van Dam and Utescher, 2016).

The link between climate, vegetation and herbivory has long been studied, including suggestions that the teeth of large herbivorous mammals capture a climatic signal. This

concept has the potential to provide quantification of climatic variables, including precipitation, in both the present and the past (Fortelius *et al*., 2014). This ability would be highly desirable to the palaeoclimate community as at many sites there is often an abundance of well-preserved mammal assemblages from well-dated contexts but a limited number of suitable proxies available to reconstruct precipitation. These assemblages often span environmental transitions on millennial to centennial timescales, as is seen in the Late Pleistocene, offering the potential to quantify precipitation and investigate rates of precipitation change in the past. This is important to validate palaeoclimate models which are used as a basis to predict rates of future climate change and associated environmental and ecological responses.

Recent work has suggested that hypsodonty (tooth crown height) of large mammalian herbivores can be used as a quantitative predictor of mean annual precipitation in both modern (Eronen *et al*., 2010a; Liu *et al*., 2012; Žliobaitė *et al*., 2016) and fossil contexts (Eronen *et al*., 2010b). This method could be directly applied to Late Pleistocene mammal assemblages to reconstruct mean annual precipitation to assess rates of aridity change and, through multi-proxy studies, assess the impact on the contemporary biotic communities. However, an issue identified by the present research is that the spatial scale of the existing models, for both the climatic and mammalian data, is too coarse for robust application to a Late Pleistocene context where discrete fossil assemblages are available from point localities, on relatively short timescales. This is in comparison to the previous palaeo applications of the method over larger spatial and temporal scales. There is also an assumption in the literature that intraspecific variation in hypsodonty is not of concern, leading to the use of ordinated per-species mean hypsodonty scores in place of actual tooth measurements. This assumption is not adequately tested in the literature and has the potential to limit the robustness of predictions and reconstructions of climate. There is a suggestion that, as hypsodonty is treated as an ecometric in these models, it captures the full community variation, without the need to consider inter- and intraspecific variation in the same way [the method is “taxon-free” (Fortelius et al., 2019)] as might be done with species-distribution modelling and transfer functions. However, if the method were to be applied to Late Pleistocene fossil localities, the discrete, spatial and time-restricted nature of the assemblages, as well as small sample sizes, may warrant a simpler, non-ecometric approach.

This thesis attempts to readdress the concept of using hypsodonty as a climatic predictor by tackling some of the concerns outlined above. The overall research aim is to develop a robust approach to reconstructing past precipitation and aridity in the Late Pleistocene using ungulate hypsodonty index as a proxy. However, it is clear from a review of the

literature that the robustness of the existing models of the modern relationship must first be tested further.

To address this aim, five hypotheses are to be tested. The first three hypotheses relate to the necessary further testing of the modern relationship:

1. Hypsodonty index values of each taxa measured in the modern dataset are normally distributed and intraspecific variability is low, which would validate the assumption of per-species mean hypsodonty.

2. Using actual raw measurements of the teeth of individual animals will predict climate as robustly (if not more robustly) than the previous ecometric approach using ordinated per-species mean hypsodonty.

3. Individual raw hypsodonty index measurements of individuals and mean hypsodonty of the community that is actually present will correlate to climate more strongly than the mean of ecoregion mammal communities (where taxa are assumed to be present or absent). Under this hypothesis, this thesis will also consider the following questions:

    - Are precipitation and aridity as important as the mechanistic understanding would suggest?
    - Or is the temperature signal reported in some of the most recent research of significance?

This research, therefore, firstly reassesses the modern relationship at a much finer spatial resolution, using raw tooth measurements (instead of per-species mean hypsodonty scores) from well provenanced museum specimens from point-localities. Measurements are constrained to only the lower third molar in order to maintain a consistent methodology compared to previous work. Intraspecific variation is investigated and considered when testing correlations between hypsodonty and climatic variables. The correlations computed under this approach do not seem to support conclusions suggested in the literature. This highlights the complex nature of the relationship between climate, environment, diet and dentition on a global scale.

The final two hypotheses relate to reconstructing past precipitation using ungulate hypsodonty index as a proxy:

4. Climate variables can be accurately and robustly quantified in the past using fossil hypsodonty index measurements.

5. Climatic or environmental signals can be seen in community average hypsodonty changes through time, regardless of correlation between hypsodonty index and climate variables.

In this application to fossils, hypsodonty is investigated at seven fossil sites from the Mediterranean, dated to the Late Pleistocene. At these sites there are well-resolved environmental proxies that exhibit signals of environmental and climatic change, with a level of chronological and stratigraphic control sufficient to test the relationship between climatic and change and hypsodonty. Changes in ungulate community hypsodonty are compared to the proxy data to attempt to elucidate climatic signals (if any) from the hypsodonty data and, to unravel some of the complexity revealed in the modern study.

1.2 Outline of thesis

This thesis adopts the following structure:

Chapter 2 presents a comprehensive review of the literature, firstly addressing the development of dentition, different forms and types of teeth and how these are related to diet, ecological niches as well as to environmental variables. Secondly, there is a focus on definitions of hypsodonty and a review of the current models used to understand the modern relationship between hypsodonty and climate and how climatic variables are quantified. Thirdly, there is a review of the application of these models to fossils and how climatic variables are quantified in the past under these methods. Finally, the research aims and hypotheses to be tested in this study are presented.

Chapter 3 outlines the methodology of the study and the materials used for both the modern and fossil application. There is also an extensive review of the literature relating to the fossil sites and their proxy data.

Chapter 4 presents the results and findings of firstly, the investigation into intraspecific variation in ungulate hypsodonty and secondly, the investigation into the relationship between hypsodonty and different climatic variables. Correlation matrices are presented, alongside descriptive statistics for multiple formats of the dataset. Results from regression analyses are also presented.

Chapter 5 discusses the results presented in Chapter 4 and, with reference to the literature, attempts to explain the relationships observed and the possible mechanisms behind these relationships. It links the new understanding of intraspecific variation with

the previous research. It also suggests appropriate ways to use this new understanding in the Late Pleistocene context in order to reconstruct palaeoclimatic information.

Chapter 6 presents the results of hypsodonty index measurements from each Late Pleistocene site in turn. Information on the specimens measured from each site is stated, covering number and state of specimens, range of taxa measured and their associated depth and chronological age. Average hypsodonty index per level/unit is presented against depth and age.

Chapter 7 discusses the hypsodonty results from the Late Pleistocene sites, highlighting methodological concerns when applying this method to fossils. This chapter also provides a synthesis of the understanding of the hypsodonty-climate relationship following both the fossil application and the modern study, highlighting strengths and weaknesses of both the approach taken in this study and the previous research. Suggestions for future work are identified.

Chapter 8 concludes the thesis, briefly readdressing the research questions.

CHAPTER 2
Literature Review

This chapter provides a comprehensive review on the current state of knowledge on dentition, diet and the environment. This is followed by a more in-depth and specific discussion of studies that have been undertaken to understand the relationship between hypsodonty and climate, including quantification of specific variables using hypsodonty index. Finally, further research opportunities arising from the analysis of the literature are then suggested.

2.1 Dentition, diet and the environment

2.1.1 The evolution of different dentitions

Teeth are uniquely found in vertebrates; in fact, most, but not all, vertebrates have teeth. Invertebrates do not have true teeth but often have structures similar in form or function. Throughout the vertebrates, it is the mammals that display the most complex forms of teeth, combined with a limited capacity for tooth renewal (Jernvall and Thesleff, 2012). Mammalian dentitions show interrelationships of growth, function and evolution (Fortelius, 1985), and are therefore suitable and important objects of study in answering many biological questions. Evolutionary studies on teeth owe much of their advancement to the robust nature, and hence preservation potential of teeth, which has led to the relative completeness of this part of the vertebrate fossil record (Jernvall and Thesleff, 2012).

Although the basic components of all mammalian teeth are similar, there is a great deal of diversity within the Class. Although some mammals, such as anteaters, are edentate (lacking teeth), there is great variation in the range of dentitions present in other Orders. This diversity greatly increases when the mammalian fossil record is included. Studies on fossils from the first known mammals (c. 225 million years ago) to the present day suggest that mammals have evolved and adapted to an extensive range of diets and environments over this time (Bergqvist, 2003). Even in the earliest mammalian fossils, there is evidence of a heterodont dentition (Kermack *et al*., 1973, 1981), with different tooth types having different functions within the different regions of the mouth. The anterior teeth such as incisors and canines have a greater range and speed of movement as they are further from the articulation of the jaw. The cheek teeth, being closer to that articulation, have restricted movement but their proximity to the muscles means that

greater pressure can be exerted (Butler, 2000).

The cheek teeth are split into premolars and molars and it is these types of teeth that exhibit diverse and complex crown shapes, often including folding. These teeth carry out the majority of work required in masticating food and therefore display the greatest diet related diversity in size, shape and also growth (DeBlasé and Martin, 1982 cited in Bergqvist, 2003).

2.1.2 Food processing and combatting tooth wear

The diversity of dentitions offers many solutions to the different challenges of obtaining and processing foods in different environments without the dentitions themselves being compromised through breakage or wear. It has been well known since the 18th century that teeth move in both the horizontal and vertical planes, based on Cuvier's work on ungulate feeding (1815, cited in Ungar, 2015). Simpson (1939) further suggested that teeth function on three levels when processing food: there is a grinding component fulfilled by horizontal motion; there is a fracturing component fulfilled by vertical motion and exertion of force from the jaw muscles as previously mentioned; and another vertical motion of sliding that shears food. Focusing particularly on herbivores, the main function of the dentition is to rupture cell walls of vegetation in order to release the nutrients that would otherwise be excreted without their necessary digestion and absorption (Wuersch *et al*., 1986). Maximum efficiency of digestive enzymes is achieved when food has been broken down in order to increase the surface area upon which these enzymes can act (Bezzobs and Sanson, 1997). This is especially true for fibrous plant material (Hanley *et al*., 1993).

Natural selection has acted on teeth in response to repeated stresses during the processing of food. Certain "dental defences" have evolved to protect teeth (Ungar, 2015, pp. 29). Mammals, in contrast to most other vertebrate Classes do not have unlimited generations of teeth; the majority have two sets at most, however, there are some exceptions (e.g. manatees) that retain the capacity to renew their dentitions at multiple times during a lifetime (Whitlock and Richman, 2013). In the case of most mammals, fracture of teeth can be catastrophic. Imperfections and damage can lead to breakage and tooth failure, which in turn can limit an individual's ability to obtain and process food and could lead to death by starvation (Ungar, 2015). One way to increase the durability of a dentition is to increase the amount of enamel exposed at the occlusal surface as this is the most resistant component of teeth. In certain mammals such as primates, suids and proboscideans, the enamel has become thicker to create a stronger crown. In others such as many ungulates, the occlusal surface area of enamel is increased by infolding the enamel many times (MacFadden, 1992). This would be advantageous as

teeth need to have the required strength to break food objects in the mouth, without being broken themselves. Indeed, it has been observed that mammals that feed on hard objects have thicker enamel (Dumont, 1995; Kay, 1981).

Another effect upon teeth is that of wear. As tooth wear will change the shape of any given tooth, it will also change the tooth function and possibly affect structural integrity, which is why tooth wear has warranted much attention in the literature to date (Ungar, 2015). Teeth that wear too quickly would be detrimental to the individual so natural selection should favour teeth that wear in a way that does not cause any decrease in functionality or food processing efficiency throughout life (Ungar and M'Kirera, 2003). It is important to note that certain mammals require some wearing of their tooth crowns in order to fracture food effectively (e.g. Fortelius and Solounias, 2000; Rensberger, 1973), with some mammals such as guinea pigs wearing their teeth through grinding in-utero, so that teeth are functional from birth (Teaford and Walker, 1983). These cases, where wear is necessary for teeth to function properly, provide examples of secondary tooth shape as described by Fortelius (1985).

Differences in enamel structure can alter a tooth's resistance to wear, but any complete or near-complete loss of this enamel from the occlusal surface of the tooth would drastically decrease functional efficiency of food fracturing (Gipps *et al*., 1984 cited in Ungar, 2015). If this occurs, some mammals will attempt to compensate by chewing food for longer or increasing the intake amount of food but this will decrease efficiency of processing the food through their entire digestive process (Kojola *et al*., 1998; Pérez-Barbería and Gordon, 1998).

Increasing the size and volume of a tooth has its advantages in managing tooth wear, however in reality, this response has not been widely selected by evolutionary processes as it would require substantial morphological and developmental changes in the cranium and other parts of the body (MacFadden, 1992). Although some groups of mammals such as some rodents (Hydrochoeridae), some artiodactyls (Camelidae, Hippopotamidae and Suidae) and higher proboscideans have evolved in this way (Janis and Fortelius, 1988), most herbivorous mammals with large teeth also have large body sizes. The isometric scaling between tooth surface area and body size indicates that in general, increasing the size and volume of a tooth is not a popular evolutionary adaptation in herbivores. A strategy for potential resistance to wear would also be to increase the number of teeth, but again this is rare and of little evolutionary advantage in many mammal clades (MacFadden, 1992).

Combatting excessive wear has been overcome in some taxa by increasing the height of their tooth crowns in order to prolong their function (Damuth and Janis, 2011; Janis

and Fortelius, 1988; Williams and Kay, 2001). This evolutionary strategy is widespread, highlighting its efficiency in resisting dietary wear. Mammalian diets are conventionally classified into the following groupings: carnivores, omnivores, herbivores, and also frugivores. In omnivores, and similarly in carnivores, teeth are brachydont (low-crowned) with long, closed roots. In herbivores, particularly those grazing on abrasive grasses, the teeth have evolved into relatively higher crowns, termed mesodont, and these teeth also have closed roots (Ungar, 2015). Hypsodont, or much higher-crowned teeth, grow for longer over an individual's lifetime and are seen in many lineages, including certain rodents, proboscideans and many extinct families. In some small insectivorous mammals and bats, only the cusps have lengthened, but in the large majority of cases, increased crown height is achieved through hypsodonty (MacFadden, 1992). In some cases, teeth become hypselodont, meaning that they are 'ever-growing' and roots remain open (Ungar, 2015), although this is relatively uncommon in mammals.

2.1.3 Hypsodonty and diet

Definitions of hypsodonty are largely agreed upon but are sometimes brief or simplistic. In simple terms, hypsodont teeth are those teeth that are high-crowned and elongated in comparison to the brachydont teeth (Damuth and Janis, 2011) seen in many carnivorous and omnivorous mammals. One of the key differences between brachydont teeth and hypsodont teeth is that in a brachydont tooth, the entire crown is above the jawline, whereas the crown of a hypsodont tooth is partially retained within the jaw and erupts later on as the crown is worn down through its use in feeding (Janis, 1988). Damuth and Janis (2011, pp. 734) aptly compare this process to "somewhat like the emergence of new lead in a mechanical pencil".

The earliest appearance of hypsodont mammals was during the Late Cretaceous and early Palaeocene of South America, but it was during the Miocene that many ungulate species (Janis and Fortelius, 1988) as well as rodents and lagomorphs became hypsodont (MacFadden, 1992). This broadly coincided with the spread of grasslands, a subject of intense focus and debate in the literature, as discussed below. It was suggested in the early twentieth century that hypsodonty was an adaptive response to the expansion of Miocene grasslands in North America, based on the concurrent radiation of *Merychippus*, a more hypsodont horse than its predecessors during the late early Miocene, around 17.5 million years ago (e.g. Matthew, 1926). Several more ungulate lineages (e.g. camels, equids and rhinoceroses) also show hypsodonty during this time and it is this combination of palaeontological evidence that has been traditionally used as a proxy for the spread of savanna-type vegetation during the Miocene. However, more recent work by Strömberg (2006) suggests from palaeobotanical evidence that grasslands in North America appeared about 4.5 million years earlier, at 22 million years

ago. On this evidence, hypsodonty of *Merychippus* as an adaptive response to grassland environments would be lagged, at least in this genus. However, rodent fossils dating from the time of the first appearance of grasslands at 22 million years ago did have hypsodont dentitions, and another equid genus, *Parahippus*, showed alterations in enamel microstructure at the inception of grassland expansion, which may have increased dental durability. So it can be argued that the fossil record from this time is showing a dental response to the origin of grasslands, albeit not directly through hypsodonty. This slow evolution of full hypsodonty has been suggested by Strömberg (2006) to be a result of weak and changing selection pressures and/or restrictions due to previous phylogenetic adaptations of certain lineages. Further work suggests that the convergent evolution of hypsodonty in multiple lineages may not be predominantly reflecting similar environmental conditions, particularly considering grassland as a driver, because the evolution of hypsodonty appears to be triggered in South America under two different floral environments, one consisting of open-habitat grasses and the other consisting of closed, ash-laden forests (Strömberg *et al.*, 2013).

Most of the focus of previous research on diet and hypsodonty has been through Christine Janis' work on ungulate faunas (Janis, 1984, 1988, 1990, 1995; Janis *et al.*, 2000). As mentioned previously, teeth have evolved and adapted to process food obtained from different habitats and environments. Janis (1984, 1988) stated that in extant ungulates, the grazers (consuming predominantly grasses) are hypsodont, whereas browsers (consuming shrubs, herbs and tree foliage) are brachydont, showing that there is a correlation between the degree of hypsodonty and diet types (grazer, fresh grass grazer, mixed feeder in open habitats, mixed feeder in closed habitats, browser, selective browser and high level browsers). This link between hypsodonty and diet is also seen in the phylogenetic study by Williams and Kay (2001) which correlated diet and hypsodonty but controlled for shared ancestry in tooth morphology and/or feeding behaviour in their investigation.

Studies from the past decade have largely considered the biological, ecological and biome level biases that affect our understanding of the mechanical relationship, as outlined above, which was the focus of earlier studies. It is important to note that the relationship between hypsodonty and diet is not simply related to presence and absence of different plant material, but specifically linked to environmental conditions that limit availability of edible plant material and the varying demands upon the dentition from consuming these different plant foods (Liu *et al*., 2012). In fact, Fortelius *et al*. (2014) suggest that hypsodonty, along with other traits, should be viewed more as "setting the boundary conditions" of habitats, and therefore diets, that are available to any particular species. In this sense, it is advantageous for a species to develop a hypsodont dentition

regardless of evolutionary cost, as in periods of environmental change such as increasing aridity and the spread of open habitats, it is almost a requirement to be hypsodont to access this increasingly important "resource" (Fortelius *et al*., 2014, p. 590). Hypsodonty is not a response to changes in the average resource availability or a species 'diet', but an adaptative response to coping with climatic and environmental extremes (Foretelius *et al*., 2014).

Outside of diet, questions of biases relating to larger spatial or temporal scales have arisen. In fact, it is important to consider regional and continental scale ecometrics to establish baseline comparisons between organism and environmental interactions, not least to discount or at least, be aware of patterns in the geographical distribution of ecometric traits that have arisen by chance and are not related to the environment. Biases from phylogenetic and spatial autocorrelations have been found not to be a significant influence on models of the relationship between hypsodonty and precipitation (Lawing *et al*., 2016; see section 2.2 for further discussion of hypsodonty and climate). A further suggestion that scale plays an important role in our understanding of the functional relationship between dental traits and climate came from Lintulaakso *et al*. (2019) who suggest that whilst faunal clusters in the relationship between dental traits and climate can be seen at any spatial scale, they are only climatically and functionally meaningful at larger scales. Their research revealed that there are eight distinct faunas in North America but only one cluster in Europe and they indicate that functional trait specialisations are likely to be barriers to large-scale mixing. This has implications when considering the applicability of models of hypsodonty-climate relationships on a global scale. This is especially important as in certain areas of the world such as South America, there are very few hypsodont taxa. Therefore, caution should be applied if applying models that only consider the trait of hypsodonty, since a model of that type is suggested not to be able to robustly resolve South American climate. However, all of these models rely on the same ordinated hypsodonty index dataset first published by Janis (1988). Implications of this are discussed further in section 2.2.

2.1.3.1 Fibrousness and toughness

One of the frequently argued points is that the relationship between hypsodonty and diet-induced tooth wear can be explained by endogenous factors. Thus, the physical properties of certain plant foods, specifically their "fibrousnness" and "toughness" (Damuth and Janis, 2011, p. 740), have been the subject of many discussions in studies on extant ungulates. "Fibrousness" is used to describe the ratio of soluble and easily digestible cell contents to the fibrous cell wall, which contains durable cellulose and lignin. Cellulose is more difficult to digest and requires bacterial fermentation to extract

nutrients that can then be digested. Lignin is largely not digestible by mammals. This has meant that “fibrousness” is almost always taken to be a measure of nutritional quality, hence many studies suggest that highly fibrous diets will lead to increased tooth wear, as the individual must consume higher quantities of poor quality food to obtain sufficient nutrition (Damuth and Janis, 2011). However, Clauss and Dierenfeld (2008, cited in Damuth and JanIs, 2011) have suggested that fibre content of browse and graze diets may not actually be that different and that variation in tooth wear rates, and thus varying levels of hypsodonty, is not due to variation in nutritional quality. Similarly, it has been suggested that “toughness”, the resistance of material to cutting, also explains the relationship between hypsodonty and feeding. Higher occlusal pressures required to process tough vegetation may be needed and this may increase the effect of abrasive particles in the food (phytoliths, grit etc – see below). However, the fibrous nature of the plant material is not likely to contribute significantly to tooth wear (Damuth and Janis, 2011) nor warrant any response in crown height.

2.1.3.2 Phytoliths

Grasses often contain phytoliths (plant silica) and these are often considered a type of defence mechanism to deter predation by herbivores, as well as provide physical support to the plant (Piperno, 2006). Grazers avoid plants with high phytolith content, as evidenced from several laboratory studies where, given the choice, and with all else equal, herbivores will choose to eat those plants with fewer phytoliths (Massey and Hartley, 2006, 2007). Damuth and Janis (2001) suggested that despite these acts of choice, and some evidence of very high phytolith content being an irritant (Laca *et al*., 2001), phytoliths generally do not deter feeding. A study on Japanese sika deer showed increases in tooth wear rate with increased consumption of silica-rich vegetation (Kubo and Yamada, 2014), although the fibre content of this vegetation must also be considered based on the discussion above. The hardness of phytoliths has also been studied and, despite original conclusions that phytoliths are harder than enamel (Baker *et al*., 1959), more recent research has concluded the opposite: that phytoliths are generally not capable of wearing tooth enamel (Sanson *et al*., 2007; Lukas *et al*., 2013; Erickson, 2014).

2.1.3.3 Exogenous dust and grit

Janis (1988) concluded that grit and dust adhering to food were more important abrasive elements than the siliceous phytoliths for a number of reasons: (1) crown height could not distinguish between grazers and mixed feeders in open habitats, (2) mixed feeders in open habitats were more hypsodont than mixed feeders in closed habitats, (3) grazers

of fresh grasses in floodplains had significantly lower degrees of hypsodonty than grazers in open habitats or mixed feeders and (4) species browsing at a high level above ground were less hypsodont than those browsing at lower levels in the same habitat. The processes through which exogenous grit and dust become ingested are frequently discussed in the hypsodonty literature (e.g. Williams and Kay, 2001; Damuth and Janis, 2011; Sanson *et al*., 2017), especially in view of Janis' conclusions mentioned above, but the role of phytoliths is usually championed. In fact, the first mentions of the role of non-plant abrasives came in the late nineteenth century (Kovalesky, 1874, cited in Damuth and Janis, 2011), but it is only recently that more empirical studies on dust, soil, grit and feeding have been completed.

Observations of herbivore feeding have revealed that some species unintentionally consume large amounts of soil that is mixed in with vegetation or adheres to the surface (Damuth and Janis, 2011). It is likely that this varies within individuals of a species as shown by many studies on domestic cattle, where soil can comprise anywhere between 1% and 18% of daily dry matter intake, depending on the season (Kirby and Stuth, 1980; Green and Dodd, 1988). For sheep, who graze closer to the ground, this can reach 33%, although averages are around 5% (Healy and Ludwig, 1965a,b), which is also comparable to wild horses (Sneva *et al.*, 1983) and bison (Beyer *et al*., 1994). In mixed feeders, the values are <2%. Different types of soil can have different effects on tooth wear, as shown by studies on sheep grazing on different soils (Healy and Ludwig, 1965a,b; Ludwig *et al*., 1968). A recent controlled laboratory study, again on sheep, shows that dust on food surfaces has little effect on teeth and that it is the endogenous properties that are acting as selection pressure for dental adaptations (Merceron *et al.*, 2016). However, soil can have many component parts and while some are relatively soft, the presence of hard quartz (when present) can abrade enamel easily. Finally, it has also been suggested that differences between soil consumption of browsers and grazers stem from the latter being unselective in their feeding (Damuth and Janis, 1988).

2.1.4 Teeth, environment and climate

Research focus on endogenous factors acting as selection pressure for hypsodonty has led to a small number of studies beginning to investigate possible environmental and climatic controls on hypsodonty, rather than diet alone. It is without question that environment and climate will control the distribution, type and quality of vegetation, so an environmental or climatic component is to be expected. The most interesting avenue of research is that which has suggested that hypsodonty itself can be used as a climate proxy. Hypsodonty has already been shown to correlate with dietary habitats from open grasslands to closed forests (Janis, 1988 – see above). Annual precipitation controls the amount of tree cover in any given habitat or environment (Janis *et al*., 2004). As

precipitation, habitat and hypsodonty are linked in this way, there is potential to predict precipitation amount statistically. Indeed, several studies have shown that mean hypsodonty index of mammalian communities is a good predictor for the level of precipitation in the habitat of the community (Damuth *et al*., 2002; Janis *et al*., 2004, Eronen *et al*., 2010a;). The development of these ideas came through significant work on Neogene fossils, using a 'per-species mean hypsodonty' (Fortelius *et al*., 2002, 2006; Janis *et al*., 2004, Eronen, 2006) and this is discussed further in the following section.

2.2 Hypsodonty and quantifying climatic variables

2.2.1 Defining hypsodonty index

Several recent studies have tested the potential for hypsodonty to predict environmental parameters such as net primary productivity (Liu *et al.*, 2012; Žliobaitė *et al.*, 2016) and climatic variables such as temperature and precipitation (Eronen *et al.*, 2010a; Liu *et al.*, 2012; Žliobaitė *et al.*, 2016). Hypsodonty data in these studies are values of 'per-species mean hypsodonty' as defined by Janis (1988). In this seminal study, average hypsodonty values were calculated for each species by measuring the 'hypsodonty index' (the ratio of tooth crown height to the width of the same tooth – see section 3.1.2.1 for further explanation) of no more than six individuals, in most cases measurements were only taken from one or two individuals (Janis, 1988). All living individuals of that species are then assumed to have that hypsodonty index. These hypsodonty indices are subsequently classified into "approximate ranges" and hypsodonty indices are parameterised as follows: brachydont teeth (those with a hypsodonty index of less than 1.5), mesodont teeth (those with a hypsodonty index between 1.5 and 3), hypsodont teeth (those with a hypsodonty index between 3 and 4.5), and highly hypsodont (any teeth with a hypsodonty index greater than 4.5) (Janis, 1988, pp. 380). Despite Janis (1988) suggesting that these parameters should not be taken as rigid, the way in which the recent studies use hypsodonty index is exactly that, with ordinated scores rather than representing hypsodonty as a continuous variable.

2.2.2 Hypsodonty index and quantifying modern climate and environment

The first study to fully explore the modern relationship between hypsodonty index and precipitation in a quantitative way was that of Eronen *et al.* (2010a), with the main aim of using new estimates in climate modelling. Using regression trees, it was shown that there is a non-linear relationship between hypsodonty and mean annual precipitation (r^2=0.581, mean error of 388mm). Eronen *et al.* (2010a) suggest that this large standard

error is in part caused by the re-invasion of more humid habitats by more hyposodont taxa that have large home ranges and broad habitat preferences. It is likely that the per-species mean hypsodonty also contributes to the low r^2 value and larger error as this uses ordinated values of hypsodonty rather than those on a continuum, which is likely to be a more representative method of measuring hypsodonty. In a sense, hypsodonty index treated in this way is acting as presence-absence data. Despite this, Eronen *et al.* (2010a) report that climate in Africa was extremely well estimated in their results (likely due to Africa being the region where mammal distribution has been subject to the least impact from humans) along with well-estimated values for Eurasia and slightly less so for the Americas. In North America, large proportions of the continent were lacking mammal data, whilst in South America there are large areas of tropical rainforest with high precipitation which seemed to prove problematic in predicting hypsodonty.

When assessing the study by Eronen *et al.* (2010a), it is important to understand the spatial distribution of different mammal taxa. The spatial resolution of their mammal distribution data is at 'ecoregion level', with ecoregions defined by the World Wildlife Fund (WWF; Olson *et al.*, 2001). Each ecoregion has a list of mammal species present within it, with the assumption that the presence of a species indicates that it is distributed throughout the entire ecoregion (Eronen *et al.*, 2010a), which may be an overestimation. As Janis (1988) gave the mean hypsodonty index per species, the average hypsodonty index of each ecoregion can be calculated. However, these studies do not take the mean hypsodonty values for each species but instead use the ordinated scores above that were not designed to be rigid. For example, the tufted deer (*Elaphodus cephalophus* Milne-Edwards, 1872) has a hypsodonty index of 1.69 and the common eland (*Taurotragus oryx* (Pallas, 1766)) has a hypsodonty index of 2.91 (Janis, 1988, Table 5, p. 386) but both would be classified as 'mesodont' and given a score of '2' (e.g. Liu *et al.*, 2012). It is this number that is used to establish the average 'class' of hypsodonty per ecoregion, rather than the actual per-species mean hypsodonty index calculated by Janis (1988). This is the case even if the hypsodonty index of the aforementioned two taxa were averaged from measurements on only three and two individuals respectively. It is therefore doubtful that this is representative of the natural mean hypsodonty index for the whole species. Furthermore, intraspecific variation is not adequately assessed for any of the taxa in Janis' dataset.

Climatic data for these studies were obtained from the high resolution WORLDCLIM dataset produced by Hijmans *et al.* (2005), for which there is now an updated version (Fick and Hijmans, 2017). To assess the relationship between climate and hypsodonty index (i.e. the average hypsodonty index of each ecoregion), it is necessary to have the two sets of data at the same spatial scale, here at the scale of the ecoregions. This

should be not confused with the spatial resolution of the datasets, which are rendered to a comparable resolution in the studies. Problems arise when certain areas classed as one ecoregion do not have the same climate across the board when considering the individual variable layers in the Hijmans *et al.* dataset. For example, the British Isles are classed as one ecoregion but, when looking at mean annual precipitation, a strong precipitation gradient exists from the wetter west coast of Ireland to the relatively dry 'climate' of East Anglia. Ecoregions are traditionally defined as areas with the same environmental conditions and climate (Eronen *et al.*, 2010a) but the datasets are at a discord with one another in these studies.

Further work was undertaken by Liu *et al.* (2012), using dental ecometric traits of loph counts and molar crown complexity in addition to hypsodonty. These traits allow estimation of net primary productivity, since this is constrained by the three interactive components of temperature, precipitation and solar radiation. As dental characteristics have been used to reveal temperature and precipitation, they should therefore also be applicable for estimation of net primary productivity in both the present and the past. For estimating temperature, using loph count and hypsodonty together as covariates provided the greatest accuracy (r^2=0.69) whereas hypsodonty alone was not useful (r^2=0.01). For estimating precipitation, hypsodonty had the highest correlation with the precipitation of the driest month and the driest quarter. In this case, high levels of hypsodonty seem to be associated with the presence of a specific dry season. Estimating net primary productivity was also shown to be successful using hypsodonty and loph count together (Liu *et al*, 2012).

Another recent study attempting to quantify environmental variables from dental traits is that of Žliobaitė *et al.* (2016). This study brought the spatial scale down from ecoregion to a more local level, focussing on thirteen national parks in Kenya and using available meteorological data and modern mammal assemblages from the past 60 years. These mammal assemblages were assessed for their dental traits/functional crown types including ordinated hypsodonty, horizodonty (tooth crown length), acute lophs, obtuse lophs, structural fortification of cusps, flat occlusal topography and coronal cementum. Least Angle Regression (LARS) models were used to test which dental traits could accurately predict climatic limits in the ecosystems of Kenya. Interestingly, hypsodonty is almost never used in the models as best predictor. It was further suggested by these authors that hypsodonty should be regarded as redundant and therefore rejected, as it is very strongly correlated with four of the other variables. Hypsodonty was deemed to be still informative but the model results indicated that the relevant information captured by hypsodonty was already captured in the model by the other predictors. The results of the models show that the minimum net primary productivity is well estimated, thereby

improving on previous studies that only estimated average or overall climate rather than the extremes or limiting conditions. The conclusions are very interesting in that they suggest that the main functional link between climate and herbivore teeth is not the properties of the average food consumed but is instead the non-availability of the preferred plant foods during dry seasons or long dry periods.

An attempt to use a more comprehensive approach was taken by Galbrun *et al.* (2018), using data mining and redescription mining. Data mining involves the analysis of pre-existing databases, whilst redescription reframes the data, giving an explanation (or a description) of it in two or more different ways. In a species distribution context this may be that a region of the earth can be first described as the area where species X is present, where the second description of the same region is its climate (Galbrun and Mietinen, 2017). This approach was used to investigate a number of dental functional traits, including hypsodonty from global occurrences of large herbivorous mammals and climatic variables (Galbrun *et al*., 2018). This was a development of the work of Eronen *et al.* (2010a) as outlined at the start of section 2.2.2, but with generated conclusions that differed among regions. Ordinated hypsodonty scores were again used, on a per-species mean hypsodonty basis, and this was derived per locality based on species presence or absence. The hypsodonty score per locality was suggested to capture the community adequately at each locality in question, however no measurements of hypsodonty index were taken from any locality. The same averaging approach was taken for other dental functional traits, which were added and tested in Galbrun *et al*.'s model. Their redescription approach involved 'querying' each locality once through bioclimatic variables, and once through the dental traits. Each pair provides two different ways (two descriptions) to characterise a single site, and these redescriptions were then characterised spatially in the same way as the conventional biome approach, but were described as "computational biomes" (Galbrun *et al.*, 2018, p.8). These computational biomes largely match the Köppen-Geiger climate classification (Kottek *et al*., 2006), and the redescriptions contain both a bioclimatic and functional trait component, instead of a bioclimatic one alone. However, as opposed to the classic biome approach, the computation biome distribution exists simply as spatial data and does not account for geographic effects such as orography.

Their results indicate that three zones can be distinguished through their redescription approach: "the boreal-temperate moist zone, the tropical moist zone and the tropical-subtropical dry zone" (Galbrun *et al.*, 2018, p.28). In their conclusions, these authors state that the boreal-temperate moist zone is characterised by seasonal cold temperatures, low hypsodonty and high percentage of species with obtuse lophs. The tropical moist zone is reportedly characterised by high temperatures, high isothermality

and high precipitation, with high hypsodonty and high horizodonty. Finally, the tropical-subtropical dry zone is characterised by high seasonality of temperature and precipitation, with high hypsodonty and high horizodonty. Additionally, and curiously, the dental traits recorded for climatically-similar sites were different, for example, moist African forests had a much higher share of hypsodont species, compared to moist North American forests. They suggested that anthropogenic effects in both these areas account for this difference, although no further explanation was given. These authors also suggested that their approach reveals that the Tibetan plateau is "covered by redescriptions from the tropical-subtropical dry group and by redescriptions from the boreal-temperate moist group" (Galbrun *et al.*, p.28), which may indicate that this area has a combination of both groups in its climate and dental functional traits. This would clearly be at odds with the traditional Köppen-Geiger climate classification of the Tibetan plateau as cold tundra (Kottek *et al*., 2006). According to the authors the redescription approach can reveal locations where a unique (spatial) relationship between dental functional traits and climate exists, although it is unclear how often this phenomenon is present in the global data, and whether this has much relevance in improving our understanding of the hypsodonty-climate relationship in this prediction modelling context.

The most recent work on hypsodonty (and other dental traits) was published by Oksanen *et al.* (2019), in which these authors create new models to estimate temperature from ordinated hypsodonty scores and loph counts. The focus here is on the higher latitudes, with the aim of incorporating more of the temperate climate zones as opposed to the previous models that concentrated more on accurately predicting climate in the tropical latitudes (e.g. Eronen *et al.*, 2010a). Additionally, temperature is the more limiting climatic factor in the temperate zones, and as seen in previous work in ecometrics, is more difficult to predict (e.g. Eronen *et al.*, 2010a; Liu *et al.*, 2012). The new models created by Oksanen *et al.* (2019) resolve better the acute lophs, which reportedly carry a temperature signal, often masked by hypsodonty as the more dominant trait. Overall, their research presents "refined" models (Oksanen *et al.*, 2019, p.1772) to predict modern temperature from dental traits, as well as suggesting an improvement to predict net primary productivity under the same methodology. The model may be refined but the underlying data is still very much a presence-absence dataset of mammals with scored traits that assume no intraspecfic variation, full distribution of specific taxa across whole biomes, and with no actual measurements of hypsodonty of individuals. Their new models were applied to Pleistocene fossil localities, which will be discussed in the following section.

2.2.3 Hypsodonty index and past climate and environment

The first study to apply the idea of hypsodonty to estimate climate quantifiably in the past was Eronen *et al.* (2010b), who directly applied their modern model to a database of Neogene fossils. Again, this is a presence-absence dataset, with ordinated hypsodonty scores given to each taxon, following Janis (1988). No measurements were acquired from fossil material, with an assumption of no intraspecific variation. These authors validated their method using available palaeobotanical information but the temporal scale of the mammalian data is very coarse, with time slices ranging from 1.4 million years for the "Early Pliocene" to eight million years for the "Early Miocene" (Eronen *et al.*, 2010b, p.238). Using presence-absence data for fossil mammal taxa in order to create a "community" that spans such lengthy time periods may not be representative, especially as it is known from the marine oxygen isotope record that climate shifts occurred on much shorter timescales, even back into the early Pliocene and beyond, although not on the scale and magnitude of Quaternary glacial and interglacial cycles (Lisiecki and Raymo, 2005). There is also a question around the source and resolution of the proxy data used to validate the hypsodonty-inferred quantifications of climate. Again, over such large time slices, there is a question as to the resolution of palaeobotantical proxies and the likelihood that climate signals may be masked or moderated as a factor of the long time span of the sample. These doubts lead to the conclusion that further testing should be done at different spatial and temporal scales.

The improved modern model created by Oksanen *et al.* (2019) was also applied to Pleistocene fossil sites. This brought the temporal scale down to a level for which more representative and comparable proxy data are available, compared to validating with proxy data across large faunal units of the Miocene and Pliocene as had been done previously by Eronen *et al.* (2010b). In this latest research, 50 Early and Middle Pleistocene mammal sites with previously-published estimates of mean annual temperature and mean temperature of the coldest month were selected. These estimates were obtained using either climatic tolerances of ectothermic vertebrates or from the mutual climatic ranges of fossil beetles or ostracods. These provide a site-by-site basis for comparison, at much higher temporal and spatial resolution than that of the previous studies. Mean annual temperature, mean minimum temperature of the coldest month and net primary productivity were estimated for these fossil sites using an ecometric approach involving hypsodonty and obtuse lophs. For the fossil sites, mean annual temperature was found to be overestimated using dental traits when compared to the proxy reconstructions, whereas mean minimum temperature of the coldest month was more similar to the proxy reconstructions; however, although the correlation was positive, it was not very strong at R^2=0.64 (p=0.03). Nevertheless, the proxy and mammal

assemblage data were averaged across the entire sequence at each site, which may have masked variation and some taxa in the mammal dataset may have been assumed to co-exist when this is not necessarily the case. It would have been interesting for Oksanen *et al.* to have applied their model to precipitation and aridity on these timescales, as precipitation is far less well-resolved on Pleistocene timescales than temperature. This provides a future line of investigation for the current research.

Faith *et al.* (2019) applied the dental ecometric approach at Late Pleistocene sites in Africa and revealed some pitfalls with the methodology. Here, these authors stressed that too much emphasis is given to the robustness of ecometric-inferred estimates of palaeoclimate variable (e.g. the mean annual precipitation at locality X at time Y). This is because the means of ecometric traits such as hypsodonty vary with sample size, meaning a skew of the mean in certain situations when the ecometric trait in question is not randomly distributed across the species abundance distribution (e.g. abundant taxa may have different traits than rare taxa). Sample size is inherently a problem in fossil contexts based on preservation, fossil recovery and other taphonomic issues. The issue is that if a trait is different in rare taxa, this difference will not be reflected in the mean until the sample size is large enough to capture the rare taxa. This may not have been a problem across the large slices of the Neogene as used by Eronen *et al.* (2010b) but with increasing spatial and temporal resolution, this becomes significant and must be considered when using ecometric approaches. Faith *et al.* suggested that the trait mean should be weighted by taxonomic abundance. However, abundance data may not be available for fossil assemblages or may be unreliable where a taphonomic or collection bias is apparent (e.g. Faith and Lyman, 2019). The ecometric approach is thus problematic and is worsened when combining dental traits in models, a procedure deemed necessary to improve model fit in modern contexts (e.g. Eronen *et al.*, 2010a,b; Liu *et al.*, 2012; Žliobaitė *et al.*, 2016; Oksanen *et al.*, 2019). A lot of factors must be considered under these approaches and the functional herbivory-morphology-climate mechanism of hypsodonty, which is simultaneously well studied but not comprehensively understood, may need to be investigated outside of the functional ecometric approach.

2.3 Summary and proposed further research questions

Although there is a large body of research published on the links between dentition and climate and hypsodonty itself, there has been an intense focus on ecometric methodologies. The opportunity thus exists to test the ability of hypsodonty alone to predict climate without using ordinated scoring and percentages of hypsodont taxa within an assemblage.

The ecometric approach and mean community ordinated hypsodonty has been defended as a way to capture the whole community in an unbiased way (Fortelius, 2019). However, it could be argued that the ecometric approach applied thus far to create models to predict climate and environment makes too many assumptions and that methods built upon successive studies have propagated uncertainties through averaging of biological variability (especially with assumptions of no intraspecific variability) and averaging of climatic variability across vast spatial and temporal scales. The building of the global model of the relationship between hypsodonty (and other dental traits) and climatic variables has been applied at large spatial scales and at coarse resolution. An improved approach would be to make the resolution of the global model much higher, at point localities. Again, the presence-absence of mammal taxa at biome scale is an approach that is perhaps too simplistic and evidence from locality-level mammal communities could be tested against climate in future, instead of assuming mammals coexist through all localities within a biome.

Questions about the hypsodonty data have thus been raised through this review. Ordinated per-species mean hypsodonty is a coarse metric and in order to refine it, measurements of hypsodonty index should be taken from individual animals and any assumption surrounding intraspecific variability should be thoroughly tested. There is also a need to standardise the idea of hypsodonty index as currently, the lower third molar has been suggested as the basis for the per-species mean hypsodonty ordinated values (as per Janis,1988) but subsequent work refers to the second molars, both upper and lower, which, in certain taxa, are very morphologically different. A more consistent approach is consequently needed. In order to permit more effective comparison with previous studies, the lower third molar may be the tooth of choice as it underlies the per-species mean hypsodonty datasets so commonly used previously, although it is worth bearing in mind that there appears to be limited robust empirical testing of which molar records a climatic (or functional) signal (if any).

The potential to predict palaeoprecipitation using hypsodonty of large herbivores is an attractive concept, since developing past precipitation proxies such as stable isotope geochemistry is often time- and resource- intensive. A high level of interest in a potential rapid, cheap proxy estimator exists in the Quaternary palaeoclimate community, especially over timescales of abrupt climate change, such as in the Late Pleistocene (Rasmussen *et al.*, 2014). An ideal palaeoprecipitation proxy would involve a method where data are collected rapidly and quantified estimates can be calculated with ease. The apparent strength of the mechanistic concept linking hypsodonty and climate, and the abundance of Quaternary fossils, especially ungulates, means that this avenue warrants exploration. The approach taken in this thesis considers only ungulates,

reflecting their abundance and predominance in Quaternary assemblages. Orders such as Primates and Proboscidea are not included in the present study, as primate and proboscidean fossils are rarely identified in Quaternary fossil sites, particularly in the Late Pleistocene test cases from the Mediterranean that are included in this thesis. Although Primate habitats are largely at the wetter end of the aridity spectrum, the absence of this Order and predominance of ungulates in most Quaternary assemblages means that an investigation solely involving ungulates is warranted. It is also suggested that changes in mean hypsodonty in Neogene Eurasia was driven by the most common ungulates of each time interval (Fortelius *et al*., 2014), highlighting their important role. However, before this model can be applied to the Quaternary palaeontological record there needs to be a reinvestigation of the fundamental correlative link between climatic variables and actual measurements of hypsodonty index, at the appropriate spatial and temporal scales, and a new model developed for the present day relationship, before it can be tested on fossil sites with the aim of reconstructing past precipitation over millennial and centennial scales of abrupt climate change.

In light of the aim of obtaining robust, reliable and rapid palaeoprecipitation estimates over abrupt timescales, this review of the literature has culminated in a number of questions that will addressed by the current research. This thesis aims to address the following hypotheses:

1. Hypsodonty index values of each taxa measured in the modern dataset are normally distributed and intraspecific variability is low, which would validate the assumption of per-species mean hypsodonty.

2. Using actual raw measurements of the teeth of individual animals will predict climate as robustly (if not more robustly) than the previous ecometric approach using ordinated per-species mean hypsodonty.

3. Individual raw hypsodonty index measurements of individuals and mean hypsodonty of the community that is actually present will correlate to climate more strongly than the mean of ecoregion mammal communities (where taxa are assumed to be present or absent). Under this hypothesis, this thesis will also consider the following:

    - Are precipitation and aridity as important as the mechanistic understanding would suggest?

    - Or is the temperature signal reported in some of the most recent research of significance?

4. Climate variables can be accurately and robustly quantified in the past using

fossil hypsodonty index measurements.

5. Climatic or environmental signals can be seen in community average hypsodonty changes through time, regardless of correlation between hypsodonty index and climate variables.

CHAPTER 3
Materials and Methods

The following sections outline the materials and methods used to collect the data to explore variations in ungulate hypsodonty across the globe in present-day and Late Pleistocene communities. The rationale behind the analytical approach that was used is stated, with reference to addressing the aims of this study.

3.1 Materials and methods for investigating variations in modern ungulate hypsodonty

3.1.1 Materials used for investigating variations in modern ungulate hypsodonty

3,788 measurements of hypsodonty index (defined below in section 3.1.2.1; see Table 4.1 for totals per taxon) were collected from specimens from the following zoological and comparative anatomy collections: Natural History Museum, London, UK, University Museum of Zoology, Cambridge, UK, Powell-Cotton Museum, Quex Park, Birchington-on-Sea, UK, Muséum national d'Histoire naturelle, Paris, France, Museum für Naturkunde, Berlin, Germany, Naturhistoriska riksmuseet, Stockholm, Sweden, Royal Belgian Institute of Natural Sciences, Brussels, Belgium and the Royal Museum of Central Africa, Tervuren, Belgium.

The criteria used for the selection of suitable specimens were as follows:

1. The specimen must be of an ungulate taxon of the Orders Perissodactyla or Artiodactyla (excluding the Family Hippopotamidae as members of this Family are semiaquatic and despite predominately eating terrestrial grasses, also consume some aquatic plants (Grey and Harper, 2002) and have shown carnivorous behaviour (Dudley, 1998) which means that they will have a different mechanistic relationship between feeding behaviour, dentition and climate). In this thesis, herbivores are defined as taxa that feed exclusively on any plant material (including lichens).
2. The specimen must be an adult with the lower third molar (M_3) present and fully erupted (the base of the crown of the M_3 is above the top of the mandible in Cervidae and in other Families, a crown is fully erupted when the third cusp is clearly above the edge of the mandible and the heights of the first two cusps are comparable to the height of the cusps of the M_2).

3. The M_3 must be unworn or only partially in a state of wear (see Figure 3.4)
4. The crown of the M_3 must not be damaged in a way to preclude the collection of measurements as outlined in detail in section 3.1.2.1.
5. The specimen must be well-provenanced (the locality where the specimen was collected in the field must be known to an appropriate level of detail such as town or longitude and latitude).

The list of specimens measured is presented in a database in Appendix 1 and the spatial extent of specimen localities is shown in Figure 3.1. Additionally approximately 5,000 additional specimens were examined but did not meet the above criteria (for example, specimens that were not labelled with an accurate locality, specimens that were too worn, specimens where the M_3 was damaged, or specimens where it was unclear whether it was wild, or appeared to be sourced from animals that resided in captivity).

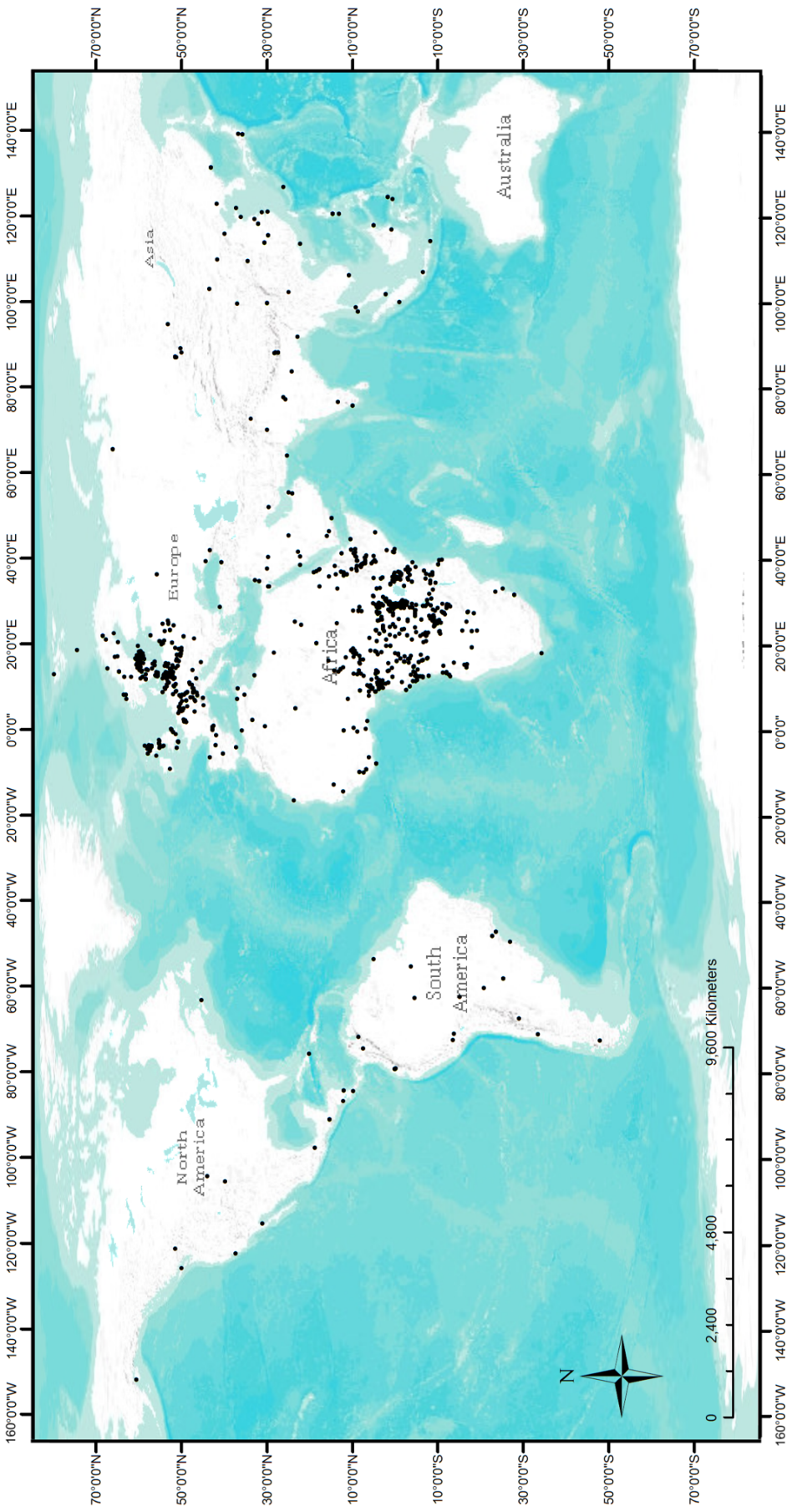

Figure 3.1: Map showing the localities (black markers) of the specimens measured for the study of modern ungulate hypsodonty index.

3.1.2 Methodology for investigating variation in modern ungulate hypsodonty

This section outlines the approach taken for collecting the measurements of hypsodonty index and then explains the analytical approach taken with the data.

3.1.2.1 Methodology for measuring hypsodonty index

Measurements of hypsodonty index were carried out following the methods outlined in Janis (1988). The height of the crown was measured on the buccal side of the M3 from the base of the enamel at the lowest point to the tip of the highest cusp. The measurements are outlined below in Figures 3.2 and 3.3. Measurements were collected for specimens from all but one collection using a digital vernier calliper (Sealey Professional Tools Model Number AK9623EV; resolution of 0.01 mm and an accuracy at <100 mm of ±0.04 mm). The Powell-Cotton Museum did not permit the use of this metal-ended calliper in order to protect their specimens from damage so specimens from this collection were measured with a plastic-tipped calliper (Carbon Fiber Composites; resolution of 0.1 mm and repeatability of 0.1 mm).

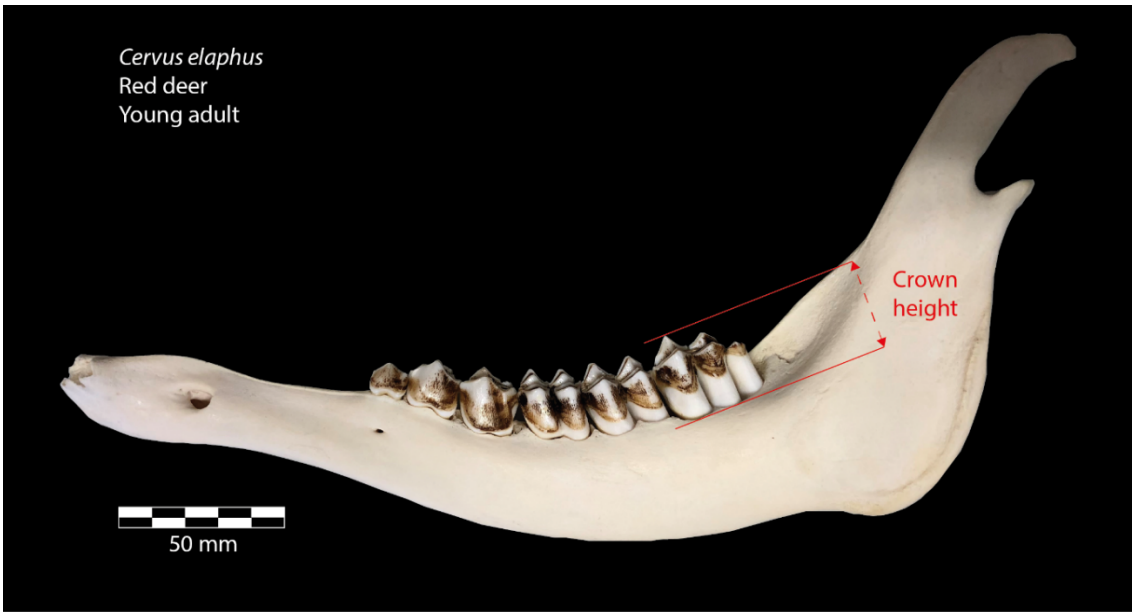

Figure 3.2: Buccal view of the left mandible of a young adult red deer (*Cervus elaphus* Linnaeus, 1758). The location for measurement of tooth crown height of the M_3 is shown in red. Specimen from the comparative collection at the Department of Geography at Royal Holloway University of London.

Figure 3.3: Occlusal view of the left mandible of a young adult red deer (*Cervus elaphus*). The location for measurement of tooth crown width of the M_3 is shown in red. Same specimen as Figure 3.1.

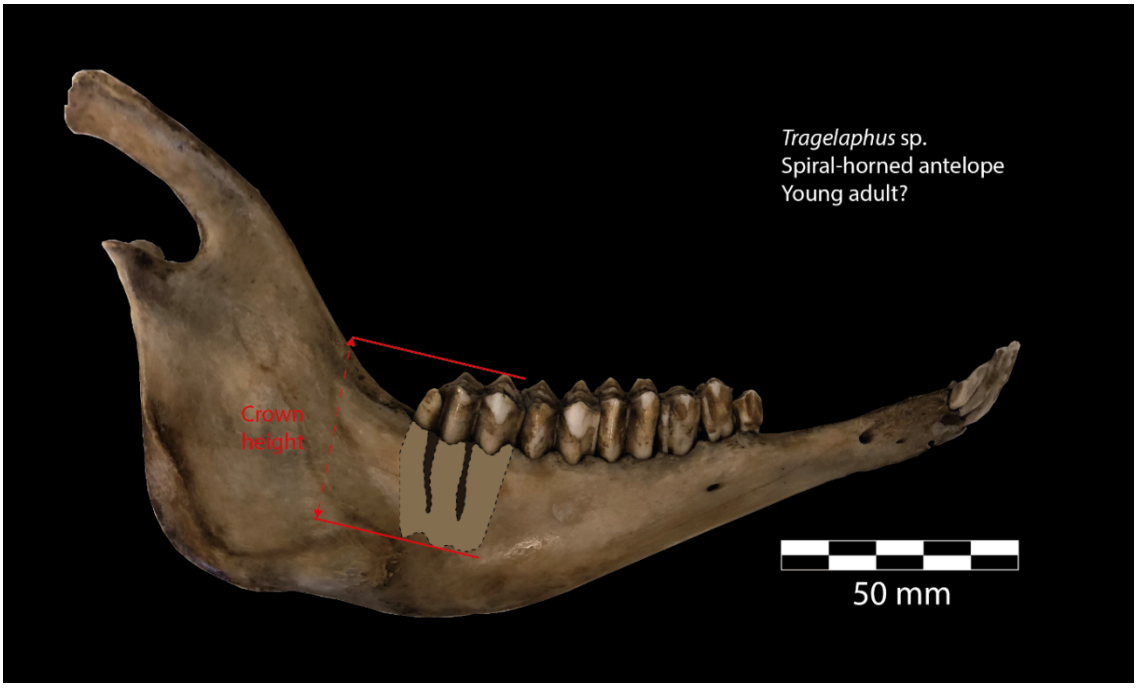

Figure 3.4: Buccal view of the right mandible of a young adult spiral-horned antelope (*Tragelaphus* sp. de Blainville 1816); the teeth are fully erupted but exhibit very little wear. The portion of the M_3 that is below the jawline is shown. The location for measurement of tooth crown height of the M_3 is shown in red. Specimen from the comparative collection in the Department of Geography, Royal Holloway University of London.

For taxa where the base of the crown of an adult M_3 is fully above the jaw line, measurements were taken as described above. For taxa where the base of the crown may be within the mandible, such as those in the family Bovidae, a different procedure was used. Following Janis (1988), the measurement of the crown height was undertaken by feeling for the base of the crown within the mandible and measuring from this point to the highest cusp (see Figure 3.4). This is a standard approach to measuring these types of teeth in studies of tooth crown height. Ideally a more precise measurement of crown height in these taxa could be undertaken using x-rays, however as this study included a very large number of specimens from many collections, the practicality, availability of appropriate equipment and temporal and financial constraints precluded the use of x-

rays in this research. The measurement of crown width in these types of teeth was undertaken as per Figure 3.3 above, using the widest part of the crown accessible above the jawline.

Measurements were recorded in a master database as crown height and crown width for each tooth measured and hypsodonty index was calculated as follows:

$$hypsodonty\ index = \frac{crown\ height}{crown\ width}$$

Calculated hypsodonty measurements are documented in the results in Chapters 4 and 6 to two decimal places to reflect the higher resolution (0.01mm) of the digital vernier calliper that was used for the majority of measurements (Sealey Professional Tools Model Number AK9623EV).

The other data recorded in the master spreadsheet were: (1) name of the collection, (2) specimen number, (3) Order, (4) Family, (5) Genus, (6) Species, (7) sub-species (if applicable), (8) sex (if known), (9) locality information, (10) side (left or right), (11) wear score and (12) date of data collection.

For recording wear, suitable specimens were scored a “1” if the tooth was unworn and “2” for those just in wear. Teeth that were too worn were discounted but could have also been assigned a score of “3”, “4”, etc. All measurements were included in first steps of analysis but differentiation of those specimens that are completely unworn and just in wear permits further subsequent analysis and exploration. Examples of suitable and unsuitable teeth are shown below in Figures 3.5-3.7.

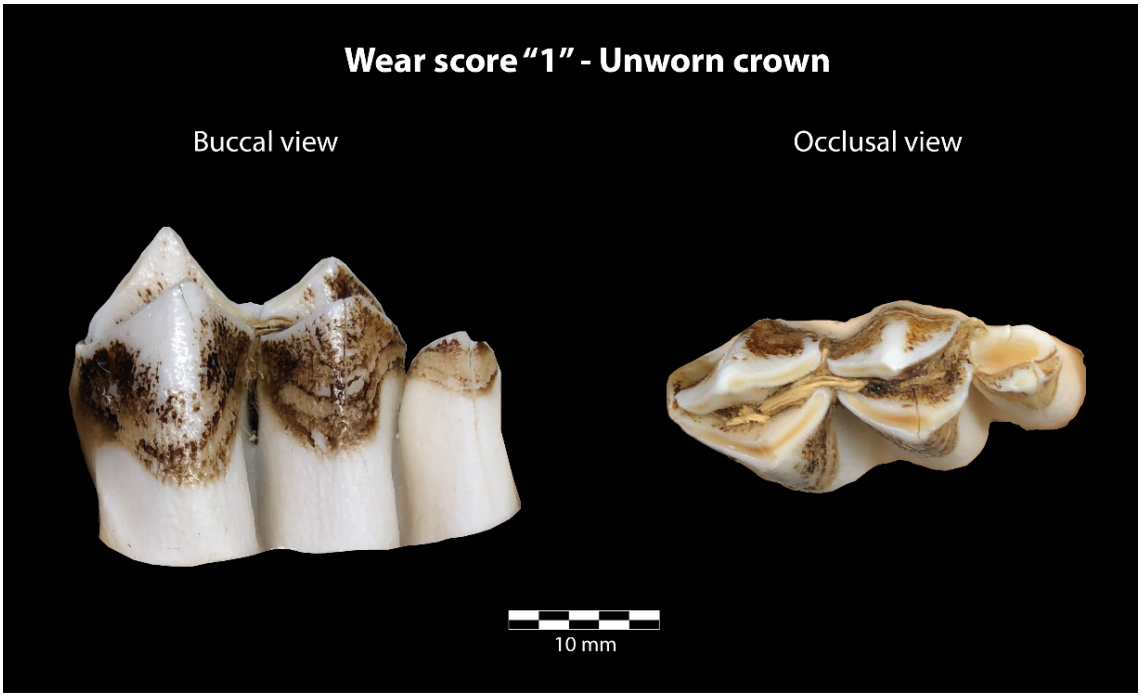

Figure 3.5: An example of an unworn *Cervus elaphus* M_3 which would be scored as "1" and therefore suitable to be measured for hypsodonty index in this study.

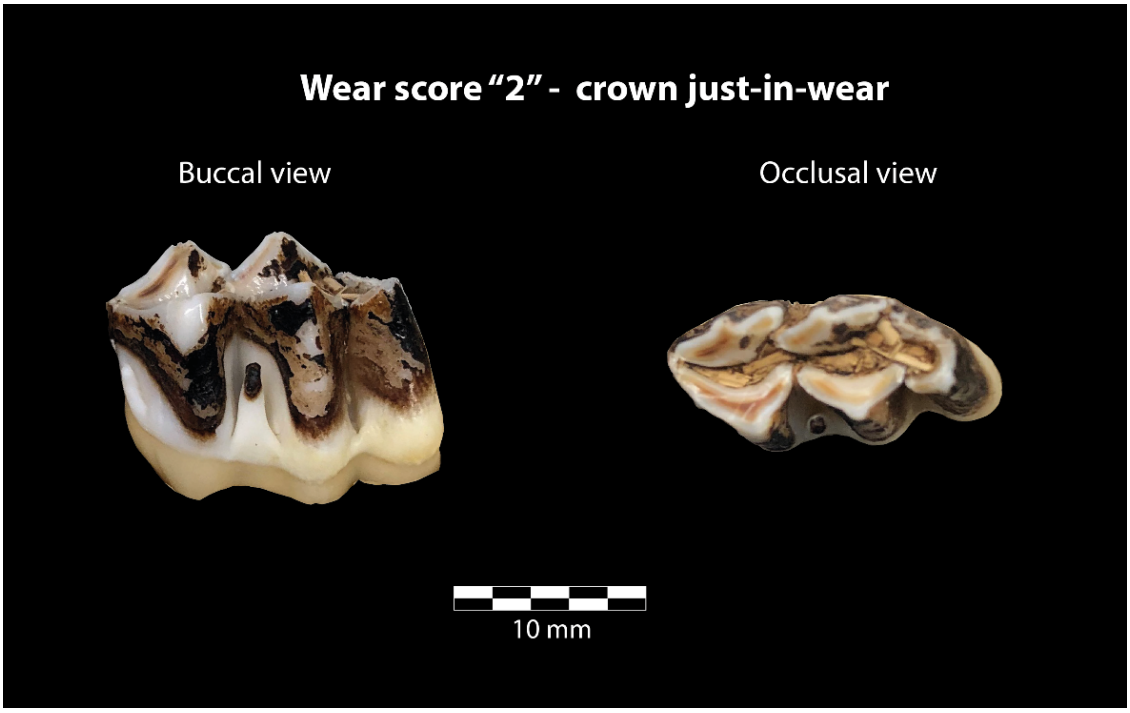

Figure 3.6: An example of a *Capreolus capreolus* (Linnaeus, 1758) M_3 exhibiting a small amount of wear and would be scored as "2" and therefore suitable to be measured for hypsodonty index in this study.

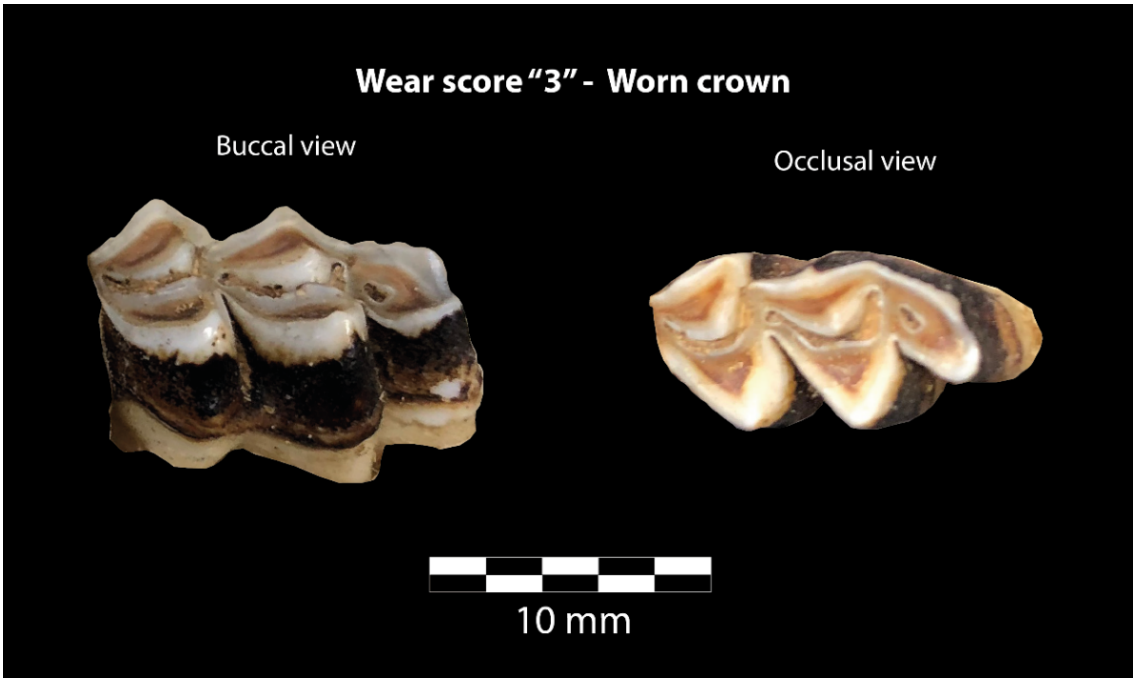

Figure 3.7: An example of a cervid M3 exhibiting a larger amount of wear and would be scored as "3" and therefore unsuitable to be measured for hypsodonty index in this study.

Figure 3.8 provides schematic line drawings of low, medium and high levels of hypsodonty to highlight examples of taxa with different crown heights.

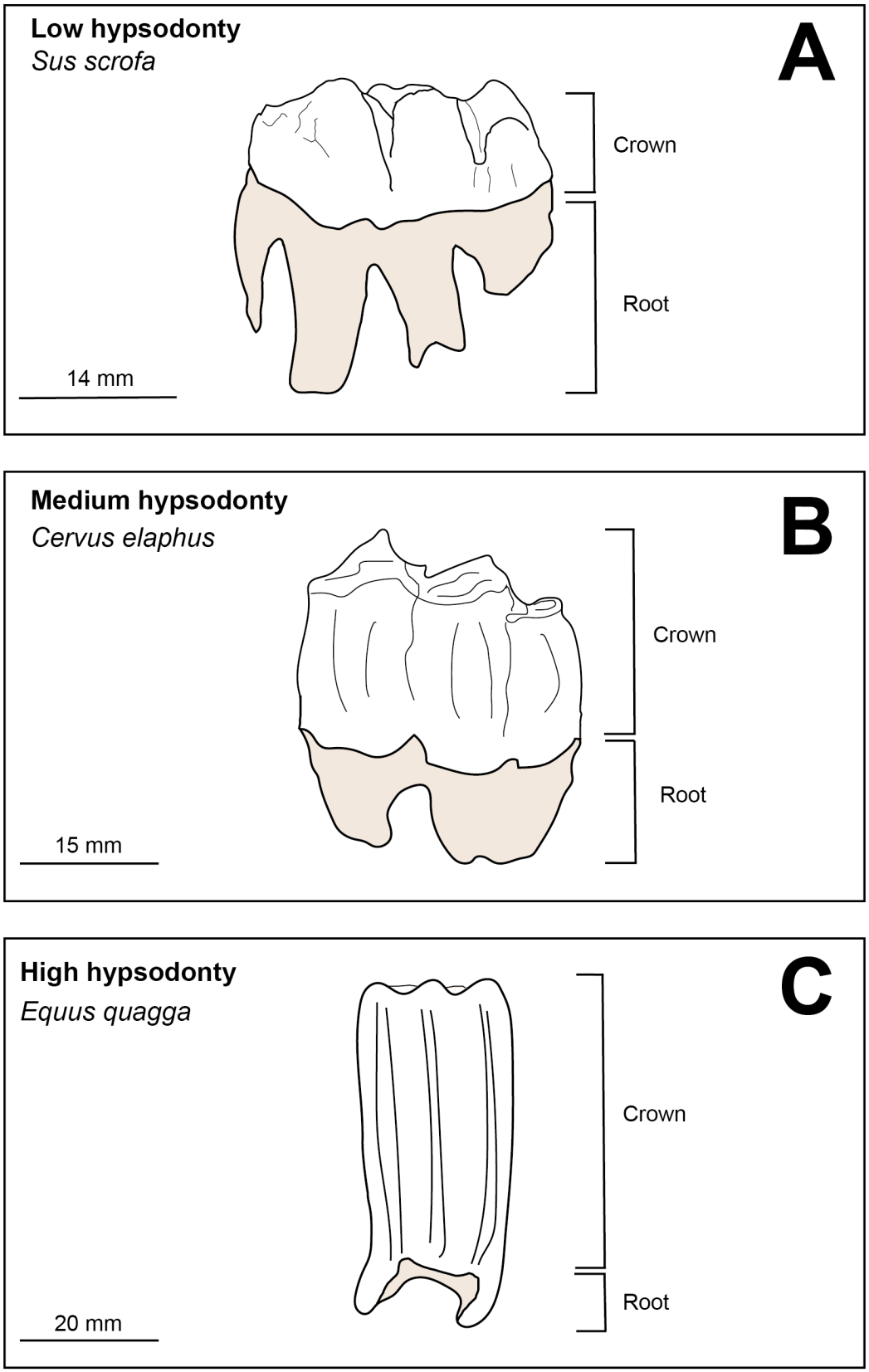

Figure 3.8: Schematic line drawing showing examples of different levels of hypsodonty in lower molars, highlighting crown height. From top: A) *Sus scrofa*; B) *Cervus elaphus* and C) *Equus quagga*. Scale on each schematic is approximate.

3.1.2.2 Methodology for investigating intraspecific variation in ungulate hypsodonty

For many taxa, a great number of measurements of hypsodonty index were collected for a large number of individuals from each taxon. To assess the assumption in the literature that all individuals of a single species can be classified into a certain hypsodonty class (e.g. Eronen *et al*., 2010a), it is necessary to investigate the nature and dispersal of the hypsodonty index measurements within each taxon.

For each Family and then each taxon, descriptive statistics (mean, median, variance, standard deviation and coefficient of variation [measure of dispersion around the mean]) were calculated for the hypsodonty index measurements and a histogram and a Q-Q plot was constructed to examine the distribution of the data. The Shapiro-Wilk test for normality was used for each taxon to confirm whether data was normally distributed or not. The Shapiro-Wilk test can be undertaken to test the supposed normality of a dataset, it evaluates the null hypothesis that a sample came from a normally distributed population (Shapiro and Wilk, 1965). If the probability (p-value) is above the critical threshold of 0.05 then the null hypothesis can be retained, and it can be assumed that the data is drawn from a normal distribution. If the p-value is below this critical value, then the null hypothesis can be rejected, and we can assume that the dataset is drawn from a distribution that significantly deviates from a normal distribution (Laerd Statistics, 2018). In this study the Shapiro-Wilk tests were undertaken in IBM SPSS Statistics v.21.

Further investigation of the distribution of any not-normal datasets was carried out using visual analysis of histograms and Q-Q plots, to look for bimodality and other types of distribution (Ford, 2015) that may help interpret the datasets. As the hypsodonty index data has a spatial component, any taxa that were indicated to be from a not normal distribution were plotted on location maps. This was to visually inspect for any clustering to see if the non-normality of the data was being influenced by different spatial populations within each taxon. Non-normality was then addressed in a geographical and ecological context for each of these taxa.

3.1.2.3 Obtaining climatic data for each locality

Modelled and interpolated climate data was downloaded from the WORLDCLIM dataset (Fick and Hijmans, 2017). This data was the most up-to-date version available, superseding that created by Hijmans *et al*. (2005) which was used in previous research on hypsodonty index and climate (see Eronen *et al*., 2010a). Nineteen bioclimatic variables, which are 50-year averages from 1950-2000, were downloaded and these are shown in Table 1.

The WORLDCLIM datasets are available at resolutions of 30 seconds (1km^2), 2.5 minutes (5km^2), 5 minutes (100km^2) and 10 minutes (340km^2) resolutions. There are advantages to using the highest resolution data, including the fact that it is then possible to differentiate, with confidence, between the climatic variables of localities which are within 1km distance of each other. This allows the testing of relationships between hypsodonty index and climate parameters at a resolution of point localities.

In spatial distribution studies, where there may be an investigation of potential environments that are suitable for a certain criterion (e.g. a species and its habitat preferences), having the highest resolution bioclimatic data would be a distinct advantage as this would reveal even small areas of suitable locations which may be masked in lower resolution datasets (larger grid sizes). There may be situations where using the highest resolution data is not appropriate or warrants caution, such as when considering variation in the home ranges of study taxa. The home ranges of certain taxa may be large enough to cause significant ecological noise in the dataset (especially if movements are seasonal) and by using larger grid sizes, this may capture the full range of movement of different taxa. However, the biological and geographical scope of the data collected in this study meant that assessing the home ranges of every taxon and incorporating them into the model testing was unfortunately impractical due to resource constraints.

Lower spatial resolution (larger grid sizes) will have the effect of averaging climatic parameters over large spatial areas. In the previous research, Eronen *et al*. (2010a) used spatial resolutions of WWF ecoregions; the disadvantages of this are discussed in section 2.2.2. The approach in this research is to use the highest spatial resolution possible in both the climate data and the provenance of mammal specimens. If lower resolution climate data were then used, it would be necessary to match the hypsodonty index data to the same resolution, thus requiring the amalgamation of data from sites which fall within 1km^2, 5km^2, 100km^2 and 340km^2 areas, depending on resolution chosen. This would not only reduce the number of one-to-one datapoint correlations in the model but would mask any spatial variation. The approach taken in this thesis is therefore not to average hypsodonty index data across different point localities in order to preserve as much of the variability as possible.

Originally the highest resolution data (1 km^2 resolution) was to be used in this study but constraints in computing power meant that the second-highest resolution of 5 km^2 was ultimately chosen. As the WORLDCLIM data is available for the entire globe, geographical coverage was not impacted by adopting resolution. All layers of climate data were imported into ESRI ArcGIS for Desktop version 10.3.

Table 3.1: The climatic variables from WORLDCLIM and their descriptions (based on O'Connell and Inglis, 2012). These represent climate averages of the years 1950 to 2000.

WORLDCLIM notation	Name of climate variable	Unit	Notes
bio1	Mean annual temperature	℃	
bio2	Mean diurnal temperature range	℃	Mean of the monthly difference between maximum temperature and minimum temperature
bio3	Isothermality		Quantification of how large the day-to-night temperatures oscillate relative to the summer-to-winter (annual) oscillations; derived by calculating the ratio of bio2 to bio7 and multiplying by 100 (O'Donnell and Ignacio, 2012).
bio4	Temperature seasonality		Standard deviation x 100 (Units: Percent)
bio5	Mean maximum temperature of the warmest month	℃	
bio6	Mean minimum temperature of the warmest month	℃	
bio7	Mean annual temperature range	℃	= bio5 - bio6
bio8	Mean temperature of wettest quarter	℃	
bio9	Mean temperature of driest quarter	℃	
bio10	Mean temperature of warmest quarter	℃	
bio11	Mean temperature of coldest quarter	℃	
bio12	Mean annual precipitation	mm	
bio13	Precipitation of the wettest month	mm	
bio14	Precipitation of the driest month	mm	
bio15	Precipitation seasonality		Coefficient of variation, Units: Percent
bio16	Precipitation of the wettest quarter	mm	
bio17	Precipitation of the driest quarter	mm	

bio18	Precipitation of the warmest quarter	mm
bio19	Precipitation of the coldest quarter	mm

3.1.2.4 Analytical and statistical approach for investigating relationship with climate

Firstly, for all the data, descriptive statistics were calculated including measures of central tendency, the minimum, maximum, the 25th and 75th percentiles, range, and measures of variance including variance, standard deviation and coefficient of variation.

As the main aim of this part of the research is to assess whether hypsodonty index can be used a predictor for climate variables, it is appropriate to use regression analysis. Regression analysis produces an equation whereby the coefficients represent the relationship between each independent variable and the dependent variable, thus allowing predictions to be made.

Regression analysis requires several steps (Bolker, 2015):

1. Checking of the relationship between each independent variable and the dependent variable using scatter plots and correlations
2. Checking of relationships among independent variables using scatter plots and correlations
3. Conducting of simple linear regressions for each independent variable/dependent variable pair
4. Use of the non-redundant independent variables in the analysis to find the best fitting model
5. Use of the best fitting model to make predictions about the dependent variable

The analytical process undertaken involves investigating the relationship between the hypsodonty index measurements in similar and additional ways to that which was attempted by Eronen *et al*. (2010). Each raw hypsodonty index measurement was first treated as a single data point, then individual animals were used as the data points (with left and right measurements averaged). Mean hypsodonty index per locality was used in a similar way to previous research but at an individual point location rather than at the ecoregion scale, as has been attempted in the past (see Eronen *et al*., 2010). The same was then attempted using the classification of hypsodonty index suggested by Fortelius

et al. (2014). All of these were carried out with the full data set and then a filtered dataset to remove migratory taxa.

Correlation matrices for each of the steps outlined above were produced for the different subsets of the dataset. The data was also $\log_{10}$ transformed to normalise skew in the data and tested in the same way. The highest correlating climate variables were then used in regression analysis. As linear regression is simplistic (Chatterjee and Hadi, 2012) and the aim of this study is to model the relationship between hypsodonty and climate in the simplest way, this was the first approach. A multivariate approach was taken as there are many interacting climate variables. As some of these climate variables may be autocorrelating and regression analysis relies on data independence (Chatterjee and Hadi, 2012; Bolker, 2015), only the strongest correlating variable (out of those that autocorrelated) was chosen for use in any model, and the other ones classed as redundant and were not used. Visual analysis of individual correlations would suggest whether there is the potential for relationships to be non-linear in nature. Linear regression itself is very sensitive to outliers and anomalies in the data, and as such, extreme values are likely to be underestimated in the output model (Bolker, 2015; Gurevitch and Nakagawa, 2015). The approach taken in this study was to model the relationship using multivariate linear regression, adding the strongest correlating independent climate variables first and then adding the remaining ones. The effect on the model output was examined to see if these variables increased or decreased model fit.

3.2 Materials and methods for investigating hypsodonty index as a proxy in the Late Pleistocene

This subsection outlines the methodology employed to investigate hypsodonty index changes at seven Late Pleistocene fossil sites from across the Mediterranean. The Mediterranean was selected as the spatial location as precipitation and moisture availability is suggested to be the key driver in environmental changes in this region, throughout the Quaternary including today, particularly primary productivity (Jongen *et al*., 2011) and the maintenance of green biomass (Ramos *et al*., 2015). The Late Pleistocene was selected as the temporal focus for this study primarily as there is abundant well-dated palaeoclimatic and palaeoenvironmental evidence for abrupt climate changes throughout this time period. These abrupt climate changes include stadial and interstadial oscillations through Marine Oxygen Isotope Stage 3, the transition into and out of the Last Glacial Maximum, and the climatic oscillations of the Last Glacial-Interglacial Transition including Greenland Stadial and Interstadial 1 (Rasmussen *et al*.,

2014). Second, as the Late Pleistocene is relatively recent in geological history, there is a highly likelihood of good fossil preservation; many of the species present in fossil sites are extant and therefore the ecologies of these taxa are well understood, which will aid interpretation of the results (Schreve, 2007). A more detailed site selection criteria is presented below, followed by an outline of the background of the selected sites and their fossil material that was used in this study.

3.2.1 Site selection criteria for fossil sites

In total, seven sites were chosen based on the following criteria:

- **Presence of fossil ungulate taxa**
    - M_3s must be present that meet the criteria for measurement outlined in section 3.1.2.1.
- **Chronology**
    - The site must be dated to the Late Pleistocene (from the end of Marine Oxygen Isotope Stage 5e to the start of the Holocene at 11,700 years b2k as defined by Walker *et al*., 2009)
    - The chronology of the site must be well constrained through high resolution dating methods(e.g. radiocarbon, thermoluminescence, electron spin resonance and uranium-series dating) undertaken on appropriate material within the last two decades to account for methodological advances (e.g. Higham, 2011) and/or age modelling using appropriate and improved methods (e.g. Bronk Ramsay, 2008) and up to date calibration (e.g. IntCal 13 radiocarbon calibration (Reimer *et al*., 2013) wherever it is appropriate and possible.
    - Multiple sites selected, where possible, with overlapping ages to allow regional comparison
- **Availability of multi-proxy palaeonvironmental evidence**
    - Chemical proxy evidence such as stable isotope records (oxygen and carbon isotopes) will be used, where available, in validating responses of hypsodonty index throughout site sequences
    - Biological proxy evidence such as palynological, palaeoentomological or vertebrate faunal evidence will be used, where available, for palaeoenvironmental reconstructions to aid interpretation of hypsodonty index changes at a site

- **Geographical spread**
    - Sites covering the Mediterranean from east to west and both north and south of the Mediterranean Sea selected, in order to cover the whole of the region that is environmentally controlled by its moisture regime

Based on the above criteria the following sites were selected for this fossil study: (1) Abric Romaní rock shelter, Spain, (2) Teixoneres cave, Spain, (3) Le Portel-Ouest cave, France, (4) Grotta del Romito, Italy, (5) Tabun cave, Israel, (6) Qafzeh cave, Israel and (7) Haua Fteah, Libya. The locations of these are presented in Figure 3.9. A summary of chronology is presented at the end of section 3.2.

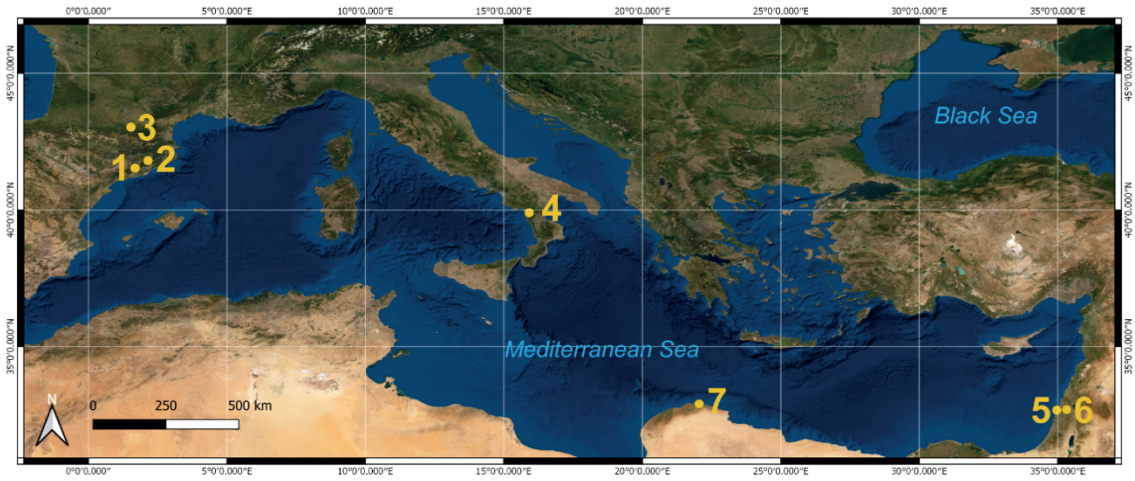

Figure 3.9: Location map showing the location of fossil sites across the Mediterranean: (1) Abric Romaní, (2) Teixoneres, (3) Le Portel-Ouest, (4) Grotta del Romito, (5) Tabun, (6) Qafzeh and (7) Haua Fteah.

3.2.2 Background to fossil sites

A brief background to previous work is presented below for each of the seven selected sites including site stratigraphy, chronology, palaeoenvironmental proxy data, faunal lists and any relevant archaeological information.

3.2.2.1 Abric Romaní (Capellades, Spain)

3.2.2.1.1 Introduction

Abric Romaní (41°32'N 1°41'E) is a rock shelter found 45 km north west of Barcelona, Spain, on the north-eastern side of the Cinglera del Capelló cliff in the town of Capellades (see Figure 3.10). It is 280m above sea level (Marín *et al*., 2017). The site lies on the edge of the River Anoia basin and the Catalan pre-littoral mountain range (Burjachs *et al*., 2012). It was discovered in 1909 by Amador Romaní and several series of excavations were carried out throughout the 20th century. The most substantial work

began in 1983 under the directions of Eudald Carbonell (Marín *et al*., 2017). The 20m thick sequence of travertine sediments is well stratified, clearly separating different archaeological levels. The site has yielded faunal and Mousterian lithic material, with evidence of hearths, indicating multiple occupation events by Neanderthals. Uranium series and radiocarbon dating places the site between 70-40kyr (Bischoff *et al*., 1988; Marín *et al*., 2017).

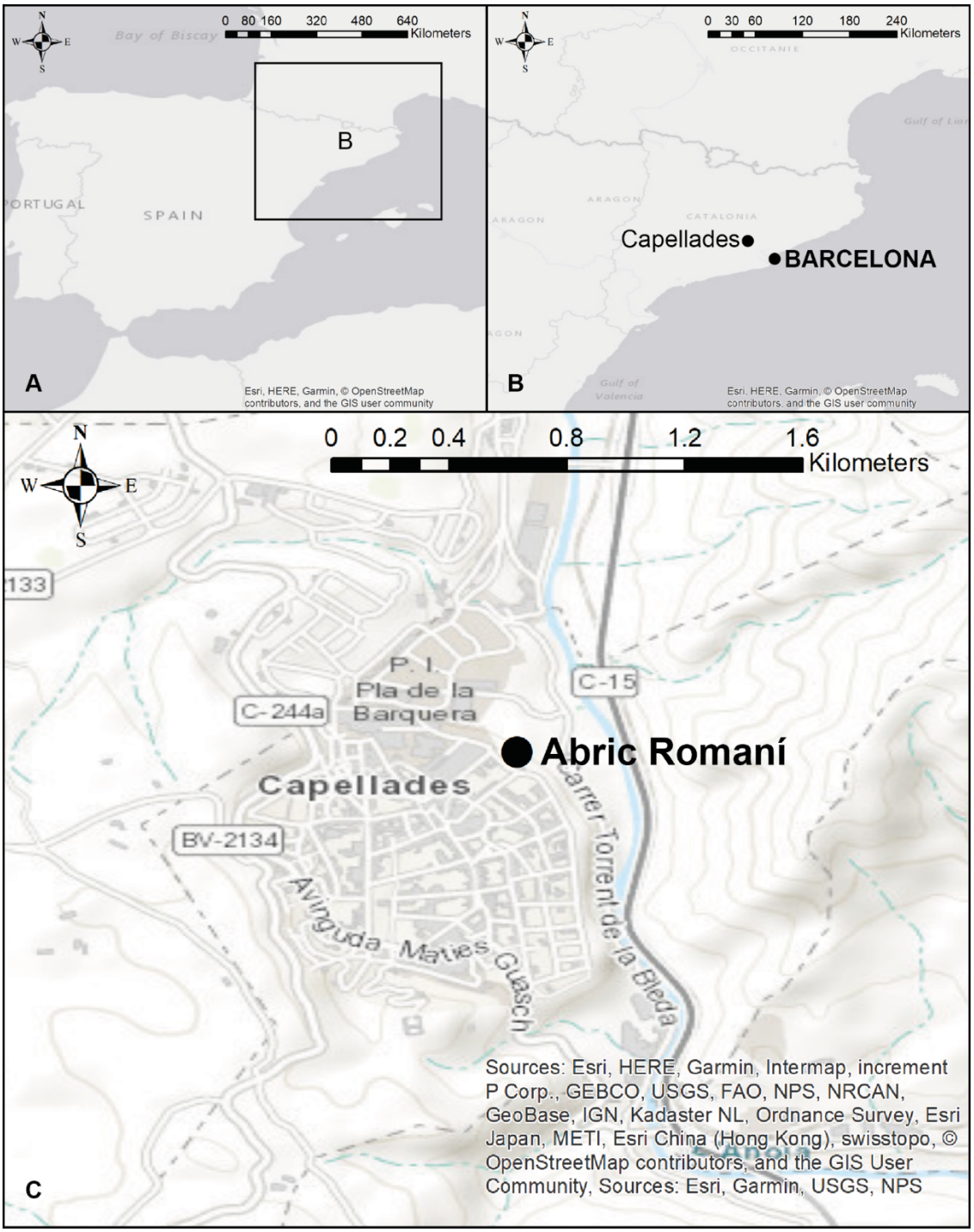

Figure 3.10: Map showing the location of Abric Romaní. A) Iberian peninsula, B) the Catalonia region showing the town of Capellades and C) the location of the Abric Romaní rock shelter within the local area of Capellades.

3.2.2.1.2 Stratigraphy and chronology

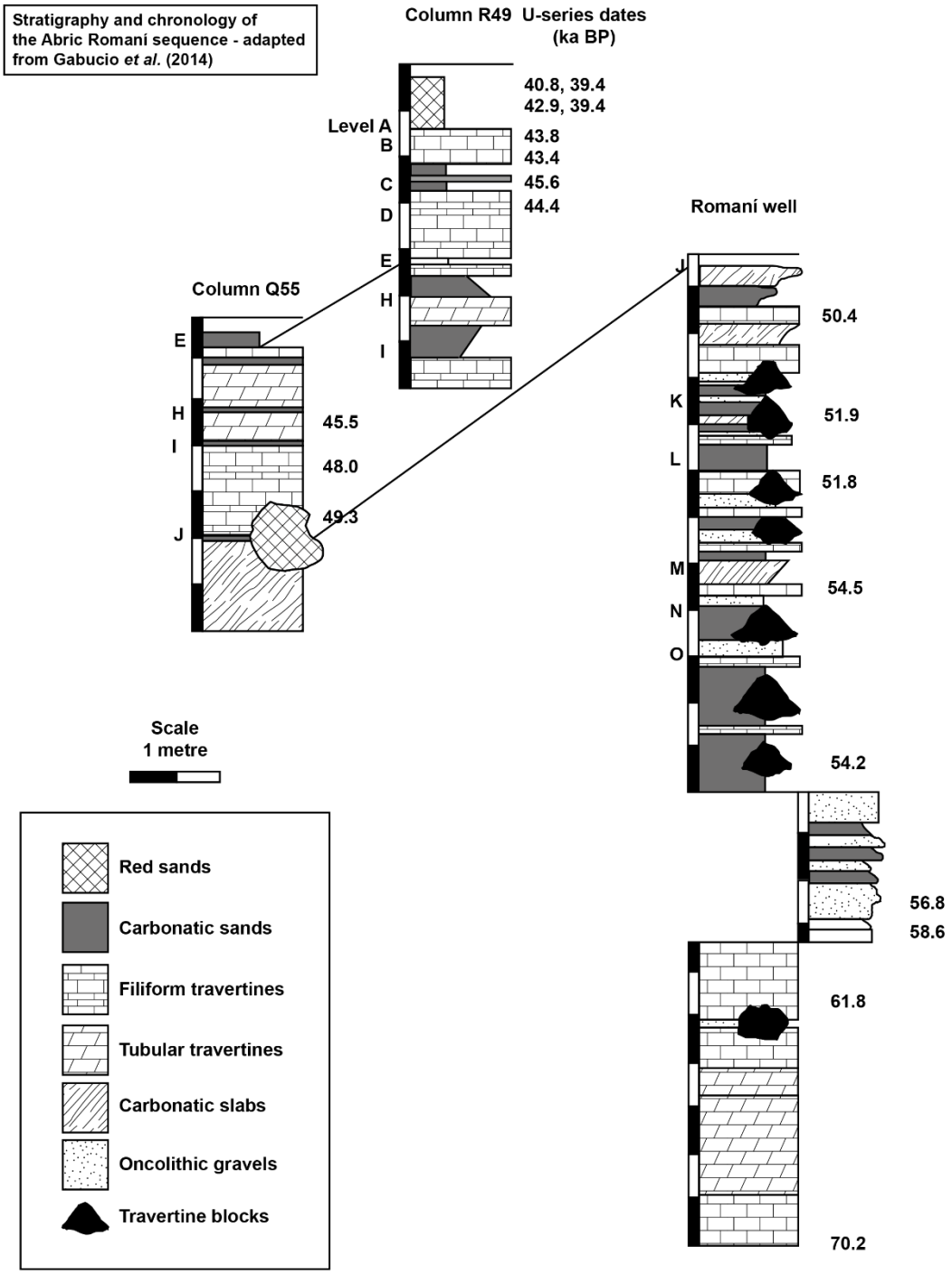

Figure 3.11: Sedimentology and stratigraphy of the Abric Romaní rock shelter. Dates from the uranium series chronology are also shown throughout the sequence (adapted from Gabucio *et al*., 2014).

The deposits in the rock shelter itself consist of approximately 20m of travertine platforms that have originated during periods of water filtration through the rock shelter walls and overhanging ledges (Giralt and Julia, 1996). During times of limited or no water flow, travertine formation was halted and replaced by the deposition of detrital material largely composed of silt and clay. Therefore, the sequence itself consists of sterile travertine

layers approximately 1 metre in thickness interspersed with the detrital layers. It is these detrital layers that have yielded archaeological material and at the time of the most current excavation, sixteen archaeological levels have been recorded (Rosell *et al*., 2012). See Figure 3.11 above for a visual summary.

The main chronology for the site was produced using Uranium-series and radiocarbon dating. The use of the two techniques in combination is a result of the site age being around the limit for radiocarbon dating as well as the need to date both inorganic and organic material. The sequence of archaeological levels has been dated to 70-40 kyr, with sedimentation rate estimated at ~0.6m/kyr (Bischoff *et al*., 1988). The uppermost archaeological level (Level A) is attributed to the Upper Palaeolithic and is dated to c. 39ka. The remainder of the levels are all attributed to the Middle Palaeolithic and the chronology indicates these levels were deposited during MIS 3 (Bischoff *et al*., 1988; Rosell *et al*., 2012). These dates are also indicated on Figure 3.11.

3.2.2.1.3 Palaeoecology and palaeoenvironment

A number of palaeoecological studies have been completed on the site of Abric Romaní including work on the palynological record (Burjachs and Julià, 1994, 1996; Burjachs *et al*., 2012) charcoal remains (Burjachs *et al*., 2012), macrofaunal remains (Rivals *et al*., 2009; Fernández-Lazo *et al*., 2010, 2011), microfaunal remains (López-García, 2008; Burjachs *et al*., 2012) and herpetofaunal remains (Burjachs *et al*., 2012). A summary of a selection of the proxy data is shown in Figure 3.12 but these are explained in more detail below.

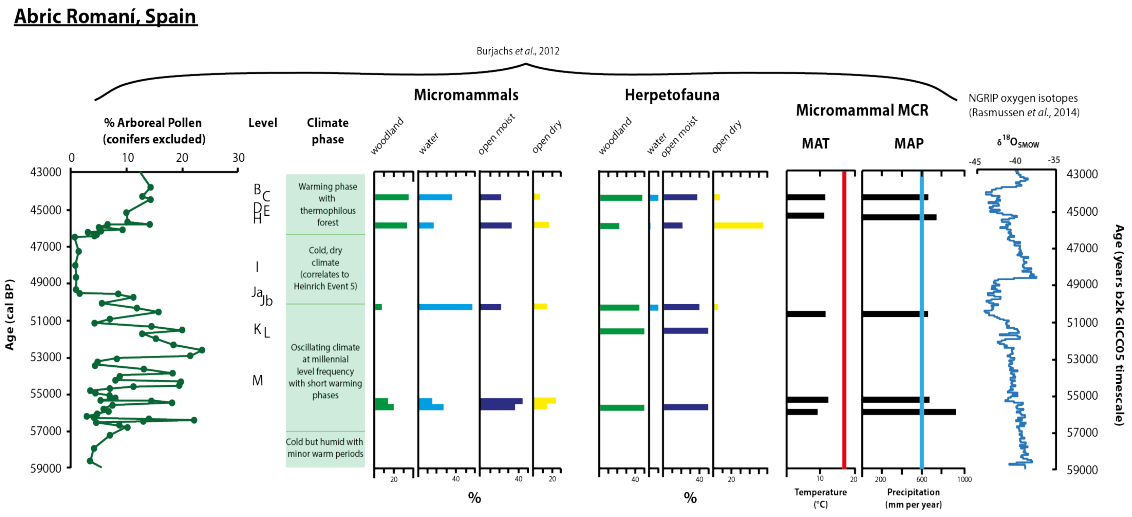

Figure 3.12: Palaeoenvironmental proxy data plotted against ages from Gabucio *et al*. (2014) alongside pollen, micromammal and herpetofaunal data and temperature and precipitation reconstructions using the Mutual Climatic Range (MCR) method. The thick red vertical line represents modern Mean Annual Temperature (MAT) for the site and the thick blue vertical line represents the modern Mean Annual Precipitation (MAP) for the site (data from and figure based upon Burjachs *et al*., 2012). Oxygen isotope data from Greenland (NGRIP; Rasmussen *et al*., 2014) is also presented.

The pollen spectra indicate that there are five distinct climatic phases recorded at the site. The samples for this analysis were taken from the entire sequence including those parts that were not excavated during archaeological studies (Burjachs *et al*., 2012; Burjachs and Julià, 1994, 1996). The results of these studies show the following sequence of climatic events: (1) ca. 70,000 – 66,000 years BP: the development of a thermophilous forest with periodic interruptions by rapid expansions of steppic vegetation and Poaceae, (2) ca. 66,000 – 57,000 years BP: a cold but humid climate dominated by Poaceae and *Artemisia* and *Pinus*, with minor warmer periods oscillating at c. 2300 year intervals, similar to the rapid expansions in the previous phase, (3) ca. 57,000 – 50,000 years BP: oscillating climatic phases at millennial frequency with short warming phases with mesothermophilous taxa, (4) ca. 50,000 – 46,000 years BP: a cold, dry climate characterised by low arboreal pollen percentage and high abundance of *Artemisia*, Asteraceae and Poaceae indicating regional steppe vegetation. This phase correlates with Heinrich event 5 in Greenland, which indicates potential long-distance teleconnections at this time (5) ca. 46,000 – 41,000 years BP: a warming phase characterised by the expansion of thermophilous forest.

Charcoal was found in all archaeological layers within the sequence with each layer yielding two taxa except Level D, which had a larger variety of taxa found. In general, the charcoal data shows low variability throughout the sequence. This indicates that firewood management is likely based on the most available and abundant species close to the site. *Pinus* charcoal is found in all the archaeological layers indicating that pine forest was growing near the site throughout the entire sequence of occupation (Burjachs *et al*., 2012).

The small mammal assemblage from the site includes insectivores, bats and rodents from levels D, E, J, N and O. The assemblage consists of three insectivores (*Crocidura russula*, *Sorex* gr. *coronatus-araneus* and *Talpa europaea*), three bats (*Miniopterus schreibersii*, *Pipistrellus pipistrellus* and *Nyctalus lasiopterus*) and eight rodents *(Microtus arvalis*, *Microtus agrestis*, *Iberomys cabrerae*, *Terricola duodecimcostatus*, *Terricola* cf. *pyrenaicus*, *Arvicola sapidus*, *Apodemus sylvaticus* and *Eliomys quercinus*). The assemblage is dominated throughout the sequence by species that inhabit open forests/forest edge environments (e.g. *I. cabrerae* (Pita *et al*., 2014), and *A. sylvaticus* (Tellería *et al*., 1991), and species with humid requirements, such as *I. cabrerae* (Pita *et al*., 2014). *A. sapidus* indicates that a permanent aquatic environment is nearby to the site as it is amphibious and inhabits wetlands (Fedriani *et al*., 2002). The Mutual Climatic Range climate reconstruction from the small mammals indicates that the Mean Annual Temperature (MAT) was 4.6-7.5 ˚C colder than the present day MAT of 16 ˚C whereas

the Mean Annual Precipitation (MAP) was 70-340 mm higher than the present day MAP of 601 mm (Burjachs *et al*., 2012).

Herpetofaunal studies on the site have identified remains in levels D, E, J, K and O. Six taxa have been identified including anurans (*Bufo bufo*, *Bufo calamita* and *Rana temporaria*), lizards (Lacertidae indet. and *Anguis fragilis*) and a snake (*Vipera aspis*) (López-García, 2008; López-García *et al*., 2009). This assemblage indicates that a colder and more humid environment existed during deposition than is found in the present day. These taxa persist in habitats such as humid meadows and small patches of moist and cold woodland. The assemblage is limit but consistent throughout the sequence with the exception of level E which shows a greater abundance of *B. calamita* which prefers slightly less humid environments. This could indicate that level E may be deposited during drier conditions or at least indicates some climatic instability that reduced humidity (Burjachs *et al*., 2012).

The palaeontological and zooarchaeological research at Abric Romaní has identified thirteen large mammal taxa throughout the sequence. The most common and numerous are red deer (*Cervus elaphus*) and horse (*Equus ferus*) but in some levels the presence of narrow-nosed rhinoceros (*Stephanorhinus hemitoechus*), aurochs (*Bos primigenius*), an undetermined Proboscidean and, to a lesser extent, chamois (*Rupicapra pyrenaica*) have been documented. Carnivore remains have been identified and these are frequently recovered from the travertine platforms and not within the archaeological levels. A table showing presence of the large mammal taxa throughout the sequence is shown in Table 3.2.

Table 3.2: The large mammals identified from the Abric Romaní sequence and their location in the stratigraphy (adapted from Rosell *et al*. (2012).

Taxon/Levels	A	B	C	D	E	F	G	H	I	J	K	L	M
Ursus sp.		■											■
Canis lupus		■			■								
Panthera leo spelaea									■				
Panthera pardus				■									
Lynx sp.	■	■			■								
Felis silvestris	■			■									■
Crocuta crocuta	■	■			■								
Proboscidea					■								
Stephanorhinus hemitoechus								■		■			
Equus ferus	■	■	■	■	■	■	■	■	■	■	■	■	■
Cervus elaphus	■	■	■	■	■	■	■	■	■	■	■	■	■
Bos primigenius	■				■				■	■	■	■	■
Rupicapra rupicapra	■	■		■	■	■	■	■		■			

The faunal remains exhibit a high level of bone fragmentation. Taphonomic study of the remains indicates excellent bone preservation and no alteration or damage by post depositional processes (Fernández-Lazo *et al*., 2010). This is attributed to the high sedimentation rate of the site (Carbonell *et al*., 1996). The bone fragmentation is consistent with intense bone processing by human occupants of the site. In levels L and M, 70% of the bone fragments are less than 3cm in size and in level K, this is 60%. In terms of the age profile of the exploited fauna, adult animals are most abundant but some juveniles and infants are represented, especially in level L. The greatest age diversity was shown in those taxa classed as medium size, and in general the number of old adults is lower than would be naturally present in these populations. The evidence for exploitation of this fauna by the occupants of the cave is present in the numerous cutmarks on the bone surfaces as well as indications of intentional breakage of bones. Many impact points are visible on bone elements with high marrow content indicating marrow consumption by the occupants was likely. Approximately half of the bone material has evidence of burning (Fernández-Lazo *et al*., 2010). The carnivore material shows no evidence of anthropogenic marks and as such the presence of these predators

is interpreted as sporadic denning or natural intrusion during periods where humans were absent (Rosell *et al*., 2012).

Studies on dental wear of large mammals included both meso- and microwear studies. Mesowear scores of dental remains from levels J to M reveal a diversity of dietary behaviour and habitats. The scores of the different species (*B. primigenius*, *E. ferus*, *C. elaphus* and *R. pyrenaica*) do not overlap indicating habitat and/or niche segregation in response to interspecific competition. Microwear analysis shows that both *B. primigenius* and *E. ferus* had diet largely composed of graze with *E. ferus* showing a high graze diet that did not vary between the levels in terms of abrasiveness. *B. primigenius* on the other hand showed an abrasive diet in the microwear but mesowear showed this taxon as having a less abrasive diet. This discrepancy is indicative of a mixed-feeder (Semprebon and Rivals, 2007) and as microwear records diet shortly before death, it was likely the individuals were hunted during a season when their diet consisted of more abrasive material. It remains to be seen whether this discrepancy will be highlighted by differences in hypsodonty which is more related to average diet over the lifetime of an individual than seasonal dietary differences. Microwear study on red deer teeth showed a change in diet from more leaf-browse in level J to a higher graze component in level K. This could be climatically driven but could also be seasonal variation in diet and the individuals in each level may have been hunted in different seasons. In summary, the dental wear studies indicate a variety of habitats in close proximity to the site and that hunting occurred in both open and more closed environments in different seasons of the year (Burjachs *et al*., 2012).

3.2.2.1.4 Regional climatic links and summary

The sequence covers MIS 4 and the first part of MIS 3 and correlates with the time period including Dansgaard-Oeschger cycles 19 to 12, including Heinrich 6 and 5. During the part of the sequence that is dated to MIS 4 there are no archaeological levels but pollen analysis indicates that the climate was not stable and was interrupted by warming events that have been correlated to GI-19 and GI-18. Following this there is a deterioration indicated by a decrease in arboreal pollen that has been correlated with Heinrich event 6. However, the arboreal pollen level does not decrease below 40% indicating that this was a cooler event rather than a cold event (Burjachs *et al*., 2012).

Following this, arboreal pollen increases and 25% of vegetation taxa are thermophiles. This has been correlated to GI-17 and at the local/regional level this begins more humid phase and ends more arid. The next climatic phase correlates to GS-17 and MAT is 7.5˚C colder than present and MAP is 350 mm higher as indicated by the micromammals. The next part of the sequence corresponds to archaeological later N and is correlated to

GI-16 and is largely similar to the previous interstadial. Charcoal indicates pines and micromammal MCR reconstructions indicate a MAT 4.6°C colder than present and a slightly higher MAP than present (+75 mm). The phase correlating with the next interstadial (GI-15) is largely the same in its climate.

The large Neanderthal occupation phases of archaeological layers M, L, K and J appear to correlate with Dansgaard-Oeschger event 14. The palaoecological data at the time indicates a pine forest with 33% warm indicator taxa. The micromammals indicate a MAT of 5.5˚C lower MAT than present, and a 60 mm per year higher MAP than present.

Archaeological layers Ja, I and H appear to correlate with Heinrich event 5. Palaeoecological data indicates this as a cold phase at the site with more arid peaks at the beginning and end with intermediate phases of open pine forests.

Finally, the archaeological levels E and D correlate with GI-12 and are shown to be less temperate than previous interstadials at the site, with only 20% of taxa being warm indicators. MAT is 5.7˚C colder than present, but MAP is up to 150 mm higher than present (Burjachs *et al*., 2012). The correlations and palaeocological data are summarised in Figure 3.12.

3.2.2.1.5 Materials used in this study

Access to faunal material from Abric Romaní was provided by the Institut Català de Paleoecologia Humana i Evolució Social (IPHES) in Tarragona, Spain. Data was collected in December 2016. Fifteen M_3s were suitable for measurement of ungulate hypsodonty index.

3.2.2.2 Teixoneres Cave (Moià, Spain)

3.2.2.2.1 Introduction

Teixoneres Cave is located in the village of Moià, Barcelona, Spain (41° 48’ 25’’ N, 2° 09’ 02’’ E, 760m asl, see Figure 3.13). Teixoneres is one cavity in the karstic system of the Toll Caves and consist of a U-shape cave that is 30m in length and is comprised of three chambers (X, Y and Z). The cave’s archaeological importance was first discovered by a local speleological group in the 1950s. This group recovered some lithics and a Pleistocene faunal assemblage. Some additional work was carried out in 1973 on palaeontological remains, but the cave remained closed until the current excavation began in 2003 (López-García *et al*., 2012; Talamo *et al*., 2016).

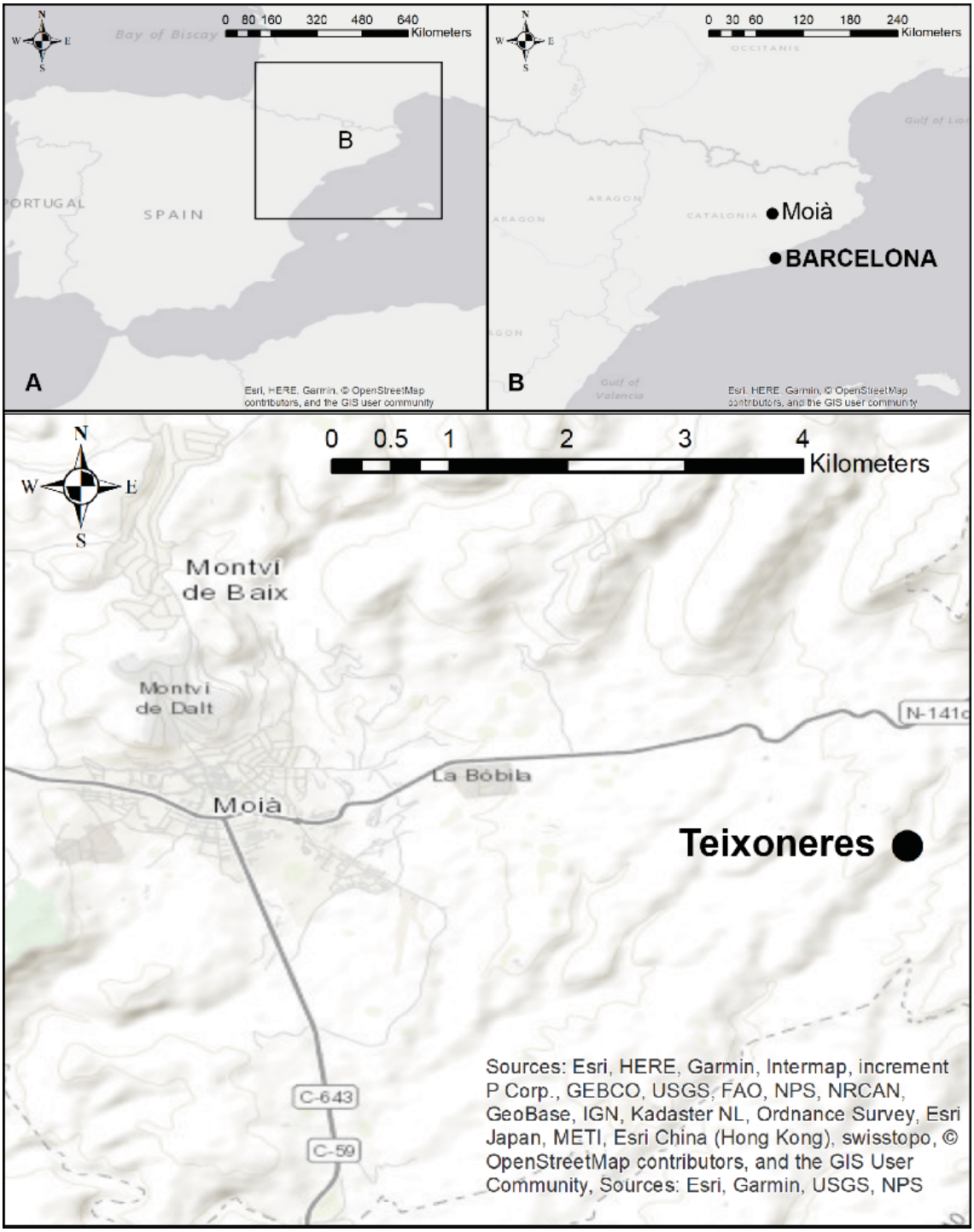

Figure 3.13: Map showing the location of Teixoneres. A) Iberian peninsula, B) the Catalonia region showing the town of Moià and bottom: the location of the Teixoneres cave within the local area of Moià.

3.2.2.2.2 Site stratigraphy and chronology

The site is filled with sediments approximately 6m in thickness containing a least 15 levels yielding archaeological or palaeontological material. Levels I to IV cover the Late Pleistocene with levels I and IV interpreted as warm and wet periods. Uranium-series dating situates level IV at an average date of 100.3± 6.1ka, within MIS 5c (Tissoux *et al*.,

2006). Level I has been dated to the Lateglacial between ca. 14-16 ka BP after some additional correction for uranium contamination of this level (see Tissoux *et al*., 2006). A schematic of the stratigraphy is shown in Figure 3.14. The biostratigraphic marker taxa of *Pliomys lenki*, *Microtus* (*Iberomys*) *cabrerae* and *Hystrix* sp. allow the age of levels II and II to be constrained between ca. 90 and 30 ka BP (López-García *et al*., 2012; see section 3.2.2.2.3 below).

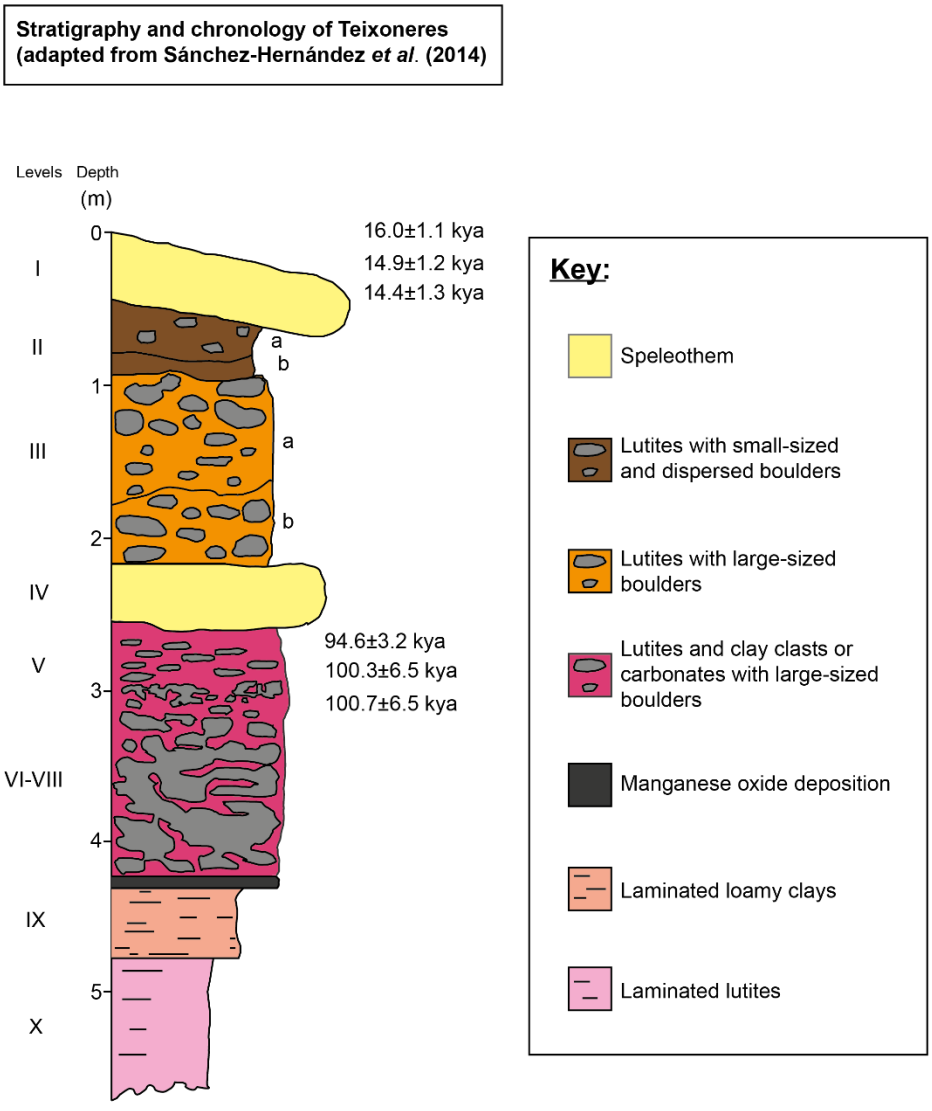

Figure 3.14: The stratigraphy of Teixoneres cave. Uranium-series dates are also shown. Adapted from Sánchez-Hernández *et al*. (2014).

3.2.2.2.3 Palaeoecology and palaeoenvironment

Palynological analysis at Teixoneres for levels II and III (i.e. the period between MIS 5c and the Lateglacial) shows that different environments existed through the sequence but that woodland and open areas were shown in both levels to varying degrees. Throughout the two levels, the arboreal pollen percentage remained above 50% (see Figure 3.15). The woodland indicator species found were pines and oaks whilst the herbaceous

vegetation was comprised of Poaceae, Chenopodiaceae and Asteraceae. Alongside these were many heliophilous taxa such as Cupressaceae, Cisteraceae, *Corylus*, *Erica* and *Ephedra*, indicating the existence of a semi-open landscape nearby (López-García *et al*., 2012). Although levels II and III show a similar vegetation assemblage in terms of presence of taxa, the abundances are different. The steppe genus *Artemisia* was only present in level II, indicating that this level was relatively dry. Level III shows a relatively moist environment, as seen in the higher levels of *Corylus* and Pteridophyta spores (López-García *et al*., 2012).

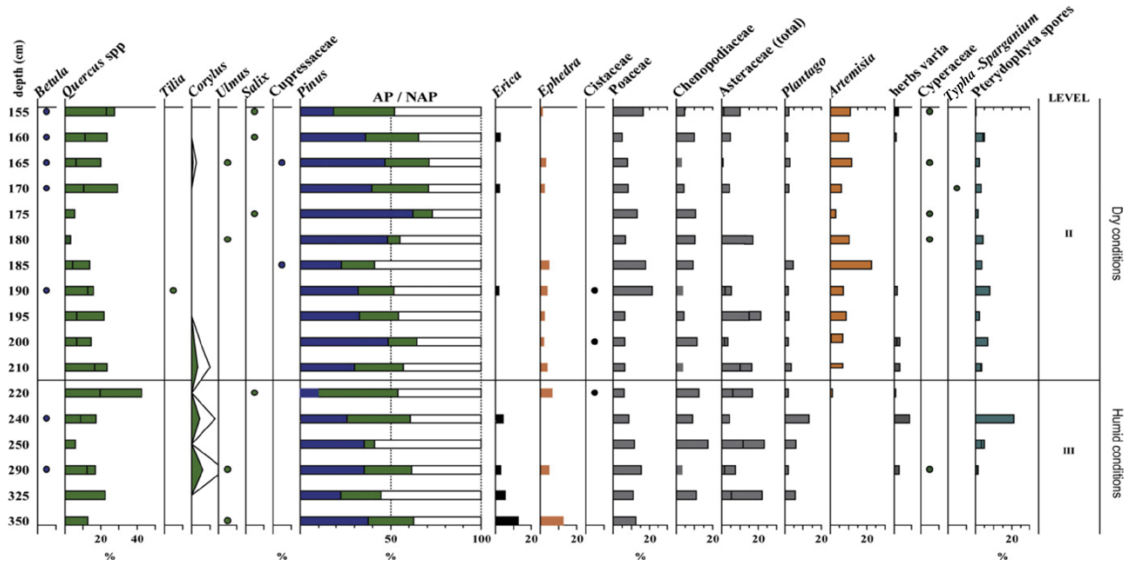

Figure 3.15: Pollen diagram for levels II and III at Teixoneres cave (figure taken from López-García *et al*., 2012).

Charcoal remains from Levels II and III revealed 4 taxa were present in close proximity to the site to be exploited by the occupants of the cave. Pines were present including *Pinus pinea*/*pinaster* and *Pinus sylvenstris* (López-García *et al*., 2012). This is not surprising as pine forests (particularly *P. sylvestris*) were the most common and widespread types of forest in the Mediterranean throughout the Late Pleistocene. It is worth noting the charcoal analysis found the presence of the mesothermophiles *Buxus sempervirens* and *Quercus* spp., showing that milder habitats existed in close proximity to the cave (Burjachs *et al*., 2012; López-García *et al*., 2012).

The small vertebrates from Teixoneres consist of both micromammal and herpetofaunal remains. Habitat weightings and the Mutual Climatic Range (MCR) were used to reconstruct palaeoenvironmental and palaeoclimatic conditions throughout Levels II and III. Biostratigraphic indicators were also used to supplement the chronology of the sequence.

The micromammal assemblage includes a large sample of six insectivore taxa, five bat taxa and 13 rodent taxa. The biostratigraphic indicator taxa of three rodent species, two

extinct (*Pliomys lenki* and *Hystrix* sp.) and one extant (*Microtus (Iberyomys) cabrerae*) indicates that Level IIb is older than 30 ka BP and Level III has an age between 90 and 60 ka BP. The presence of *Apodemus sylvaticus* in all levels is consistent with woodland above 60% throughout the sequence. However, within this the micromammals indicate two clear environmental phases: (1) Level III has evidence for higher levels of humidity with more meadows and water streams in the vicinity; (2) a drier phase recorded in Level IIb with an increase in dry meadows and rocky areas with a progressive decrease in the number of water streams nearby (López-García *et al*., 2012). The MCR analysis indicates temperatures were between 8.3 and 5.3˚C lower than today and the precipitation was between 181 and 322 mm higher than today. Changes throughout the sequence can be seen in Figure 3.16.

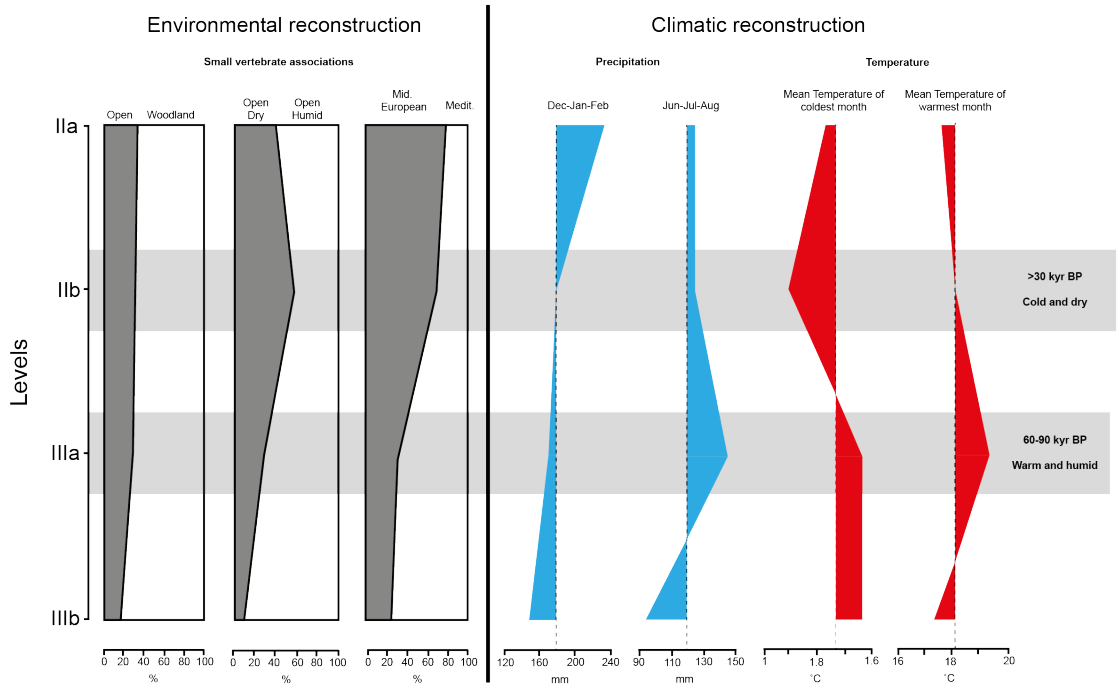

Figure 3.16: Environmental and climatic reconstructions for Teixoneres Cave for levels II and III. Environmental reconstructions show percentage change in the environmental associations of small vertebrate taxa within the Teixoneres sequence. Climate reconstruction shows from left to right: precipitation reconstruction in blue for December-January-February (winter) and June-July-August (summer), temperature reconstruction in red for the coldest and warmest months. The dotted lines shown in the climatic reconstructions represent the mean through the sequence for each respective variable. Figure adapted from López-García *et al*. (2012).

Thirteen herpetofauna taxa were identified throughout the sequences giving an overall indication of temperate, humid meadows alongside woodlands. As well as woodlands being well developed near to the cave, there are indication of water bodies nearby. Although there are temperate to cold humid conditions throughout the levels the representation of open-dry habitat indicators increases from the base of Level III to the top of Level II. The presence of the thermophilous snake *Malpolon monspessulanus* in Level IIb (López-García *et al*., 2012) indicates that the temperature did not decrease

below 10˚C (Blásquez and Pleguezuelos, 2002) during the deposition of this level. The presence of *Salamandra salamandra* in Levels II and IIb (López-García *et al*., 2012) gives an indication that the environment during this time was not especially dry as this species does not survive in areas with prolonged periods of aridity (Buckley and Alcobendas, 2002).

The large vertebrate faunal record is diverse which is concordant with the previously discussed proxy evidence for a mosaic landscape with wet forest and meadows (López-García *et al*., 2012). The most represented specimens at Teixoneres are leporids (namely *Oryctolagus cuniculus*), horses (*Equus ferus* and *E. hydruntinus*), red deer (*Cervus elaphus*) and large bovids (*Bos*/*Bison*), followed by roe deer (*Capreolus capreolus*), wild boar (*Sus scrofa*), chamois (*Rupicapra rupicapra*), ibex (*Capra pyrenaica)* which are present in fewer numbers. There are also remains of woolly rhinoceros (*Coelodonta antiquitatis*) and woolly mammoth (*Mammuthus primigenius*), rarely seen in Iberian sites of this age. There is also a significant presence of carnivores in the cave, especially cave bears (*Ursus spelaeus*) and spotted hyaenas (*Crocuta crocuta*). Wolves (*Canis lupus*), foxes (*Vulpes vulpes*), lynx (*Lynx* sp.) and badgers (*Meles meles*) are also present in the assemblage (Talamo *et al*., 2016).

Taphonomic analysis indicate that the assemblage was formed by alternating agents of Neanderthal groups and large carnivores (hyaenas and cave bears). The material exhibiting anthropogenic markings was mostly found near the entrance to the cave whereas that material that appears to be accumulated by carnivores is found in the inner cave. Most of the fossils are highly fragmented with only 11.9% identifiable in Unit II and 4.6% in Unit III. Out of a total of 1465 identified specimens, 1263 of these are ungulates. Despite the high fragmentation, preservation of the remains is good (Álvarez-Lao *et al*., 2017).

Unit III has been dated from >51,000 ^{14}C BP to 44,210 cal BP (dating on the bottom of Unit III is beyond the oldest part of the IntCal13 calibration curve of Reimer *et al*., 2013) and Unit II has been dated 44,210 to 33,060 cal BP (Talamo *et al*., 2016), both corresponding to MIS 3 which is characterised by many abrupt climatic oscillations. Unit III is of palaeoecological interest due to the presence of woolly rhinoceros and woolly mammoth, both cold-adapted species. Unit II also includes woolly rhinoceros but woolly mammoth is absent. The presence of both of these species from >51,000 ^{14}C years BP to 44,210 cal years BP is worthy of note as this is somewhat older than most Late Pleistocene occurrences previously documented in Iberia (see Àlvarez-Lao and Garcìa, 2010).

Unit III also contains a number of temperate species which are not ordinarily seen in assemblages containing woolly mammoth and woolly rhino. This suggests that these species may have only reached the Iberian Peninsula occasionally during the very coldest climatic oscillations and cohabited with the local faunas rather than replacing them entirely. Either way, the faunal assemblage at Teixoneres suggests that during MIS 3 there was a mosaic landscape with areas of steppe-like environment, open forested areas and the presence of chamois and ibex also indicates more bare and rocky environs (Álvarez-Lao *et al*., 2017).

3.2.2.2.4 Materials used in this study

Access to faunal material from Teixoneres was provided by the Institut Català de Paleoecologia Humana i Evolució Social (IPHES) in Tarragona, Spain. Data was collected in December 2016. 21 M_3s were suitable for measurement of ungulate hypsodonty index.

3.2.2.3 Le Portel-Ouest (Ariège, France)

3.2.2.3.1 Introduction

The site of Portel was discovered in 1908 and consists of two caves: Portel-Est, famous for its cave paintings and Portel-Ouest where, during excavations between 1949 and 1987, 34 Neanderthal remains were discovered alongside more than 200,000 lithic artefacts and bones distributed around the site. It has since been revealed that there are approximately twenty levels attributed to the Late Pleistocene. The site itself is situated at coordinates 43° 1'53.68"N 1°32'21.07"E in the department of Ariège in south west France, approximately 10 km north west of the town of Foix (see Figure 3.17). The 5 m thick sequence of 14 beds (subdivided into a total of 21 beds) has been dated by Uranium-series dating, given an age of ca. 135 ± 9 ka (Ajaja, 1994 cited in Vézian, 2014) to the postglacial period ca. 23.1 ± 3.5 ka (Tissoux, 2004, cited in Vézian, 2014), although deposition does not appear to be continuous. See below for detailed stratigraphic and chronological information.

The site of Portel was discovered in 1908 and consists of two caves: Portel-Est, famous for its cave paintings and Portel-Ouest where, during excavations between 1949 and 1987, 34 Neanderthal remains were discovered alongside more than 200,000 lithic artefacts and bones distributed around the site. It has since been revealed that there are approximately twenty levels attributed to the Late Pleistocene. The site itself is situated at coordinates 43° 1'53.68"N 1°32'21.07"E in the department of Ariège in south west France, approximately 10 km north west of the town of Foix (see Figure 3.17). The 5 m thick sequence of 14 beds (subdivided into a total of 21 beds) has been dated by Uranium-series dating, given an age of ca. 135 ± 9 ka (Ajaja, 1994 cited in Vézian, 2014)

to the postglacial period ca. 23.1 ± 3.5 ka (Tissoux, 2004, cited in Vézian, 2014), although deposition does not appear to be continuous. See below for detailed stratigraphic and chronological information.

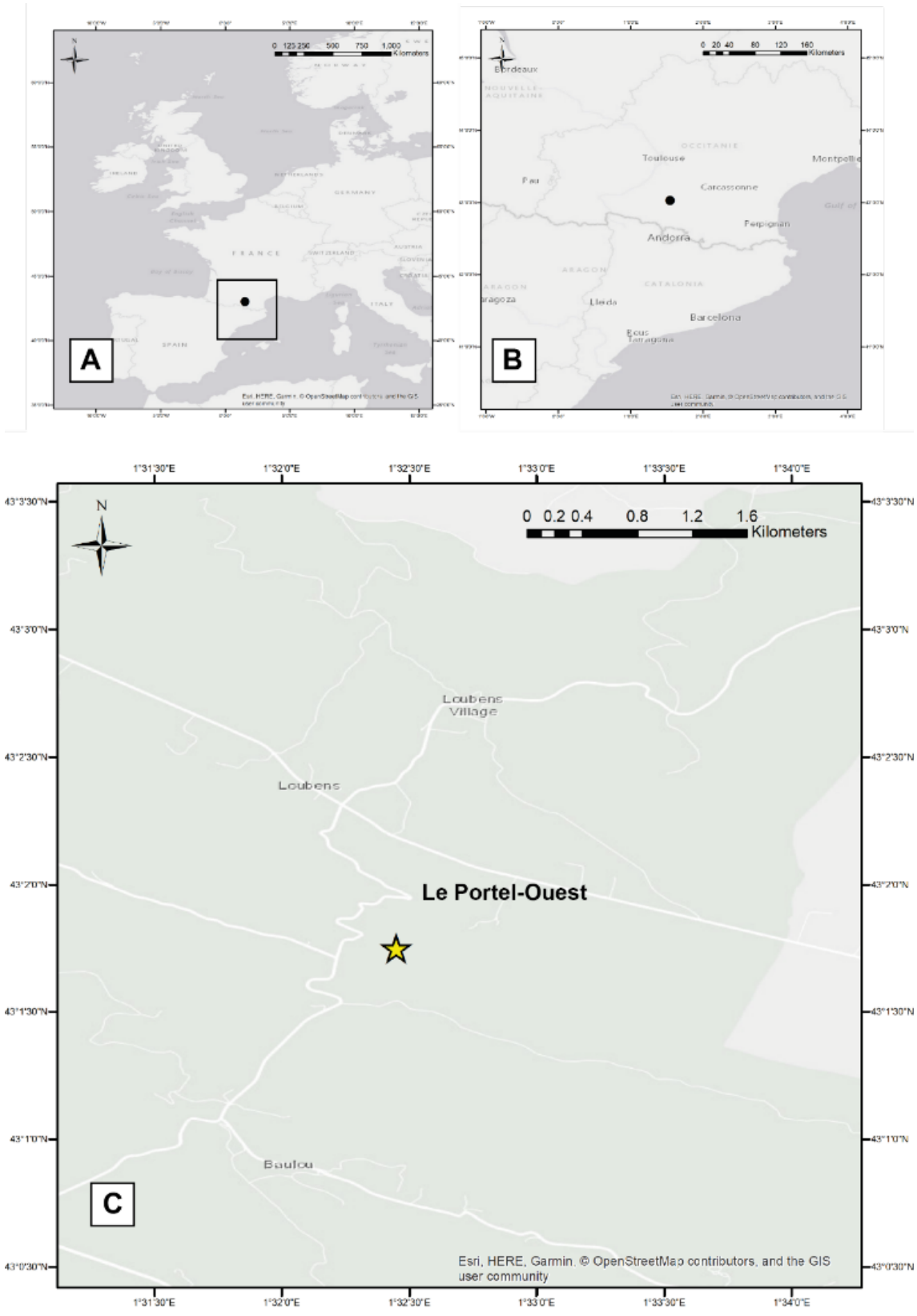

Figure 3.17: Location map of Le Portel-Ouest. A) Location within France, the square box represents B. B) Location within the Pyrenees region. C) Location within the Loubens village region.

3.2.2.3.2 Site stratigraphy and chronology

The 5m sequence consists of beds with a total of 21 subdivisions, grouped by Vézian (2014) into four archaeostratigraphic groups: the basal units (M, L, K, J, I), the first Mousterian assemblage (H, G, F3, F2, F1, F), the second Mousterian assemblage (D1, D, C) and the Upper Palaeolithic assemblage (B1A, B1, B). A schematic diagram of the stratigraphy is presented in Figure 3.18.

- Bed M is the base of the sequence and has not been reached in excavations to date.
- Bed L consists of a discontinuous stalagmite platform found at a depth of 4.6 m. This platform has been dated by uranium-series dating to 135 ± 9 ka (Ajaja, 1994 cited in Vézian, 2014) and provides the oldest constraining absolute age for the Portel-Ouest sequence.
- Bed K (4.6-3.95 m depth) is of a yellowish material and is subdivided into K1 and K2. K2 contains some calcareous clastic material proposed to be cryogenic. Bed K1 is composed of clays showing evidence of soil development indicating a cessation of infilling of sediment for an unknown duration. Sedimentological study of this bed (Menzhi, 1994) has suggested this was formed during a humid period, but conflicting ecological tolerances of fauna found in this level suggest that multiple climatic episodes may be recorded here.
- Bed J (3.95-3.88 m) is a reddish black sandy-clay layer resembling an accumulation of organic matter with a high percentage of calcium carbonate (Djerrab *et al*., 2001, cited in Vézian, 2014). This layer is ecologically sterile (Vézian, 2014).
- Bed I (3.88-3.68 m) is a reddish brown and contains karstic limestone pebbles, bones exhibiting evidence of rolling and smoothed, shiny quartz grains. Whitish concretions are present as the base. Wild boar and reindeer are present along with small lithics (Vézian, 2014).
- Bed H (3.68-3.28 m) is also reddish brown colour but composed of limestone fragments in a clay suggested to be a product of decalcification. Lithics are limited and reindeer is the only faunal species present (Vézian, 2014).
- Bed G (3.28-3.13 m) is dark brown in colour and is a thin layer with an important stony fraction and a number of karstic pebbles. The lithics and fauna are more abundant, with many cold-adapted species (reindeer, chamois and alpine ibex) and open landscape taxa such as horse and bison (Vézian, 2014).

- Bed F (3.13-2.31 m) consists of 5 sub-divisions (F3, F3, F1A, F1 and F, all archaeologically distinct but sedimentologically similar (Djerrab *et al*., 2001 cited in Vézian, 2014). Thousands of lithic and faunal remains are present including 34 Neanderthal remains. The majority of the faunal assemblage consists largely of reindeer, horse and bison and the bones exhibit many examples of human modification (Gardeisen, 1997). The first ESR and uranium-series dating for F3 and F2 by Ajaja (1994) indicated an age of 38.4 ± 6 ka but this was not confirmed by the subsequent dating by Tissoux (2004), using an improved ESR and uranium-series technique, reporting a slightly older age of 44.0 ± 6.6 ka for the same part of the sequence. However, the age uncertainties of both reported ages overlap.

- Bed E (2.31-2.06 m) is a brown layer that marks the boundary between the Lower and Upper Mousterian with silt and clays dominant and very little archaeology and fauna.

- Bed D (2.06-1.66 m) is a reddish grey unit with a high proportion of sand and limestone fragments (with higher corrosion of those in D compared to D1. This is interpreted as a cold and drier period. The lithic assemblage is richer in denticulate tools (Prince, 2000, cited in Vézian, 2014).

- Bed C (1.66-1.01 m) is a yellowish colour and consists of silt and clays. The lithics vary from the base to the top of this layer where there are more lithics associated with the Acheulian type B industry. Cold-adapted and montane faunal elements such as reindeer, chamois and alpine ibex dominate the assemblage followed by open-landscape fauna such as horse and bovids. There is also an important proportion of forest adapted taxa such as red deer and roe deer (Gardeisen, 1997).

- Bed B (1.01-0.11 m) contains a lithic industry corresponding to the Châtelperronian overlying a less abundant Gravettian assemblage. This bed is subdivided into B, B1, B1A and B2. B2 consists of large blocks reaching 1m across in a yellow clay and lithics and faunal remains are scarce. B1A is composed of a yellowish-brown material with corroded limestone pebbles. The lithics in B1A are a mixture of Mousterian and Upper Palaeolithic industries. B1 also contains an Upper Palaeolithic industry (Vézian, 2014).

- Bed A is not archaeological in nature and is not of significant importance.

The main Neanderthal occupation is therefore situated during MIS 3 (Gardeisen, 1999).

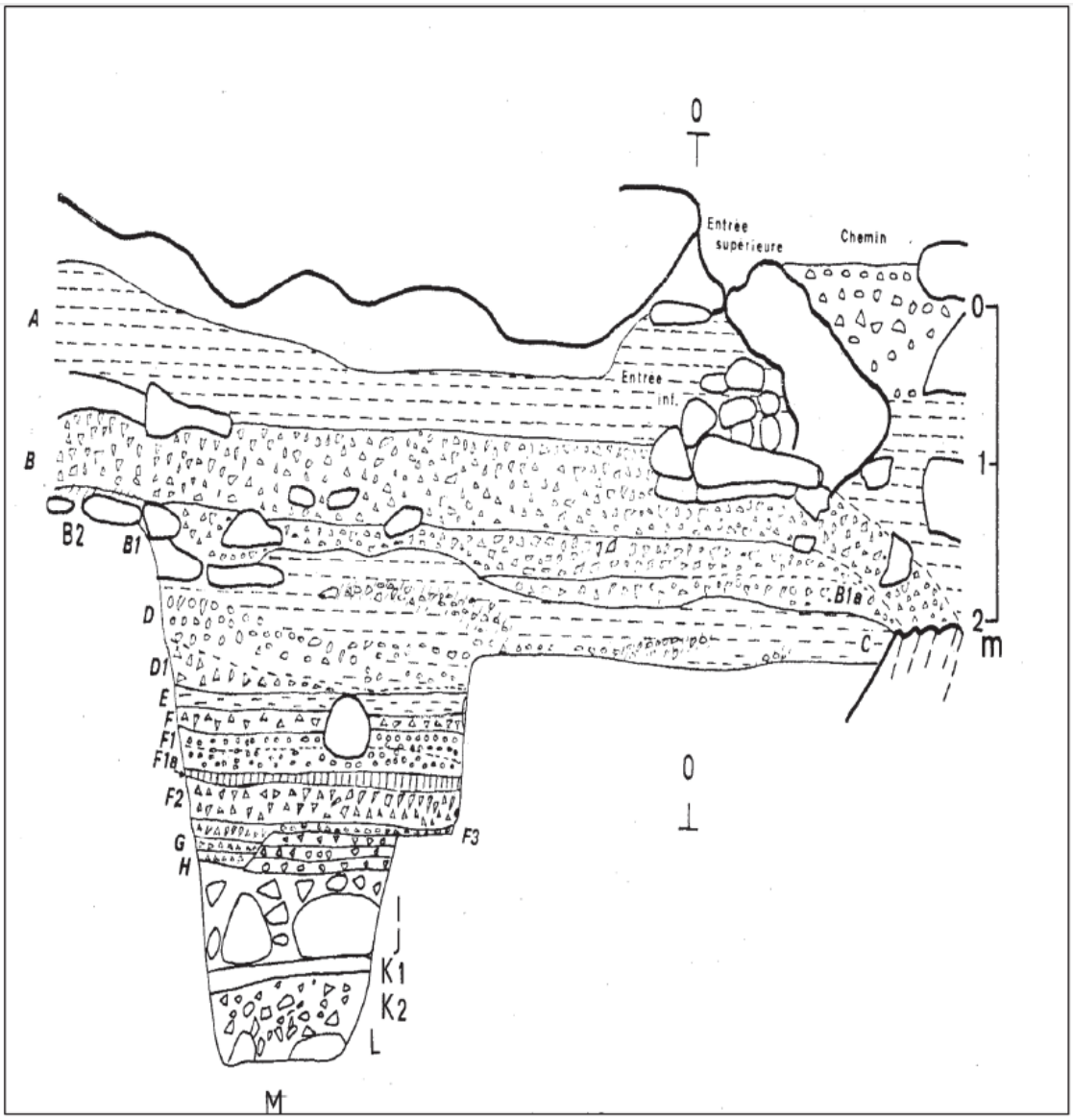

Figure 3.18: The stratigraphy of Portel-Ouest (taken from Vézian, 2014).

3.2.2.3.3 Palaeoenvironmental and palaeoecological proxies

A palynological study of Portel-Ouest was published in 1998 (Renault-Miskovsky and Girard, 1998, cited in Vézian, 2014). Pollen taxa found in beds K to C are indicative of cold and dry climate with open-landscapes present, but also some warm climate indicators are present. Pollen grains from the upper beds (C to B) are indicative of a colder climate and a more open landscape that coincides with the start of the Upper Palaeolithic in the sequence (Vézian, 2014).

Extensive palaeontological and archaeozoological investigations at Portel-Ouest have been carried out by Gardeisen (1985, 1986, 1988, 1994, 1996, cited in Vézian, 2004; Gardeisen, 1997, 1999). Large mammal faunal remains per bed are presented below in Table 3.3. The abundant fauna varies throughout the sequence. Herbivores are represented primarily by reindeer, horse, bison and red deer followed by a minority of

roe deer, chamois, alpine ibex, *Megaloceros*, woolly rhinoceros and mammoth (Vézian, 2014). Wild boar is reported in the literature but there appears to be no recording of specimen numbers for this taxon. Carnivores are represented mostly by red fox and wolf, especially in bed F. Bear, badger, hyaena and cave lion are also present at the site (Vézian, 2014).

Table 3.3: Table of the large mammal fauna from Portel-Ouest. Numbers shown are Number of Individual Specimens (NISP) per taxon, per bed (from Gardeisen, 1998).

Taxon/Bed	B	C	D	E	F	F1	F2	F3	G	H	I	J	K	Total
Ursus spelaeus	54	13	13	1	2	4	6	3					23	119
Canis lupus	1	13	13	1	8	13	168	40	5				21	283
Vulpes vulpes	113	30	15		19	46	560	158	63				106	1110
Panthera (Leo) spelaea	2	1					3						2	8
Felix sylvestris	1													1
Lynx lynx	2													2
Meles meles	87	5	4				2	4					4	106
Mustela putorius								1				2		3
Martes sp.	1													1
Crocuta spelaea	276	39	106		7	25	67						15	535
Rangifer tarandus	55	28	132		191	187	2970	1705	137		3		18	5426
Megaloceros sp.						1	3		2					6
Cervus elapus	101	20	37		33	74	605	85	85	8			2	965
Capreolus capreolus					6		14	5					35	60
Bison sp.	277	21	169	4	94	178	1084	191	5				4	2027
Capra caucasica	18	4	13		8	5	86	46	29				9	218
Rupicapra rupicapra	39	1	8			1	36	6						91
Equus caballus cf. *germanicus*	47	2	190	5	194	243	2075	766	31				1	3554
Coelodonta antiquitatis	2		4											6
Mammuthus sp.								1						1
Total	1076	177	704	11	562	777	7679	3011	280	0	3	0	242	14522

The faunal remains are very fragmented, either by human activity or by carnivores, however, the specimens have a high level of preservation, especially in bed F. Features on the remains reveal the different occupants of the cave: cutmarks, impact and fracture marks, carnivore gnaw marks and also evidence of trampling and transportation (Vézian, 2014). The taphonomic studies have permitted an understanding of activities at the cave throughout the deposition of the sequence. Middle Palaeolithic Neanderthals periodically occupied the cave during autumn and winter, practicing an opportunistic hunting strategy. Based on body part distribution and bone damage, it is suggested that animals were exploited in sophisticated and systematic manner from skinning to extraction of bone marrow. Alternating with Neanderthal presence were periods of carnivore occupation, especially hyaenas (Gardeisen, 1999).

3.2.2.3.4 Materials used in this study

Access to the materials from Portel-Ouest was granted by the Centre Européen de Recherches Préhistoriques (CERP) in Tautavel, France. Data was collected in February 2017. 44 M_3s were suitable for measurement of ungulate hypsodonty index.

3.2.2.4 Grotta del Romito (Calabria, Italy)

3.2.2.4.1 Introduction

The cave of Grotta del Romito is located in Calabria, southern Italy, at coordinates 39° 54′N, 15° 55′E. It is approximately 25 km inland from the Tyrrhenian Sea at an altitude of 275 m above sea level, in the Lao Valley (Craig *et al*., 2010). The entrance of the cave is at the bottom of a rock cliff on the right bank of a small tributary of the Lao River (see figure 3.19), about seven metres above the present river level. The site consists of an inner cave 25-30 m in length in an east-west direction and around 4 m high (Ghinassi *et al*., 2009) and also a partially collapsed outer rockshelter (Blockley *et al*., 2018). The site was first excavated in the 1960s with a trench in both the cave and rockshelter (Graziosi, 1962, 1971). Further investigations in the 21st century have expanded the cave trench to reveal well-preserved Palaeolithic and Mesolithic levels (Martini and Lo Vetro, 2005a,b, 2007, 2011; Martini *et al*., 2007, 2016).

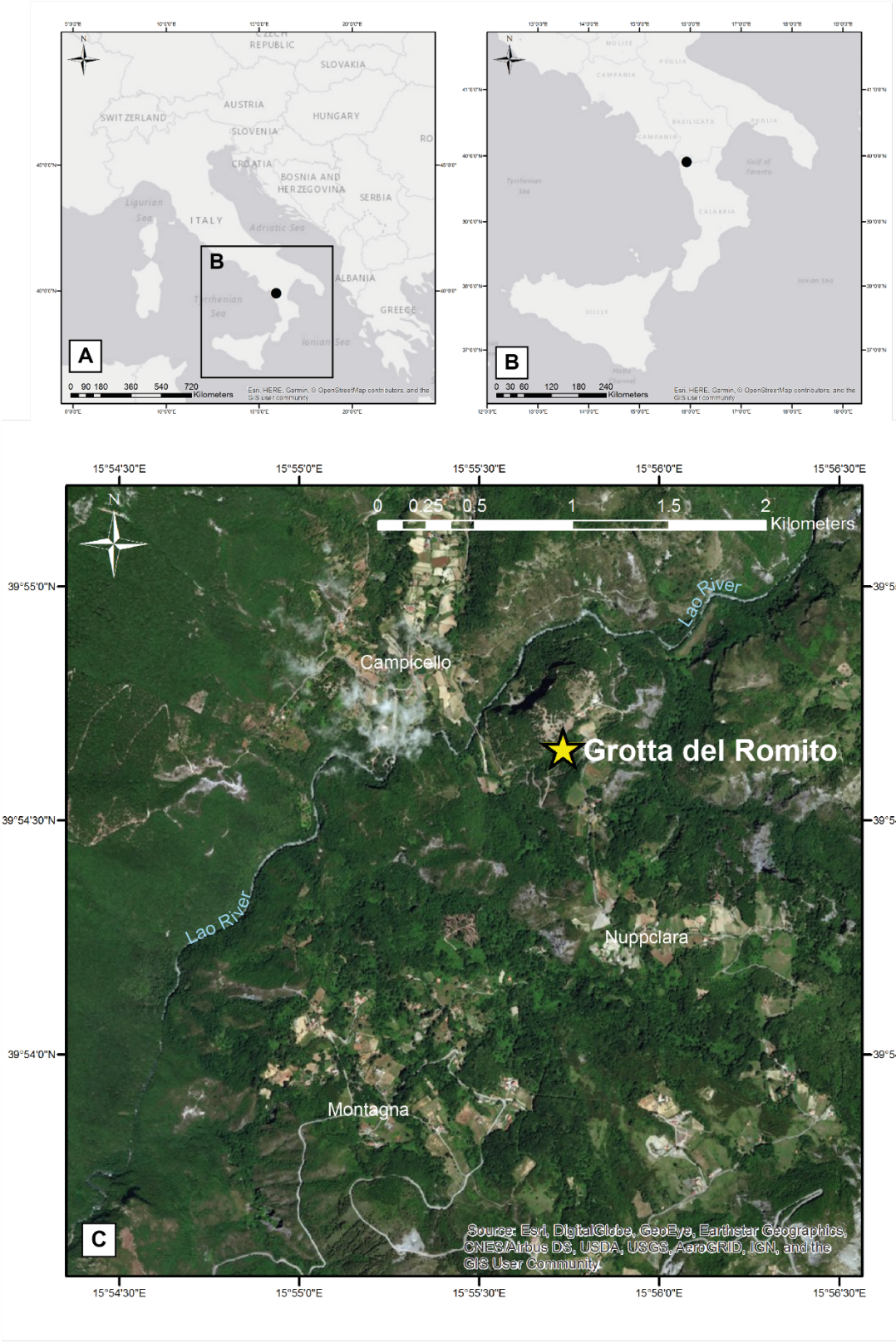

Figure 3.19: Location map of Grotta del Romito: A) within central southern Europe, B) within southern Italy and C) within the Lao River valley.

3.2.2.4.2 Site stratigraphy and chronology

The 21st century investigations have revealed twelve archaeological units (Layers N-A; see Figures 3.20 and 3.21). These main units are divided on the basis of changes in lithology whilst sub-units are defined by changes in archaeology (Blockley *et al*., 2018). The chronology of the site has been constructed using radiocarbon dating, Bayesian age modelling and tephrostratigraphy and the sequence spans ca. 33-27.3 ka cal BP to ca. 12-11.3 ka cal BP (Blockley *et al*., 2018).

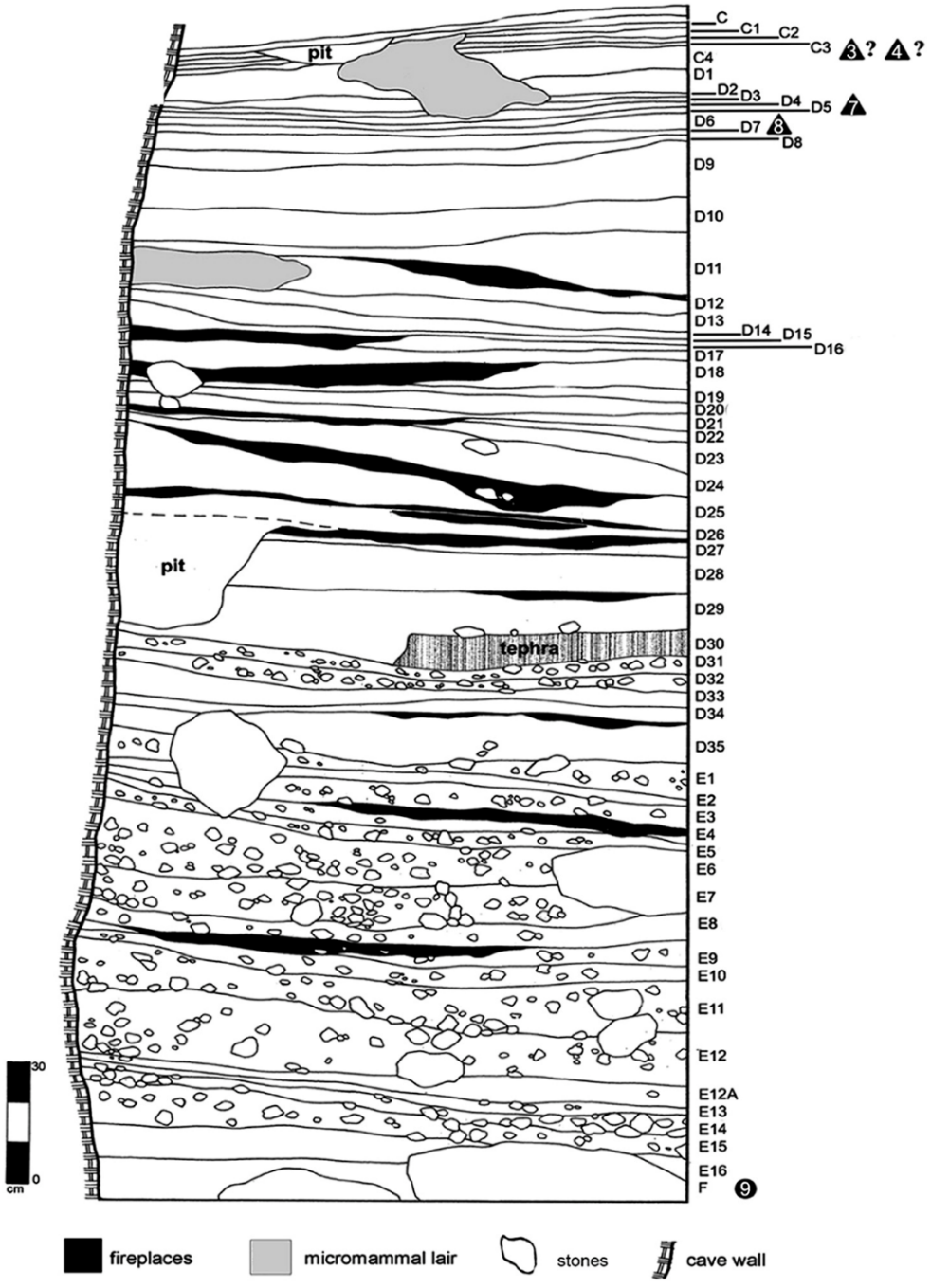

Figure 3.20: The upper part of the sequence from Grotta del Romito (taken from Blockley *et al*., 2018). The triangle and circle symbols represent the burials.

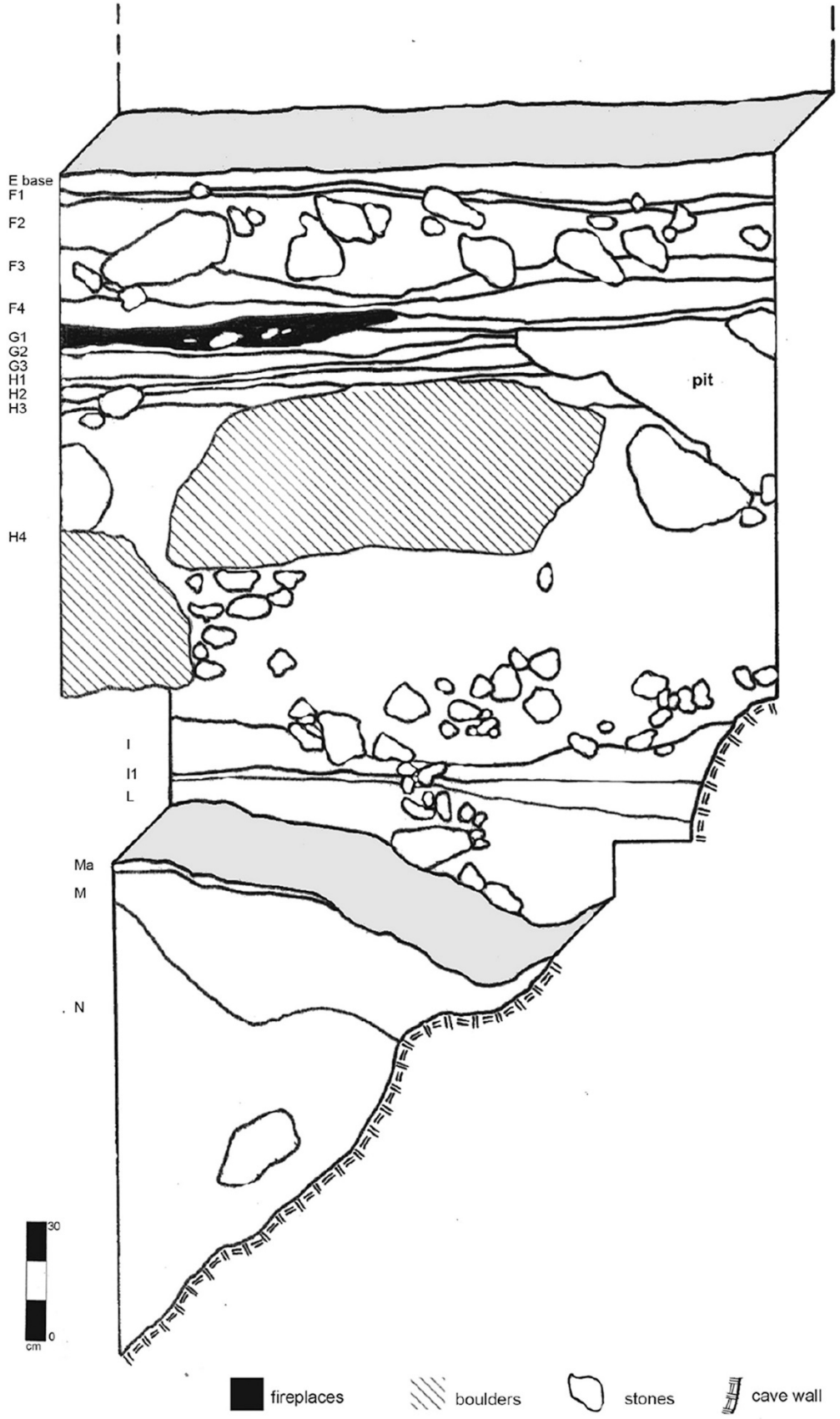

Figure 3.21: The lower part of the sequence from Grotta del Romito (taken from Blockley *et al*., 2018).

Sedimentological studies have revealed that the layers are predominantly coarse- to fine-grained cave sediments originating from the weathering of limestone and in-washing

from outside of the cave. Occasionally, there are additional large clasts of limestone. There appears to be a notable change in sedimentology from alluvial to anthropogenic origin between units E and D (Ghinassi *et al*., 2009), reflecting an increase in intensity of occupation after water flow in the cave ceases, as represented by the end of alluvium deposition (Blockley *et al*., 2018). The sequence and its units are reasonably intact, although the presence of burials and pits has disturbed the sequence in the upper part (especially units D and C). Neolithic and historical activities in the upper most layers (units B and A) have caused heavy disturbance of the sediments. Unit D30 contains a visible tephra layer (ROM-D30) dated to 15,792 – 15,318 cal BP, however it has not been attributed to any known and dated volcanic eruption. The rockshelter contains some Early Holocene deposits overlying a Late Epigravettian deposit that matches that of the upper sequence in the inner cave (Blockley *et al*., 2018).

Cultural phases of Grotta del Romito are designated as follows: Middle/Late Gravettian (H1-H4,I-I1, L), Late Gravettian (G1-G13), Early Epigravettian (F1-F4), Middle/Late Epigravettian (E1-E16), Late Epigravettian (D-D35) and a second Late Epigravettian phase (C-C4) (Bertini Vacca, 2012).

3.2.2.4.3 Palaeoenvironmental and palaeoecological evidence

Snail shells have been recovered from the archaeological deposits and these were analysed for their stable isotopic composition and identified taxonomically. These reveal considerable environmental changes in the Epigravettian part of the sequence. The oxygen isotope record created by Colonese *et al*. (2007) has now been placed by Blockley *et al*. (2018) onto a newly constructed chronology, covering much of the Lateglacial interstadial, from ca. 14,300 to ca. 13,000 cal BP (see Figure 3.22). It can be seen that there is a clear correspondence between the oxygen isotope composition of the land snails at Grotta del Romito and that seen in the NGRIP ice core record (Rasmussen *et al*., 2006), showing abrupt isotopic shifts from GI-1e through the reversal of GI-1d and back to warmer conditions of GI-1c. The age of the GI-1d event in the GICC05 event stratigraphy is 14,025 ± 169 years BP and this matches closely the age of 14,217-14,016 cal BP from the revised chronology for the mid-point of the molluscan oxygen isotope excursion from Grotta del Romito (Blockley *et al*., 2018).

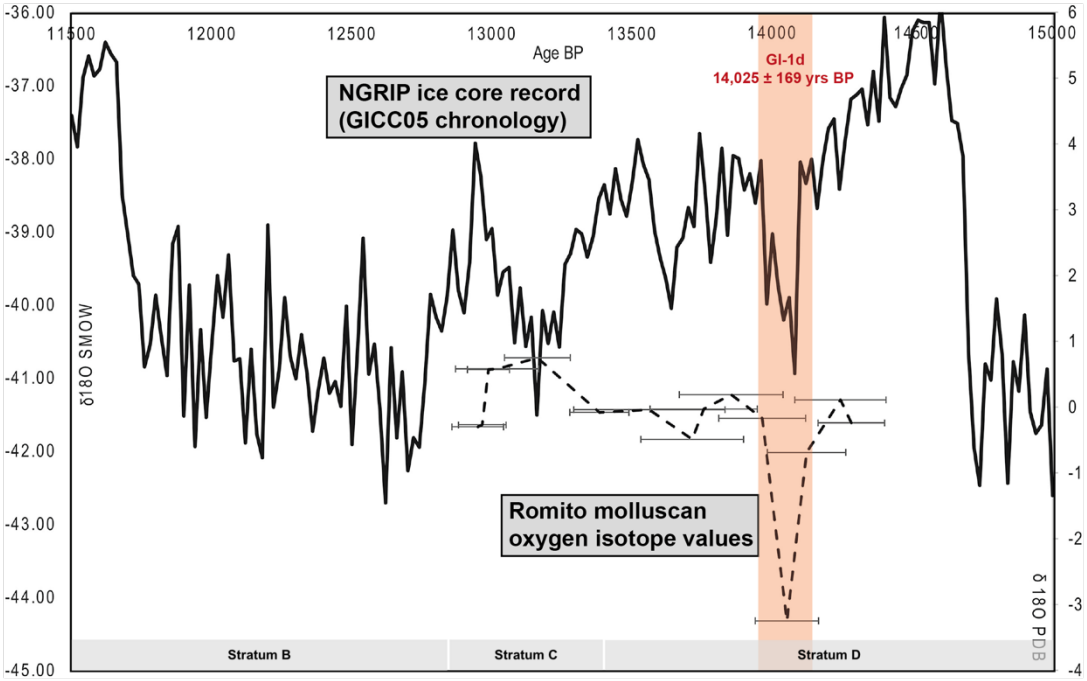

Figure 3.22: Molluscan shell oxygen isotope values (from Colonese *et al*., 2007) plotted on the latest chronology (Blockley et al., 2018) compared to the NGRIP ice core record (Rasmussen *et al*., 2006, 2014). Figure modified from Blockley *et al.* (2018).

Recent investigations of the small mammal material from Grotta del Romito has revealed palaeoenvironmental changes (López-García *et al*., 2014) and this information has also been placed by Blockley *et al*. (2018) onto their revised chronology (see Figure 3.23). The small-mammals appear to shift significantly to a dominance of woodland adapted taxa after the Heinrich 1 event (from about ca. 15,800 cal BP with an intensification after 15,000 cal BP; Rasmussen *et al*., 2006, 2014). This abrupt shift in small mammals occurs at Grotta del Romito between layer D29 (15,756 - 15,228 cal BP) and layer D11 (14,317 - 14,103 cal BP) and appears coincidental with the abrupt transition into GI-1e in the NGRIP record. The micromammal transition from dry to woodland adapted taxa appears synchronous with the shift from steppe to woodland taxa in the southern peninsula of Italy as shown in the pollen record from Lago Grande di Monticchio (Blockley *et al.*, 2018). The ROM-D30 tephra coincides with changes in micromammal fauna at Romito and is chronologically close to the start of increases in woody tree taxa at Lago Grande di Monticchio. It has therefore been suggested that the ROM-D30 tephra can be used as a marker for environmental amelioration in southern Italy during the Lateglacial (Blockley *et al*., 2018).

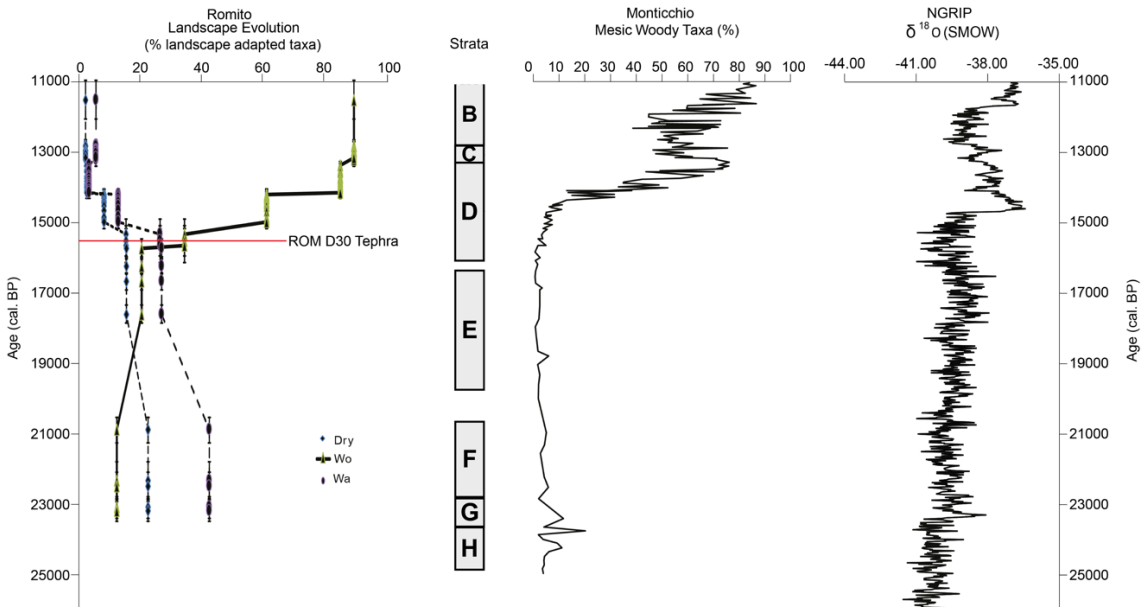

Figure 3.23: From left to right: percentages of small mammal taxa with reference to their habitat preferences (Dry, Woodland (Wo) and Water (Wa)) plotted on the revised Blockley *et al*. (2018) timescale with the position of the ROM-D30 tephra also marked, original small mammal data from López-García *et al*. (2014); the strata labels showing the position of each stratum on the revised chronology; percentage of mesic woody taxa in the pollen record from Lago Grande di Monticchio published by Brauer *et al*.(2007) and the NGRIP oxygen isotope record plotted on the GICC05 chronology (Rasmussen *et al*., 2006; Rasmussen *et al*., 2014).

During the excavations from 2000 to 2007, many large mammal remains were recovered from the sequence. It was observed that although many remains are highly fragmented, they are well-preserved. Considering the entire sequence as a whole, 98% of the specimens are ungulates whilst carnivores, lagomorphs, rodents and insectivores are represented by only a few remains. In order of importance, the ungulates are represented by ibex (*Capra ibex*), wild boar (*Sus scrofa*), chamois (*Rupicapra* sp.) and red deer (*Cervus elaphus*) with roe deer (*Capreolus capreolus*), aurochs (*Bos primigenius*) and wild horse (*Equus ferus*) being a minor quantitative component. The frequency of the six most represented species per layer is shown in Figure 3.24. During the Middle Gravettian cultural phase (Layers M, L and I; 33,007 – 23,733 cal years BP, date from Layer I only; Blockley *et al*., 2018) , the primary food sources for the occupants of Grotta del Romito were ibex (73% of the whole assemblage), red deer (14%) and chamois (9; Bertini-Vacca, 2012). At the transition from the Middle to Late Gravettian (27,592 – 23,733 cal years BP; Blockley *et al*. 2018), ibex increases in percentage (Bertini-Vacca, 2012). In the Late Epigravettian (16, 375 – 15, 549 to 12,985 – 12,805 cal years BP; Blockley *et al*., 2018), the best represented species changes to wild boar (~35% in layers D and C) whilst ibex becomes less important (31% in layers D and C) (Bertini Vacca, 2012).

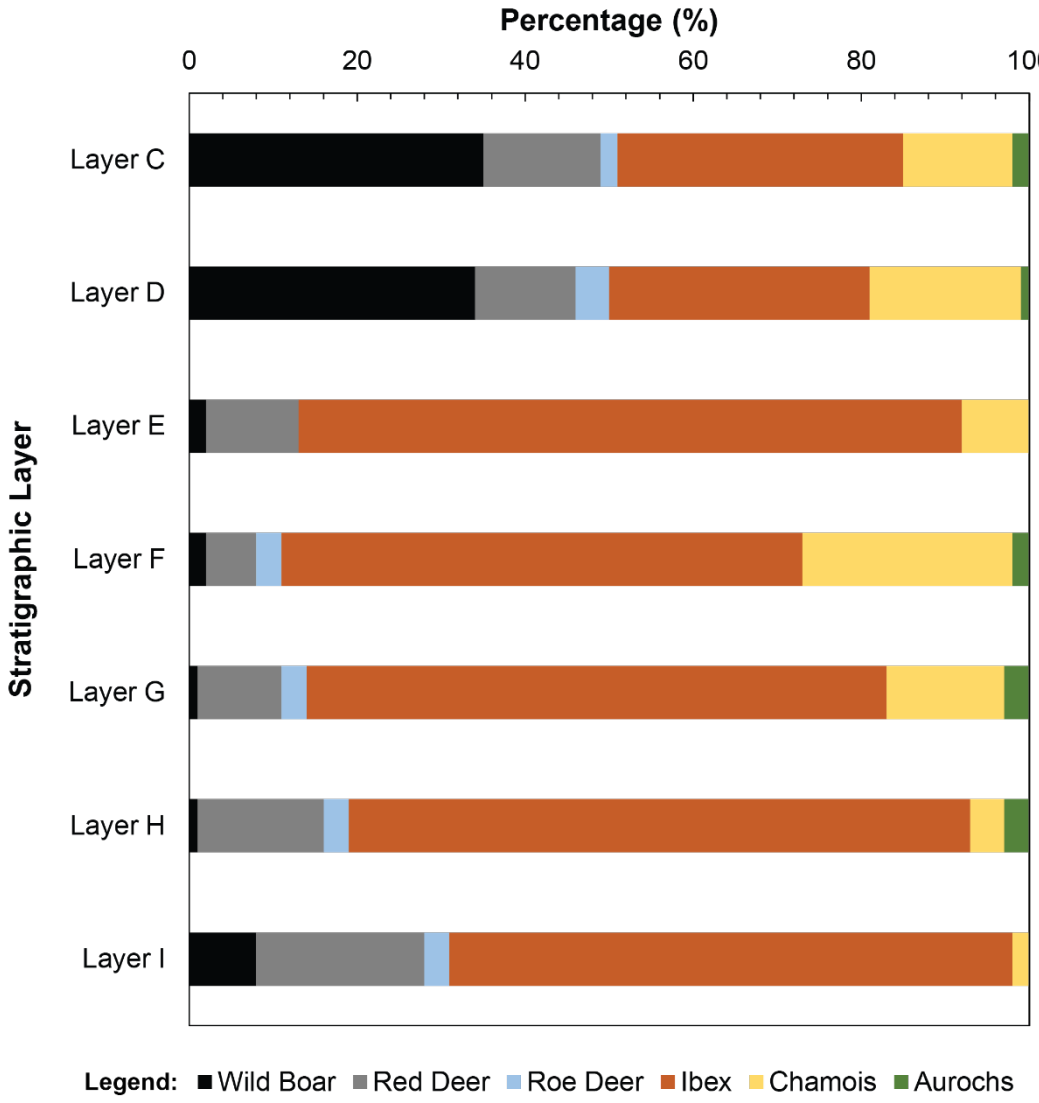

Figure 3.24: Variation in the frequency by percentage NISP (Number of Individual Specimens) of the six most represented taxa throughout the Grotta del Romito sequence (modified from Bertini Vacca, 2012).

3.2.2.4.4 Materials used in this study

The faunal material was made available for use in this study by the Museo e Istituto Fiorentino di Preistoria "Poalo Graziosi" and the Dipartimento di Storia, Archeologia, Geografia, Arte e Spettacolo at Università degli Studi di Firenze in Florence, Italy. 56 M_3s were suitable for measurement of ungulate hypsodonty index.

3.2.2.5 Tabun cave (Mount Carmel, Israel)

3.2.2.5.1 Introduction

Tabun Cave (32° 40′ 13.8″ N, 34° 57′ 55.8″ E) is located in the Mount Carmel region of Israel (see Figure 3.25), first excavated in the 1930s (Garrod and Bate, 1937), followed by further investigations between 1967 and 1972 (Jelinek *et al.*, 1973) and others since 1975.

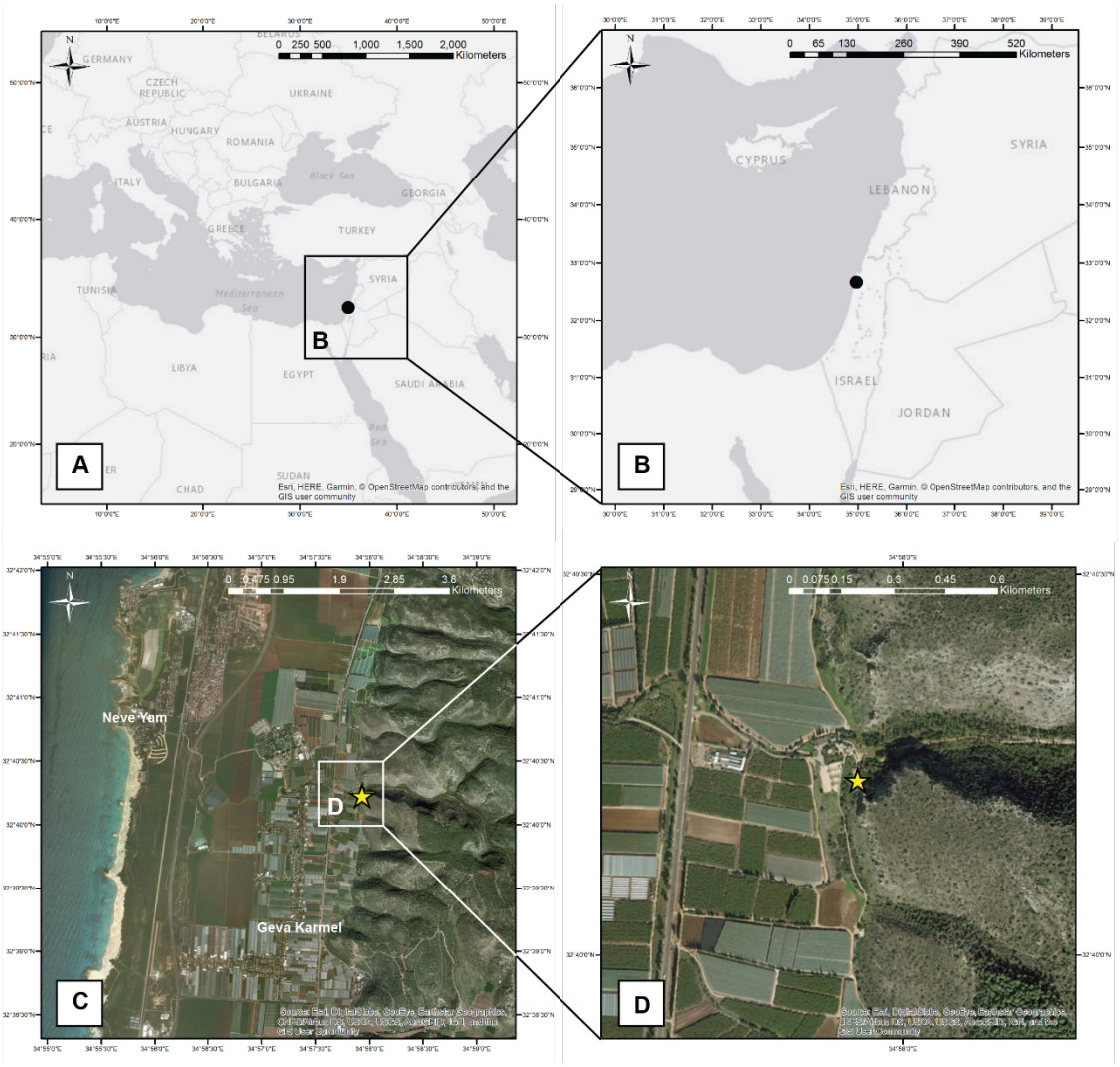

Figure 3.25: Location of Tabun cave**:** A) within the Middle East region, B) within Israel, C) within the Mount Carmel locality, D) at a local level.

The sequence is 25 metres in thickness and covers the Lower and Middle Palaeolithic. It has yielded the remains of a Neanderthal-like hominid (Tabun C1) along with remains of Anatomically Modern Humans (AMH) and rich lithic materials and is therefore regarded as one of the most important reference sites in the Levant (Mercier and Valladas, 2003). The site is situated at an elevation of c. 60m a.s.l. and consists of an outer chamber with rock walls but open to the sky and a closed inner chamber with a wide 'chimney' feature (Jelinek *et al.*, 1973).

3.2.2.5.2 Stratigraphy and chronology

The original excavation by Garrod and Bate (1937) identified six major archaeological layers from the external chamber and the chimney. Jelinek *et al.* (1973) reassessed the stratigraphy and regrouped the levels into three units (Units I, II and III), mainly based on sedimentological differences between the upper two levels and those underlying them (Albert *et al*., 1999) rather than archaeological differences (see Table 3.4). The following descriptions are taken from Jelinek *et al*. (1973, p.158): "Unit I (= Level B) – Red clay washed in from the plateau and limestone blocks from the ceiling; Unit II (= Level C) – alternating layers of ash, charred materials and baked soil, intercalated with thin beds of sediment like that of Unit I; Unit III (= Levels D through G) Eolian sand, increasingly silty upwards; the top part of II is strongly disturbed by erosional channels and slumping". There is a sharp erosional surface marking the contact between Unit III and the overlying Unit II, whereas the transition from Unit II into Unit I is very gradual (Jelinek *et al*., 1973).

Table 3.4: Layers designated by Garrod and Bate (1937) and the regroupings by Jelinek *et al*. (1973).

Garrod and Bate (1937)			**Jelinek *et al*. (1973)**
Layer	**Cultural designation**		**Unit**
A			
B	Upper Levalloiso-Mousterian		I
C	Lower Levalloiso-Mousterian	Neanderthal burial (Tabun I) and mandible (Tabun II)	II
D			
E	Acheuleo-Yabrudian		III
F	Late Acheulian		
G	Tayacian		

Jelinek (1982) appears to have subdivided the layers I, II and III (see Table 3.4 above) into a total of fourteen layers (I-XIV), although it is unclear in the literature how Jelinek's two unit naming systems are clearly related (see Figure 3.26). Subsequent work by A. Ronen created a 6 m extension below Jelinek's trench, and as of 2014, the Tabun sequence extends to 16 m in depth and contains a sequence of 100 archaeological layers (Shimelmitz *et al*., 2014; see Figure 3.27).

Age-estimates for the Tabun sequence have been obtained through U-series dating (Mercier and Valladas, 2003), electron spin resonance and U-series absolute dating (Grün and Stringer, 2000), with various revisions over time due to methodological improvements. Despite these improvements, the TL and ESR dates are not totally in agreement with each other as can be seen in Table 3.5.

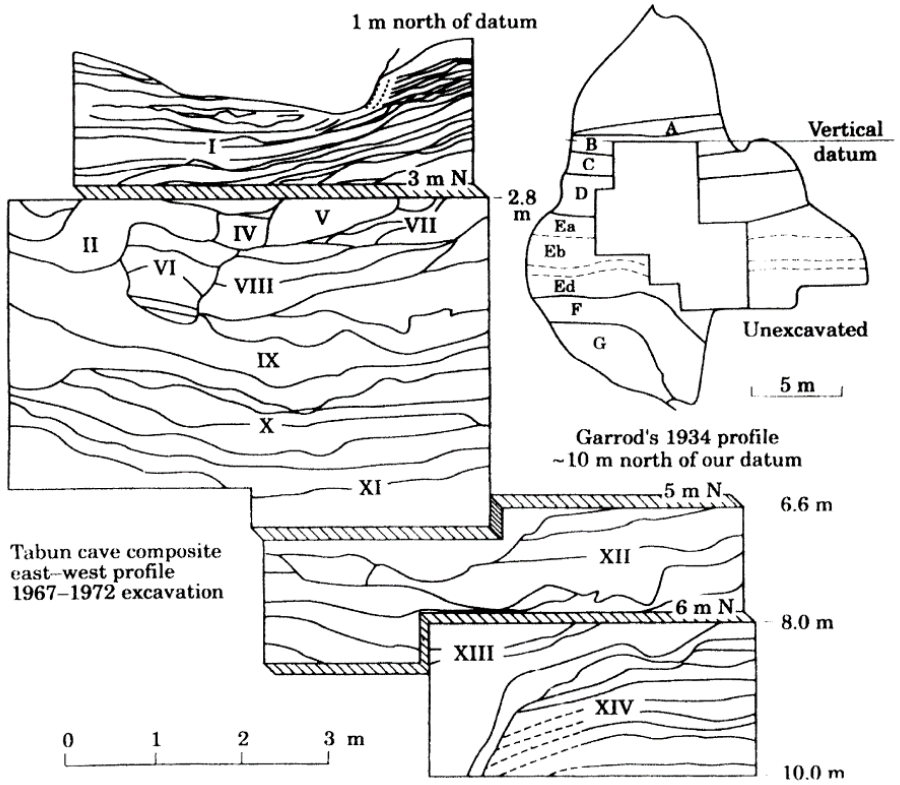

Figure 3.26: Diagram of the stratigraphy of Tabun Cave showing both Garrod and Jelinek's excavation (taken from Mercier and Valladas, 2003).

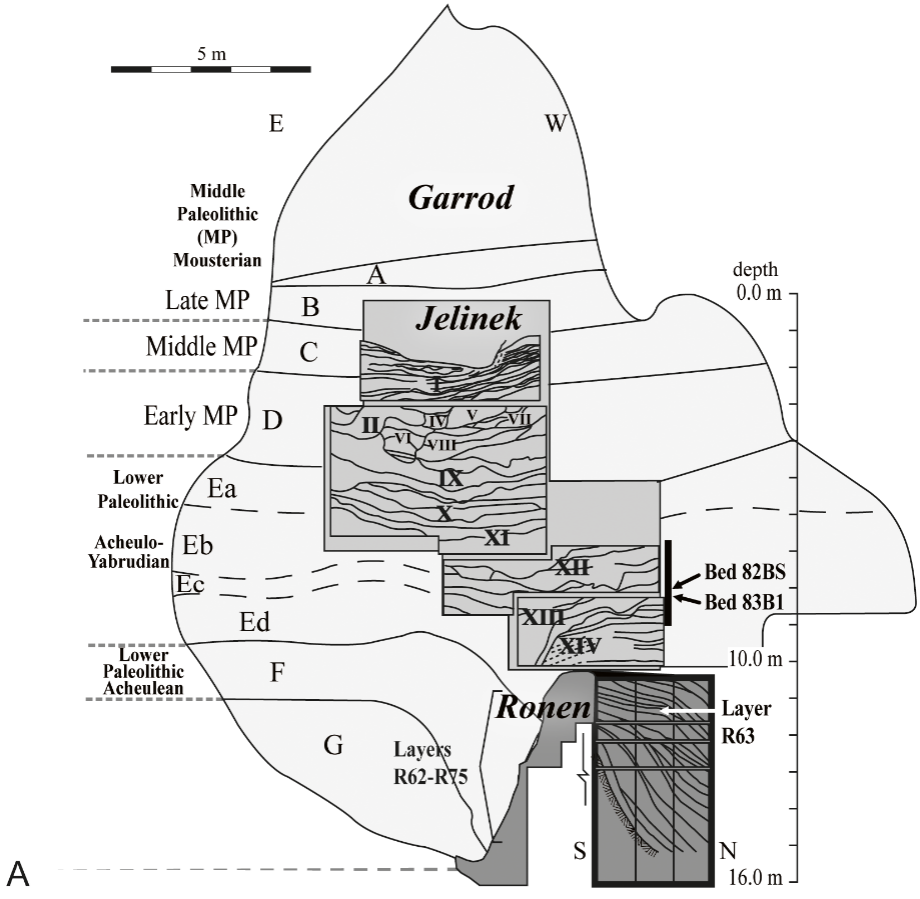

Figure 3.27: The latest stratigraphy from Tabun showing the extension of the sequence by Ronen and the relation between the three excavations (taken from Schimelmitz *et al.*, 2014).

Table 3.5: Thermoluminescene, U-series and ESR chronologies for Tabun.

Unit/layer	TL Mean age (ka) (Mercier and Valladas, 2003)	U-series and ESR Mean age (ka) (Grün and Stringer, 2000)
Unit B		104^{+33}_{-18}
Unit I/C	165 ± 16	135^{+60}_{-30}
Unit II/D	196 ± 21	
Unit V/D	222 ± 27	143^{+41}_{-28}
Unit IX/D	256 ± 26	
Unit X/Ea	267 ± 22	208^{+102}_{-44}
Unit XI/Ea	264 ± 28	
Unit XII/Eb	324 ± 31	
Unit XIII/Ed	302 ± 27	

3.2.2.5.3 Palaeoenvironmental and palaeoecological evidence

A large number of macrofaunal remains have been recovered from Tabun, mainly during the original Garrod excavation. In a reassessment of the assemblage by Marin-Arroyo (2013), 3,402 specimens were accounted for, with two-thirds belonging to level B. The high level of taxonomic and anatomic identification (99%) is attributed to recovery bias in the original excavations. A total of 25 mammal species were identified with a dominance of ungulates and a low frequency of carnivores. The three most dominant species, in order of number of individual specimens (NISP) are *Dama mesopotamica*, *Gazella gazella* and *Bos primigenius*. Tabun B is completely dominated by *D. mesopotamica* (78.5% NISP) compared to Tabun C (8.9%) and Tabun D (31.3%). The percentage of *G. gazella* decreases through time from 41.5% in Tabun D to only 15.1% in Tabun B. This stark difference of Tabun B was interpreted by Bate (1937) as a result of climatic differences. The accumulation of Tabun B is shown to be mainly natural. Other ungulates are represented in the deposit (see Table 3.6), but the very largest mammals such as *Dicerorhinus mercki* (= *Stephanorhinus kirchbergensis*) and *Hippopotamus amphibius* appear only in Tabun D and C (Marin-Arroyo, 2013).

Taphonomic analysis indicates that carnivore activity was very scarce and Marrín-Arroyo (2013) suggests that at least in Tabun D and C, humans were the primary accumulating agent and the remains could have been the result of primary consumption. The appearance of the bone assemblage in Tabun B, however, is completely different. The

bones in Tabun B show evidence for water pooling, dissolution and sub-aerial weathering and many elements are articulated suggesting that the assemblage accumulated naturally by animals falling through the roof of the cave. Breakage of the bones is typical of that which occurs naturally through pressure within a deposit. That being said, Tabun B is not devoid of taphonomical evidence of human exploitation. Cut marks on bones from this level hint that although Tabun B is a natural trap at this time, it was known to humans and they took advantage of both the ungulates and carnivores that had fallen and perished (Marín-Arroyo, 2013).

Further palaeoclimatic inferences can be made from understanding the flora at Tabun. A pollen study of the cave sediments was presented by Horowitz in 1979 and a summary diagram is presented below in Figure 3.28. The sequence has been split into two zones. A lower zone comprising Layers G, F and E (Garrod and Bate's designations) consists of low percentages of arboreal pollen, even lower than the present day. There are also very high percentages of Chenopodiaceae in comparison to grasses and sedges, together with relatively elevated proportions of Asteraceae, although in general these layers have a low species diversity.

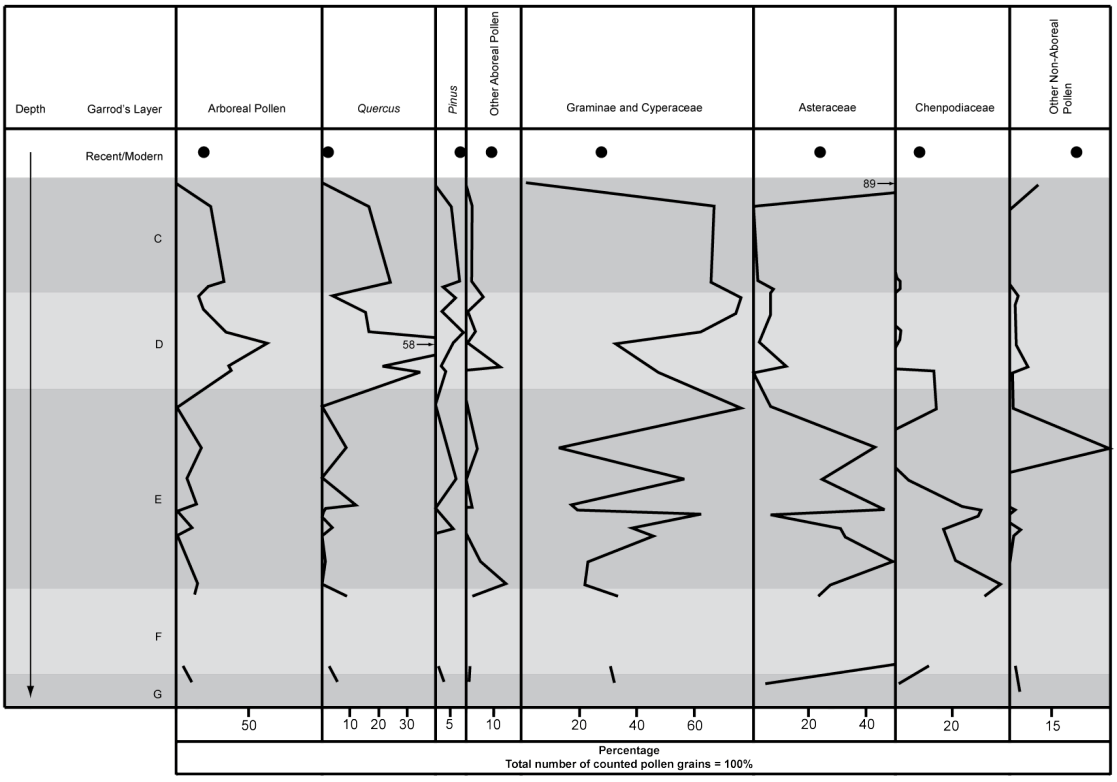

Figure 3.28: Summary pollen percentage diagram for Tabun (modified from Horowitz, 1979).

The upper zone (Beds D and C) contains a much higher percentage of arboreal pollen than in the lower beds (and higher than in the present day vegetation which sits at approximately 19% but is highly skewed by the cultivation of cypresses and Horowitz (1979) suggests this is likely to be half of this percentage). There is almost no

Chenopodiaceae present and rather low numbers of Asteraceae but grasses and sedges are much higher. There are some open field indicators but it is clear the vegetation at this time is dominated by trees, namely oak and pine.

The pollen spectra from the upper part of Bed F and all of Bed E represent “very dry, interpluvial conditions” (Horowitz, 1979, p.253) where higher sea levels caused flooding of the coastal plain, stopping the development of open field vegetation. This, along with the scarcity of trees, led to the dominance of halophilic vegetation (such as Chenopodiaceae) typical of sand dunes and coastal plains in the pollen signal. Beds D and C, however, are interpreted as representing “pluvial conditions” (Horowitz, 1979, p.253) with a forest on Mount Carmel that is much more developed than that found in the region today.

Table 3.6: The faunal assemblage of Tabun Cave (data from Marin-Arroyo, 2013). NISP = Number of Individual Specimens; MNE = Minimum Number of Elements; MNI = Minimum Number of Individuals.

Taxon	Tabun D			Tabun C			Tabun B		
	NISP	MNE	MNI	NISP	MNE	MNI	NISP	MNE	MNI
Dicerorhinus mercki	12	11	2	26	26	2			
Hippopotamus amphibius	7	5	1	35	31	3			
Bos primigenius	31	31	3	100	97	3	49	45	3
Equus hydruntinus							39	39	3
Equus hemionus	3	3	1	4	4	2	4	4	1
Equus ferus				11	11	2			
Camellus sp.				1	1	1			
Cervus elaphus	46	37	3	21	17	2	17	17	2
Dama mesopotamica	141	115	11	43	38	3	1,729	1,599	78
Capreolus capreolus	5	5	1				3	3	1
Capra sp.	6	6	1	15	14	2	21	21	5
Gazella gazella	187	162	11	187	174	8	332	318	23
Sus scrofa	13	13	2	38	36	3	9	9	1
Lepus capensis				2	2	1			
Procavia capensis				3	2	2	1	1	1
Hystrix indica	25	25	1				13	13	1
Hyaena hyaena	1	1	1				9	9	2
Crocuta crocuta	5	5	2	2	2	1			
Panthera pardus				2	2	1	48	46	4
Felis cf. silvestris	1	1	1				2	2	1
Canis aureus	2	2	1				4	4	1
Canis lupus	27	27	2				2	2	1

Vulpes vulpes				6	6	1	42	42	6
Ursus arctos	2	2	1	15	15	1			
Martes foina							3	3	1
Megafauna size				17	6				
Large mammal size				13	10				
Medium mammal size				3	2		3	3	
Small mammal size				10	8				
Indeterminate				1	1		3	3	
Total Ungulates	432	372	33	420	392	26	2,203	2,055	117
Total Carnivores	38	38	8	25	25	4	110	108	16
% Ungulates	84	82	73	76	78	68	94	94	87
Total	**514**	**451**	**45**	**555**	**505**	**38**	**2,333**	**2,183**	**135**

3.2.2.5.4 Materials used in this study

The faunal material was made available for use in this study by the Natural History Museum, London. 117 M_3s were suitable for measurement of ungulate hypsodonty index.

3.2.2.6 Qafzeh cave (Mount Precipice, Israel)

3.2.2.6.1 Introduction

Qafzeh Cave (32° 41′ 17.59″ N, 35° 19′ 5.67″ E) is situated at an altitude of 220m a.s.l. on the left bank of the Wadi el-Haj in the hills of Lower Galilee, close to the town of Nazareth, Israel (Rabinovich *et al*., 2004; Shea and Bar-Yosef, 2005; see Figure 3.29). The first excavations were carried out by Neuville and Stekelis between 1932 and 1935 (Neuville, 1951) and were halted by an avalanche. In 1936, the site was bombed by the British as it was serving as a hide-out for gangs during the Great Arab Revolt (Anon., 2018). Excavations were renewed in 1965 by a French team headed by Vandermeersch and these continued until 1979 (Vandermeersch, 1966, 1969a,b, 1970, 1972, 1981).

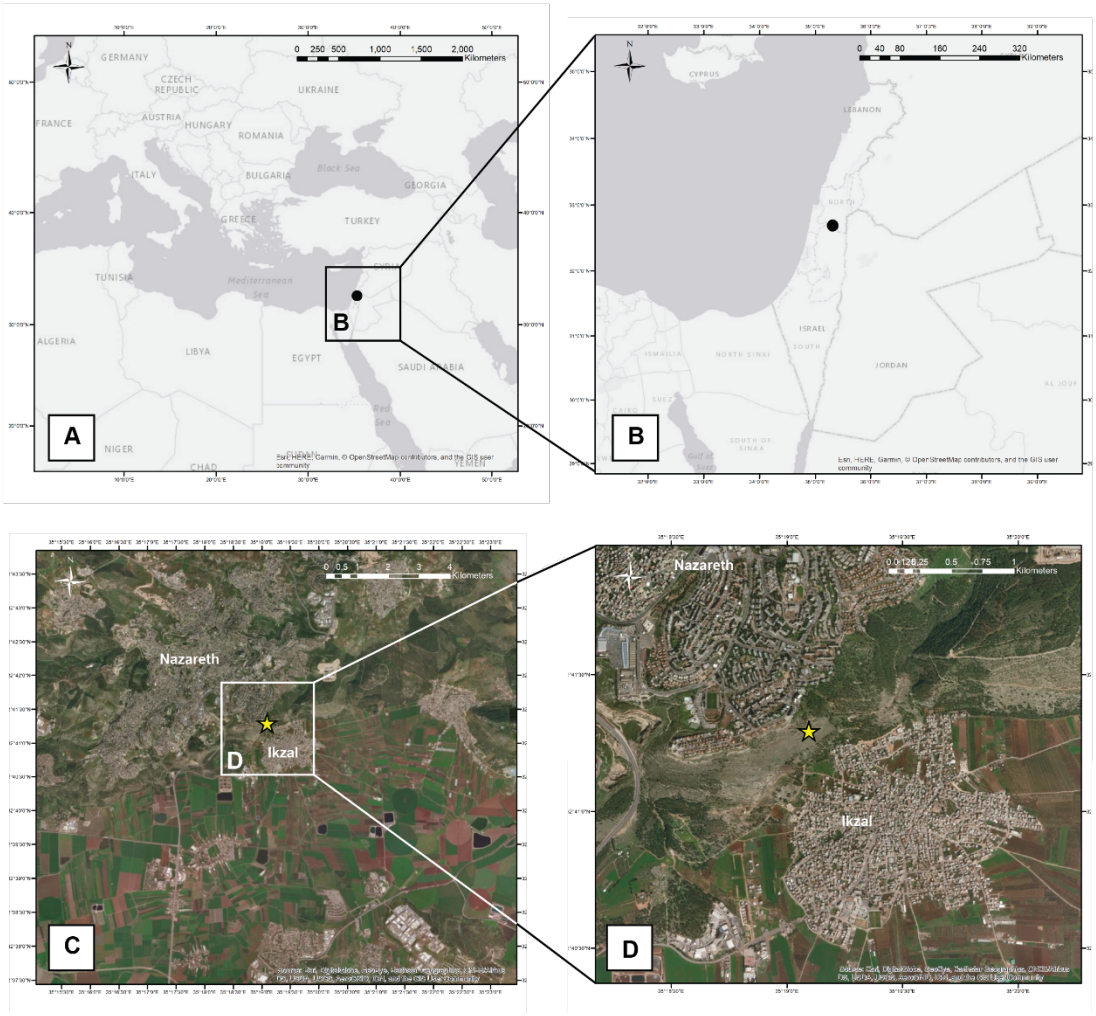

Figure 3.29: Location of Qafzeh cave: A) within the Middle East region, B) within Israel, C) within the Mount Nazareth locality, D) at a local level.

The cave consists of “a large, high-vaulted inner chamber, some 21 by 12 m” (Farrand, 1979, p. 377) that is connected by a corridor type structure (“vestibule”; Farrand, 1979, p.377) to a terrace in the open air. The “vestibule” has a high abundance of remains including human burials. The inner chamber has karstic features including a second

opening to the exterior. A chimney is present but filled with material that opens out into a talus feature inside the cave (Farrand, 1979).

3.2.2.6.2 Stratigraphy and chronology

The cave consists of “a large, high-vaulted inner chamber, some 21 by 12 m” (Farrand, 1979, p. 377) that is connected by a corridor type structure (“vestibule” (Farrand, 1979, p.377) to a terrace in the open air. The “vestibule” has a high abundance of remains including human burials. The inner chamber has karstic features including a second opening to the exterior. A chimney is present but filled with material that opens out into a talus feature inside the cave (Farrand, 1979).

The original early excavations documented the stratigraphy as follows (Neuville, 1951; Bar-Yosef and Belfer-Cohen, 2004; see Figure 3.30):

- Layer E: c. 0.75 m thick, brownish, no gravels but with hearths and rich in lithics
- Layer D: c. 0.60-0.85 m thick, reddish brown with an abundance of small calcareous fragments and numerous faunal remains and hearths.
- Layer C: c. 1.5-2.0 m in thickness, containing many calcareous fragments with larger surface rockfall material. A few hearths were present, along with faunal remains and the skull of Homo 2 (the second hominin skull as described by Neuville (1951), now attributed to archaic *Homo sapiens* (Bar-Yosef and Belfer-Cohen, 2004)).
- Layers A and B: historical deposits

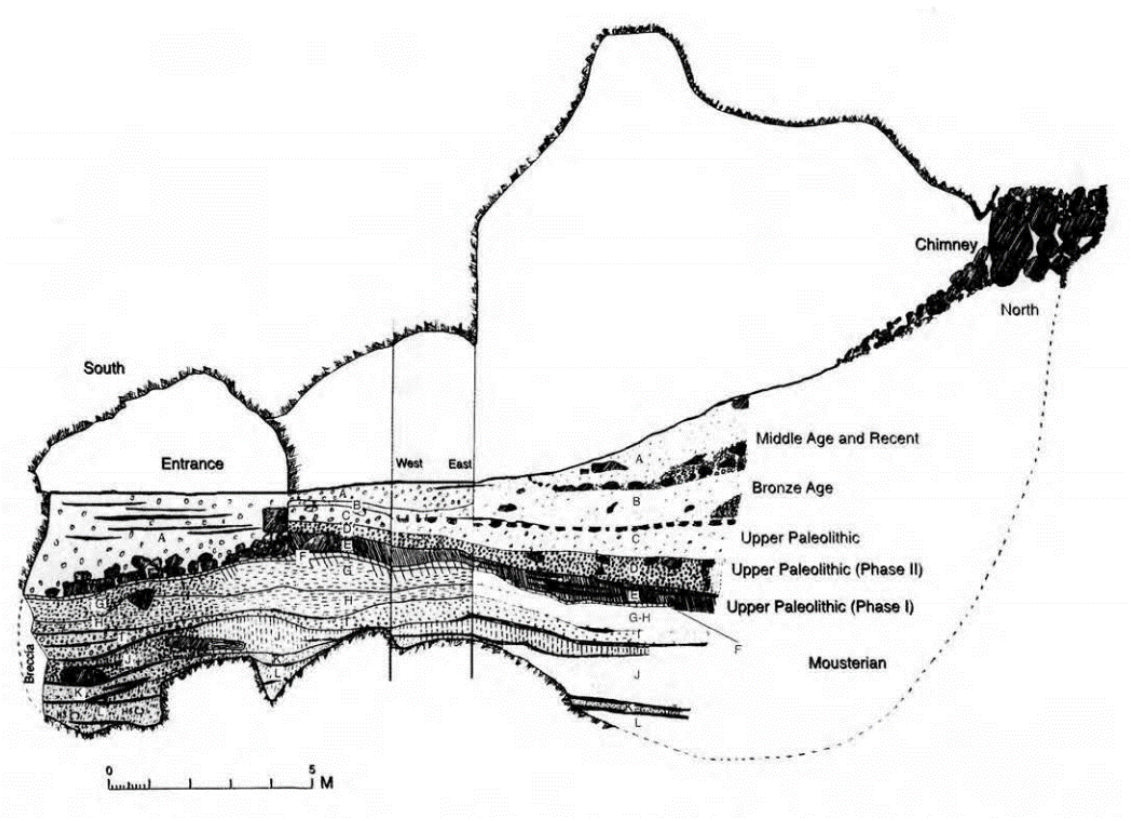

Figure 3.30: Site stratigraphy of the Upper Palaeolithic levels of Qafzeh cave from the original excavation (Neuville, 1951); taken from Bar-Yosef and Belfer-Cohen (2004), originally modified from Vandermeersch (1981).

The second set of excavations by Vandermeersch and colleagues largely confirmed the stratigraphy outlined by Neuville (1951) and documented the stratigraphy as follows, subdividing into thinner units (Bar-Yosef and Belfer-Cohen, 2004; see Figure 3.31):

- Layer 11: brown silt with occasional grey bands and few calcareous fragments, very few finds
- Layer 10: brown silt with occasional grey bands and few calcareous fragments, very few finds
- Layer 9: reddish clayey silt with small calcareous fragments and residues of hearths and confirmed Upper Palaeolithic lithics
- Layer 8: reddish clayey silt with heavily weathered calcareous fragments and residues of hearths and confirmed Upper Palaeolithic lithics
- Layer 7: reddish clayey silt with small calcareous fragments and residues of hearths and confirmed Upper Palaeolithic lithics decreasing in number.
- Layer 6: numerous large calcareous fragments with poor but unweathered finds
- Layer 5: numerous large calcareous fragments with poor but unweathered finds

- Layer 4: reddish brown slit with some weathered stones and some undetermined lithics
- Layers 2 and 3: larger rocks and ceramic fragments, presumably dating to the Bronze Age. A limestone slab floor marks the base of Layer 3
- Layer 1: modern/ recent historical

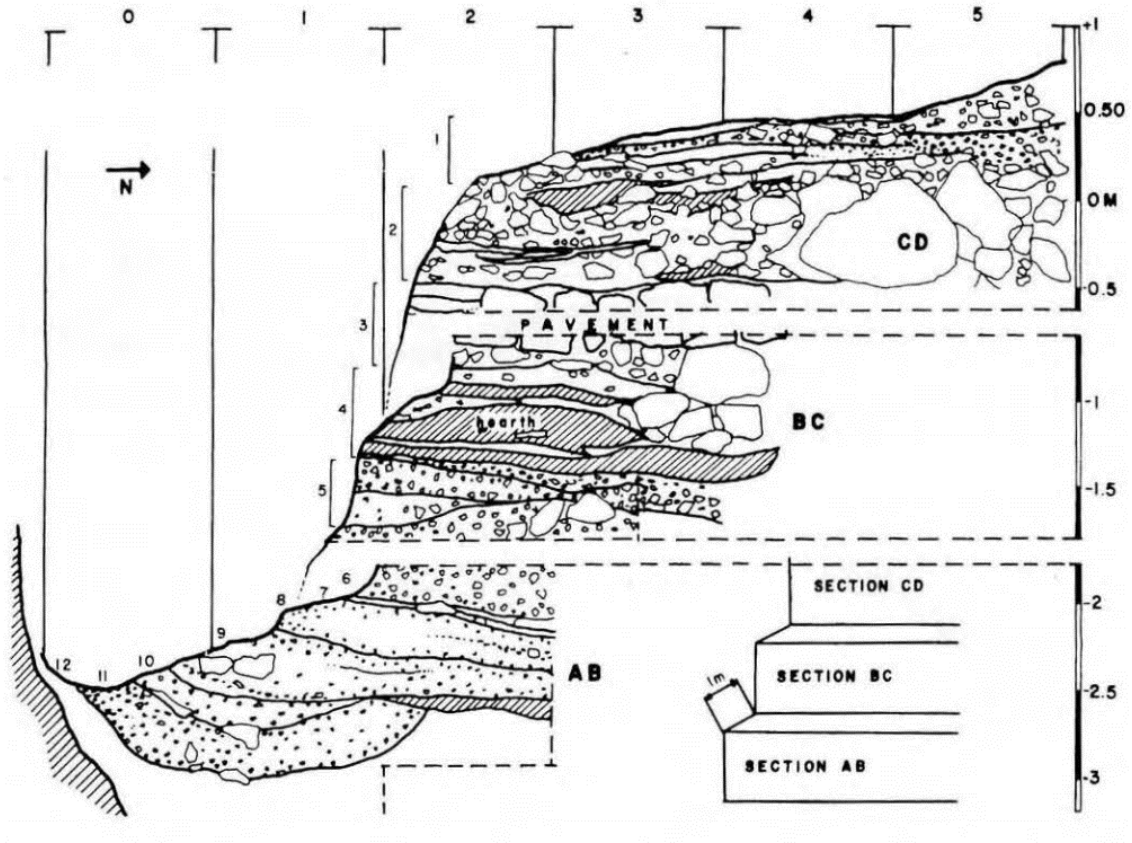

Figure 3.31: Stratigraphy of the Upper Palaeolithic levels of Qafzeh cave from the second set of excavations (Vandermeersch); taken from Bar-Yosef and Belfer-Cohen (2004) modified from Vandermeersch and Ronen (1972).

The cave was not fully described in the literature from either the 1930s or the post-1965 excavations and an attempt was made by Farrand (1979) to correlate and summarise the two excavations described above as well as providing some more detailed sedimentological descriptions. Farrand notes that the sediments in the inner chamber are strongly different than those in the “vestibule” and terrace areas.

The terrace sediments are “uniquely limestone bedrock rubble” (Farrand, 1979, p. 377) which is mostly angular, with minor amounts of a sand-silt-clay matrix and apparently unaffected by chemical weathering. Below the present dripline of the cave, these sediments are fully cemented into a concrete-like deposit. However, above the dripline these sediments are loose and very friable. It is worth noting that some of the human burials are lying in both the cemented and loose sediments. The terrace sediments

appear to contain only Mousterian finds, whilst the inner cave contains Mousterian, Upper Palaeolithic and “post-paleolithic” industries. The sedimentological characteristics described above indicate that the terrace deposit accumulated rapidly with evidence of freeze-thaw activity around the cave entrance. The cementing of the material is likely to have occurred as a result of rainfall exposure creating calcium carbonate soon after deposition, with no evidence of post-depositional weathering (Farrand, 1979). Tillier and Vandermeersch (1976, cited in Farrand, 1979) distinguished 24 individual beds in the terrace deposits, all with a similar style of deposition and all containing Mousterian lithics. However, there is an unconformity between beds VII and IX, in a similar fashion to that found inside the cave between beds 11 and 12 (Farrand, 1979).

Beds 11 to 7 are suggested by Farrand to be a single grouping due to their similarity: they are strong brown in colour, have rounded and porous clasts, most of them smaller than 2 mm. Clays and heavy minerals indicate that these beds are not as heavily weathered as beds 12 and 13, although postdepositional weathering is still significant. Bones and bone fragments are common in these layers, and a high abundance of *Gazella* in beds 7 to 9, which indicates drier environmental conditions, hints that the different degrees of weathering had a climatic control.

Farrand also notes that there is likely to have been considerable sediment transport from outside the cave, although it is unlikely that these sediments are aeolian in origin. Beds 6 to 11 and possibly 12 and 13 are likely to be products of this sediment transport from outside the cave. The reddish brown colour of beds 6 to 11 “might be attributed” to subaerially reworked soils above the cave chimney, similar to what is suggested for the origin of beds B and C at Tabun cave in the Carmel Mountains (Farrand, 1979, p.179).

Bed 6 appears to be more of the chimney colluvium. It is suggested by Farrand that there is a hiatus (possibly small) between bed 7 and the overlying bed 6.

The upper levels of Qafzeh begin with bed 4 being suggested by Farrand as Neolithic in age with the presence of hearths and the overlying levels begin the historical deposits with bed 3 having a stone pavement with pottery and bronze objects. The sediments in these beds also appear to be chimney colluvium with more angular clasts present (Farrand, 1979).

The chronological control of Qafzeh cave will be discussed below but it is suggested that stratigraphic correlation of some parts of the Qafzeh sequence with the Tabun sequence is possible. The Mousterian lithic industries of the terrace and inner cave deposits generally appear to correlate with Tabun D and/or C. Haas (1972) worked on microvertebrate remains from Qafzeh and has suggested that the Mousterian at Qafzeh is older than that found at Tabun D/C but this will be further discussed below. The

unconformity between beds 11 and 12 at Qafzeh and the unconformity at Tabun C and D are sedimentologically similar, with both sites having underlying beds that are heavily weathered and the unconformities themselves both showing water action. However, there is a proposition that local changes in the cave configuration at Tabun may have played a role in this unconformity, so this suggested correlation is tentative and unexplored (Farrand, 1979).

Developing an understanding of the timing of deposition at Qafzeh has been a primary goal of the research at the site, mainly due to the presence of hominin remains. The first estimates of the age of the hominins was based on the correlation of Qafzeh micromammalian remains with those from five other sites in the local region which were laid down during a high sea-level stand dating to the Last Interglacial (≥85 ka) (Tchernov, 1981; Bar-Yosef and Vandermeersch, 1981; Schwarcz *et al*., 1988). Amino acid racemisation ages of bone fragments from Qafzeh indicated ages of 73 ± 5 to 51 ±4 kyr for beds XXII to XVII (the beds in which the hominin burials were found) (Schwarcz *et al*., 1988).

In the late 1980s, two methods were used to attempt to close the debate on the ages of the Qafzeh hominins. Thermoluminescence (TL) dating of burnt flints from layers XXIII, XXII, XXI, XIX, XVIII, and XVII, yielding a mean age of 92± 5 kyr BP (Valladas *et al*., 1988; see Figure 3.32).

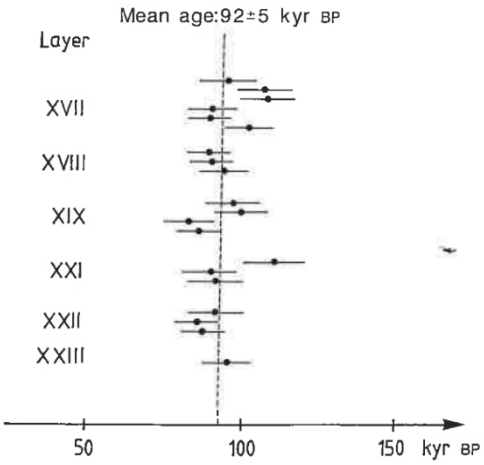

Figure 3.32: Thermoluminescene ages of burnt flints from Qafzeh cave (taken from Valladas *et al*., 1988).

Electron spin resonance (ESR) dating of enamel of the teeth of large mammals from the hominin-bearing layers gives an age of 115 ± 5 kyr BP (Schwarcz *et al*., 1988; see Table 3.7). These dates are significant as it indicates that the Qafzeh hominins are one of the earliest remains of anatomically modern humans outside Africa (Bar-Yosef and Vandermeersch, 1993; Rabinovich *et al*., 2004). However, a recent discovery of *Homo sapiens* fossils in Greece dated to 170-220 kyr (Harvati *et al*., 2019) indicates that the

Qafzeh hominins were just one of potentially many early migrations out of Africa. The 4.5 m thick Mousterian unit (terrace) is subdivided into upper and lower units but the dating methods above could not resolve the ages and all the dates fall within Marine Oxygen Isotope Stage (MIS) 5d-a (Hallin *et al*., 2012). However, recent work by Ambrose (2018) using geochemical isochrons ($\delta^{18}O$ and $\delta^{13}C$) suggests that level XXI may date to 119-128 ka BP, which correlates to MIS 5e rather than MIS 5d-a (see Figure 3.33).

Table 3.7: Electron Spin Resonance (ESR) dates for enamel from Qafzeh. EU = early uptake of uranium by enamel and dentin; LU = linear uptake of uranium by enamel and dentine (modified from Schwarcz *et al*., 1988).

		ESR ages (kyr)	
Sample	Layer	EU	LU
370A	XV	92.1	112.0
370B		94.2	114.0
373	XV	94.7	116.0
372	XVII	95.2	103.0
368A	XIX	87.7	106.0
368B		99.7	112.0
368C		102.0	117.0
368D		111.0	124.0
371A	XIX	107.0	128.0
371B		119.0	145.0
371C		82.0	101.0
369A	XXI	95.9	118.0
369B		118.0	143.0
369C		73.7	94.0
369D		74.2	89.1
369E		95.3	116.0
Averages:		96 ± 13	115 ± 15

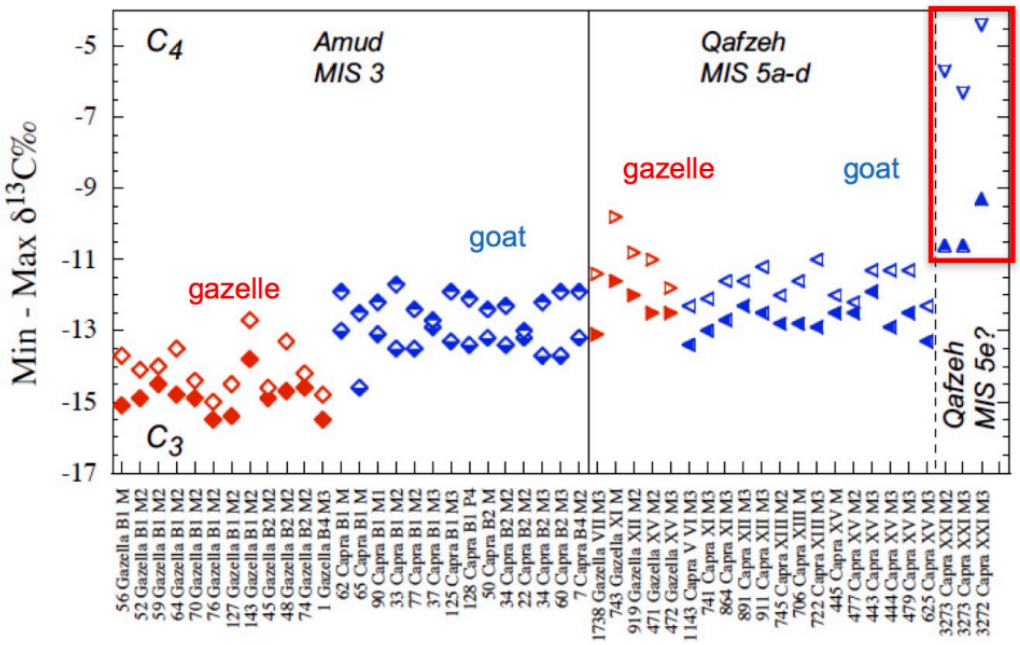

Figure 3.33: Carbon isotope ($\delta^{13}C$) data from goat and gazelle tooth enamel from Amud and Qafzeh caves. Figure taken from Ambrose (2018) and original data is from Hallin *et al*. (2012).

Dating for the Upper Palaeolithic sequence of Qafzeh has been undertaken using radiocarbon methods. In 1997, charcoal samples were collected from the western section of the Upper Palaeolithic deposits (Bar-Yosef and Belfer-Cohen, 2004). These dates are presented below in Table 3.8.

Table 3.8: Radiocarbon dates from the Upper Palaeolithic deposits at Qafzeh cave (taken from Bar-Yosef and Belfer-Cohen, 2004).

Layer	Square	Age B.P.	Lab. Number
8	Z24c 15/20	27,510 ± 340	GifA-98229
8	Z24c 15/20	27,080 ± 270	AA-27294
8	Z24d 20/25	26,720 ± 300	GifA-97336
8	Z24d 20/25	27,000 ± 280	AA-27289
8	Z24 25/30	28,460 ± 360	GifA-98231
8	Z24 25/30	26,540 ± 280	AA-27293
9	Z24b 35/45	28,340 ± 360	GifA-97337
9	Z24b 35/45	28,020 ± 320	AA-27291
9	B23 20/30	29,060 ± 390	GifA-98230
9	B23 20/30	28,380 ± 330	AA-27292
11	B22b-d 30/40	31,520 ± 490	GifA-97338
11	B22b-d 30/40	29,320 ± 360	AA-27290

3.2.2.6.3 Palaeoenvironmental and palaeoecological evidence

It has already been noted that Qafzeh cave contains both Middle and Upper Palaeolithic levels. 27 human fossils were recovered from the Middle Palaeolithic deposits in the terrace section of the site (Shea and Bar-Yosef, 2005). Additional remains were discovered in the main cave itself, in the Upper Palaeolithic levels (Neuville, 1951; Ronen and Vandermeersch, 1972). Almost all of the burials were found in layer XVII, with one burial (H. 11) uncovered in layer XXII (Bar-Yosef Mayer *et al*., 2009). The skeletal morphology of the remains is quite variable, and despite all being identified as anatomically modern humans (*Homo sapiens*), some display "primitive" features in the cranial morphology (Vandermeersch, 1981; Stringer, 1978; Stringer and Trinkaus, 1981).

A large study of the faunal remains was undertaken by Rabinovich *et al*. (2004). In this work it was clear that there was variation between the levels in terms of both the faunal remains and associated lithic assemblages. Some levels were combined to increase sample size and focussing only on macrofauna in a combined Middle Palaeolithic assemblage (consisting of 1,470 identified bones) and a combined Upper Palaeolithic assemblage (consisting of 716 identified bones). The species list is presented in Table 3.9. In the Middle Palaeolithic levels, there is a dominance of red deer and fallow deer with a low frequency of gazelle. Large mammals such as aurochs, three species of equid and narrow-nosed rhinoceros are also present and relatively common. In the Upper Palaeolithic, the dominance of red deer and fallow deer drops but these taxa are still relatively common. Instead, gazelle is most dominant at 19.5% of the assemblage. No rhinoceros is present but there are a few remains of large mammals such as aurochs, equids and hartebeest.

Table 3.9: Number of Individual Specimen (NISP) counts for the Middle and Upper Palaeoltihic assemblages at Qafzeh. Total NISP per taxon is shown along with NISP counts per body size categories. Table modified from Rabinovich *et al*. (2004, p. 629).

Taxon/body size class	Middle Palaeolithic (Levels 12-15)	Upper Palaeolithic (Levels 5-9)
Gazella gazella	91	140
Capra aegagrus	97	15
Bos primigenius	171	29
Alcelaphus buselaphus	7	15
Sus scrofa	62	43
Cervus elaphus	198	57
Dama mesopotamica	193	5
Capreolus capreolus	5	5
Equus undet.	46	-
Equus caballus	4	-

Equus hydruntinus	1	-
Equus tabeti	27	-
Dicerorhinus (= Stephanorhinus) hemitoechus	35	-
Canis lupus	1	-
Canis aureus	1	3
Vulpes vulpes	2	7
Vormela peregusna	-	1
Hyaena hyaena	-	3
Crocuta crocuta	15	29
Hyaenidae undet.	1	-
Panthera leo	2	2
Panthera pardus	2	1
Felidae undet.	1	-
Carnivora undet.	1	3
Very large sized mammals (e.g. *Bos/Rhinoceros*)	165	46
Large-medium sized mammals (e.g. *Dama/Cervus*)	63	102
Medium sized mammals (e.g. *Capra*)	33	-
Small sized mammals (e.g. *Gazella/Capreolus*)	177	170
Very small sized mammals (e.g. *Lepus/Vulpes*)	4	6
Unidentified mammals	65	34
TOTAL	1470	716

Micromammals was only recovered from the very lowest part of the sequence (layers XXIV-XV). The taxa present here includes *Sciurus*, *Spalax*, *Myomimus*, *Gerbillus*, *Meriones*, *Microtus*, *Apodemus*, *Rattus* and *Mus*. It was also reported by Tchernov (1991) that from the Middle to the Upper Palaeolithic levels, there was a reduction in numbers of *Mus musculus*, which was interpreted by Rabinovich *et al*. (2004) to reflect the more ephemeral nature of the occupation of Qafzeh during the Upper Palaeolithic. Haas (1972) also reports the presence of Amphibia, Reptilia, Aves and Chiroptera at Qafzeh although these orders are not considered here.

The presence of carnivores including juvenile spotted hyaena remains suggests that Qafzeh was periodically used not only as a carnivore den but also as a maternity den for spotted hyaenas in both the Middle and Upper Palaeolithic. Taphonomic study of the faunal remains revealed carnivore damage, human modification and burning. It is suggested that Qafzeh was the site of sporadic human occupations interspersed with carnivore denning across the Middle and Upper Palaeolithic (Rabinovich *et al*., 2004).

Palaeoecological and palaeoclimatic interpretations of the faunal assemblage at Qafzeh are interesting as there is a contrast of both open and woodland indicator taxa. Rabinovich *et al*. (2004) report that red deer, fallow deer and aurochs dominate the sequence which is interpreted as an indicator of woodland in the local area, whereas the micromammals (particularly in the lower levels) suggest a more open and dry environment (Hallin *et al*., 2012; Rabinovich and Tchernov, 1995). There is a strong signal from many sites in the Levant of this age of a significant northward shift of the Saharo-Arabian belt during MIS 5 (Rabinovich and Tchernov, 1995). At Qafzeh, the woodland indicators may represent small microenvironments of woodland in close proximity to the cave itself rather than more regional tree development. During MIS 5, the Levant has been suggested to be both relatively humid (Shea, 2008; based on speleothem data) and more arid (Frumkin *et al*., 2011). Data from the contemporaneous sapropel deposition in the south east Aegean Sea (S5) suggests that MIS 5 was certainly not stable (Rohling *et al*., 2015) and it is this instability that may explain the data that indicates both humid and arid conditions during this time.

Carbon and oxygen stable isotope ratios from gazelle and goat tooth enamel from Qafzeh indicate that during MIS 5d-a, the region around the cave was more open than the present day. There was no significant difference in stable isotope ratios between the Middle and Upper Palaeolithic levels. The isotope results also suggest that the Qafzeh region experienced a rainfall regime similar to that found in present day south-western Cape region of Africa. The presence of open environment taxa of goats and gazelles in many levels, alongside the woodland-adapted large mammals, suggests that there were several different habitats in proximity to the site (Hallin *et al*., 2012).

3.2.2.6.4 Materials used in this study

The faunal material was made available for use in this study by the National Natural History Collections of the Hebrew University of Jerusalem, Israel. 27 M_3s were suitable for measurement of ungulate hypsodonty index.

3.2.2.7 Haua Fteah (Cyrenaica, Libya)

3.2.2.7.1 Introduction

Haua Fteah is a large limestone karstic cave situated c. 10 km east of Sousa and c. 20km north of the ancient Greek city of Cyrene at coordinates 32°53′59″N 22°03′05″E. The cave is on the lowest series of terraces that forms the Gebel Akhdar (Green Mountain), an upland area lying between the Mediterranean Sea and the Sahara and has a Mediterranean type climate. The cave faces north towards the sea and has a 20 m high entrance and an 80 m wide interior (Barker *et al*., 2007).

The original excavations were carried out in 1950, 1951 and 1955 by Charles McBurney of the University of Cambridge and revealed a uniquely deep and rich series of human occupation in North Africa. The age of the oldest occupation at the site could not be determined at the time as the original excavations failed to reach the base of the sequence and stopped at around 13 m below the ground surface. McBurney estimated the lowest units in his excavation were deposited during the Last Interglacial (c. 120 kya). The upper levels were dated using radiocarbon methods and in all, seven major cultural phases were identified spanning from the Middle Palaeolithic to the historic period (Barker *et al*., 2007). Advancements in methodologies since the 1950s mean that it is now suggested that the lower levels of the McBurney excavation may be up to 195 kyr in age (Moyer, 2003).

The most recent excavations began in 2007, led by Graeme Barker, also of the University of Cambridge and continued through eight field seasons until 2015. These excavations focused on cleaning and accurately recording the original sections from the McBurney excavations (Upper and Middle Trenches (Trench U and M, respectively)) as well as excavating new trenches and extending McBurney's Deep Sounding (plus Trench D, S) downwards by 1.25 m to determine any presence of earlier cultural material (Jacobs *et al*., 2017). Full overviews of the field seasons from the latest excavations are published in *Libyan Studies* (Barker *et al.*, 2007, 2008, 2009, 2010, 2012; Rabett *et al.*, 2013; Farr *et al*., 2014).

3.2.2.7.2 Stratigraphy and chronology

The 1950s excavations revealed approximately 14 m of deposits. McBurney excavated what is now known as the Upper Trench (ground surface to c. 2 m depth), the Middle Trench (c. 2-7m) and the Deep Sounding (c. 7-14 m depth). The latest excavations since 2007 excavated new areas alongside McBurney's trenches as well as extending the depth of the deep sounding.

Five main sedimentary facies (see Figure 2) have been recognised in the Upper and Middle Trenches based on (1) particle size, (2) calcium carbonate analysis, (3) loss on ignition analysis, (4) magnetic susceptibility and (5) micromorphology. See Douka *et al*., (2014) for detailed descriptions.

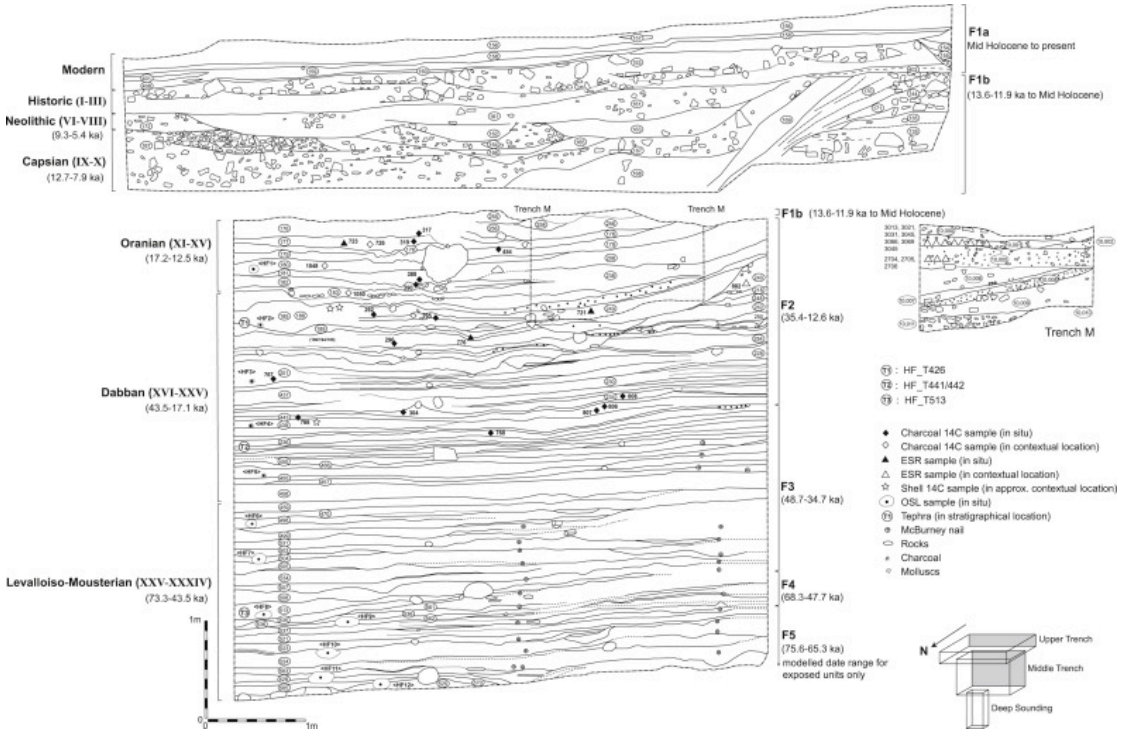

Figure 3.34: The stratigraphic context of the upper 7.5m of deposits at Haua Fteah. The facies are shown F1a-F5. Taken from Douka *et al*. (2014).

In order to date the sequence at Haua Fteah, a number of dating techniques have been used comprising radiocarbon, optically stimulated luminescence (OSL), electron spin resonance (ESR) and tephrochronology. Douka *et al*. (2014) carried out a chronological study on the upper 7.5m consisting of the Upper and Middle Trenches. This study used radiocarbon dating of charcoal, land snails and marine shells along with optical dating of quartz grains, ESR of tooth enamel and tephrochronology. From this work they report that Facies 5 dates to approximately 75-65 ka, correlating to MIS 4. However, they admit that this facies extended down into the Deep Sounding which was out of the scope of their work. Facies 4 dates to c. 68-47 ka, Facies 3 to c. 47-35 ka and Facies 2 to c. 35-12ka, meaning that Facies 4, 3 and 2 correlate to the period MIS 4-2. Material from the

Deep Sounding and an additional lower trench (S) was dated subsequently by Jacobs *et al*. (2017). This research revealed a hiatus in sediment deposition between c. 70-50 ka that was not taken into account in the age model of Douka *et al*. (2014)) and managed to reach the base of the Deep Sounding and gave a date of c. 150 ka for the start of accumulation of sediment. Occupation at the site continues through MIS 5e where there is a marked increase in artefact density reflecting increased presence at the site during the Last Interglacial (Jacobs *et al*., 2017).

Archaeology and cultural stratigraphy

McBurney (1967) recognised seven cultural stratigraphic units (outlined in: Klein and Scott, 1986):

1. *Historic*: Layers I-V. Wheel-made pottery and metal artefacts with Greco-Roman potsherds occur in situ in layer I-II and older postherds in layers III-V.

2. *Neolithic*: Layers VI-VIII. First occurrence of potsherds, pressure-flaked stone artefacts, rough hoe-shaped limestone implements and “grinding equipment”. Neolithic pottery of “Caspian Tradition”. Radiocarbon dates of layers VI and VIII date this culture between 7000 and 4700 BP.

3. *Libyco-Caspian*: Layers IX and X. Backed bladelets, numerous true microliths, occasional notched and strangulated blades and bone and ostrich eggshell artefacts. Correlated to the Maghreb cultures and radiocarbon to rougly 10,000 to 7,000 BP.

4. *Iberomaurusian*: Layers XI-XV. Abundance of well-made, very thin, backed bladelets and the rarity of other stone tools. Divided into and early and late phase: the early phase (layers XIV and XV in which “reverse trimmed” back bladelets are rare; layer phase (layers XIII and XII and X in which these bladelets are abundant. Oldest formal bone artefacts at the site, dated between 15,000 and 10,000 BP on limited radiocarbon dates.

5. *Dabban*: Layers XVI-XXVI. The earliest appearance of “punched” or “true” blades. Divided into two phases: early phase layers XXV-XXE and a late phase layers XXD-XVI on changes in too-type frequencies. Dated 50,000 to 20-18,000 BP based on radiocarbon and correlation to the Dabban industry at ed Dabba.

6. *Mousterian:* Layers XXXV-XXVI. A series of flake assemblages subdivided by McBurney into an “Evolved Hybrid Mousterian” (layers XXXV and XXXIV), an early Levalloiso-Mousterian (layer XXXIII), a possible Aterian (layers XXXII and XXXI) and a later Levalloiso-Mousterian (layers XXX-XXVI). The Mousterian sequence is beyond the radiocarbon timescale.

7. *Pre-Aurignacian*: Deep Sounding. This is distinguished by the abundance of crude angle burins and by scrapers and other tools often made on elongated flakes or flake-blades. Precise age unknown (as of 1986).

Two partial human mandibles were found associated with Levalloiso-Mousterian artefacts between layers XXXII and XXXIII.

3.2.2.7.3 Palaeoenvironmental and palaeoecological evidence

Tens of thousands of bones have been excavated, many of which were highly fragmented. 9068 bones were identified to skeletal element and to taxon level. These included 8003 from mammals, 425 from birds, 619 from tortoises, three from snakes and 18 from fish. Focussing on the mammalian finds, the finds were presented per cultural unit by Klein and Scott (1986) (see Table 3.10) as the individual layers generally contained too few bones for meaningful analyses.

The presence of abundant artefacts and hearths suggests that it is most probable that humans are responsible for the accumulation of faunal material at the site. Taphonomic studies revealed that there are very few bones with damage of any kind (humans, carnivores or rodents). The evidence of carnivore and porcupine in the assemblage could suggest minor accumulation by these animals, but the lack of human modifications to bones may be because humans may have avoided bone with their stone tools to avoid blunting or damaging their tools rather than bone being resistant to damage from tools. It is also possible that human modification may be present on some of the thousands of fragments that were unidentified and not studied in any detail (Klein and Scott, 1986).

The molluscan oxygen isotope record from Haua Fteah shows that during the latest Pleistocene and late glacial the Gebel Akhdar region was only slightly more arid that the present day. This conclusion is also suggested by data from other palaeoenvironmental proxies which suggest that the environment and climate were largely stable. Even the most arid phase at Haua Fteah appears to have coincided with an increase in human occupation at the site, perhaps indicating that Haua Fteah was used a coastal refugium within a more arid region. Conditions became more humid during the Holocene, but this was punctured by two arid phases at c. 8.0 ka and c. 7.3 ka that have been linked to more regional changes in the Mediterranean (Prendergast *et al.*, 2016).

Carbon isotopes from caprid and bovid tooth enamel indicated that there was a dominance of C_3 plant species during the last glacial period and early Holocene (namely the Levalloiso-Mousterian to the Caspain period at Haua Fteah). C_4 plants appear only from the mid Holocene onwards indicating that for much of the period of occupation at Haua Fteah the paleoenvironmental conditions were relatively constant. However, there

is an indication that there was lower precipitation before the Last Glacial Maximum (Reade *et al*., 2016). The overall stability indicated from the mammal and molluscan isotope studies slightly contrasts with that seen in the sedimentological study of the cave which suggests more instability (Inglis, 2012). Reade *et al*. (2016) suggest that this is a factor of differing spatial and temporal resolutions of the different studies rather than any true climatic or environmental disparity. A more recent study on the caprid tooth enamel from Haua Fteah suggests that there is an increase in the seasonality of the climate throughout the sequence, with a peak in seasonality in the late glacial (Oranian phase). It is suggested that the control on this seasonality change at Haua Fteah was a result of changes in winter precipitation levels and the strength of the summer dry season (Reade *et al*., 2018).

3.2.2.7.4 Materials used in this study

The faunal material was made available for use in this study by the Museum of Archaeology and Anthropology, University of Cambridge. Twelve M_3s were suitable for measurement of ungulate hypsodonty index.

Table 3.10: The number of identifiable mammalian specimens and the minimum number of individuals represented in successive cultural units at Haua Fteah (modified from Klein and Scott, 1986).

	Number of Identifiable Specimens (Minimum Number of Individuals)											
Taxon	**Pre-Aurignacian**	**Hybrid Mousterian**	**Evolved Levalloiso-Mousterian**	**Aterian**	**Levalloiso-Mousterian**	**Early Dabban**	**Late DABBAN**	**Early Ibero-Maurusian**	**Late Ibero-Maurusian**	**Libyo-Capsian**	**Neolithic**	**Historic**
Lepus capensis	-	-	-	-	-	-	-	-	3(1)	3(1)	-	-
Oryctolagus cuniculus	-	-	-	-	-	-	-	1(1)	-	-	-	-
Lagomorphs gen.	-	-	-	1(1)	1(1)	1(1)	1(1)	1(1)	3(1)	3(1)	2(1)	-
Hystrix cristata	1(1)	-	-	-	-	-	-	-	-	1(1)	17(4)	-
Ursus sp.	-	-	-	-	-	-	-	-	-	-	1(1)	-
Canis lupus familiaris	-	-	-	-	-	-	-	-	-	1(1)	4(2)	5(2)
Vulpes vulpes	-	-	1(1)	-	-	-	-	2(1)	6(1)	4(1)	4(1)	-
Small mustelid	1(1)	-	-	-	-	-	-	1(1)	-	-	-	-
Crocuta crocuta	-	-	-	-	-	-	1(1)	-	-	3(1)	-	-
Hyaenidae	-	-	-	-	1(1)	-	1(1)	-	2(1)	3(1)	-	-
Felis sylvestris	-	-	-	-	-	-	-	1(1)	-	-	2(1)	-
Loxodonta sp.	2(1)	-	-	-	-	-	-	-	1(1)	-	-	-
Stephanorhinus kirchbergensis	3(1)	5(1)	1(1)	3(1)	-	1(1)	1(1)	-	-	-	-	-
Ceratotherium simum	-	-	-	-	1(1)	-	-	-	-	-	-	-
Rhinoceros	3(1)	5(1)	1(1)	3(1)	3(1)	1(1)	2(1)	-	-	-	-	-

Equus sp.	-	-	-	-	-	5(1)	5(1)	8(1)	1(1)	-	2(1)	1(1)
Sus scrofa	-	-	-	-	-	-	-	-	-	-	1(1)	4(1)
Taurotragus oryx	-	-	-	-	-	-	-	-	1(1)	-	-	-
Alcelaphus buselaphus	3(1)	1(1)	5(1)	8(1)	-	2(1)	4(1)	47(4)	121(6)	33(2)	35(2)	-
Gazella sp.	29(2)	2(1)	5(1)	4(1)	4(1)	12(2)	11(1)	65(3)	127(5)	41(3)	56(7)	4(1)
Ammotragus lervia	33(1)	2(1)	62(4)	5(1)	1(1)	29(5)	148(13)	659(25)	1295(52)	1149(41)	2349(41)	35(2)
Capra aegagrus hircus	-	-	-	-	-	-	-	-	-	1(1)	421(19)	78 (8)
Ovis aries ?	-	-	-	-	-	-	-	-	12(5)	4(1)	124(8)	2(1)
Bos sp.	13(4)	36(2)	4(1)	4(1)	4(2)	20(2)	25(4)	30(2)	189(7)	228(13)	38(3)	7(1)

3.2.3 Summary of chronologies

A summary diagram of the ages of the fossil sites in this study is presented below (Figure 3.35) for clarity.

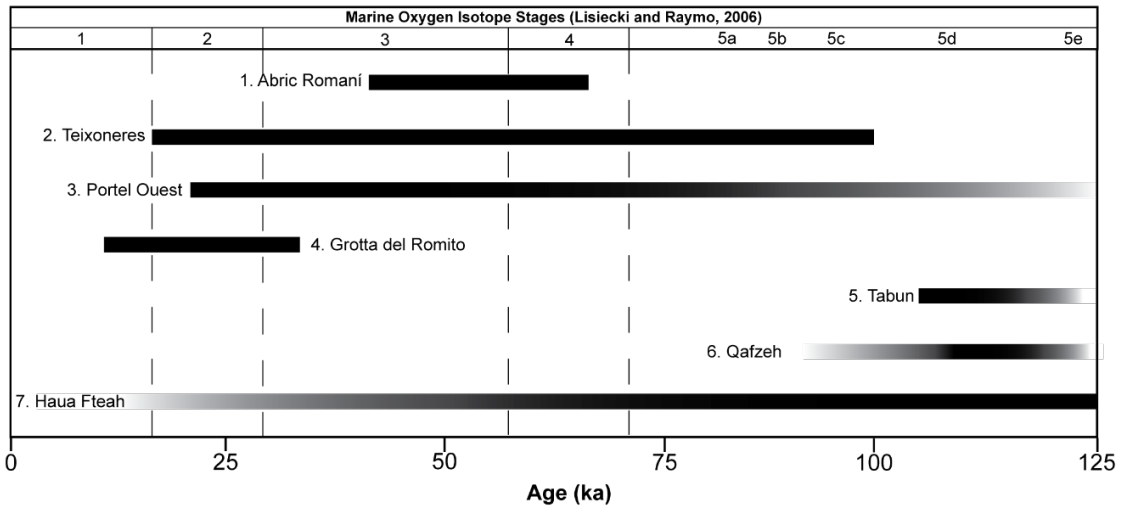

Figure 3.35: A schematic diagram summarising the ages of the Late Pleistocene fossil sites in this study**.**

CHAPTER 4
Results – intraspecific variation and modern herbivore hypsodonty as a climatic predictor

This chapter presents the results of the investigation of intraspecific variation in hypsodonty index followed by an examination of herbivore hypsodonty as a predictor of a number of climate variables.

4.1 Intraspecific variation of hypsodonty index

4.1.1 Preliminary analysis of variation and distribution of the data

As noted in the previous chapter, 3,788 raw hypsodonty index measurements were collected from modern specimens. In total this included individuals from 148 different ungulate taxa from the Families Bovidae, Cervidae, Equidae, Moschidae, Suidae, Tayassuidae and Tragulidae.

Descriptive statistics of these hypsodonty index measurements were calculated for each taxon. These are presented below in Table 4.1.

Table 4.1: Descriptive statistics for the hypsodonty index results for each taxon, split by Family (*n* = sample size, SD = standard deviation, CV = coefficient of variation).

Taxon name	n	Minimum	Mean	Median	Maximum	SD	Variance	CV
Bovidae								
Addax nasomaculatus	3	2.32	2.69	2.40	3.34	0.46	0.21	0.17
Aepyceros melampus	38	1.87	2.71	2.67	3.33	0.39	0.15	0.14
Alcelaphus buselaphus	62	1.93	3.09	2.57	5.28	1.05	1.11	0.34
Alcelaphus cokei	2	2.23	2.30	2.30	2.36	0.07	0.00	0.03
Alcelaphus sp.	2	3.71	3.90	3.90	4.08	0.19	0.03	0.05
Ammotragus lervia	4	1.78	2.61	2.58	3.51	0.77	0.59	0.30
Bison americanus	2	1.18	1.32	1.32	1.45	0.14	0.02	0.10
Bison bonasus	2	1.80	1.81	1.81	1.81	0.01	0.00	0.00
Bubalus mindorensis	2	2.03	2.05	2.05	2.07	0.02	0.00	0.01
Bubalus sp.	6	1.72	1.97	1.92	2.28	0.23	0.05	0.12
Capra aegagrus	5	1.65	1.93	1.91	2.22	0.23	0.05	0.12
Capra falconeri	2	2.17	2.22	2.22	2.26	0.05	0.00	0.02
Capra ibex	6	1.97	3.18	3.66	4.09	0.86	0.74	0.27

Capra nubiana	4	2.08	2.27	2.31	2.37	0.12	0.01	0.05
Capra pyrenaica	5	1.76	2.34	2.54	2.86	0.41	0.17	0.17
Cephalophus callipygus	30	1.94	2.31	2.35	2.64	0.20	0.04	0.09
Cephalophus castaneus	22	1.61	1.93	1.92	2.19	0.16	0.03	0.08
Cephalophus dorsalis	29	1.46	2.15	1.96	2.94	0.43	0.18	0.20
Cephalophus harveyi	6	1.90	2.00	1.98	2.15	0.09	0.01	0.05
Cephalophus leucogaster	8	2.05	2.25	2.24	2.47	0.14	0.02	0.06
Cephalophus monticola	30	1.58	1.85	1.85	2.12	0.15	0.02	0.08
Cephalophus natalensis	2	2.10	2.22	2.22	2.34	0.12	0.01	0.05
Cephalophus niger	12	1.80	2.16	2.20	2.62	0.27	0.07	0.12
Cephalophus nigrifrons	6	2.24	2.32	2.32	2.41	0.06	0.00	0.03
Cephalophus ogilby	2	2.49	2.52	2.52	2.54	0.03	0.00	0.01
Cephalophus rufilatus	8	1.82	2.10	1.97	2.73	0.31	0.10	0.15
Cephalophus sp.	71	1.49	1.84	1.84	2.21	0.15	0.02	0.08
Cephalophus sylvicultor	20	1.44	1.94	1.77	2.80	0.42	0.17	0.22
Cephalophus weynsi	2	1.99	2.06	2.06	2.13	0.07	0.01	0.03
Connochaetes taurinus	18	2.01	2.37	2.25	2.93	0.32	0.10	0.13
Damaliscus hunteri	6	2.16	2.41	2.36	2.80	0.20	0.04	0.09
Damaliscus korrigum	11	2.44	2.75	2.81	3.14	0.21	0.04	0.08
Damaliscus lunatus	8	1.85	2.61	2.44	3.44	0.57	0.33	0.22
Eudorcas thomsonii	1	4.00	4.00	4.00	4.00	0.00	0.00	0.00
Gazella bennettii	4	1.75	1.96	1.93	2.23	0.18	0.03	0.09
Gazella cuvieri	2	2.33	2.49	2.49	2.64	0.16	0.02	0.06
Gazella dorcas	36	1.45	2.21	2.25	2.86	0.33	0.11	0.15
Gazella gazella	24	1.60	2.22	2.23	2.62	0.22	0.05	0.10
Gazella granti	4	1.83	2.14	2.16	2.39	0.26	0.07	0.12
Gazella izabella	2	1.71	1.77	1.77	1.83	0.06	0.00	0.03
Gazella leptoceros	4	2.22	2.63	2.63	3.05	0.30	0.09	0.12
Gazella marica	4	1.84	1.97	1.90	2.25	0.17	0.03	0.08
Gazella rufifrons	4	2.27	2.33	2.34	2.36	0.04	0.00	0.02
Gazella saudiya	2	2.42	2.52	2.52	2.62	0.10	0.01	0.04
Gazella sp.	2	2.10	2.21	2.21	2.31	0.11	0.01	0.05
Gazella spekei	2	2.12	2.26	2.26	2.40	0.14	0.02	0.06
Gazella subgutturosa	3	1.61	2.49	2.87	2.99	0.62	0.39	0.25
Gazella thomsoni	16	2.08	2.33	2.32	2.71	0.19	0.04	0.08
Gazella tilonura	2	1.59	1.82	1.82	2.05	0.23	0.05	0.13
Hippotragus equinus	58	1.14	2.24	2.28	2.75	0.28	0.08	0.13

Hippotragus niger	18	1.83	2.70	2.56	4.04	0.58	0.34	0.21
Kobus anselli	12	3.04	3.38	3.25	3.67	0.23	0.05	0.07
Kobus defassa	26	1.71	2.02	2.00	2.45	0.19	0.04	0.09
Kobus ellipsiprymnus	76	1.31	2.61	2.46	4.06	0.51	0.26	0.20
Kobus kob	180	1.68	2.66	2.76	4.05	0.59	0.35	0.22
Kobus leche	10	2.13	2.76	2.85	3.18	0.35	0.12	0.13
Kobus megaceros	4	2.87	3.02	2.99	3.23	0.14	0.02	0.05
Kobus sp.	10	1.59	1.96	1.99	2.28	0.23	0.05	0.12
Kobus vardonii	26	2.35	3.02	3.02	3.99	0.40	0.16	0.13
Litocranius walleri	8	1.33	2.35	2.62	2.86	0.58	0.33	0.24
Madoqua gueutheri	12	2.28	2.70	2.78	2.98	0.20	0.04	0.08
Madoqua saltiana	12	2.47	2.86	2.85	3.15	0.21	0.04	0.07
Nanger dama	2	2.63	2.64	2.64	2.65	0.01	0.00	0.00
Nanger soemmerringii	16	1.43	2.71	2.64	3.91	0.62	0.39	0.23
Nemorhaedus goral	3	2.18	2.36	2.38	2.51	0.14	0.02	0.06
Neotragus batesi	54	1.84	2.70	2.70	3.42	0.31	0.10	0.12
Oreotragus oreotragus	2	2.76	3.02	3.02	3.28	0.26	0.07	0.09
Oryx besia	6	1.67	2.16	2.35	2.42	0.31	0.10	0.14
Oryx gazella	2	2.28	2.34	2.34	2.40	0.06	0.00	0.03
Ourebia ourebi	34	2.28	3.07	3.09	3.81	0.37	0.14	0.12
Philantomba maxwelli	4	2.24	2.39	2.38	2.56	0.15	0.02	0.06
Philantomba monticola	185	1.28	1.66	1.60	2.66	0.26	0.07	0.16
Procapra gutturosa	5	1.73	1.95	1.92	2.18	0.15	0.02	0.08
Procapra picticaudata	18	1.75	2.08	2.06	2.54	0.19	0.04	0.09
Redunca arundinum	77	1.67	3.09	3.17	3.94	0.52	0.27	0.17
Redunca fulvorufula	17	1.89	2.19	2.19	2.49	0.18	0.03	0.08
Redunca redunca	96	1.64	2.49	2.35	3.68	0.45	0.20	0.18
Redunca sp.	10	1.76	1.96	1.90	2.15	0.13	0.02	0.07
Rupicapra pyrenaica	2	2.01	2.03	2.03	2.05	0.02	0.00	0.01
Rupicapra rupicapra	74	1.73	2.21	2.09	4.83	0.46	0.21	0.21
Sigmocerus lichtensteini	8	4.28	4.63	4.47	5.22	0.33	0.11	0.07
Sigmocerus sp.	2	4.21	4.49	4.49	4.76	0.28	0.08	0.06
Sylvicapra grimmia	85	1.38	2.56	2.54	4.47	0.55	0.30	0.21
Syncerus caffer	245	0.95	2.87	2.90	4.05	0.52	0.27	0.18
Taurotragus derbianus	2	2.17	2.30	2.30	2.43	0.13	0.02	0.06
Taurotragus oryx	9	2.15	2.39	2.26	2.70	0.21	0.04	0.09
Taurotragus strepsiceros	6	2.06	2.18	2.20	2.22	0.06	0.00	0.03

Tragelaphus buxtoni	6	1.74	2.20	2.01	2.92	0.47	0.22	0.21
Tragelaphus olivaeus	2	2.10	2.13	2.13	2.16	0.03	0.00	0.01
Tragelaphus derbianus	6	1.81	2.02	2.02	2.20	0.13	0.02	0.06
Tragelaphus eurycerus	12	1.32	2.02	1.99	2.69	0.38	0.15	0.19
Tragelaphus imerbis	2	2.25	2.29	2.29	2.32	0.04	0.00	0.02
Tragelaphus oryx	2	1.58	1.71	1.71	1.83	0.13	0.02	0.07
Tragelaphus scriptus	176	1.01	2.28	2.23	3.79	0.38	0.15	0.17
Tragelaphus sp.	6	1.97	2.06	2.06	2.21	0.08	0.01	0.04
Tragelaphus spekii	30	1.58	2.17	2.04	2.88	0.34	0.11	0.16
Tragelaphus strepsiceros	10	1.73	2.11	2.14	2.57	0.24	0.06	0.11
Cervidae								
Alces alces	129	0.88	1.23	1.22	1.52	0.14	0.02	0.11
Blastocerus dichotomus	3	1.16	1.21	1.21	1.27	0.05	0.00	0.04
Capreolus capreolus	512	1.01	1.42	1.40	2.81	0.16	0.03	0.11
Capreolus pygargus	2	1.36	1.41	1.41	1.46	0.05	0.00	0.04
Cervus dama	4	1.22	1.47	1.47	1.73	0.25	0.06	0.17
Cervus elaphus	279	1.16	1.77	1.76	2.47	0.28	0.08	0.16
Cervus mariannus	2	1.66	1.68	1.68	1.70	0.02	0.00	0.01
Cervus nippon	15	1.35	1.59	1.60	1.87	0.14	0.02	0.09
Cervus unicolor	6	1.25	1.48	1.51	1.65	0.15	0.02	0.10
Dama dama	34	1.15	1.51	1.50	1.99	0.19	0.04	0.12
Elaphodos sp.	2	1.35	1.39	1.39	1.43	0.04	0.00	0.03
Hippcamelus antisensis	2	1.57	1.62	1.62	1.67	0.05	0.00	0.03
Hippocamelus bisulcus	2	1.50	1.53	1.53	1.55	0.03	0.00	0.02
Hydropotes inermis	34	1.08	1.45	1.43	1.82	0.14	0.02	0.10
Mazama americana	4	1.26	1.36	1.36	1.45	0.07	0.01	0.05
Mazama gouazoubira	12	0.93	1.23	1.22	1.64	0.17	0.03	0.14
Mazama nemorivaga	2	1.36	1.38	1.38	1.40	0.02	0.00	0.01
Mazama rufina	2	1.49	1.49	1.49	1.49	0.00	0.00	0.00
Mazama sp.	19	1.10	1.28	1.24	1.59	0.15	0.02	0.12
Muntiacus muntjak	17	1.13	1.35	1.37	1.63	0.12	0.02	0.09
Muntiacus reevesi	2	1.64	1.66	1.66	1.68	0.02	0.00	0.01
Odocoileus virginianus	15	1.18	1.34	1.31	1.54	0.10	0.01	0.07
Odocoileus hemionus	7	1.12	1.80	2.00	2.27	0.44	0.19	0.25
Ozotoceros bezoarticus	2	1.40	1.43	1.43	1.45	0.03	0.00	0.02
Pudu pudu	2	1.38	1.41	1.41	1.43	0.03	0.00	0.02

Rangifer tarandus	36	1.23	1.47	1.44	1.92	0.14	0.02	0.10
Rusa mariana	10	1.28	1.59	1.66	1.80	0.17	0.03	0.11
Rusa timorensis	2	1.87	1.88	1.88	1.89	0.01	0.00	0.01
Rusa unicolor	10	1.45	1.59	1.56	1.81	0.10	0.01	0.07
Equidae								
Equus grevyi	4	2.97	3.12	3.15	3.22	0.09	0.01	0.03
Equus heminonus	10	3.67	4.00	3.98	4.35	0.22	0.05	0.06
Equus quagga	41	3.07	4.22	4.45	5.16	0.60	0.36	0.14
Equus zebra	2	3.09	3.32	3.32	3.55	0.23	0.05	0.07
Moschidae								
Moschus moschiferus	16	1.56	1.77	1.77	1.97	0.12	0.01	0.07
Suidae								
Babyrousa babyrussa	4	0.77	0.81	0.81	0.84	0.03	0.00	0.04
Hylochoereus meinertzhageni	34	0.78	1.03	1.02	1.34	0.14	0.02	0.13
Phacochoerus aethiopicus	18	0.76	1.06	1.03	1.39	0.17	0.03	0.16
Potamochoerus larvatus	4	0.86	0.95	0.92	1.08	0.09	0.01	0.09
Potamochoerus porcus	24	0.67	0.81	0.80	0.96	0.08	0.01	0.09
Sus barbatus	6	0.86	0.92	0.92	0.96	0.03	0.00	0.03
Sus scrofa	148	0.62	0.89	0.90	1.22	0.11	0.01	0.12
Sus verrucosus	2	0.77	0.80	0.80	0.83	0.03	0.00	0.04
Tapirus pinchaque	2	0.76	0.78	0.78	0.80	0.02	0.00	0.03
Tayassuidae								
Catagonus wagneri	2	0.80	0.82	0.82	0.84	0.02	0.00	0.02
Pecari tajacu	6	0.80	0.87	0.88	0.92	0.05	0.00	0.06
Tayassu pecari	16	0.63	0.78	0.80	0.90	0.07	0.01	0.09
Tayassu tajacu	14	0.74	0.89	0.90	1.01	0.08	0.01	0.09
Tragulidae								
Hyemoschus aquaticus	10	1.02	1.25	1.31	1.46	0.15	0.02	0.12
Tragulus javanicus	4	1.40	1.55	1.56	1.69	0.11	0.01	0.07
Tragulus sp.	36	1.07	1.30	1.32	1.53	0.13	0.02	0.10

It is clear that the sample size varies greatly between different taxa and this is considered in subsequent analysis. Normality and dispersal of the data is discussed below in sections 4.2.1.2 and 4.2.1.3.

4.1.1.1 Variation in hypsodonty index

Firstly, hypsodonty index data from this study are presented below, organised and summarised by family.

Table 4.2: Descriptive summary statistics for hypsodonty index measurements arranged by biological family (*n* = sample size, SD = standard deviation, CV = coefficient of variation).

Family name	*n*	Minimum	Mean	Maximum	SD	CV
Bovidae	2191	0.95	2.43	5.28	0.63	0.26
Cervidae	1158	0.88	1.49	2.47	0.26	0.18
Equidae	57	2.97	4.07	5.16	0.61	0.15
Moschidae	16	1.56	1.77	1.97	0.12	0.07
Suidae	238	0.62	0.92	1.40	0.13	0.15
Tayassuidae	38	0.63	0.83	1.01	0.08	0.10
Tragulidae	50	1.02	1.31	1.69	0.15	0.12

From Tables 4.1 and 4.2 above, it is clear that the family with the largest hypsodonty index values is Equidae (mean hypsodonty index of 4.07) whereas the family with the smallest hypsodonty index values is Tayassuidae (mean hypsodonty index of 0.83). However, it can be seen that when looking at the individual raw values that the highest hypsodonty index is 5.280 which is found in the family Bovidae, belonging to *Alcelaphus buselaphus*. This extreme value is over twice the mean value recorded for this family. The minimum recorded hypsodonty index value is 0.62 from the family Suidae and belongs to *Sus scrofa*.

When grouping the data at family level (as seen in Table 4.2), the data appear to be normally distributed and not highly dispersed as can be seen from the standard deviation and the coefficient of variation. None of the families' data has a coefficient of variation higher than 33% of the mean value, indicating low dispersal. When looking at species level, the highest variation is present in bovid taxa, with *Alcelaphus buselaphus* being the most variable, followed by *Capra ibex* and *Ammotragus lervia*, however, the last two have a very low sample size of four and six, respectively which may contribute to the apparent variability. The taxa with the lowest variation also have very low sample sizes of only a handful of individuals. When considering only those taxa with sample sizes of

at least twenty measurements the lowest variability is recorded in *Potamochoerus porcus*, *Equus quagga* and *Cephalophus castaneus*.

4.1.1.2 Histograms and Q-Q plots

To explore intraspecific variability further, the hypsodonty index data collected for each taxon was investigated for its normality, firstly by visual analysis of histograms and Q-Q plots. The full set of histograms and Q-Q plots are presented in the appendix. From the visual analysis, it is clear that the hypsodonty index measurements are most likely normally distributed for all but ten taxa (*Alcelaphus buselaphus*, *Cephalophus callipygus*, *Cephalophus castaneus*, *Cephalophus niger*, *Cephalophus rufiatus*, *Hippotragus niger*, *Hyemoschus aquaticus*, *Kobus leche*, *Nanger soemmeringii*, and *Procapra picticaudata*). Out of those not normally distributed, all but *A. buselaphus* have very small sample sizes (i.e. fewer than 30 measurements) and it is this low sample size that can artificially produce a false distribution. The histograms and Q-Q plot for *A. buselaphus* is presented below in Figure 4.1.

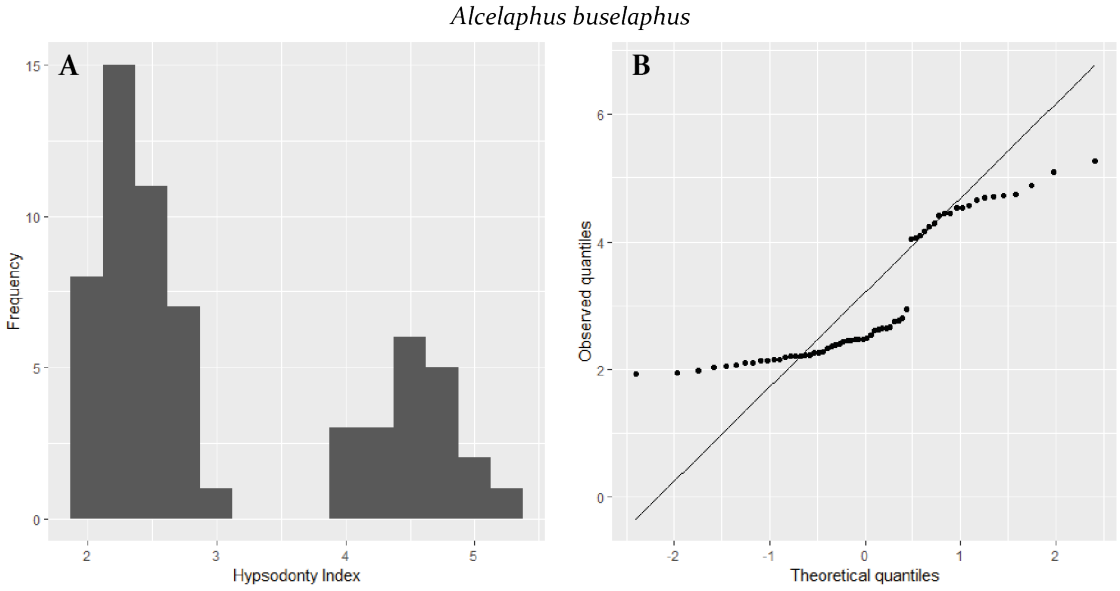

Figure 4.1: A) Histogram showing the frequency distribution of the hypsodonty index measurements of *Alcelaphus buselaphus.* B) Q-Q plot of hypsodonty index measurements of *Alcelaphus buselaphus*. It may be assumed that this shows a bimodal distribution but it is likely that the low sample size is affecting the appearance of the distribution of the data and that there is a portion of data missing and not captured in sampling. It is likely that with an increased sample size that this dataset would be closer to a normal distribution.

From visual analysis of the histograms, Q-Q plots and revisits to the raw data, a limited number of outliers was removed from the dataset. In most cases any extreme values that were clearly not due to errors in measurement or data recording were kept in the dataset as they are likely to represent real biological variation in hypsodonty index within an individual taxon.

4.1.1.3 Shapiro-Wilk tests for normality

Following the visual analysis from histograms and Q-Q plots, the hypsodonty index measurements for each taxon were statistically tested for normality using the Shapiro-Wilk test. These tests were undertaken in IBM SPSS Statistics v.21 and the results of these tests are shown in Table 4.2. The hypsodonty index measurements for the taxa highlighted in red were indicated by the Shapiro-Wilk test to be non-normal in their distribution. 22 taxa were identified as having hypsodonty index measurements that were not normally distributed, a larger number than identified from the visual analysis. Of these 22 taxa, nine had sample sizes smaller than twenty measurements, leaving thirteen taxa showing non-normal distributions in their hypsodonty index: *Alcelaphus buselaphus*, *Cephalophus* sp., *Hippotragus equinus*, *Kobus ellipsiprymnus*, *Kobus kob*, *Ourebia ourebi*, *Philantomba monticola*, *Redunca redunca*, *Rupicapra rupicapra*, *Sylvicapra grimmia*¸ *Syncerus caffer*, *Tragelaphus scriptus*, and *Rangifer tarandus*.

Table 4.3: Results of the Shapiro-Wilk tests for each taxon. The taxa highlighted in red are those with a p-value of less than 0.05 and are therefore not normally distributed. The blank rows for the Shapiro-Wilk test are those with sample sizes too small and a distribution too dispersed for SPSS to calculate the results of the test.

		Shapiro-Wilk test		
Taxon name	**n**	**W Statistic**	**df**	**p-value**
Bovidae				
Addax nasomaculatus	3	0.808	3	0.135
Aepyceros melampus	36	0.958	36	0.184
Alcelaphus buselaphus	62	0.833	66	0.000
Alcelaphus cokei	2			
Alcelaphus sp.	2			
Ammotragus lervia	4	0.836	4	0.185
Bison americanus	2			
Bison bonasus	2			
Bubalus mindorensis	2			
Bubalus sp.	6	0.997	3	0.900
Capra aegagrus	5	0.899	5	0.406
Capra falconeri	2			
Capra ibex	6	0.771	6	0.032
Capra nubiana	4	0.861	4	0.265
Capra pyrenaica	5	0.917	5	0.511
Cephalophus callipygus	30			
Cephalophus castaneus	21			
Cephalophus dorsalis	29			

Cephalophus harveyi	6			
Cephalophus leucogaster	8			
Cephalophus monticola	30			
Cephalophus natalensis	2			
Cephalophus niger	12			
Cephalophus nigrifrons	6			
Cephalophus ogilby	2			
Cephalophus rufilatus	8			
Cephalophus silvicultor	2			
Cephalophus sp.	71	0.956	247	0.000
Cephalophus sylvicultor	18			
Cephalophus weynsi	2			
Connochaetes taurinus	18	0.854	18	0.010
Damaliscus hunteri	6			
Damaliscus korrigum	11	0.980	25	0.876
Damaliscus lunatus	8			
Eudorcas thomsonii	1			
Gazella bennettii	4			
Gazella cuvieri	2			
Gazella dorcas	36	0.992	110	0.789
Gazella gazella	24			
Gazella granti	4			
Gazella izabella	2			
Gazella leptoceros	4			
Gazella marica	4			
Gazella rufifrons	4			
Gazella saudiya	2			
Gazella sp.	2			
Gazella spekei	2			
Gazella subgutturosa	3			
Gazella thomsoni	15			
Gazella tilonura	2			
Hippotragus equinus	58	0.851	76	0.000
Hippotragus niger	18			
Kobus anselli	8	0.845	8	0.084
Kobus defassa	26	0.957	26	0.338
Kobus ellipsiprymnus	76	0.914	76	0.000

Kobus kob	180	0.950	180	0.000
Kobus leche	10	0.900	10	0.218
Kobus megaceros	4	0.940	4	0.657
Kobus sp.	10	0.929	10	0.442
Kobus vardonii	25	0.963	25	0.484
Litocranius walleri	8	0.783	8	0.019
Madoqua guentheri	12	0.955	24	0.351
Madoqua saltiana	12			
Nanger dama	2			
Nanger soemmerringii	16	0.916	16	0.147
Nemorhaedus goral	3	0.985	3	0.767
Neotragus batesi	54	0.972	54	0.234
Oreotragus oreotragus	2			
Oryx besia	6	0.751	6	0.020
Oryx gazella	2			
Ourebia ourebi	31	0.927	31	0.037
Philantomba maxwelli	4			
Philantomba monticola	181	0.829	185	0.000
Procapra gutturosa	5			
Procapra picticaudata	17	0.969	22	0.681
Redunca arundinum	77			
Redunca fulvorufula	17			
Redunca redunca	93	0.951	197	0.000
Redunca sp.	10			
Rupicapra pyrenaica	2			
Rupicapra rupicapra	74	0.585	76	0.000
Sigmocerus lichtensteini	8			
Sigmocerus sp.	2	0.903	10	0.239
Sylvicapra grimmia	85	0.926	85	0.000
Syncerus caffer	245	0.982	245	0.003
Taurotragus derbianus	2			
Taurotragus oryx	9	0.815	17	0.003
Taurotragus strepsiceros	6			
Tragelaphus buxtoni	6			
Tragelaphus olivaeus	2			
Tragelaphus derbianus	6			
Tragelaphus eurycerus	12			

Tragelaphus imerbis	2			
Tragelaphus oryx	2			
Tragelaphus scriptus	176	0.952	247	0.000
Tragelaphus sp.	6			
Tragelaphus spekii	25			
Tragelaphus strepsiceros	10			
Cervidae				
Alces alces	129	0.989	129	0.407
Blastocerus dichotomus	3	0.997	3	0.900
Capreolus capreolus	507	0.997	3	0.900
Capreolus pygargus	2	0.991	509	0.003
Cervus dama	4			
Cervus elaphus	279	0.764	4	0.052
Cervus mariannus	2	0.984	279	0.003
Cervus nippon	14			
Cervus unicolor	6	0.978	14	0.964
Dama dama	32	0.897	6	0.354
Elaphodos sp.	2	0.971	32	0.532
Hippcamelus antisensis	2			
Hippocamelus bisulcus	2			
Hydropotes inermis	33	0.938	33	0.058
Mazama americana	4	0.966	4	0.818
Mazama gouazoubira	11	0.897	11	0.169
Mazama nemorivaga	2			
Mazama rufina	2			
Mazama sp.	19	0.828	19	0.003
Muntiacus muntjak	17	0.950	19	0.388
Muntiacus reevesi	2			
Odocoileus virginianus	15	0.807	22	0.001
Odocoileus hemionus	7			
Ozotoceros bezoarticus	2			
Pudu pudu	2			
Rangifer tarandus	36	0.937	36	0.042
Rusa mariana	10	0.899	10	0.216
Rusa timorensis	2			
Rusa unicolor	10	0.900	10	0.221

Equidae				
Equus burchelli	19	0.970	19	0.773
Equus grevyi	4	0.890	4	0.382
Equus heminonus	10	0.932	10	0.468
Equus quagga	22	0.919	22	0.074
Equus zebra	2			
Moschidae				
Moschus moschiferus	16	0.965	16	0.762
Suidae				
Babyrousa babyrussa	4			
Hylochoereus meinertzhageni	31	0.970	31	0.519
Phacochoerus aethiopicus	18	0.929	18	0.187
Potamochoerus larvatus	4			
Potamochoerus porcus	23	0.953	27	0.252
Sus barbatus	6	0.981	6	0.957
Sus scrofa	148	0.982	148	0.056
Sus verrucosus	2			
Tapirus pinchaque	2			
Tayassuidae				
Catagonus wagneri	2			
Pecari tajacu	6	0.874	6	0.243
Tayassu pecari	16			
Tayassu tajacu	14	0.815	17	0.003
Tragulidae				
Hyemoschus aquaticus	8	0.926	8	0.482
Tragulus javanicus	4	0.951	4	0.725
Tragulus sp.	36	0.966	36	0.326

For the thirteen taxa listed above as having a non-normal distribution (and with large enough sample sizes) maps were created to investigate whether the distribution of their data had a spatial component, and these will be discussed in Chapter 5.

4.2 Hypsodonty as a climatic predictor

Following the cleaning of the dataset (removal of datapoints where no clear locality could be plotted), the data were used in a number of ways as a whole dataset and modified datasets (see Chapter 3 for details in order to investigate the link between hypsodonty index and climatic variables and the potential (or not) for hypsodonty index to be used as a predictor of certain components of the climate. The full raw datasets used here are presented in Appendix 1.

4.2.1 Summary of modern ungulate hypsodonty index measurements

Before analysis was undertaken, the data were explored in a similar way to that outlined in section 4.1. This section presents descriptive statistics of the different datasets followed by histograms and Q-Q plots to visually assess the distribution of the data. The Shapiro-Wilk test was also performed on each dataset to test statistically for normality and these results are also presented for each dataset.

4.2.1.1 Each hypsodonty index value as a single data point (individual teeth)

Table 4.4 shows the descriptive summary statistics for the dataset of hypsodonty index calculated for each individual tooth and considered as one dataset of 3,788 measurements.

Table 4.4: Descriptive summary statistics for the dataset of hypsodonty index values of all of the individual teeth measured (*n* = number of measurements, SD = standard deviation, CV = coefficient of variation).

Statistic	Value
n	3,788
Minimum	0.62
1st Quartile	1.44
Median	1.94
Mean	2.04
3rd Quartile	2.49
Maximum	5.28
Range	4.66
SD	0.78
Variance	0.61
CV	0.38

This is the largest dataset considered in this analysis with 3,788 hypsodonty index values, for 148 different taxa from 950 unique localities. The histogram and Q-Q plot for this dataset are presented below in Figure 4.2.

Figure 4.2: A) Histogram of hypsodonty index values of all individual teeth. B) Q-Q plot of hypsodonty index values of all individual teeth.

From the histogram, it is clear that the dataset is skewed towards the lower end. This is also evident in the summary statistics as the mean of 2.04 is much closer to the minimum value of 0.62 than the maximum value of 5.28. The Q-Q plot also suggests that the dataset is not normally distributed, and this is also suggested from the Shapiro-Wilk test (see Table 4.5 below) as the *p*-value is $<2.2 \times 10^{-16}$, much lower than the value of 0.05 which is the cut-off for rejecting the null-hypothesis that the data are from a normal distribution.

Table 4.5: Shapiro-Wilk statistics for the dataset of hypsodonty index values of each individual tooth measured.

W-statistic	***p*-value**
0.95588	$<2.2 \times 10^{-16}$

4.2.1.2 *Each hypsodonty index value as a single data point (individual teeth with migratory taxa removed)*

Table 4.6 shows the descriptive summary statistics for the dataset of each hypsodonty index calculated for each individual tooth with the migratory taxa removed.

Table 4.6 Descriptive summary statistics for the dataset of hypsodonty index values of each individual tooth measured with migrant taxa removed (*n* = number of measurements, SD = standard deviation, CV = coefficient of variation).

Statistic	Value
n	2,254
Minimum	0.62
1st Quartile	1.59
Median	2.13
Mean	2.13
3rd Quartile	2.63
Maximum	5.28
Range	4.66
SD	0.78
Variance	0.60
CV	0.37

The histogram and Q-Q plot for this dataset are presented below in Figure 4.3.

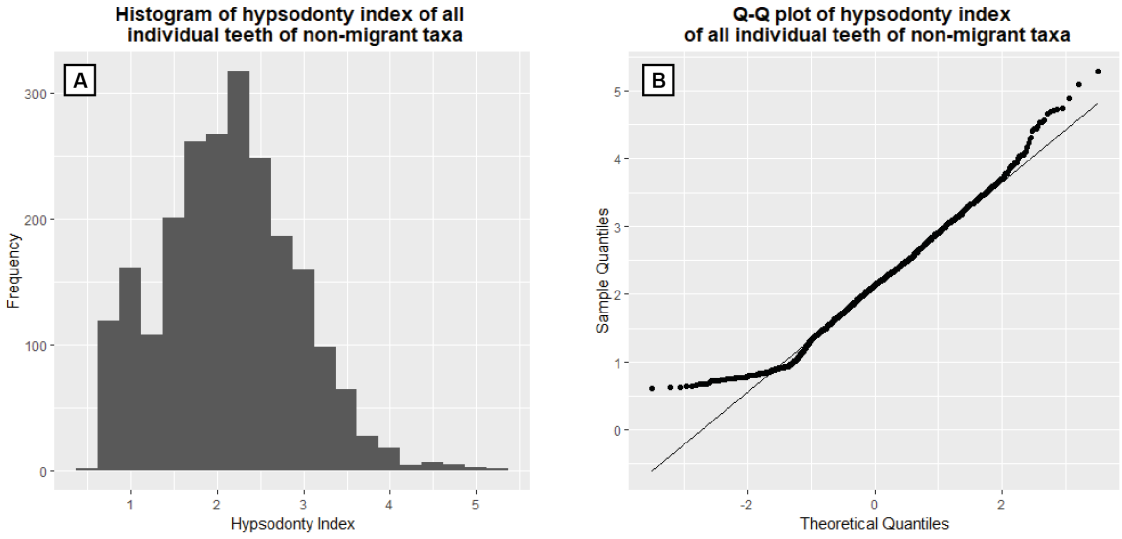

Figure 4.3: A) Histogram of hypsodonty index values of all individual teeth of non-migrant taxa. B) Q-Q plot of hypsodonty index values of all individual teeth of non-migrant taxa.

The histogram shows this dataset is also skewed to the lower end of values but less so than with migratory taxa included. Here, the mean value is higher whilst the minimum and maximum values remain the same. The Q-Q plot also shows this skew and suggests that the data are not normally distributed. The Shapiro-Wilk test (see Table 4.7) calculates a *p*-value of 3.899×10^{-14} and the null-hypothesis that the data are drawn from a normal distribution can be rejected.

Table 4.7: Shapiro-Wilk statistics for the dataset of hypsodonty index values of each individual tooth measured with migrant taxa removed.

W-statistic	***p*-value**
0.98590	3.899×10^{-14}

4.2.1.3 Each hypsodonty index value as a single data point (individual teeth with averaged left and right teeth from the same animal)

Table 4.8 shows the descriptive summary statistics for the dataset of each hypsodonty index calculated for each individual tooth but the hypsodonty index of left and right teeth from the same individual have been averaged.

Table 4.8: Descriptive summary statistics for the dataset of hypsodonty index values of each individual animal measured with left and right averaged (*n* = number of measurements, SD = standard deviation, CV = coefficient of variation).

Statistic	**Value**
n	2,000
Minimum	0.63
1st Quartile	1.44
Median	1.93
Mean	2.03
3rd Quartile	2.46
Maximum	5.15
Range	4.52
SD	0.77
Variance	0.60
CV	0.38

The histogram and Q-Q plot for this dataset are presented below in Figure 4.4.

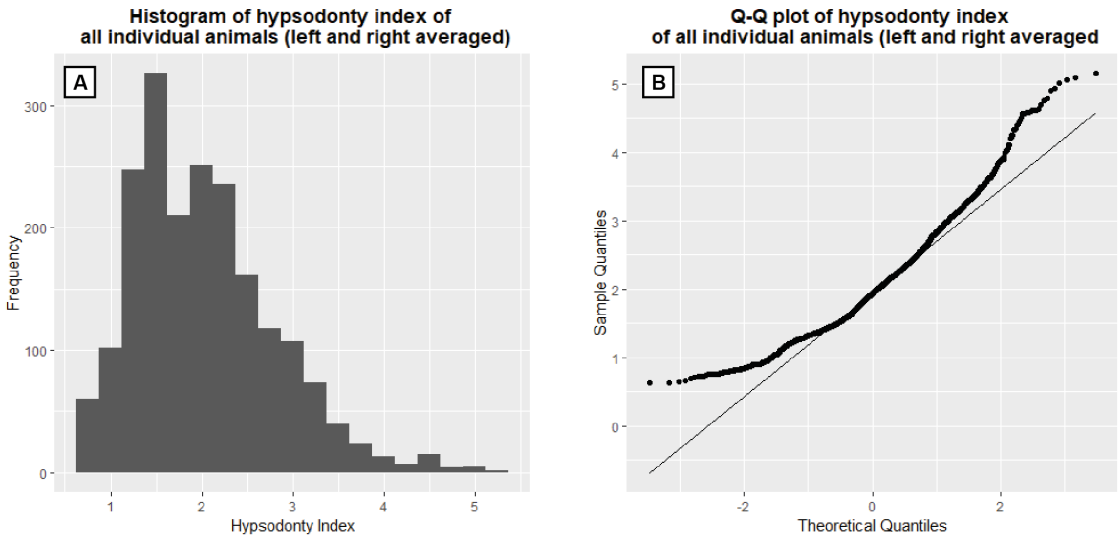

Figure 4.4: A) Histogram of hypsodonty index values of all individual teeth with left and right teeth averaged for individual animals. B) Q-Q plot of hypsodonty index values of all individual teeth with left and right teeth averaged for individual animals.

The histogram in Figure 4.4 shows that the dataset is, again, skewed to the lower end of the hypsodonty index values. The Q-Q plot suggests that the dataset is not drawn from a normal distribution and this is also suggested by the Shapiro-Wilk test *p*-value of $<2.2x10^{-16}$ (see Table 4.9) which rejects the null-hypothesis that the data is normally distributed.

Table 4.9: Shapiro-Wilk statistics for the dataset of hypsodonty index values of all individual teeth with left and right teeth averaged for individual animals.

W-statistic	***p*-value**
0.95425	$<2.2x10^{-16}$

4.2.1.4 Each hypsodonty index value as a single data point (individual teeth with averaged left and right teeth from the same animal with migrant taxa removed)

Table 4.10 shows the descriptive summary statistics for the dataset of each hypsodonty index calculated for each individual tooth but the hypsodonty index of left and right teeth from the same individual have been averaged, but with migrant taxa removed.

Table 4.10: Descriptive summary statistics for the dataset of hypsodonty index values of each individual animal measured with left and right averaged with migrant taxa removed (*n* = number of measurements, SD = standard deviation, CV = coefficient of variation).

Statistic	Value
n	1,167
Minimum	0.63
1st Quartile	1.61
Median	2.14
Mean	2.13
3rd Quartile	2.62
Maximum	5.09
Range	4.46
SD	0.77
Variance	0.59
CV	0.36

The histogram and Q-Q plot for this dataset are presented below in Figure 4.5.

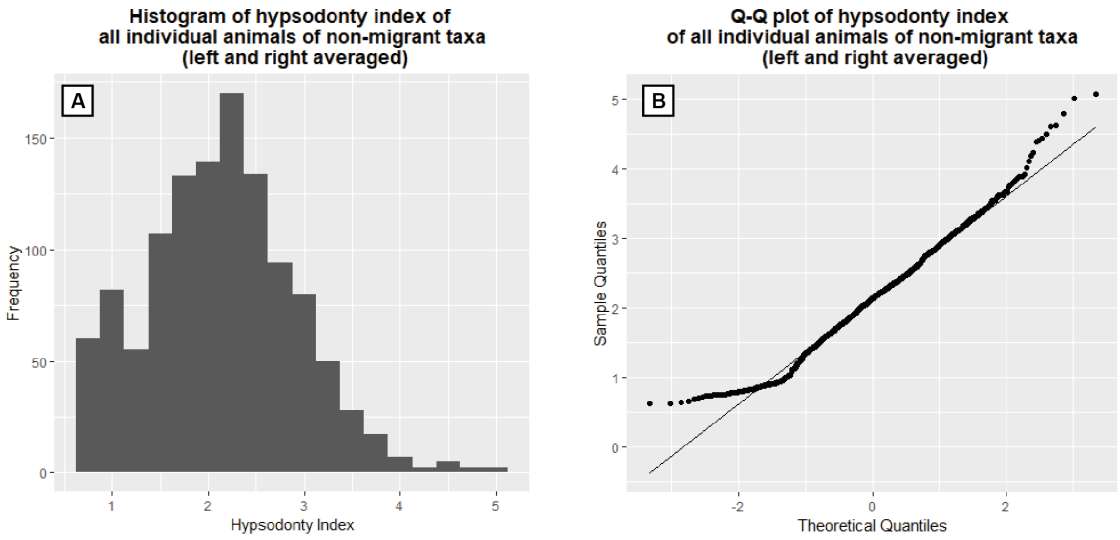

Figure 4.5: A) Histogram of hypsodonty index values of all individual teeth with left and right teeth averaged for individual animals with non-migrant taxa removed. B) Q-Q plot of hypsodonty index values of all individual teeth with left and right teeth averaged for individual animals with migrant taxa removed.

The histogram in Figure 4.5 shows that the dataset is skewed, and the Q-Q plot indicates that the dataset is likely to be not normally distributed. The results of the Shapiro-Wilk test (see Table 4.11) support this with the *p*-value being 2.881×10^{-9} and rejecting the null-hypothesis that the data are drawn from a normal distribution.

Table 4.11: Shapiro-Wilk statistics for the dataset of hypsodonty index values of all individual teeth with left and right teeth averaged for individual animals with migrant taxa removed.

W-statistic	***p*-value**
0.98574	2.881×10^{-9}

4.2.1.5 Data as mean hypsodonty index values per locality

Table 4.12 shows the descriptive summary statistics for the dataset of each hypsodonty index averaged at each locality. There are 950 localities and hence 950 mean hypsodonty index values.

Table 4.12: Descriptive summary statistics for the dataset of mean hypsodonty index values per location (*n* = number of measurements, SD = standard deviation, CV = coefficient of variation).

Statistic	Value
n	950
Minimum	0.63
1st Quartile	1.41
Median	1.92
Mean	1.99
3rd Quartile	2.45
Maximum	4.61
Range	3.98
SD	0.74
Variance	0.54
CV	0.37

The histogram and Q-Q plot for this dataset are presented below in Figure 4.6.

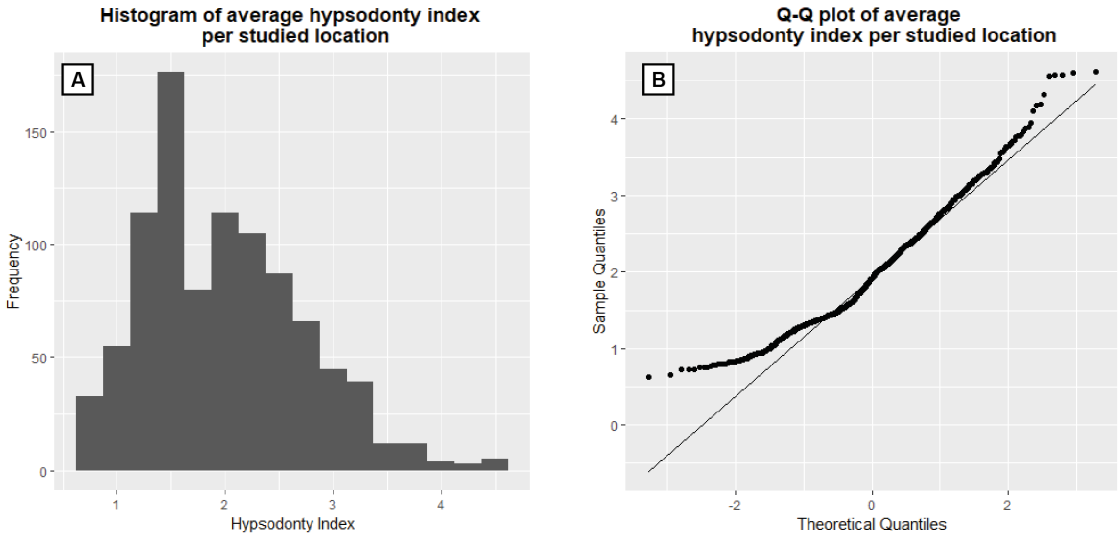

Figure 4.6: A) Histogram of average hypsodonty index values per locality studied. B) Q-Q plot of average hypsodonty index values per locality studied.

The histogram and Q-Q plot in Figure 4.6 show that the dataset is skewed to the lower end of the values and is not normally distributed. The Shapiro-Wilk test gives a *p*-value of 4.023×10^{-14} (see Table 4.13) and suggests that the null-hypothesis that the data is drawn from a normal distribution should be rejected.

Table 4.13: Shapiro-Wilk statistics for the dataset of mean hypsodonty index per locality.

W-statistic	***p*-value**
0.9658	4.023×10^{-14}

4.2.1.6 Data as mean hypsodonty index values per locality with migrant taxa removed

Table 4.14 shows the descriptive summary statistics for the dataset of each hypsodonty index averaged at each locality with migratory taxa removed. These taxa were removed to test whether seasonal migration patterns to areas with potentially differing climate conditions were creating biological noise in the dataset and obscuring any correlations between hypsodonty index and climate.

Table 4.14: Descriptive summary statistics for the dataset of mean hypsodonty index values per location with migratory taxa removed (*n* = number of measurements, SD = standard deviation, CV = coefficient of variation).

Statistic	**Value**
n	577
Minimum	0.63
1st Quartile	1.59
Median	2.15
Mean	2.12
3rd Quartile	2.63
Maximum	4.80
Range	4.17
SD	0.75
Variance	0.57
CV	0.36

The histogram and Q-Q plot for this dataset are presented below in Figure 4.7.

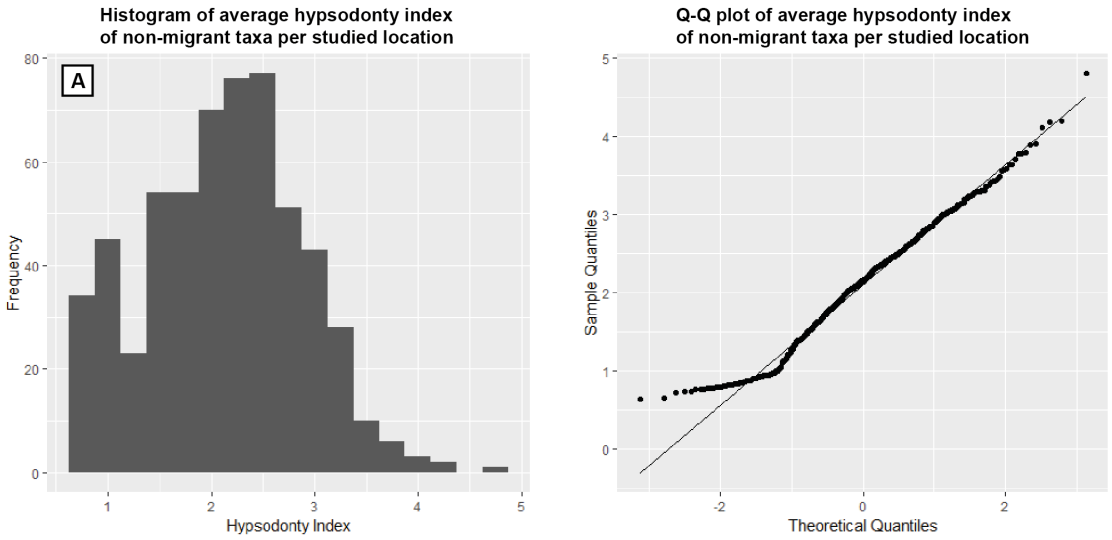

Figure 4.7: A) Histogram of average hypsodonty index values per locality studied with migrant taxa removed. B) Q-Q plot of average hypsodonty index values per locality studied with migrant taxa removed.

Again, the histogram in Figure 4.7 shows a dataset skewed towards lower hypsodonty values and this can also be seen in the Q-Q plot although there does appear to be a distribution closer to what would be expected from a normal distribution. However, the Shapiro-Wilk test (*p*-value of 8.238×10^{-6}; see Table 4.15) indicates that the null-hypothesis that this dataset is normally distributed should be rejected.

Table 4.15: Shapiro-Wilk statistics for the dataset of mean hypsodonty index per locality with migrant taxa removed.

W-statistic	***p*-value**
0.9845	8.238×10^{-6}

4.2.1.7 Data classified into hypsodonty scores

The data were also classified into different hypsodonty index scores as done in previous studies (e.g. Eronen *et al*., 2010a). This resulted in almost all values being classified as '2' or 'mesodont', thereby eliminating the biological variation in the datasets (see the appendix for the full classification data). This approach was not considered further in investigating relationships between hypsodonty index and climate.

4.2.2 Correlations with climatic variables – with untransformed datasets

Each of the datasets described above in Section 4.2.1 was imported into QGIS v3.4.1 along with the bioclimatic data at 5km^2 spatial resolution. Each dataset has a different number of spatial locations depending on how the data has been filtered and modified as per Section 4.2.1. For each spatial location in a dataset, the raw values were extracted for each climate layer and tables of climate data at each location were created.

Relationships between hypsodonty index at these locations and the different climate variables are explored in this section. For full details of the climate data see Chapter 3.

For each of the six datasets it was necessary to check the relationship between the dependent variable (hypsodonty index) and each independent variable (the nineteen climate parameters). Following this, it was necessary to check relationships among independent variables to check for autocorrelation.

4.2.2.1 Each hypsodonty index measurement as a single data point

Pearson correlation coefficients were calculated between hypsodonty index (the dependent variable) and all nineteen climate variables (the independent variables) and these are presented in the first row of the correlation matrix shown in Figure 4.8. The p-values indicate that all calculated Pearson correlation coefficients were statistically significant ($p<=0.05$).

The strongest correlations (see Figure 4.9) were between hypsodonty index (HI) and mean diurnal temperature range (bio2; R=0.45), temperature seasonality (bio4; R=-0.44), isothermality (bio3; R=0.43) and mean temperature of the coldest quarter (bio11; R=0.42).

The weakest correlations (see Figure 4.10) were between hypsodonty index (HI) and mean annual precipitation (bio12; R=0.01), precipitation of the coldest quarter (bio19; R=0.02), precipitation of the warmest quarter (bio18; R=-0.07) and precipitation of the wettest quarter (bio16; R=0.08).

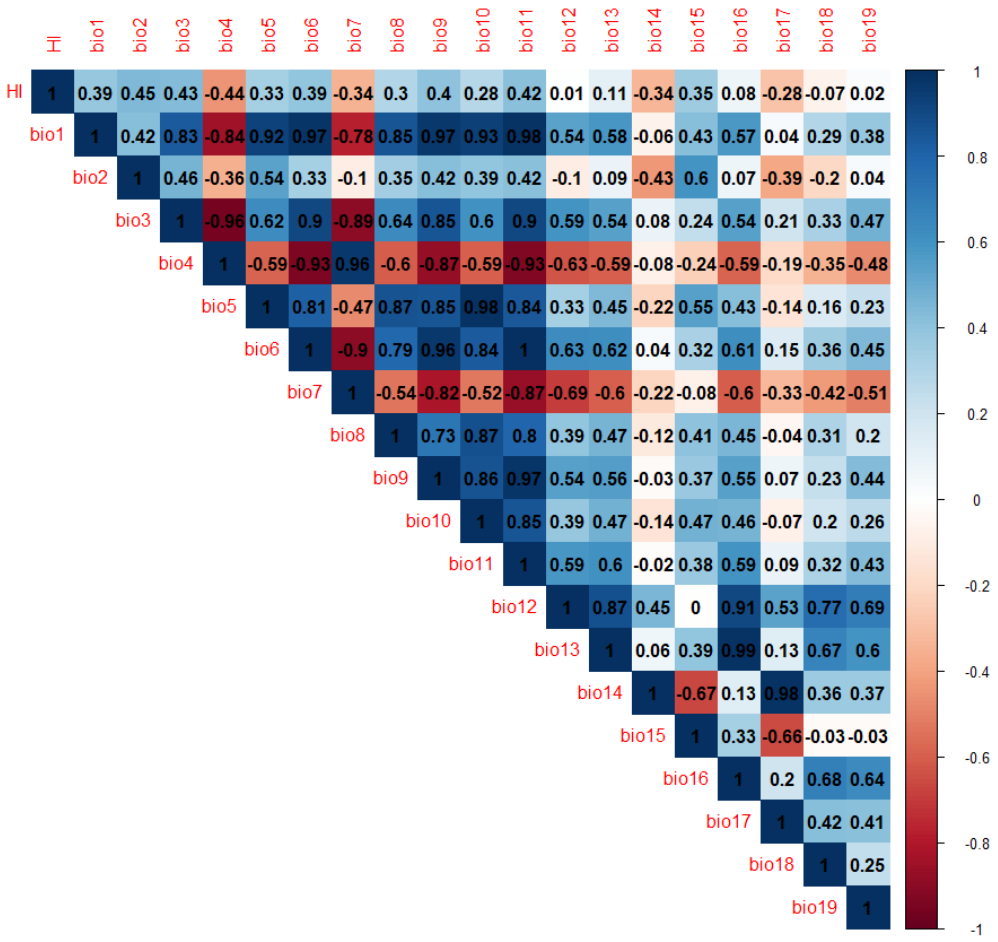

Figure 4.8: Correlation matrix showing Pearson correlation coefficients between hypsodonty index (HI) as individual data points against the nineteen climate variables (see section 3.1.2.3 for more information on notation). The colour ramp indicates the strength of the correlation as shown in the figure legend on the right-hand side.

Correlation coefficients between the independent variables are shown in the remainder of the matrix in Figure 4.8. The strongest correlations were between minimum temperature of the warmest month (bio6) and mean temperature of the coldest quarter (bio11; *R*=1), precipitation of the wettest month (bio13) and precipitation of the wettest quarter (bio16; *R*=0.99), maximum temperature of the warmest month (bio5) and mean temperature of the coldest quarter (bio10; *R*=0.98) and mean annual temperature (bio1) and mean temperature of the coldest quarter (bio 11; *R*=0.98). As seen in Figure 4.8, there are a number of autocorrelated climate variables with *R* values higher than 0.5 (both positive and negative correlation coefficients).

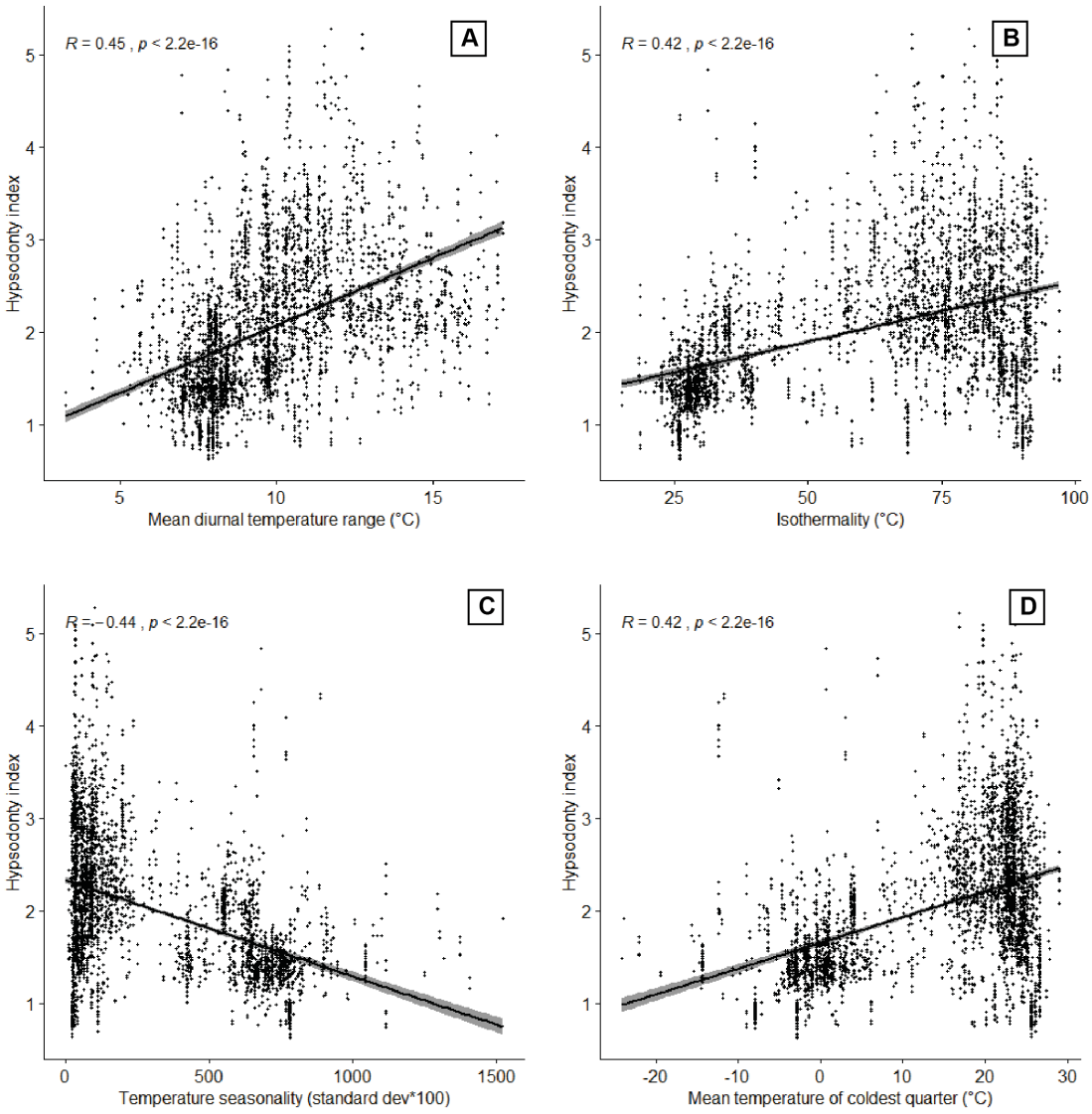

Figure 4.9: Scatter plots of the climate variables that are most strongly correlated with this hypsodonty index dataset (full dataset of individual teeth) A) mean diurnal temperature range (bio2), B) isothermality (bio4), C) temperature seasonality (bio3) and D) mean temperature of the coldest quarter (bio11). The black line represents a line of best fit and the grey band represents a 95% confidence interval around this line. Pearson's R and the associated p-value is also shown on each scatter plot.

For the purpose of linear regression for this dataset it was necessary to look at the climate variables that are most highly correlated with hypsodonty index and to discount those climate variables that are autocorrelated. Therefore, the climate variable that could be considered for regression against hypsodonty index for this dataset is mean diurnal temperature range (bio2; R=0.45) as this has the highest correlation coefficient; other climate variables that are either weakly or strongly correlated with hypsodonty index were found to autocorrelate with mean diurnal temperature range.

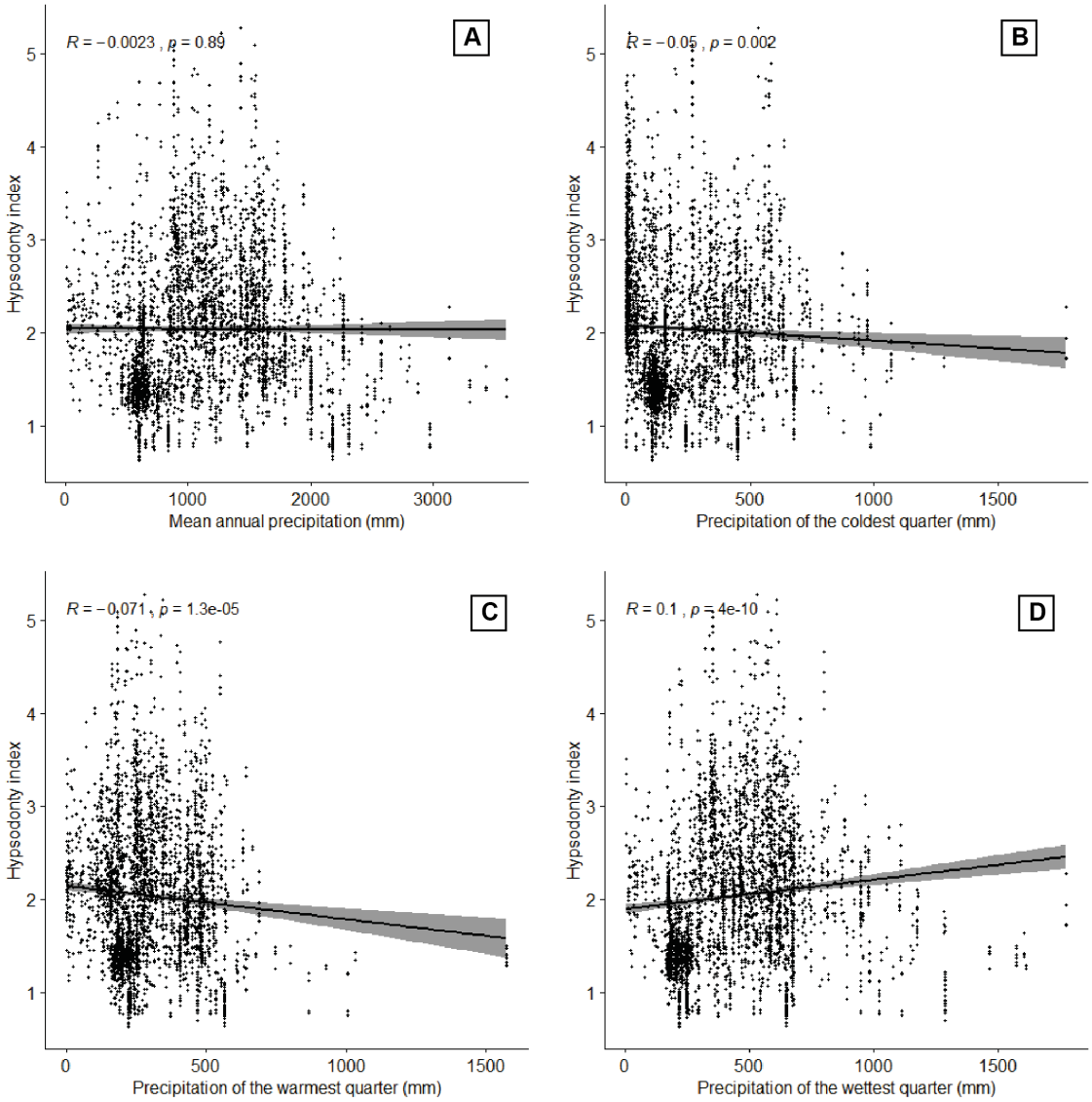

Figure 4.10: Scatter plots of the climate variables that are most weakly correlated with this hypsodonty index dataset (full dataset of individual teeth) A) mean annual precipitation (bio12), B) precipitation of the coldest quarter (bio19), C) precipitation of the warmest quarter (bio18) and D) precipitation of the wettest quarter (bio16). The black line represents a line of best fit and the grey band represents a 95% confidence interval around this line. Pearson's R and the associated p-value is also shown on each scatter plot.

4.2.2.2 *Each hypsodonty index value as a single data point (individual teeth with migratory taxa removed)*

For the second dataset with migratory taxa removed, Pearson correlation coefficients were calculated between hypsodonty index (the dependent variable) and all nineteen climate variables (the independent variables) and these are presented in the first row of the correlation matrix shown in Figure 4.11. The p-values indicate that all calculated Pearson correlation coefficients were statistically significant (p<=0.05). The correlation coefficients this time are all showing a weaker relationship between hypsodonty index and climate variables when the migrant taxa are removed from the dataset.

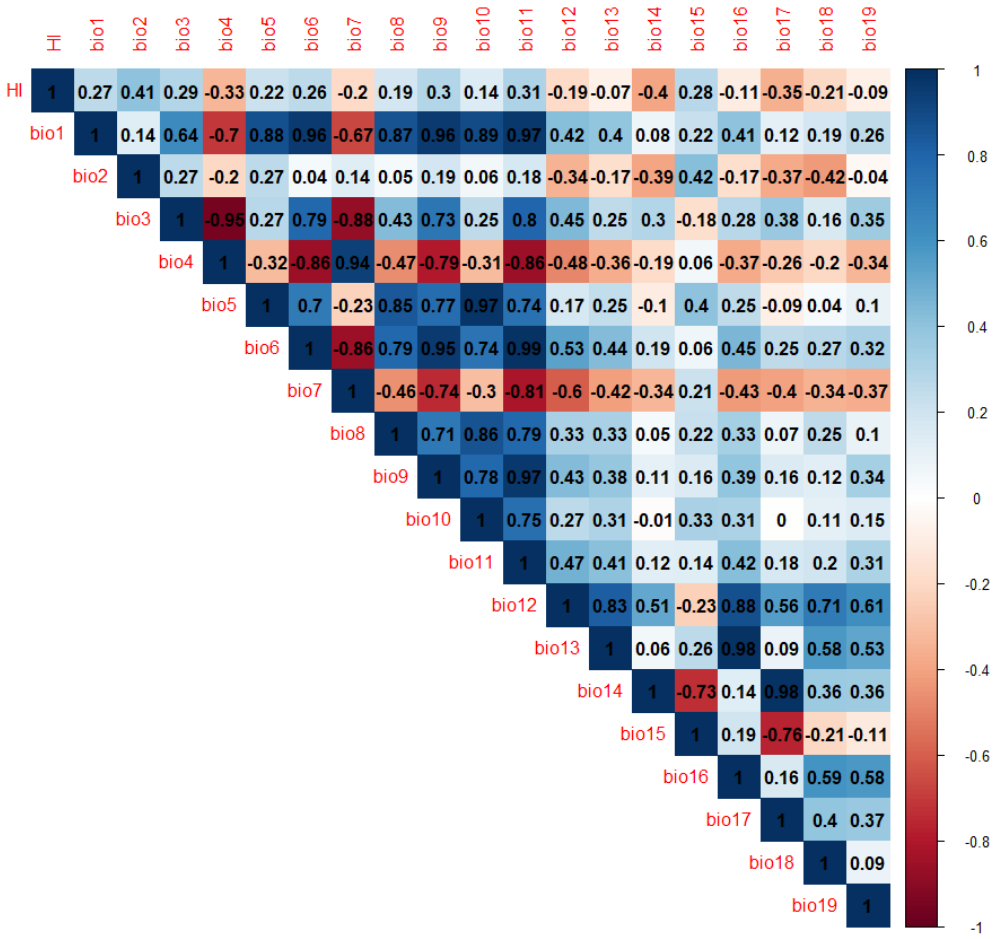

Figure 4.11: Correlation matrix showing Pearson correlation coefficients between hypsodonty index (HI) as individual data points with migrant taxa removed against the nineteen climate variables (see section 3.1.2.3 for more information on notation). The colour ramp indicates the strength of the correlation as shown in the figure legend on the right-hand side.

The strongest correlations (see Figure 4.12) were between hypsodonty index (HI) and mean diurnal temperature range (bio2; *R*=0.41), precipitation of the driest month (bio14; *R*=-0.4) precipitation of the driest quarter (bio17; *R*=-0.35) and temperature seasonality (bio4; *R*=-0.33). With the migrants removed, there appears to be both correlations with temperature and precipitation variables compared to the full dataset where the strongest correlations were with solely temperature climatic variable.

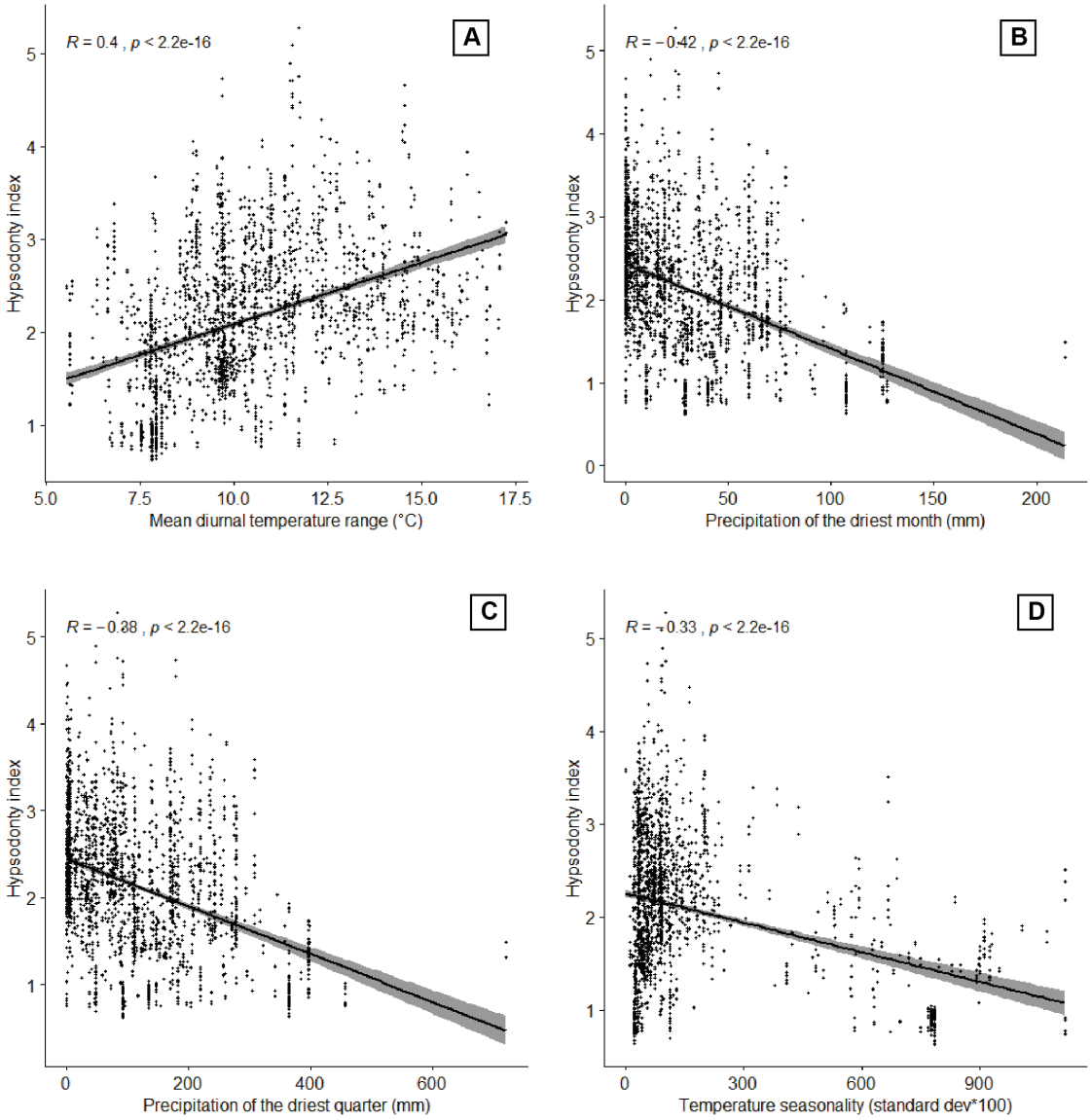

Figure 4.12: Scatter plots of the climate variables that are most strongly correlated with this hypsodonty index dataset (full dataset of individual teeth with migrant taxa removed) A) mean diurnal temperature range (bio2), B) precipitation of the driest month (bio14), C) precipitation of the driest quarter (bio17) and D) temperature seasonality (bio4). The black line represents a line of best fit and the grey band represents a 95% confidence interval around this line. Pearson's R and the associated p-value is also shown on each scatter plot.

The weakest correlations (see Figure 4.13) were between hypsodonty index (HI) and precipitation of the wettest month (bio13; *R*=-0.07) precipitation of the coldest quarter (bio19; R=-0.09), precipitation of the wettest quarter (bio16; *R*=-0.11) and mean temperature of the warmest quarter (bio10; *R*=0.14). The weakest correlations here, are stronger with the migrants removed than the corresponding correlation value are with full dataset. Here, the weakest correlations are also a mixture of temperature and precipitation variables compared to the full dataset where the weakest correlations were all with precipitation variables.

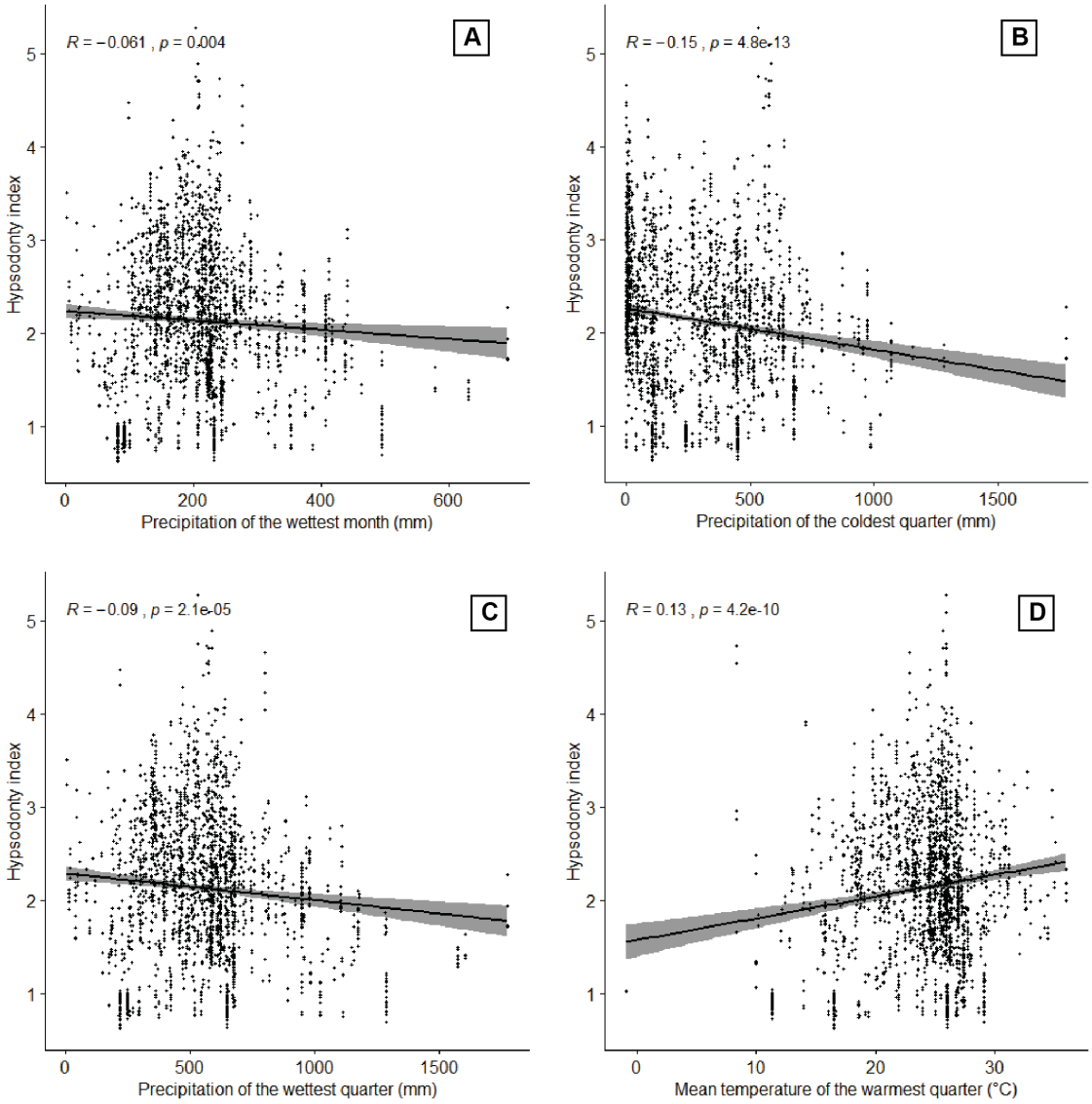

Figure 4.13: Scatter plots of the climate variables that are most weakly correlated with this hypsodonty index dataset (full dataset of individual teeth with migrant taxa removed) A) precipitation of the wettest month (bio13), B) precipitation of the coldest quarter (bio19), C) precipitation of the wettest quarter (bio16) and D) mean temperature of the warmest quarter (bio10). The black line represents a line of best fit and the grey band represents a 95% confidence interval around this line. Pearson's R and the associated p-value is also shown on each scatter plot.

As the strongest correlations with the dataset with migrants removed is weaker than correlations between climatic variables and the full dataset it is not useful to consider this dataset further for regression analysis.

4.2.2.3 *Each hypsodonty index value as a single data point (individual teeth with averaged left and right teeth from the same animal)*

For the third dataset, which contained all taxa with left and right teeth averaged, Pearson correlation coefficients were calculated between hypsodonty index (the dependent variable) and all nineteen climate variables (the independent variables). These are presented in the first row of the correlation matrix shown in Figure 4.14. The p-values indicate that all calculated Pearson correlation coefficients were statistically significant ($p<=0.05$). The correlation coefficients this time show a similar pattern to the full dataset, although it appears that averaging the left and right teeth (when both were measured from the same individual) has very slightly increased the strength of the correlations.

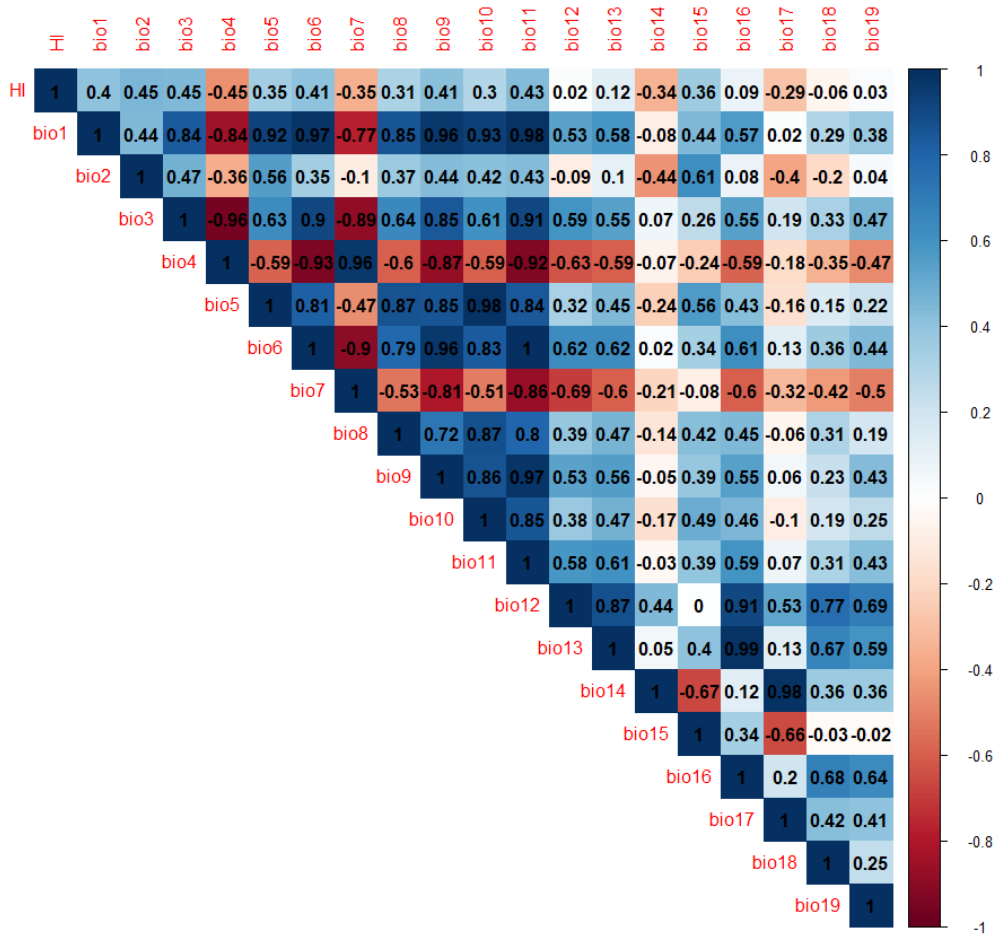

Figure 4.14: Correlation matrix showing Pearson correlation coefficients between hypsodonty index (HI) as individual data points (but with left and right teeth averaged for individual animals) against the nineteen climate variables (see section 3.1.2.3 for more information on notation). The colour ramp indicates the strength of the correlation as shown in the figure legend on the right-hand side.

The strongest correlations (see Figure 4.15) were between hypsodonty index (HI) and mean diurnal temperature range (bio2; R=0.45), isothermality (bio3; R=0.45), mean temperature of the coldest quarter (bio11; R=0.43) and minimum temperature of the warmest month (bio6; R=-0.41). As with the full, unfiltered dataset the strongest correlations are all with temperature related variables.

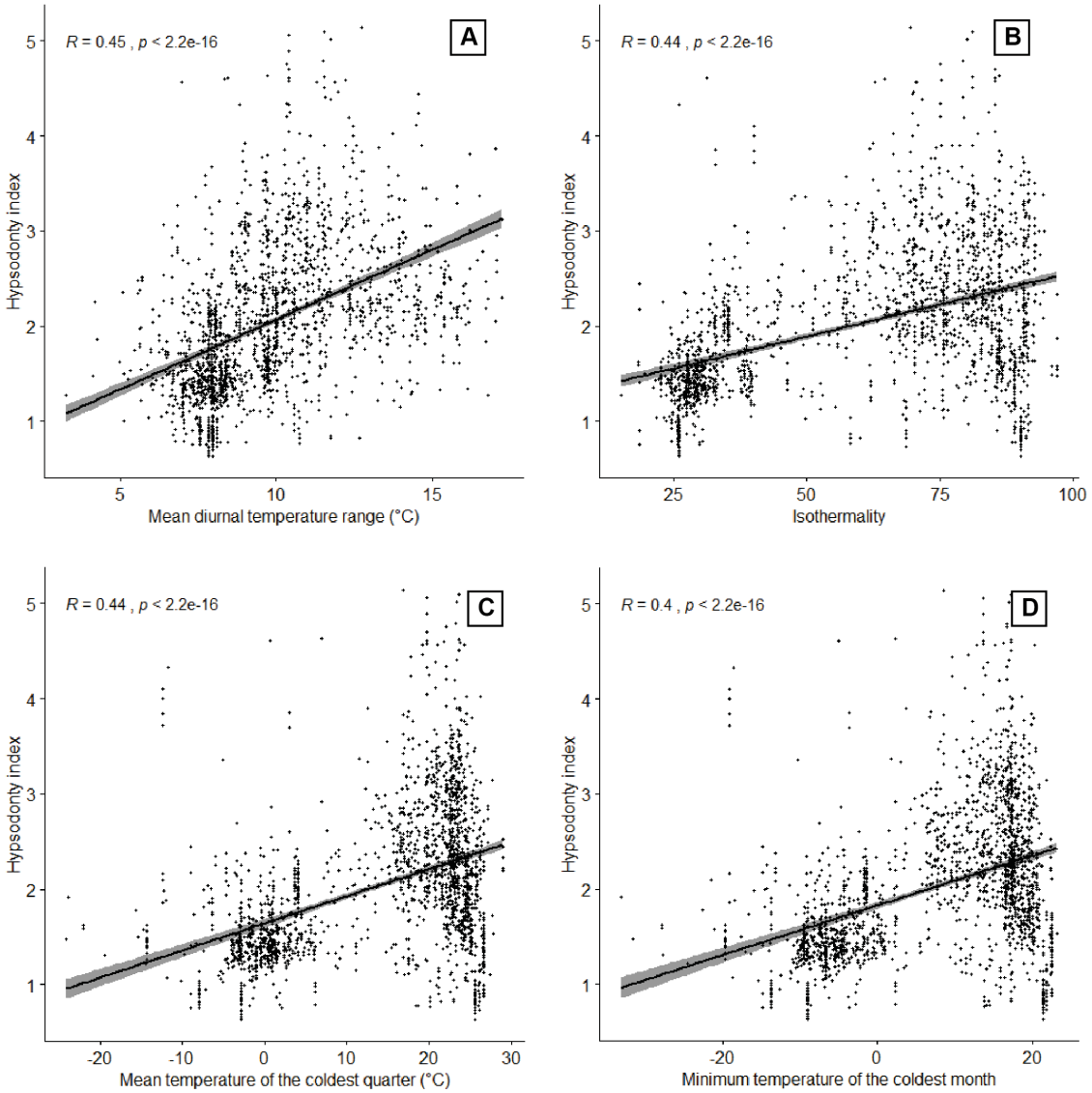

Figure 4.15: Scatter plots of the climate variables that are most strongly correlated with this hypsodonty index dataset (individual data points but with left and right teeth averaged for individual animals) A) mean diurnal temperature range (bio2), B) isothermality (bio3), C) mean temperature of the coldest quarter (bio11) and D) minimum temperature of the coldest month (bio6). The black line represents a line of best fit and the grey band represents a 95% confidence interval around this line. Pearson's R and the associated p-value is also shown on each scatter plot.

The weakest correlations (see Figure 4.16) were between hypsodonty index (HI) and mean annual precipitation (bio12; *R*=0.02), precipitation of the coldest quarter (bio19; R=0.03), precipitation of the warmest quarter (bio18; *R*=--0.06) and precipitation of the wettest month (bio13; *R*=0.12). As with the full, unfiltered dataset, the weakest correlations were all with precipitation variables.

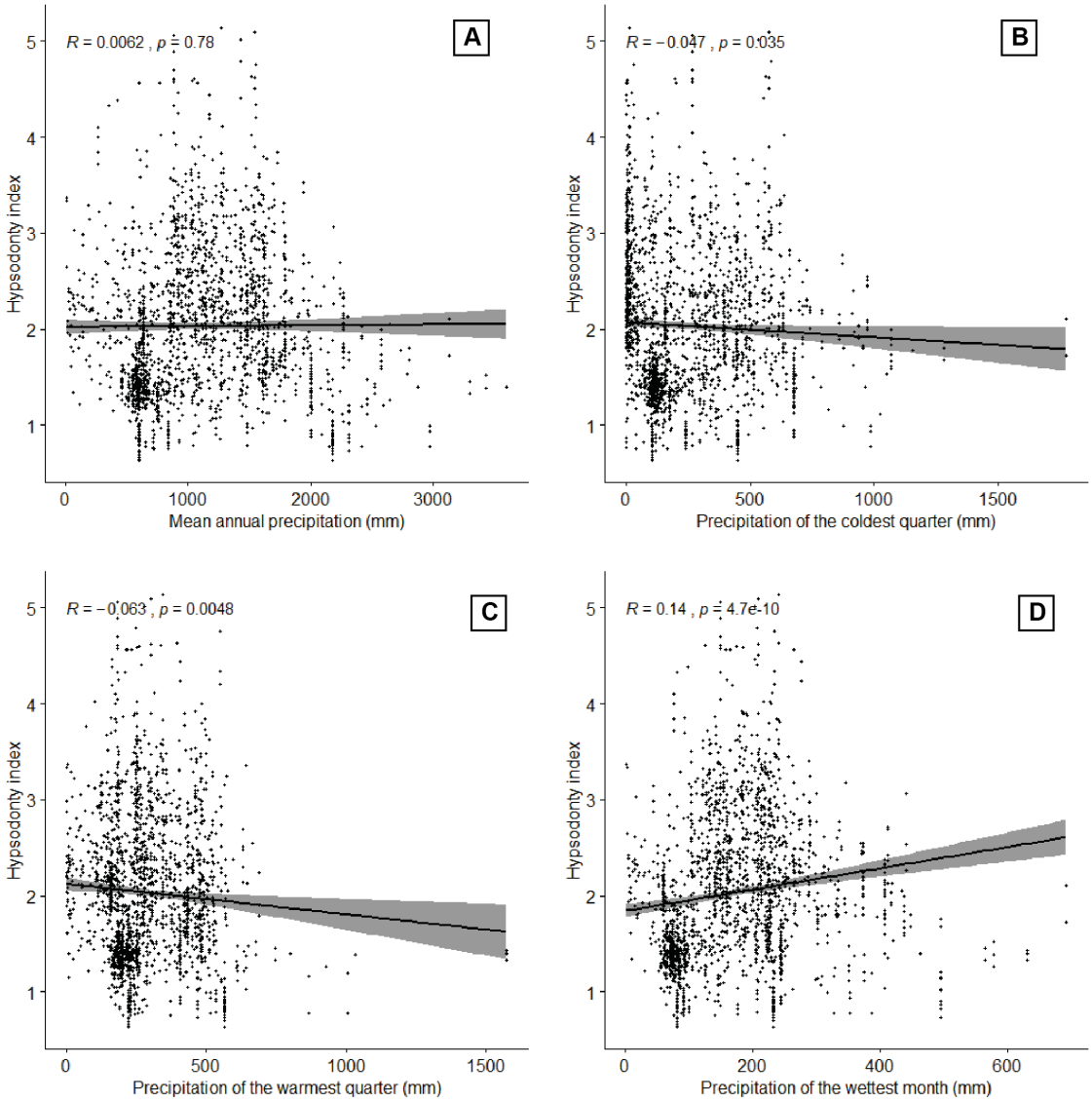

Figure 4.16: Scatter plots of the climate variables that are most weakly correlated with this hypsodonty index dataset (individual data points but with left and right teeth averaged for individual animals) A) mean annual precipitation (bio12), B) precipitation of the coldest quarter (bio19), C) precipitation of the warmest quarter (bio18) and D) precipitation of the wettest month (bio13). The black line represents a line of best fit and the grey band represents a 95% confidence interval around this line. Pearson's R and the associated p-value is also shown on each scatter plot.

As there is an increase in the strength of the strongest correlations with this version of the dataset, it could be considered in regression analysis but it is, again, necessary to discount those climatic variables that are autocorrelated. Of those with the strongest correlations with hypsodonty index, the following could be considered in further analysis: mean diurnal temperature range (bio2) and minimum temperature of the warmest month (bio6).

4.2.2.4 *Each hypsodonty index value as a single data point (individual teeth with averaged left and right teeth from the same animal with migrant taxa removed)*

For the fourth dataset, where left and right teeth were averaged for individual animals but migrant taxa were removed, Pearson correlation coefficients were calculated between hypsodonty index (the dependent variable) and all nineteen climate variables (the independent variables). These are presented in the first row of the correlation matrix shown in Figure 4.17. The p-values indicate that all calculated Pearson correlation coefficients were statistically significant (p<=0.05).

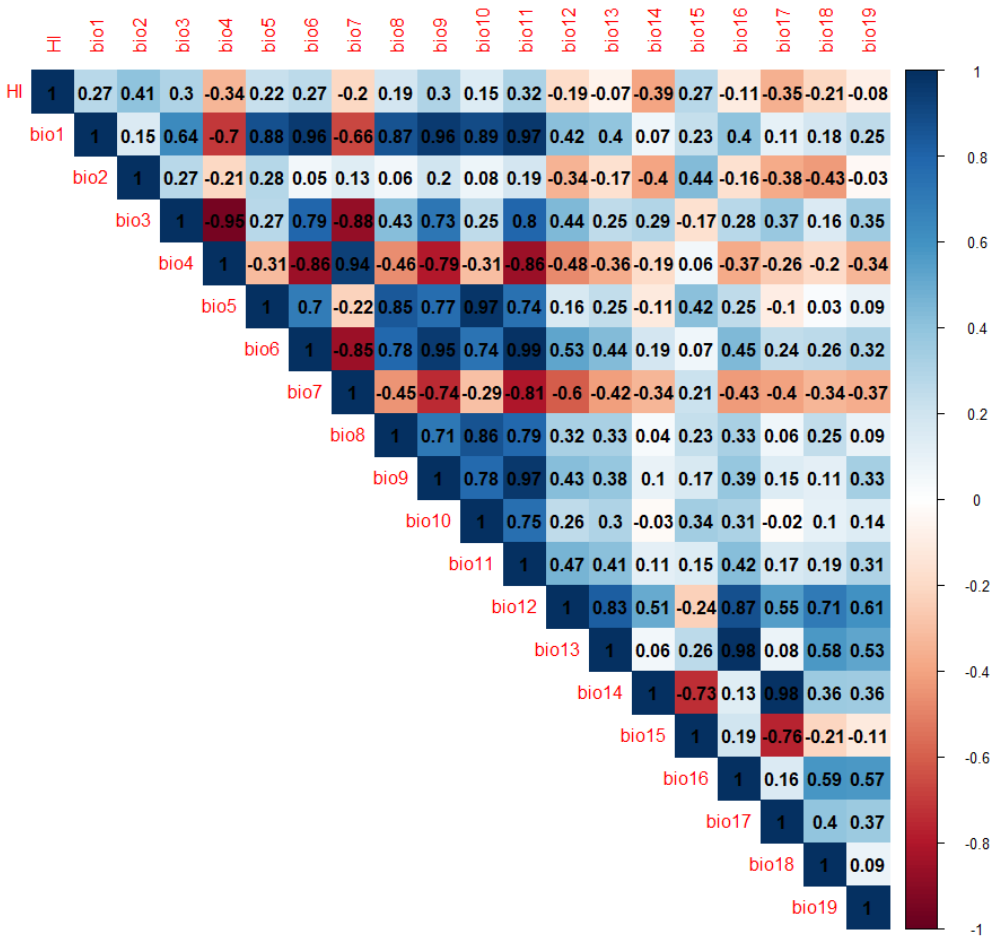

Figure 4.17: Correlation matrix showing Pearson correlation coefficients between hypsodonty index (HI) as individual data points (but with left and right teeth averaged for individual animals and migrant taxa removed) against the nineteen climate variables (see section 3.1.2.3 for more information on notation). The colour ramp indicates the strength of the correlation as shown in the figure legend on the right-hand side.

The strongest correlations (see Figure 4.18) were between hypsodonty index (HI) and mean diurnal temperature range (bio2; *R*=0.41), precipitation of the driest month (bio14; *R*=-0.39), precipitation of the driest quarter (bio17; *R*=-0.35) and mean temperature of the coldest quarter (bio11; *R*=0.32). Again, as with the second dataset (the full dataset with migrant taxa removed), the strongest correlations are with both temperature and precipitation climatic variables, however, these correlations are weaker than the

strongest correlations found in the previous dataset (full dataset but left and right averaged).

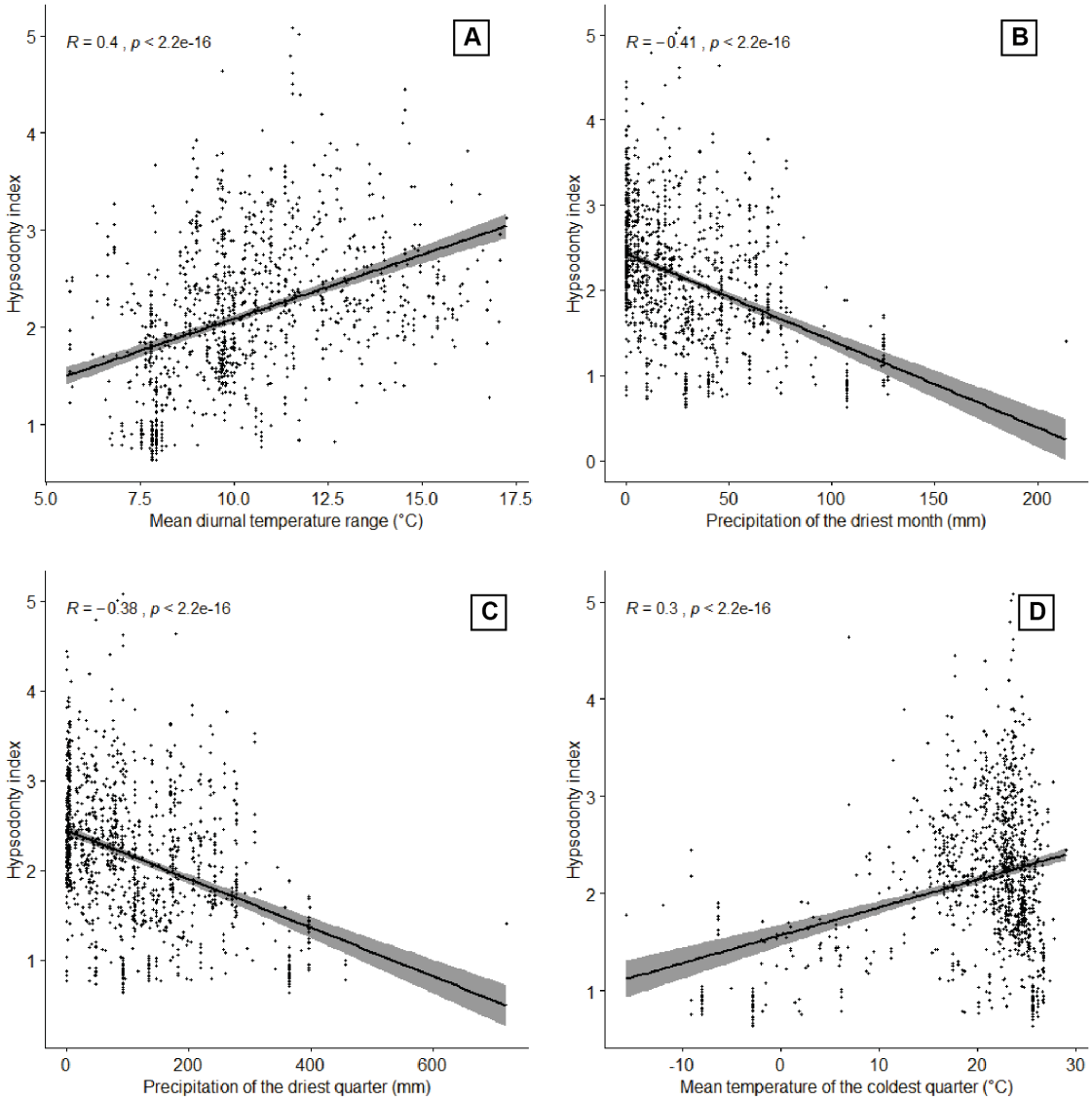

Figure 4.18: Scatter plots of the climate variables that are most strongly correlated with this hypsodonty index dataset (individual data points but with left and right teeth averaged for individual animals, but with migrant taxa removed) A) mean diurnal temperature range (bio2), B) precipitation of the driest month (bio14), C) precipitation of the driest quarter (bio17) and D) mean temperature of the coldest quarter (bio13). The black line represents a line of best fit and the grey band represents a 95% confidence interval around this line. Pearson's R and the associated p-value is also shown on each scatter plot.

The weakest correlations (see Figure 4.19) were between hypsodonty index (HI) and precipitation of the wettest month (bio13; *R*=-0.07), precipitation of the coldest quarter (bio19; *R*=-0.08), precipitation of the wettest quarter (bio16; *R*=--0.11) and mean temperature of the warmest quarter (bio10; *R*=0.15). As with the second dataset (with migrant taxa removed) the weakest correlations were all with both precipitation variables and temperature. It is worth noting that across all climate variables the correlations are very similar to each other in terms of magnitude of the correlations.

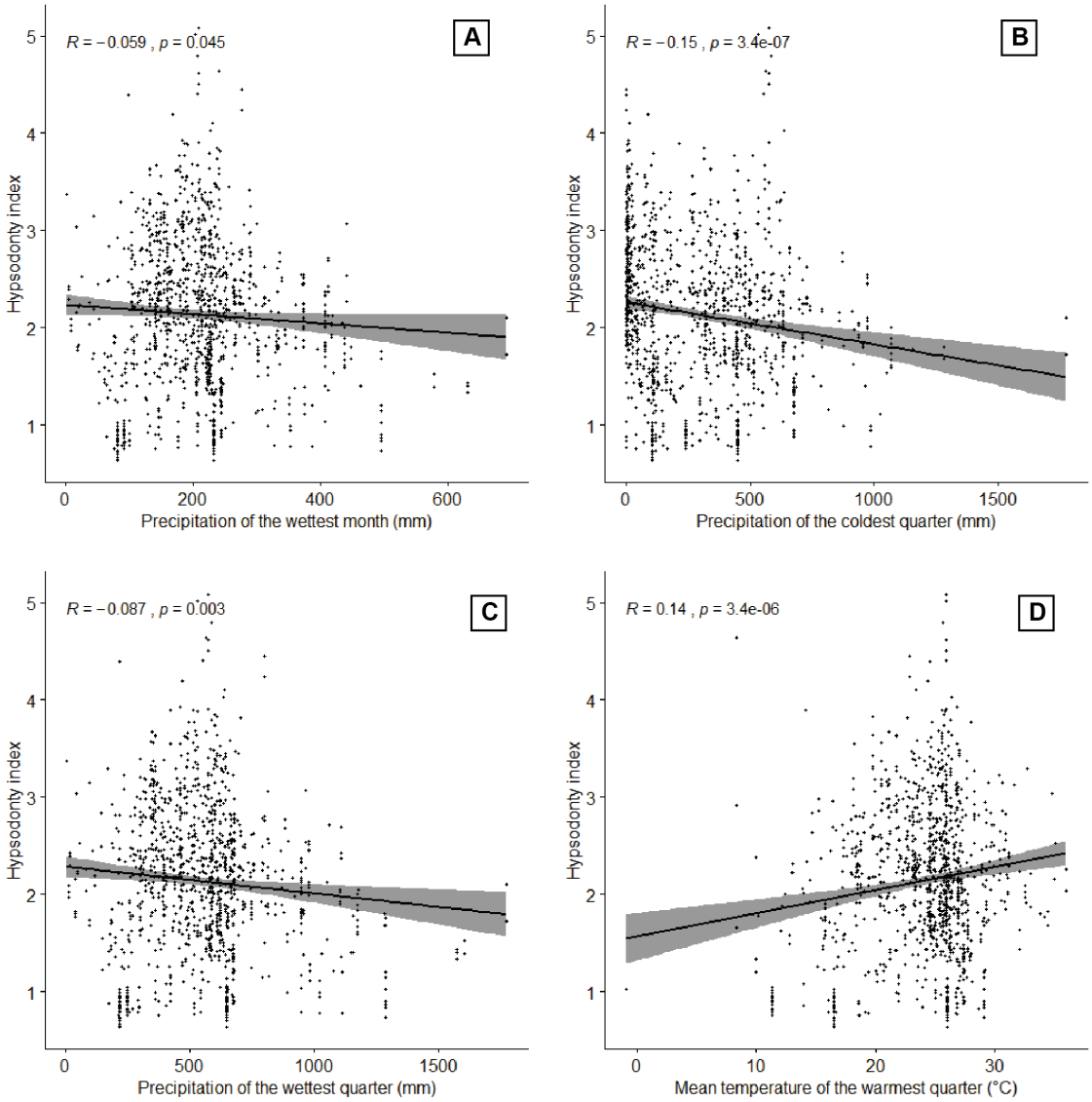

Figure 4.19: Scatter plots of the climate variables that are most weakly correlated with this hypsodonty index dataset (individual data points but with left and right teeth averaged for individual animals, but with migrant taxa removed) A) precipitation of the wettest month (bio13), B) precipitation of the coldest quarter (bio19), C) precipitation of the wettest quarter (bio16) and D) mean temperature of the warmest quarter (bio10). The black line represents a line of best fit and the grey band represents a 95% confidence interval around this line. Pearson's R and the associated p-value is also shown on each scatter plot.

4.2.2.5 Data as mean hypsodonty index values per locality

For the fifth dataset, where mean hypsodonty index values per locality were calculated, Pearson correlation coefficients were calculated between hypsodonty index (the dependent variable) and all nineteen climate variables (the independent variables). These are presented in the first row of the correlation matrix (see Figure 4.20).

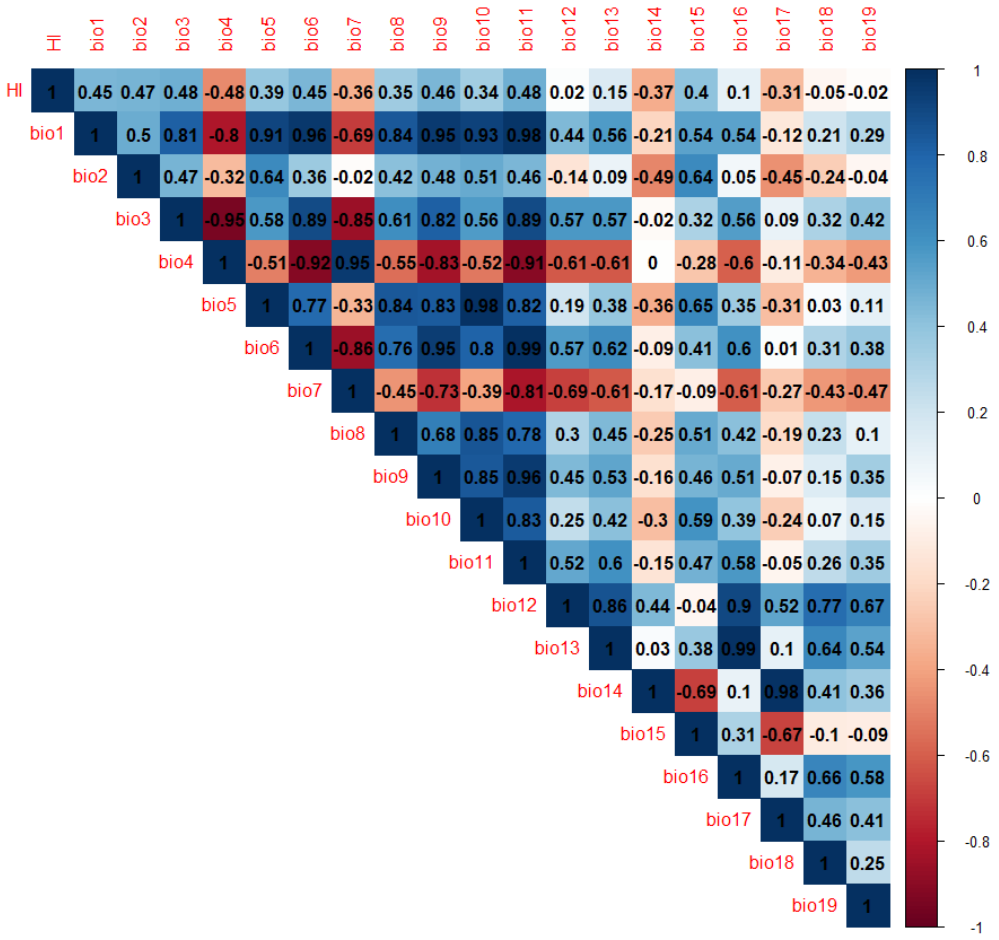

Figure 4.20: Correlation matrix showing Pearson correlation coefficients between average hypsodonty index (HI) per locality against the nineteen climate variables (see section 3.1.2.3 for more information on notation). The colour ramp indicates the strength of the correlation as shown in the figure legend on the right-hand side.

The strongest correlations (see Figure 4.21) were between hypsodonty index (HI) and isothermality (bio3; *R*=0.48), mean temperature of the coldest quarter (bio11; *R*=0.48), temperature seasonality (bio4; *R*=-0.48) and mean diurnal temperature range (bio2; *R*=0.47).

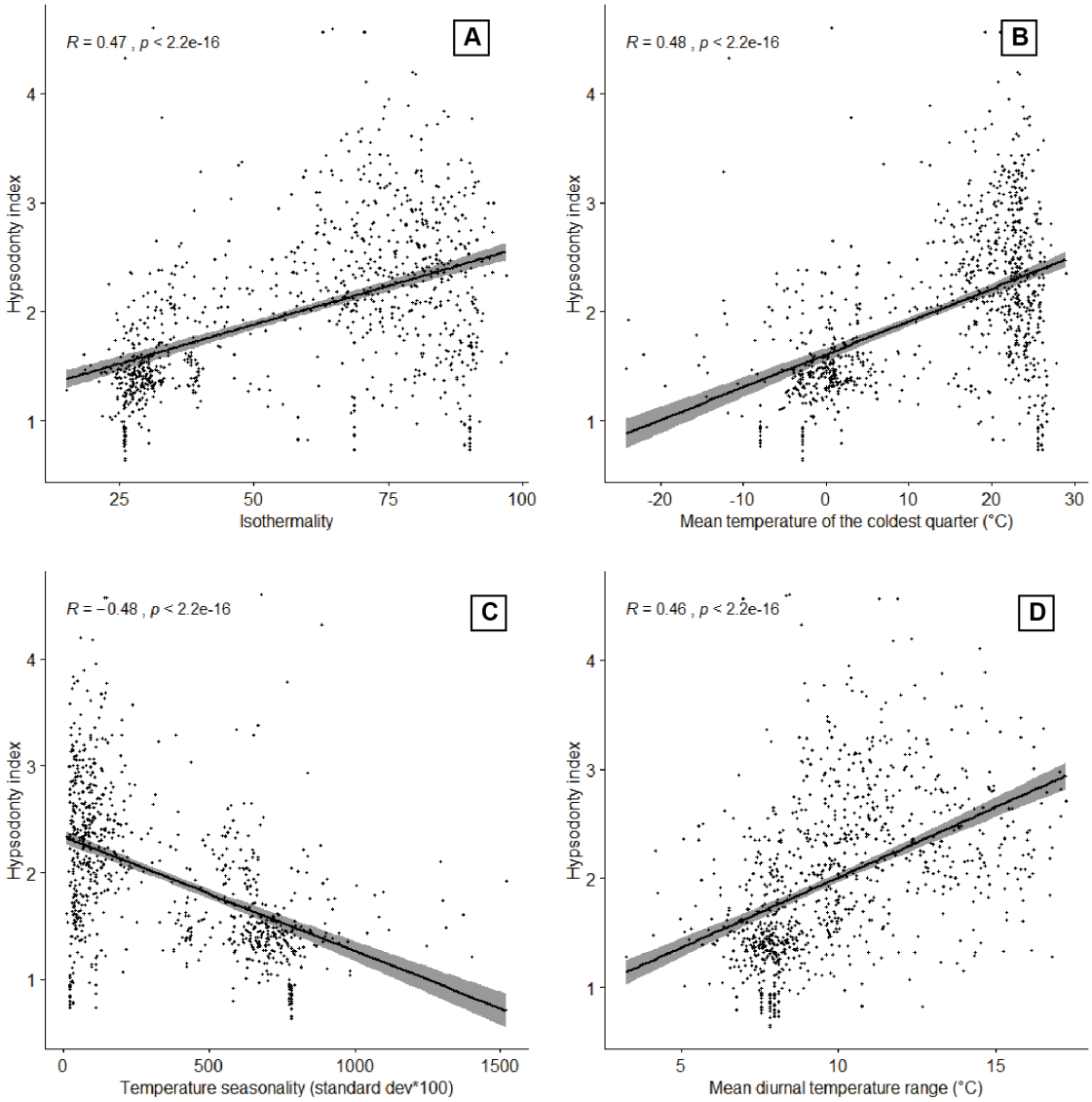

Figure 4.21: Scatter plots of the climate variables that are most strongly correlated with this hypsodonty index dataset (full dataset of hypsodonty index averaged per location) A) isothermality (bio3), B) mean temperature of the coldest quarter (bio11), C) temperature seasonality (bio4) and D) mean diurnal temperature range (bio2). The black line represents a line of best fit and the grey band represents a 95% confidence interval around this line. Pearson's R and the associated p-value is also shown on each scatter plot.

The weakest correlations (see Figure 4.22) were between hypsodonty index (HI) and mean annual precipitation (bio12; *R*=0.02), precipitation of the coldest quarter (bio19; *R*=-0.02), precipitation of the warmest quarter (bio18; *R*=-0.05) and precipitation of the wettest quarter (bio16; *R*=0.1). All of the weakest correlations are with precipitation variables although it is worth noting that precipitation seasonality (bio15) is the strongest correlation out of the precipitation variables, not much weaker than the strongest correlations which are temperature variables (including temperature seasonality).

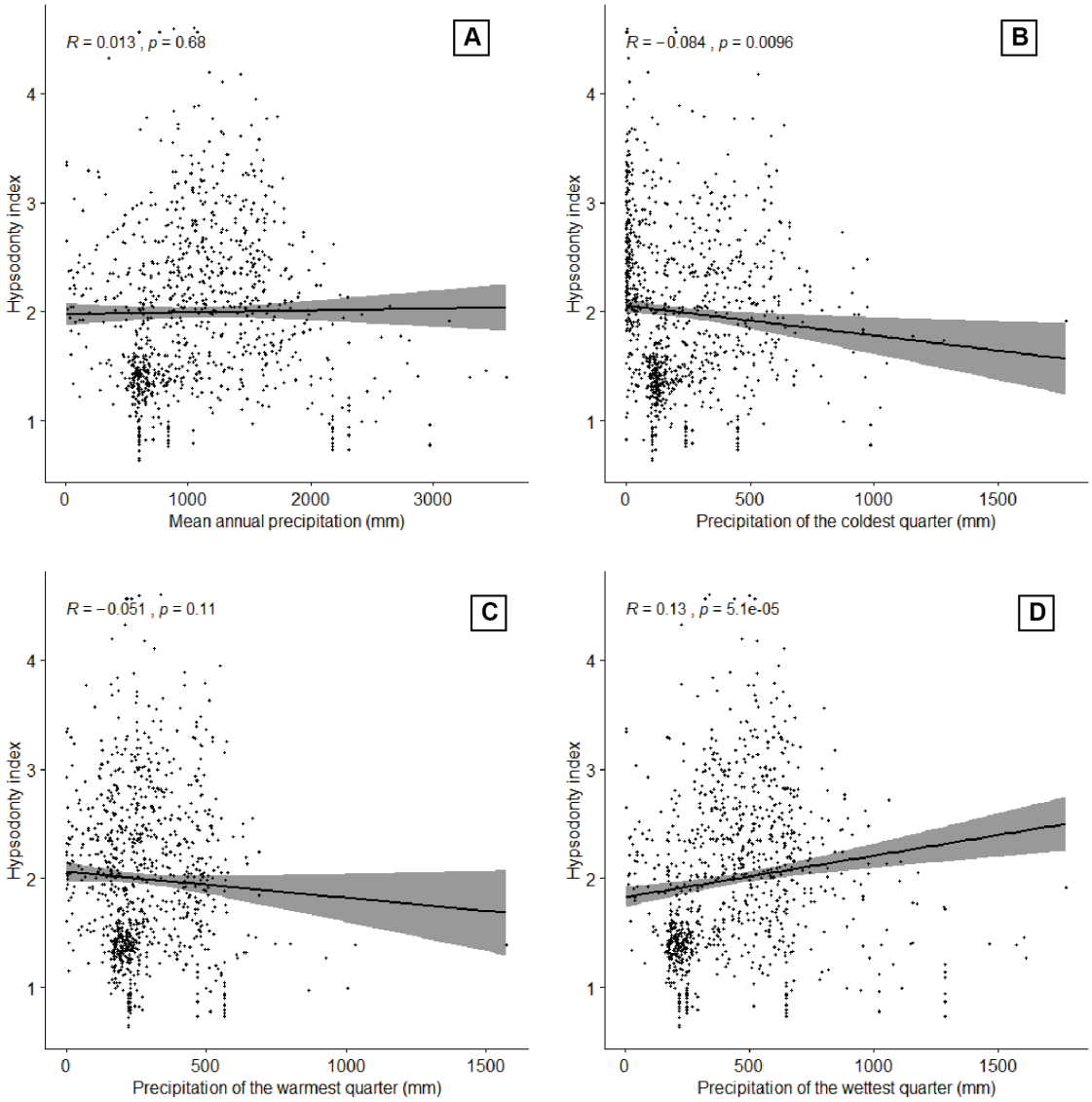

Figure 4.22: Scatter plots of the climate variables that are most weakly correlated with this hypsodonty index dataset (full dataset of hypsodonty index averaged per location) A) mean annual precipitation (bio12), B) precipitation of the coldest quarter (bio19), C) precipitation of the warmest quarter (bio18) and D) precipitation of the wettest quarter (bio16). The black line represents a line of best fit and the grey band represents a 95% confidence interval around this line. Pearson's R and the associated p-value is also shown on each scatter plot.

The strongest correlations for this dataset are the most pronounced thus far out of all the versions of the dataset examined. It is therefore useful to highlight the correlations that may be applicable in subsequent regression analysis. Isothermality itself is calculated from other climatic variables and thus is not useful for regression. The next strongest correlation is with mean temperature of the coldest quarter (bio11), but this is associated with the next two strongest correlates (temperature seasonality (bio4; *R*=-0.51) and mean diurnal temperature range (bio2; *R*=0.51). For subsequent analysis, it is therefore necessary to consider the nature of these variables in order to select the most appropriate for regression analysis in the context of this study.

4.2.2.6 Data as mean hypsodonty index values per locality with migrant taxa removed

For the sixth dataset, where mean hypsodonty index values per locality were calculated, Pearson correlation coefficients were calculated between hypsodonty index (the dependent variable) and all nineteen climate variables (the independent variables). These are presented in the first row of the correlation matrix (see Figure 4.23).

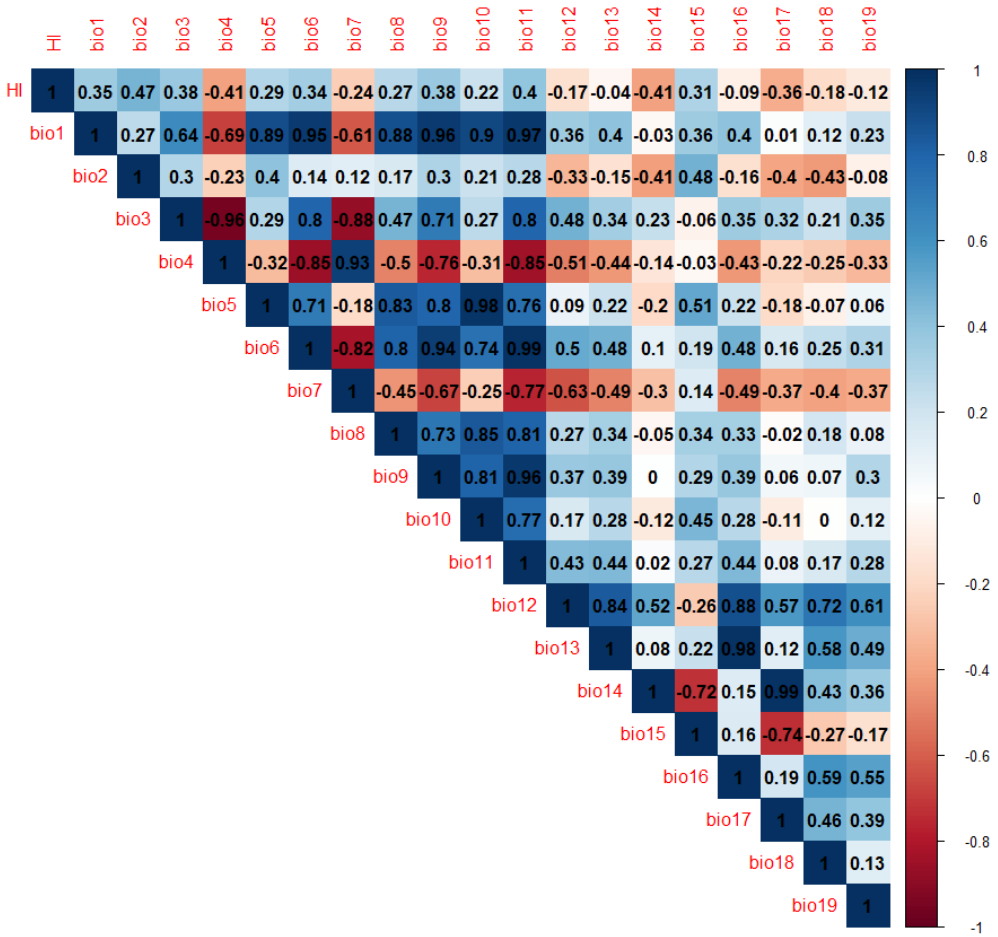

Figure 4.23: Correlation matrix showing Pearson correlation coefficients between average hypsodonty index (HI) per locality with migrant taxa removed against the nineteen climate variables (see section 3.1.2.3 for more information on notation). The colour ramp indicates the strength of the correlation as shown in the figure legend on the right-hand side.

The strongest correlations (see Figure 4.24) were between hypsodonty index (HI) and mean diurnal temperature range (bio2; *R*=0.47), precipitation of the driest month (bio14; *R*=-0.41), temperature seasonality (bio4; *R*=-0.41) and mean temperature of coldest quarter (bio11; *R*=0.4).

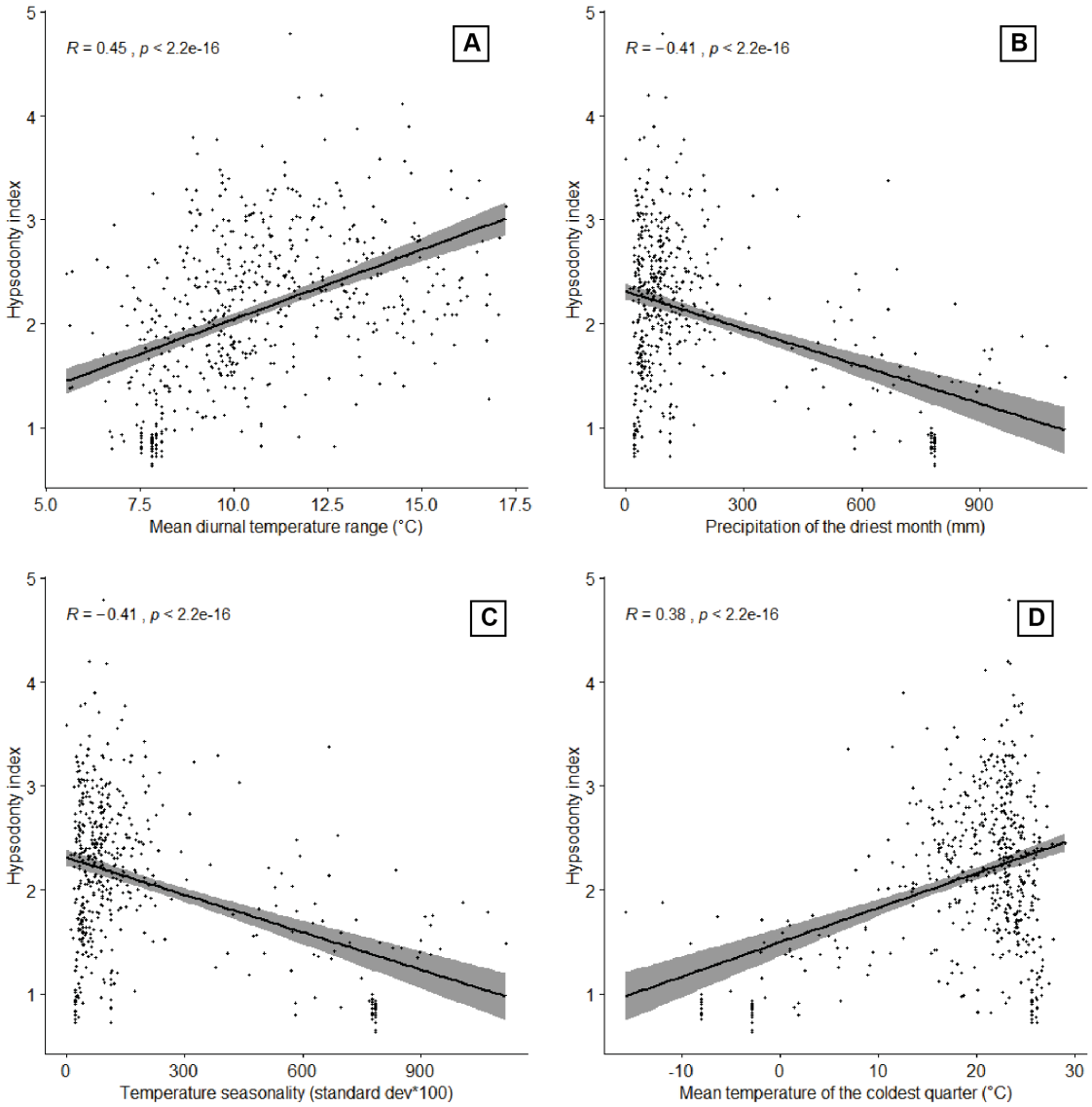

Figure 4.24: Scatter plots of the climate variables that are most strongly correlated with this hypsodonty index dataset (full dataset of hypsodonty index averaged per location with migrant taxa removed) A) mean diurnal temperature range (bio2), B) precipitation of the driest month (bio14), C) temperature seasonality (bio4) and D) mean temperature of the coldest quarter (bio11). The black line represents a line of best fit and the grey band represents a 95% confidence interval around this line. Pearson's R and the associated p-value is also shown on each scatter plot.

The weakest correlations (see Figure 4.25) were between hypsodonty index (HI) and the precipitation of the wettest month (bio13; *R*=-0.04), precipitation of the wettest quarter (bio16; *R*=-0.09), precipitation of the coldest quarter (bio19; *R*=-0.12) and mean annual precipitation (bio12; *R*=-0.17). The weakest correlations are slightly stronger than those seen in the full but location-averaged dataset but even so, these correlations are very weak.

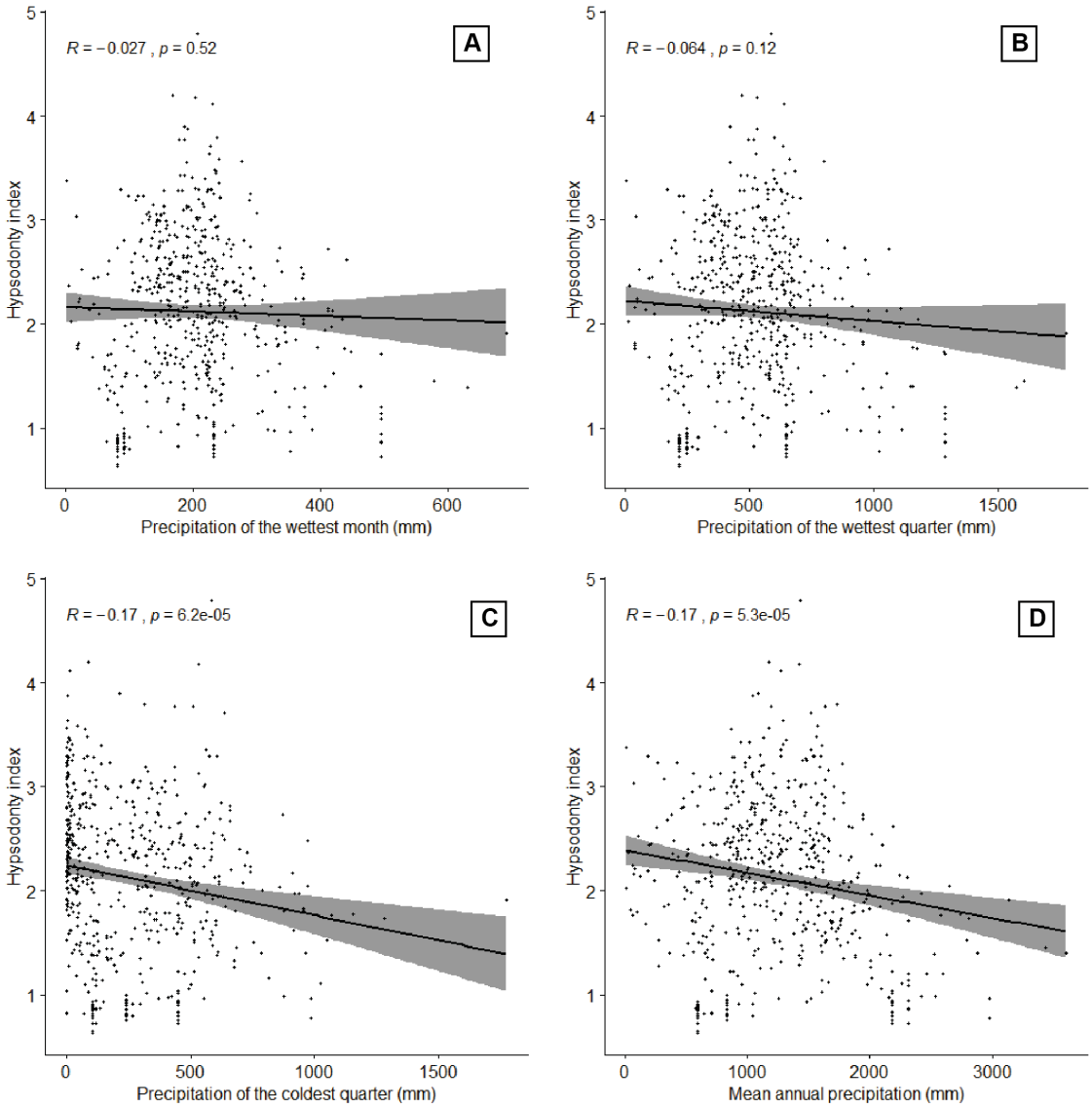

Figure 4.25: Scatter plots of the climate variables that are most weakly correlated with this hypsodonty index dataset (full dataset of hypsodonty index averaged per location with migrant taxa removed) A) precipitation of the wettest month (bio13), B) precipitation of the wettest quarter (bio16, C) precipitation of the coldest quarter (bio19) and D) mean annual precipitation (bio12). The black line represents a line of best fit and the grey band represents a 95% confidence interval around this line. Pearson's R and the associated p-value is also shown on each scatter plot.

4.2.2.7 Summary

From looking at correlations between the untransformed datasets and the climate variables, the most common variable that is most strongly correlated is mean diurnal temperature range (bio2), followed by other temperature variables. The most common weakest correlated variables are both mean annual precipitation (bio12) and precipitation of the wettest month (bio13), followed by mostly other precipitation variables. Of all the datasets, it is the full dataset where the hypsodonty index values have been averaged per location that has stronger correlations with most of the climate variables. Therefore, it is this dataset that will be considered in subsequent analysis.

4.2.3 Correlations with climatic variables – with log10 transformed dataset

As seen in the exploratory analysis outlined in section 4.2.1 the hypsodonty index datasets were largely skewed to the lower end of the hypsodonty index values. To adjust for this skew, it is appropriate to log-transform the dataset to remove some of this skewness and create a distribution closer to normality (Feng *et al*., 2014). A correlation matrix can then be computed to check if this changes the correlations that were found with the untransformed dataset. As previously noted, the dataset with mean hypsodonty index values per studied location gave the strongest correlations with the climatic variables. This dataset was log-transformed, and the correlation matrix recalculated. This is presented below in Figure 4.26. Many correlations had a *p*-value of <=0.05 and are therefore statistically significant but where there was an *R* value close to zero the *p*-value increased above the threshold for statistical significance (0.05; see the appendix for the full dataset).

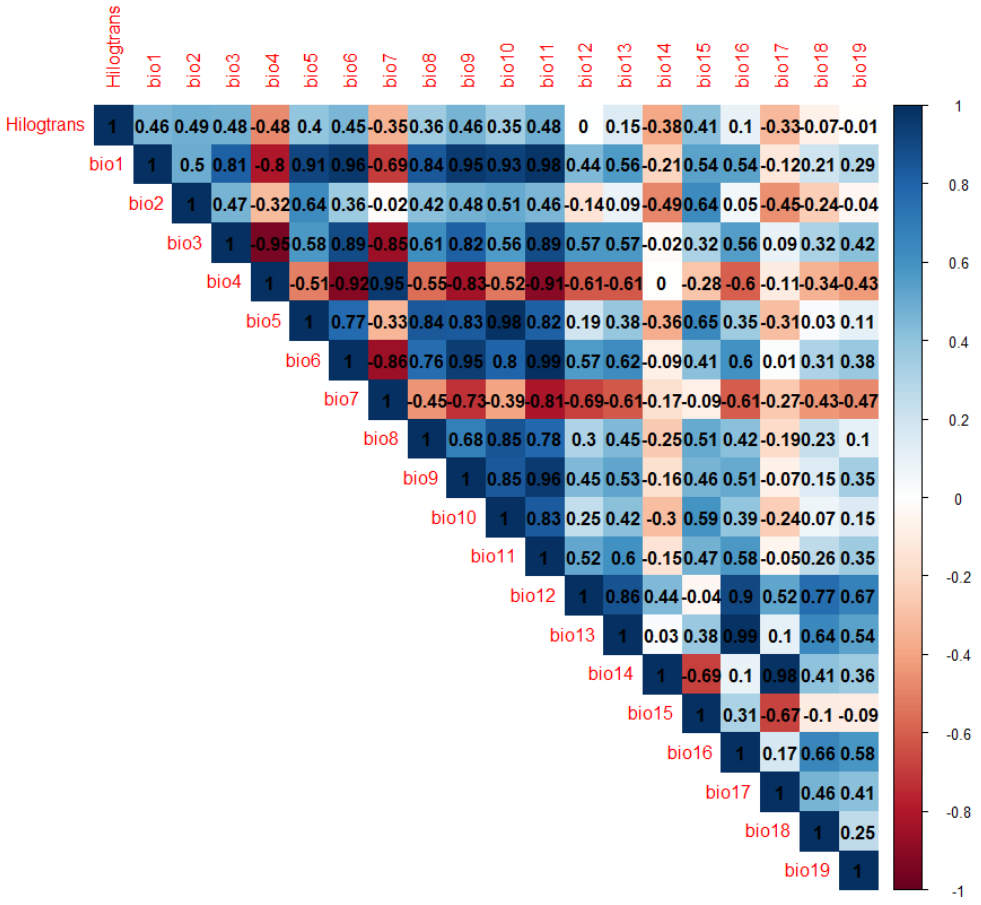

Figure 4.26: Correlation matrix showing Pearson correlation coefficients between log-transformed average hypsodonty index (HI) per locality against the nineteen climate variables (see section 3.1.2.3 for more information on notation). The colour ramp indicates the strength of the correlation as shown in the figure legend on the right-hand side.

The strongest correlations for the log-transformed data are similar to the untransformed data, with the strongest four correlating variables being the same, albeit a fraction stronger in *R* values. The strongest correlation was between log-transformed hypsodonty index and mean diurnal temperature range (bio2; *R*=0.49), followed by isothermality (bio3; *R*=0.48), temperature seasonality (bio4; *R*=-0.48) and mean temperature of the coldest quarter (bio11; *R*=0.48). Again, the strongest correlated climate variables were all temperature-related. Scatter plots of these relationships are shown below in Figure 4.27.

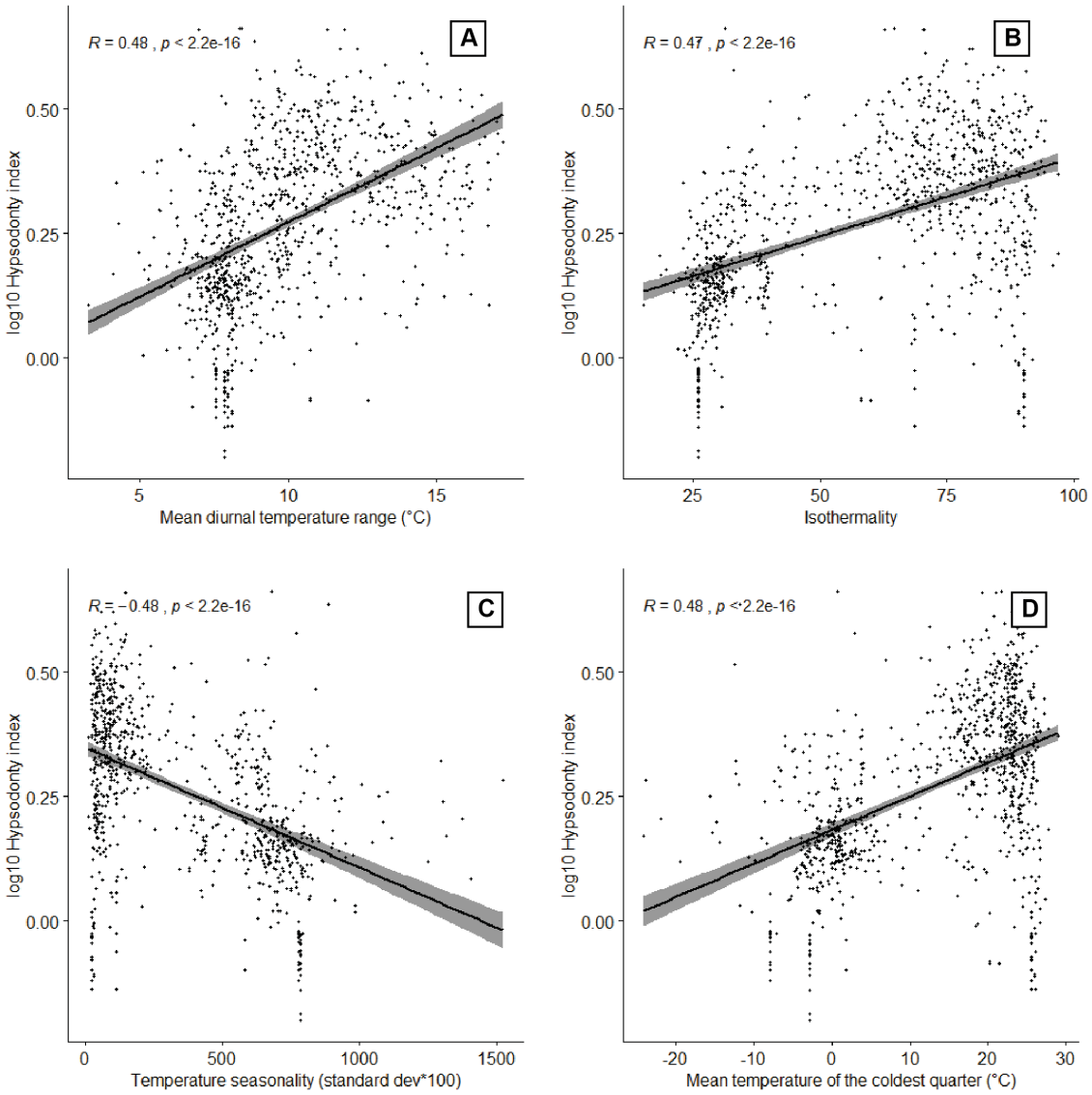

Figure 4.27: Scatter plots of the climate variables that are most strongly correlated with log-transformed average hypsodonty index per location. A) mean diurnal temperature range (bio2), B) isothermality (bio3), C) temperature seasonality (bio4) and D) mean temperature of the coldest quarter (bio11). The black line represents a line of best fit and the grey band represents a 95% confidence interval around this line. Pearson's R and the associated p-value is also shown on each scatter plot.

A similar pattern is observed with the weakest correlating climate variables. The four weakest correlating climate variables are the same for the transformed and untransformed datasets. With the transformed dataset, the climate variables that have

the weakest correlations with hypsodonty index were mean annual precipitation (bio12; *R*=0), followed by precipitation of the coldest quarter (bio19; *R*=-0.01), precipitation of the warmest quarter (bio18; *R*=-0.07) and precipitation of the wettest quarter (bio16; *R*=0.1). For these variables the *R* values are so low, they indicate there is no relationship between average hypsodonty index per locality and these climatic variables. Scatter plots of these relationships are shown below in Figure 4.28.

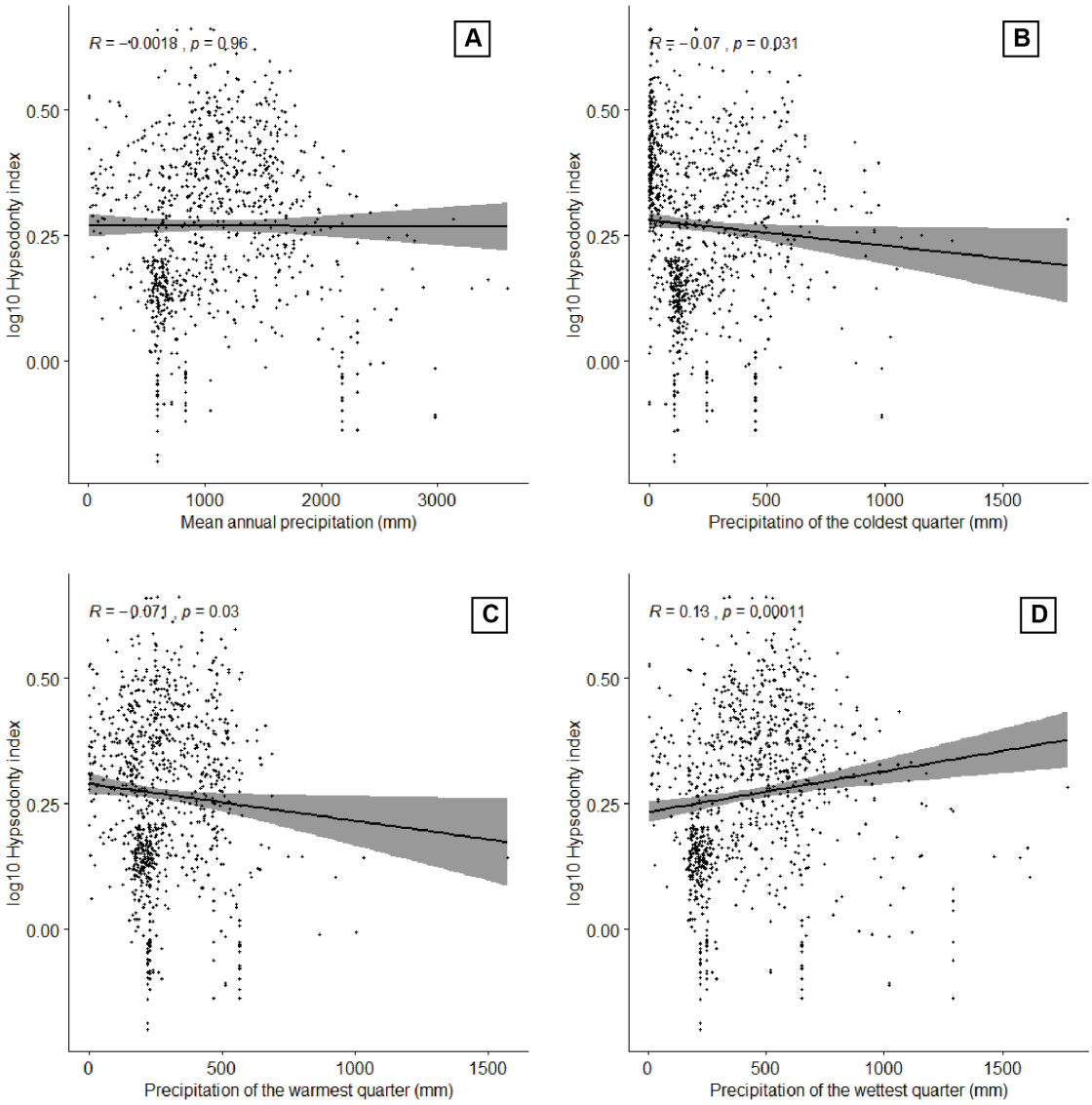

Figure 4.28: Scatter plots of the climate variables that are most weakly correlated with log-transformed average hypsodonty index per location. A) mean annual precipitation (bio12), B) precipitation of the coldest quarter (bio19), C) precipitation of the warmest quarter (bio18) and D) precipitation of the wettest quarter (bio16). The black line represents a line of best fit and the grey band represents a 95% confidence interval around this line. Pearson's R and the associated p-value is also shown on each scatter plot.

To assess which relationships and correlations could be taken further into regression analysis it is essential to discount those that are autocorrelated. Of the top four strongest correlations the variables are all autocorrelated, so it is pertinent to select only the strongest correlating variable out of these four, which is mean diurnal temperature range (bio2). Subsequent regression analysis may find that some of the other slightly weaker

but non-autocorrelated variables can explain some of the variation in hypsodonty index. This is further discussed in section 4.2.5.

In the correlation matrix (Figure 4.26), it is clear that the strongest correlations exist between log-transformed mean hypsodonty index and a number of temperature-related variables, but within the precipitation variables, there is a moderately positive correlation with precipitation seasonality. It is pertinent to examine the relationship between log-transformed mean hypsodonty index and an index of aridity (other than the coefficient of variation of precipitation as per the Bioclim dataset). Therefore, correlation between log-transformed mean hypsodonty index and a calculated aridity index (mean annual precipitation ÷ potential evapotranspiration) was calculated. The *R* value was calculated to be -0.29 showing a weak negative correlation with aridity index. The scatter plot is shown below in Figure 4.29.

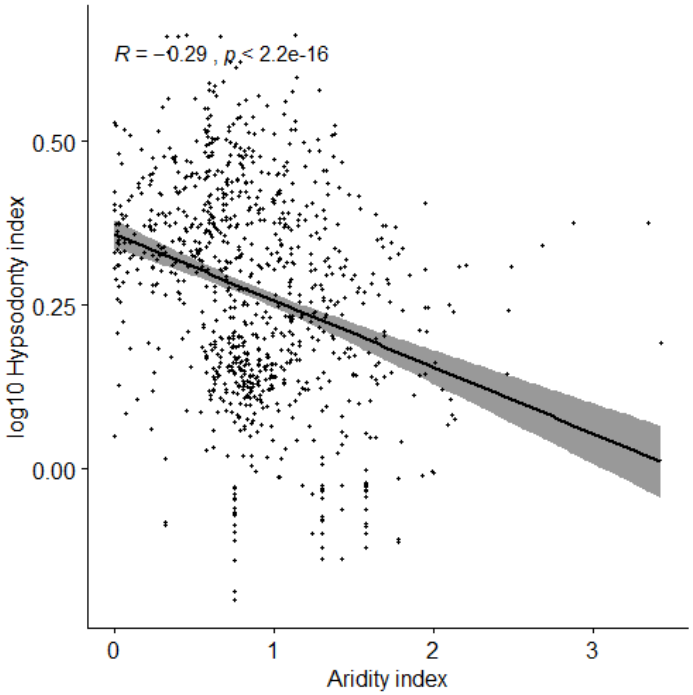

Figure 4.29: Scatter plot of log-transformed average hypsodonty index per location against aridity index. The black line represents a line of best fit and the grey band represents a 95% confidence interval around this line. Pearson's R and the associated p-value is also shown.

4.2.4 Regression modelling

Using the log-transformed dataset of mean hypsodonty index per locality, multiple linear regression was attempted using the non-redundant climate variables in order to construct an initial predictive model. After examining autocorrelating climate variables that appear to show the strongest *R* values, the following were chosen for the analysis:

- Mean diurnal temperature range (bio2)
- Annual temperature range (bio7)
- Precipitation seasonality (bio15)

```
Residuals:
     Min       1Q   Median       3Q      Max
-0.44536 -0.06546  0.00862  0.07899  0.50132

Coefficients:
                   Estimate Std. Error t value Pr(>|t|)
(Intercept)       0.1250833  0.0198141   6.313 4.21e-10 ***
subsetlog5$bio2   0.0238725  0.0021696  11.003  < 2e-16 ***
subsetlog5$bio7  -0.0067756  0.0005451 -12.429  < 2e-16 ***
subsetlog5$bio15  0.0007891  0.0001746   4.519 7.01e-06 ***
---
Signif. codes:  0 ‘***’ 0.001 ‘**’ 0.01 ‘*’ 0.05 ‘.’ 0.1 ‘ ’ 1

Residual standard error: 0.1312 on 942 degrees of freedom
Multiple R-squared:  0.3611,   Adjusted R-squared:  0.359
F-statistic: 177.5 on 3 and 942 DF,  p-value: < 2.2e-16
```

These results are statistically significant, with these three climatic variables used as independent variables in the regression. The p-value for the model also indicates that the results are statistically significant, and that a larger sample size would not improve or change the output of the model. The R^2 value (“Multiple R-squared”) of 0.3611 shows that 36.11% of the variation in the hypsodonty index is explained by the model involving these three variables. Precipitation of the driest month (bio14) and precipitation of the driest quarter (bio17) were added as further independent variables in an attempt to improve the model and while this did increase the model’s R^2 value to 0.431, neither of these coefficients were statistically significant. The results output is shown below.

```
Residuals:
     Min       1Q   Median       3Q      Max
-0.45671 -0.06087  0.00102  0.07769  0.53246

Coefficients:
                   Estimate Std. Error t value Pr(>|t|)
(Intercept)       0.3037567  0.0287178  10.577   <2e-16 ***
subsetlog5$bio2   0.0231876  0.0021580  10.745   <2e-16 ***
subsetlog5$bio7  -0.0087676  0.0006875 -12.752   <2e-16 ***
subsetlog5$bio14 -0.0006993  0.0010433  -0.670   0.5028
subsetlog5$bio15 -0.0004697  0.0002236  -2.101   0.0359 *
subsetlog5$bio17 -0.0004050  0.0003238  -1.251   0.2113
---
Signif. codes:  0 ‘***’ 0.001 ‘**’ 0.01 ‘*’ 0.05 ‘.’ 0.1 ‘ ’ 1

Residual standard error: 0.1258 on 940 degrees of freedom
```

```
Multiple R-squared:  0.4131,   Adjusted R-squared:   0.41
F-statistic: 132.3 on 5 and 940 DF,  p-value: < 2.2e-16
```

4.3 Summary

This chapter has presented the results from first, the investigation of intraspecific variation of hypsodonty in ungulates. It is clear that most of the taxa investigated in this study have hypsodonty index measurements that are drawn from normal distributions. There are a selected few taxa that appear to have datasets drawn from not-normal distributions and this will be discussed in Chapter 5. Secondly, the results of the investigation of links between hypsodonty and a large number of bioclimatic variables were presented. It is evident that correlations of different climate variables with hypsodonty index are mostly weak, with temperature related bioclimatic variables more strongly correlated that precipitation-related variables. These correlations are also varied when using the different datasets and subsets of the data, with the log-transformed whole dataset of hypsodonty index measurements of individual teeth resulting in the strongest *R* values but still weakly correlated. Taking the strongest correlating variables forward to regression modelling, it is clear that whilst statistically significant, the regression model output indicates that only 36% of variation in hypsodonty index is explained by the three strongest correlating climate variables and that adding the next strongest correlating variables did not improve the model. Mechanisms behind these results and their implications are discussed in Chapter 5.

CHAPTER 5
Discussion – intraspecific variation and the utility of modern hypsodonty index as a climate predictor

This chapter discusses the results of both the investigation into intraspecific variation in hypsodonty index and a wider discussion on how modern ungulate hypsodonty index is related to climate and environment in light of the results presented in Chapter 4.

5.1 Modern ungulate ecology and effects on hypsodonty

A large number of interacting and competing aspects of ungulate ecology and landscape- and biome-level effects must be taken into account when assessing the results of this investigation into both intraspecific ungulate hypsodonty and the relationship between hypsodonty and climate. Abiotic and biotic factors must be considered and there may be impacts on dental traits that introduce bias into the hypsodonty index data. The key aspects include, but are not limited to: (1) interspecific interactions and coexistence; (2) movements and home ranges of ungulates; (3) seasonal behaviour; (4) food selection and forage availability; and (5) life history traits such as sex, age, dimorphism, reproductive behaviour and group size.

5.1.1 Interspecific interactions and herbivore community coexistence

Carrying capacity is important to consider and in a grazing system with relatively predictable levels of rainfall (and hence stable primary production), ungulate populations are density-regulated through resource competition. If populations are near carrying capacity and there is a drought event, they are likely to experience a population crash. The long recovery time of populations after crashes means that population size cannot closely track climatic parameters such as rainfall during the following years (Vetter, 2005). If community mean hypsodonty index is correlated with mean annual precipitation (Eronen *et al*., 2010a,b; Liu *et al*., 2012; Žliobaitė *et al*., 2016) then during these unpredictable time periods, community mean hypsodonty may be in a state of flux and there may be an uncoupling of the hypsodonty index and climate relationship. Evidence of this was not tested for in this study but it is worth noting that as the climate data is averaged over 50 years, the effect of extreme events would be muted in the datasets. The effect of extreme events and the use of climate data over shorter timescales might reveal a different correlation between hypsodonty index and climate. Intraspecific changes in hypsodonty index over short timeframes may also have an effect on the

relationship between dental traits and diet and climate but this has not been tested in the literature or in this study.

Niche separation at single localities may have an impact on community hypsodonty. In many herbivore communities, there is an element of feeding facilitation (a type of niche separation where certain taxa limit their diets to specific sections of the plant community or even parts of individual plants, which in turn facilitates access to different plants or parts of those plants for other herbivore taxa). This is in contrast to direct competition for the same plant resource. In many communities there is a necessary balance of facilitation and competition over the annual cycle (Arsenault and Owen-Smith, 2002). Practices of feeding facilitation and competition can impact mean community hypsodonty index as a hypsodont taxon may feed on plant material that is not as mechanistically demanding as it is capable of eating. Similarly, even if abrasive plant material is available, it may not be being consumed due to waxing and waning levels of competition and/or feeding facilitation.

5.1.2 Home ranges

Herbivore movement is a key consideration as there are three broad categories that divide ungulates according to mobility: sedentary, migratory and nomadic. The determinants of each range type are related to spatial variability in resources (Müller *et al*., 2008) and resource availability (Teitelbaum *et al*., 2015). Sedentary ranges are facilitated by little spatial variability in resources, migratory ranges are facilitated by predictable seasonal variability in resources and nomadic movement is linked to unpredictable variability in resources (Müller *et al*., 2008).

It is those taxa that move in a nomadic fashion that have the potential to add bias into the hypsodonty index data. Unpredictable variability in resources can be caused by extreme adverse events such as drought. For example, when food or water runs out, animals may wander beyond their usual range limits (Owen-Smith *et al*., 2010). This has implications for the modern ungulate hypsodonty index dataset as when a specimen was collected from a locality, it is difficult to determine whether this locality is within or outside its normal home range. The impact of this may be that at the time of death, the individual may have been living in a locality that was sub-optimal and not consuming its “typical” diet. Therefore, there may be no mechanistic link between the dental traits of that individual and the vegetation at the particular locality where the specimen was collected. The effect of migration on the relationship between hypsodonty index and climate parameters is discussed in section 5.3.1.

5.1.3 Seasonal behaviour

Ungulate behaviour varies between seasons and this may have an impact on hypsodonty index. Often these behavioural changes relate to feeding as variability and spatial heterogeneity in forage quality and quantity is influenced by seasonal changes in climate (Vetter, 2005). There can be significant declines in digestible nutrients in winter or in dry seasons and conversely, high intake of plant material in summer or in the rainy seasons (Parker *et al*., 2009). Whilst hypsodonty index may be seen as an average over an individual's lifespan (Janis, 1984; Fortelius, 1985), there is evidence that periods of poor diet leads to more time spent foraging for food, as is the case for kudus (*Tragelaphus* sp.) during dry seasons (Parker *et al*., 2009). This may mean that populations of a certain taxon require increased dental durability (and hence increased hypsodonty) to resist wear during extended periods of consumption of lower quality plant food.

5.1.4 Food selection and forage availability

Energy requirements are an important determinant not only for food selection but also for habitat preferences in general, since vegetation cover acts as a thermal cover from heat and cold. Regarding locomotion, energy expenditure is higher when snow cover is higher. Metabolic rates for northern ungulates are therefore higher due to the need to maintain higher body mass, as this enables tissue synthesis in short summer season. The lower energy requirement for white-tailed deer (*Odocoileus virginianus* (Zimmermann, 1780)) in more southern environments is an adaptation to semi-arid environments with limited primary productivity (Parker *et al.*, 2009) whereas their northern conspecifics have increased energy demands as a response to the seasonal abundance of forage (Strickland *et al*., 2005). Metabolic demands may preclude foraging in areas with low forage amounts of poor nutritional value (Parker *et al*., 2009). However, although individuals may not forage on plants that provide a poor energy return, it does not mean that they frequent localities with exclusively homogenous high-quality plant material. On the other hand, high quality plant material may occur at a particular site, but it does not mean that it is automatically available for consumption (Gaillard *et al*., 2010); this may be either through physical barriers, or because of competition from other taxa. This is important to consider when investigating hypsodonty, along with other dental traits, as tooth form is correlated with the most mechanistically challenging foods that are only occasionally consumed, and not reflective of the typical diet (Evans and Pinena-Munoz, 2018). Hypsodonty should be viewed more as "setting the boundary conditions" in what is available to individuals as habitats, and therefore diets (Fortelius *et al*., 2014) and is not necessarily related to presence or absence of particular vegetation types. This is a key consideration when examining the relationship between hypsodonty index and

climate variables as hypsodonty may only be able to predict extremes rather than average conditions.

Spatial heterogeneity of vegetation is controlled by different factors depending on spatial scales. For example, on broad spatial scales, patterns of savanna vegetation are primarily determined by spatial differences in abiotic variables such as rainfall and nutrient availability. However, when looking at finer spatial scales, vegetation patterning is linked to herbivory, fires and other disturbance, surface water processes and soil nutrients and organic matter (De Knegt *et al*., 2008). There is a likelihood that the factors operating at finer scales have more of an impact on the plant community and vegetation development during times when the landscape or ecosystem is not in a balanced equilibrium state and responding stochastically (for example, to environmental perturbations). It has been suggested that foraging at any locality should relate to the vegetation at larger spatial scales, and that the situation at a very localised level is not of significance in terms of plant-herbivore interactions (De Knegt *et al*., 2008). This remains to be tested robustly in the literature, but in the context of this research, it is important to bear in mind that as the spatial resolution of the hypsodonty index data is at a locality level (each locality is treated as a 'community'), it may be the wider vegetation-climate signal that is captured. Accordingly, the 'community' will also be more spatially extensive. This may go a long way to explaining the wider scatter in the hypsodonty-climate correlations shown in section 4.2.

Faunal clusters or 'pools' that result from investigations into dental functional traits such as hypsodonty are indicative that associated functional trait specialisations are likely to be barriers to large-scale mixing between regions (Lintulaakso *et al*., 2009). This may explain some of the results seen in section 4.2 when correlations between climate variables and hypsodonty index (when approached from a 'global' scale including all localities) are shown to be weak, yet statistically significant in almost all co-variate pairings and in the regression modelling. Results of the climate correlations are discussed in more detail in section 5.3.

5.1.5 Life history traits

Intraspecific dietary differences exist in many ungulate taxa, typically differences between the sexes. Different levels of food intake are related to reproductive behaviour with different diet selection and habitat segregation between reproductive and non-reproductive females and males (Parker *et al*., 2009). In terms of hypsodonty, it is an allometric phenomenon and hypsodonty index as a metric removes any effect of body size. As such, there is no evidence of differences in hypsodonty index between males and females, regardless of the existence of sexual dimorphism in body size in any taxon.

However, it is yet to be established whether increased food intake in pregnant females is of any consequence for hypsodonty. As the aim of this research is to develop hypsodonty index as a proxy for Late Pleistocene climate, and it is impossible to determine sex from isolated fossil teeth, this is not followed as an avenue of investigation in this thesis.

Group size impacts the number of herbivores present on the landscape and has a similar effect on vegetation as climate. Duringtimes of drought, this pushes the vegetation to pioneer stage, whereas periods of higher rainfall push the plant community toward climax stage. These effects interact and are exacerbated by the number of grazers on the landscape, creating thresholds above which the landscape is no longer in an equilibrium state (Vetter, 2005). This may mean that the hypsodonty-climate relationship becomes difficult to model when communities go through successive phases of equilibrium and non-equilibrium. Species diversity was included by Damuth *et al*. (2002) in a study of the relationship between hypsodonty index and mean annual precipitation and this may go some way to mitigate the effect of exceeding community carrying capacity and ecosystem disequilibrium.

5.1.6 Considerations to carry forward

Both Chapter 2 and the points made above highlight the multiplicity of interacting biological and ecological factors in operation. The presence-absence approach used by a number of studies (e.g. Eronen *et al*., 2010a; Liu *et al*., 2012, Žliobaitė *et al*., 2016) may turn out to be the most appropriate for modelling hypsodonty, diet and climate relationships, but full exploration of locality-level spatial scales for both hypsodonty index and climate variables has not been undertaken before. The latter approach will, therefore, discussed in detail in the remainder of this chapter.

5.2 Interspecific and intraspecific variation of hypsodonty index

This study considered as many ungulate taxa as possible when undertaking measurements and this is reflected in the unique size and breadth of the full set of hypsodonty index measurements. Measurements were collected from 148 different taxa across seven families in an effort not only to establish comprehensive understanding of the natural variations in ungulate hypsodonty index but also to assess the assumption that each taxon has sufficiently little variation to permit classification of the whole taxon as one class of hypsodonty (see Fortelius *et al.*, 2002).

5.2.1 Equidae

The family with the largest hypsodonty index values is the Equidae (mean hypsodonty index of 4.07). This is to be expected as taxa that are predominantly grazers (as is the case for the equids) have hypsodont dentitions (Janis, 1984, 1988; Williams and Kay, 2001). When examining the equids at taxon level, however, there are some notable differences. The most hypsodont taxon is the plains zebra (*Equus quagga* Boddaert, 1785), from which 41 measurements were taken in the present study. Although this is a relatively small number of individuals compared to some taxa in other families that will be discussed later in this section, this is the largest number of measurements of the equids in this study. The coefficient of variation is 0.14, which is low, showing the data tend close to the mean. Along with a normal distribution, it can therefore be seen that intraspecific variation of *E. quagga* is low. The relatively high level of hypsodonty in this species is likely related to the fact that its diet consists of approximately 92% grasses (Lamprey, 1963). Grasses are fibrous and tough, but as discussed by Damuth and Janis (2011), the fibrous nature of plant material is not likely to contribute significantly to tooth wear, so the fibrous nature of grasses is unlikely to be contributing to the high level of hypsodonty in this case. Grasses often contain phytoliths (Piperno, 2006) but the effect on tooth wear is debated with opposing views present in the literature (Baker *et al*., 1959, cited in Damuth and Janis, 2011; Erickson, 2014; Lucas *et al*., 2013) and it is generally assumed that exogenous dust and grit is a contributor to tooth wear (Janis, 1988), with quartz content in soils a potentially significant abrasive agent (Damuth and Janis, 1988).

Zebra are highly migratory and are known to follow sources of water. It has been suggested that zebra, when feeding, have a slight preference for fresher as opposed to dry grasses (Estes, 1991). This may mean that zebra actively avoid the driest areas and therefore intake of exogenous dust and highly abrasive, dry vegetation may be minimal. However, if the teeth are revealed as highly hypsodont, and this is supposedly reflective of higher levels of these abrasive factors, perhaps the sheer volume of grasses consumed may contribute to hypsodonty rather than the exact nature of the material consumed. In areas with low rainfall, it has been suggested that zebra consume grass with tall swards, despite its lower quality, to maximise forage intake when higher quality short swards are in low supply. Tall swards of lower quality may be more abrasive so individuals with more hypsodont teeth may be more successful in foraging to meet their metabolic demands (Mwasi *et al*., 2017), especially when there are additional stressors such as episodic droughts. From the other equid taxa in this dataset, the sample size is too small (below ten individuals) to assess confidently any potential intraspecific variation.

5.2.2 Bovidae

The largest number of hypsodonty index values in this study come from the Bovidae family, across 97 different taxa. Across the whole family, there is a large range of hypsodonty index values, from a minimum of 0.95 to a maximum of 5.28, likely reflecting the large range in diets eaten by different bovid taxa. 83 of the 97 taxa showed a normal distribution although 86% of taxa had very low sample numbers (below 30 measurements, which is the average sample size required to deliver a repeatable mean within one standard deviation across all taxa) so this cannot be totally conclusive in these cases. Of the seventeen cases where the distribution of hypsodonty index values within a taxon was not normally distributed, there were thirteen cases where there were adequate sample numbers (at least 30 measurements) for further investigation. Some taxa presented histograms where it is clear that there is no evidence of bimodality and it is consequently assumed that the variation is limited. However, some taxa presented histograms suggesting perhaps more than one mode in the data; these were also suggested to be not normal from the Shapiro-Wilk test. These cases are discussed below.

5.2.2.1 Alcelaphus buselaphus Pallas, 1776

There is interesting variation within the measurements taken on individuals of hartebeest in this study. Out of the 62 individual measurements, there are two apparently separate groupings of values. 32 out of 44 (68%) of the measurements fall between 1.9 and 2.8, the remaining minority of measurements are much more hypsodont (between 4.4 and 5.27) and a large gap is present between the two groupings. Measurement error and misidentification has been discounted and it may be that these different groups of values may represent two geographically distinct populations. A location map of *A. buselaphus* values is shown below (Figure 5.1) and the higher hypsodonty index values (dark orange and red dots) are concentrated mostly on the border of South Sudan and the Democratic Republic of Congo with another few on the Uganda-Kenya border.

Climatic or environmental factors may be driving these differences as it has already been suggested in the literature that there are links between hypsodonty index and temperature, precipitation and net primary productivity (Liu *et al*., 2012). When these locations are subsequently plotted on a basemap of mean annual temperature (Figure 5.2), it appears that the lower hypsodonty index values are present in regions with temperatures higher than 25°C, whereas the high hypsodonty index values seem to be present in areas with mean annual temperatures in the 20.1-25.0°C band. However, there is no unequivocal trend with temperature as some of the mid-to-higher hypsodonty

values are also present in small pockets of temperatures between 10 and 20°C (also higher elevation localities).

Figure 5.3 shows the localities plotted against a basemap of mean annual precipitation and here it can be seen more clearly that the higher hypsodonty index values are present in the wetter region (>1500mm per year), compared to the lower hypsodonty index values, which are present in the drier regions with less than 1500mm precipitation per year. This is contrary to the view put forward in the literature that hypsodonty index is positively correlated with mean annual precipitation (e.g. Eronen *et al*., 2010a). It is reported in regions without abundant fresh drinking water, hartebeest are known to eat roots and tubers (Estes, 1991). The ingestion of less abrasive food material may have some influence on lowering overall hypsodonty in the regions where precipitation is lower, although there may be increased likelihood of consuming abrasive soil particles when consuming roots and tubers. However, it may be that the sample size of 62 is too low to capture the range of natural variation and that this separate spatial cluster of higher values on the South Sudan-Democratic Republic of Congo border is a product of this small sample size. Further work needs to be undertaken to test suitable minimum sample sizes for each individual taxon. Combined with high levels of migratory behaviour on even short timescales (hartebeest are known to migrate away from areas after rainfall events [Estes, 2004]), the hartebeest dataset may have a great proportion of biological “noise” that precludes a clear understanding of hypsodonty variation.

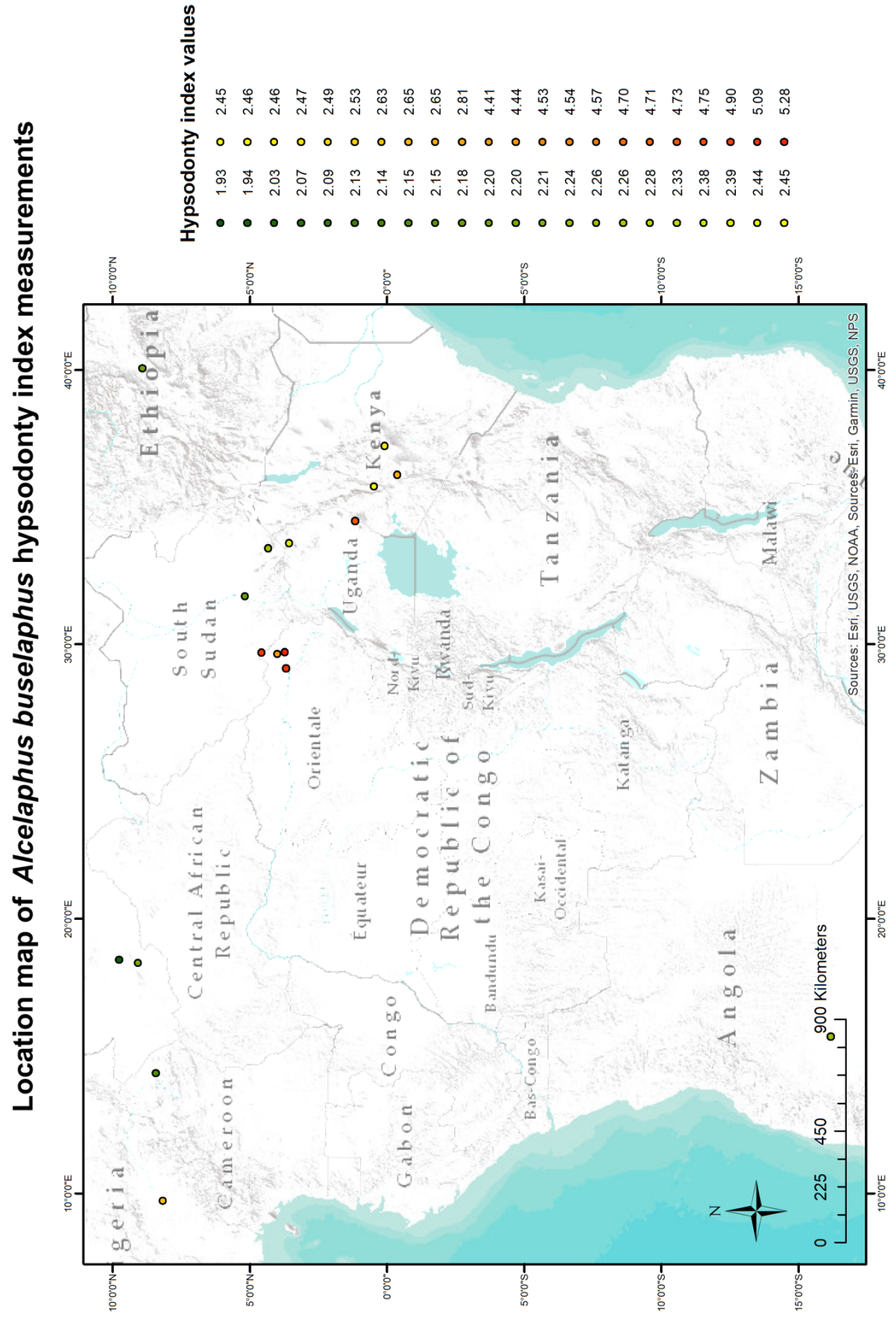

Figure 5.1: Location map of hypsodonty index measurements of *Alcelaphus buselaphus*.

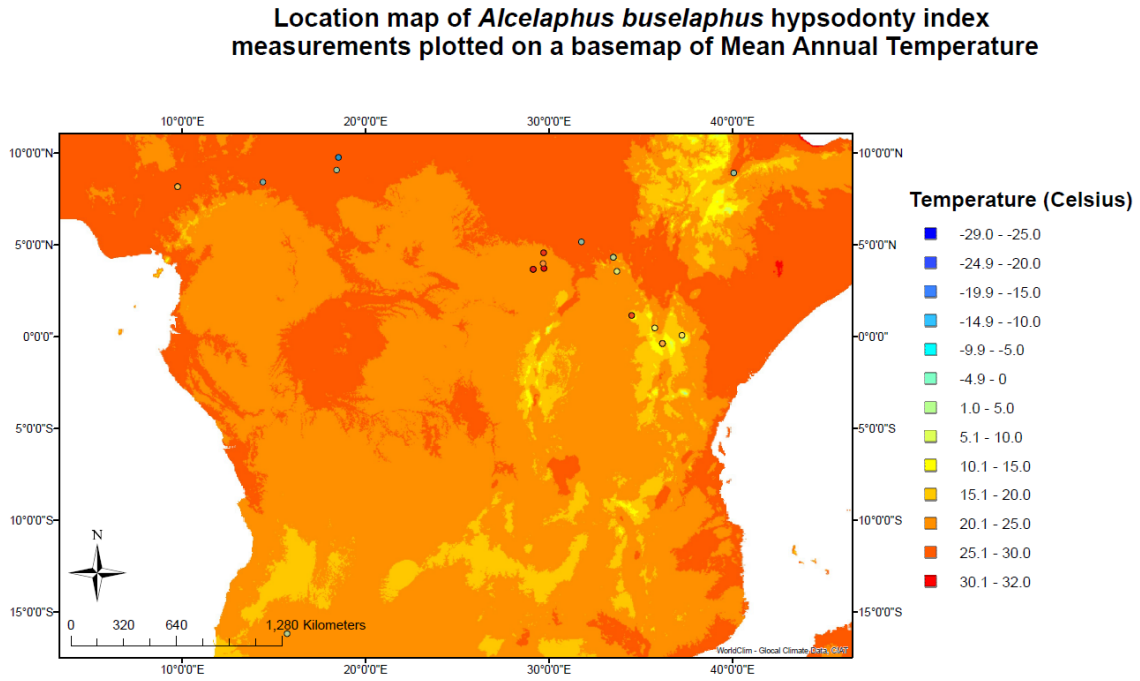

Figure 5.2: Location map of hypsodonty index measurements of *Alcelaphus buselaphus* plotted on a basemap of mean annual temperature. See Figure 5.1 for legend for hypsodonty index measurements.

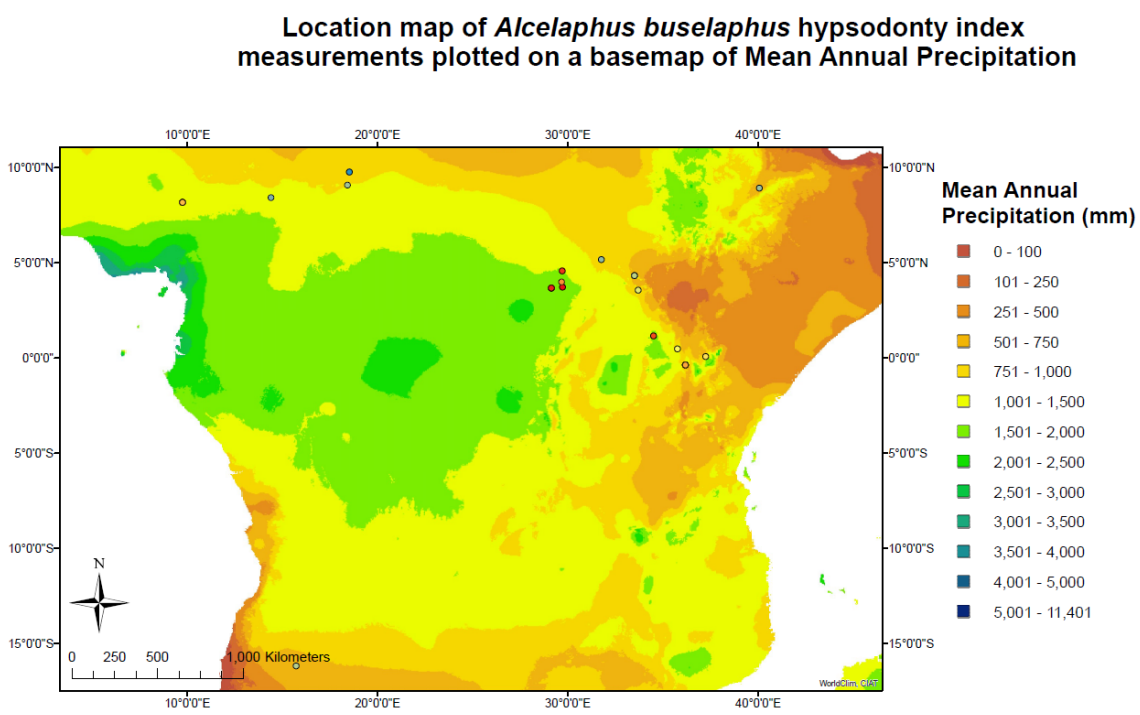

Figure 5.3: Location map of hypsodonty index measurements of *Alcelaphus buselaphus* plotted on a basemap of mean annual precipitation. See Figure 5.1 for legend for hypsodonty index measurements.

5.2.2.2 Cephalophus sp.

Fourteen different species of duiker were measured in this study but there were also 71 individuals that could not be identified to species level. The diets of different duiker taxa are broadly similar, as is their geographical distribution and habitat preferences (IUCN, 2008) so it is not clear at first glance why hypsodonty index measurements for *Cephalophus* sp. are not normally distributed according to the Shapiro-Wilk test. The coefficient of variation is low, which indicates a close dispersal around the mean. The histogram indicates that the distribution does resemble a normal distribution but there is a clear gap in the histogram that could be a manifestation of the sample size. The highest hypsodonty index values at the edge of the histogram consist of only two datapoints filling the uppermost bin. As can be seen from the location maps in Figures 5.4-6, the highest hypsodonty index values for *Cephalophus* sp. are located in Cameroon (2.208) and southern Tanzania (2.150). There is also another relatively high hypsodonty value of 2.012 plotting in central-eastern Tanzania, which is interesting as all the other *Cephalophus* sp. were located in the rainforests of Cameroon. From the map against mean annual temperature (Figure 5.2) it can be seen that there appears to be no relationship between hypsodonty of duikers and temperature. Interestingly, as suggested by previous research (e.g. Janis, 1988), the highest hypsodonty index values are plotting in an area with lower mean annual precipitation. Without resolving to species level, it is difficult to assess the relationships seen between hypsodonty index and climate as different duiker taxa inhabit quite different environments. For example, the bush duiker is never found in deep forest, in contrast with the forest duikers that are adapted to living in deep bush forests of central Africa (IUCN, 2018). It is worth noting that the magnitude of difference between the highest few values is only 22% above the mean value indicting only a marginal difference.

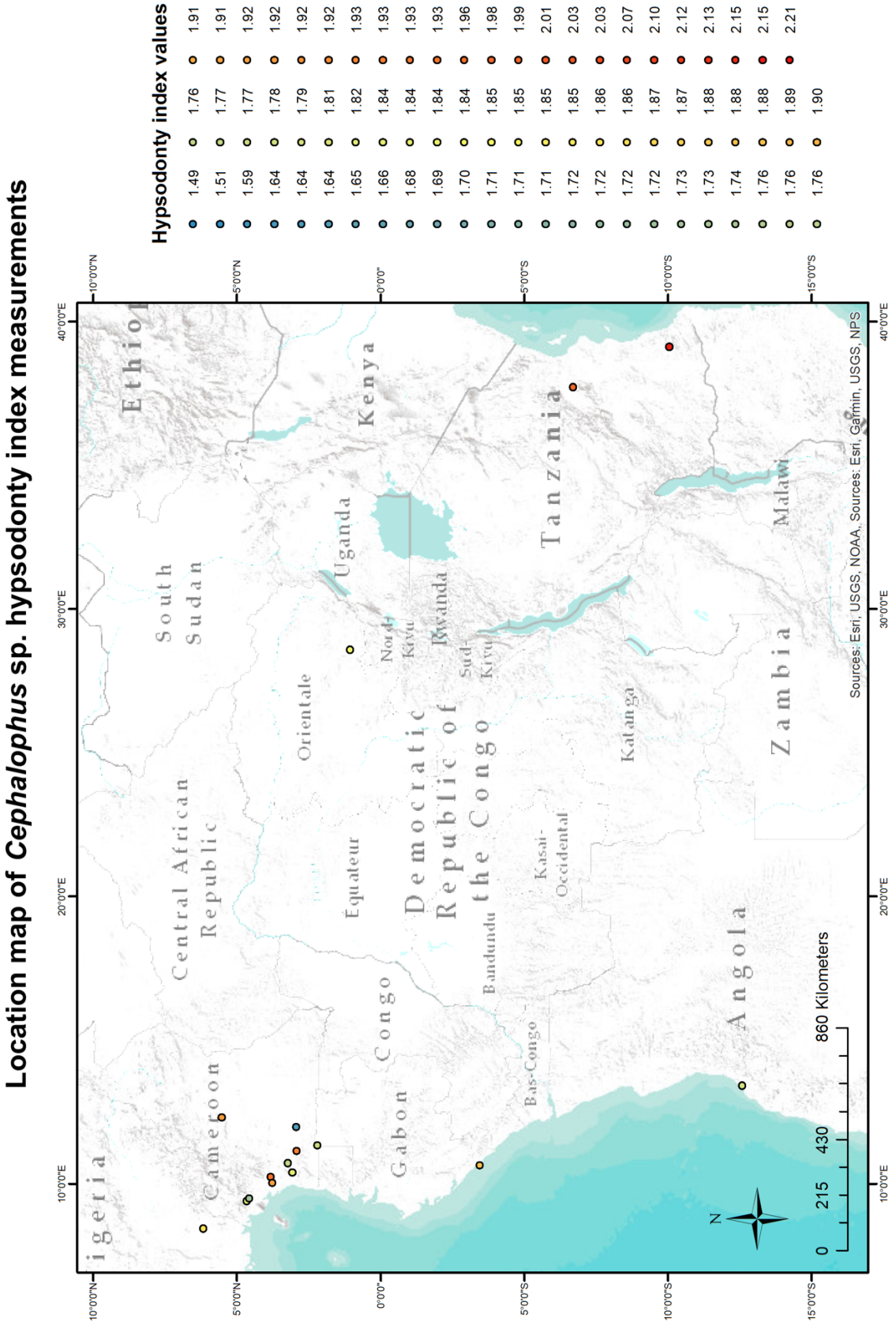

Figure 5.4: Location map of hypsodonty index measurements of *Cephalophus* sp.

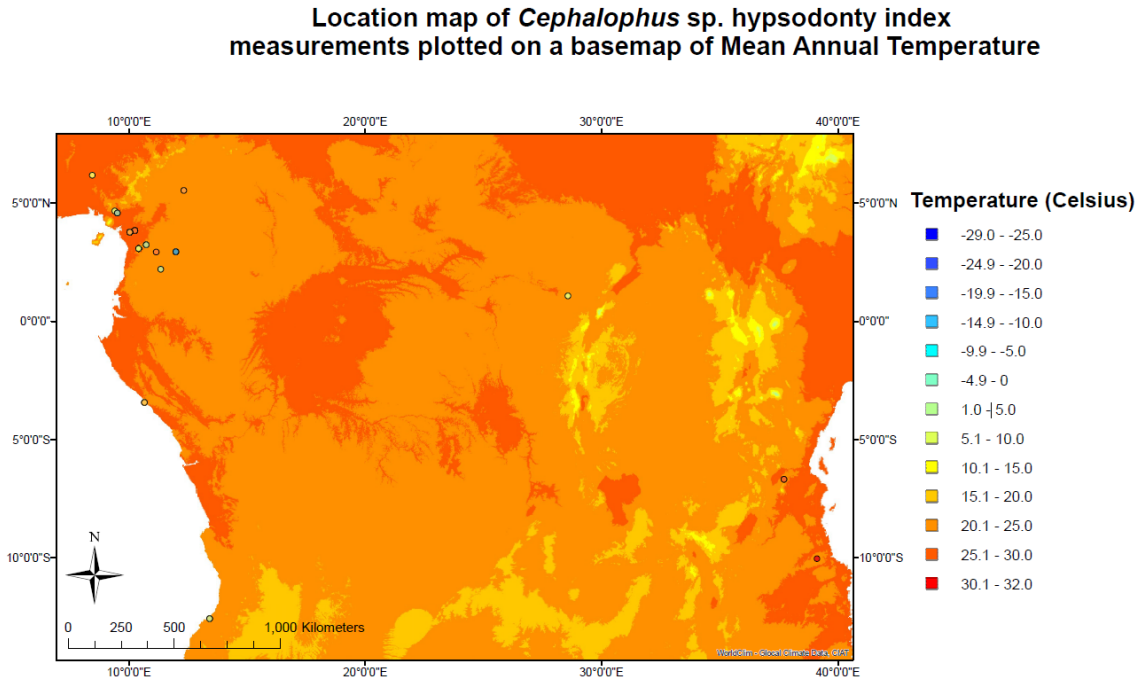

Figure 5.5: Location map of hypsodonty index measurements of *Cephalophus* sp. plotted on a basemap of mean annual temperature. See Figure 5.4 for legend for hypsodonty index measurements.

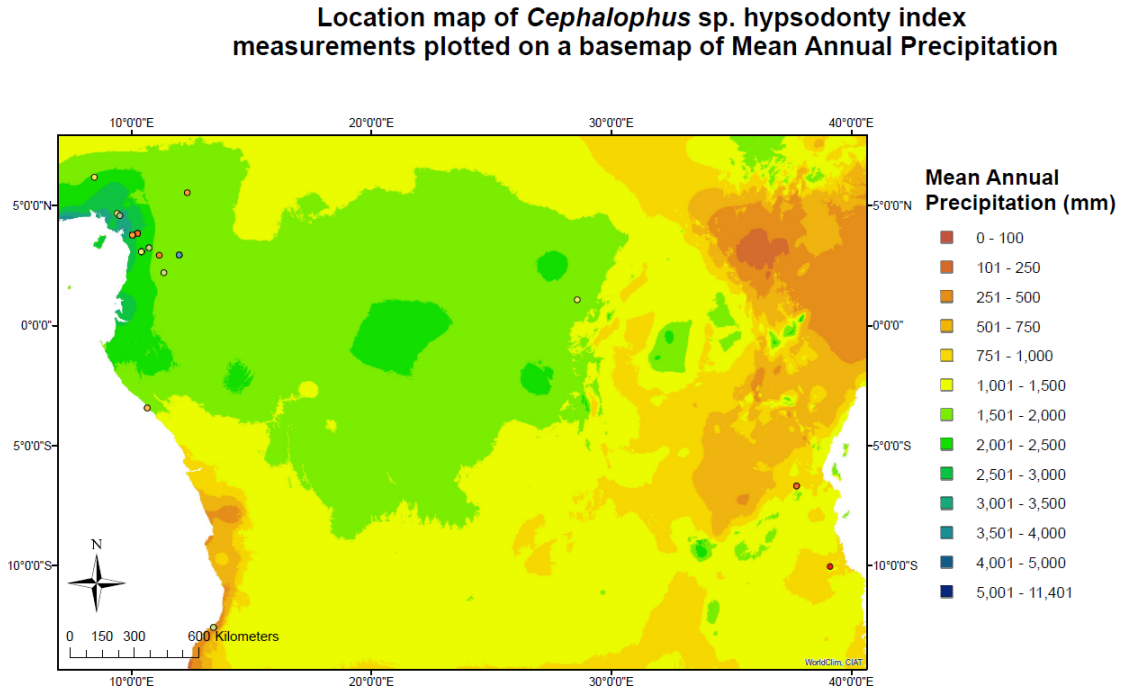

Figure 5.6: Location map of hypsodonty index measurements of *Cephalophus* sp. plotted on a basemap of mean annual precipitation. See Figure 5.4 for legend for hypsodonty index measurements.

5.2.2.3 Hippotragus equinus Harris, 1838

The histogram for the hypsodonty index values for the roan antelope (*Hippotragus equinus*) indicates that the distribution is not normal and could be bimodal, with most of the values forming one lower mode whilst a second mode of higher hypsodonty index values may be present. The sample of just 58 individual measurements may be a factor in this apparent bimodality as the geographical distribution does not appear to show any clustering of separate populations (see Figure 5.7).

There does not appear to be a pattern with temperature either as both lower and higher hypsodonty index values are equally located within the 15.1 -20.0 and the 20.1 to 25.0 °C temperature bands (see Figure 5.8). Additionally, all of the localities plot within the same band of mean annual precipitation (see Figure 5.9). Roan antelope are known to graze on mid-length grasses (up to 90%) but also to browse on leaves. Their feeding habitats have been described as very specific as they focus on grasses at heights of 40-140mm above the ground, suggested to be related to the neck length and angle of the jaw (Spinage, 1986). Despite the potential of dust and grit from soil being ingested from feeding at these heights, their frequent visits and close proximity (no less than two miles) to watering holes or rivers (Estes, 1993) may mediate the amount of wear that acts on the teeth. It is therefore possible that (small sample size aside) differing amounts of wear are created through varying percentages of grass and herbaceous foliage intake and/or variable frequencies of visits to waterholes, or local differences in soil.

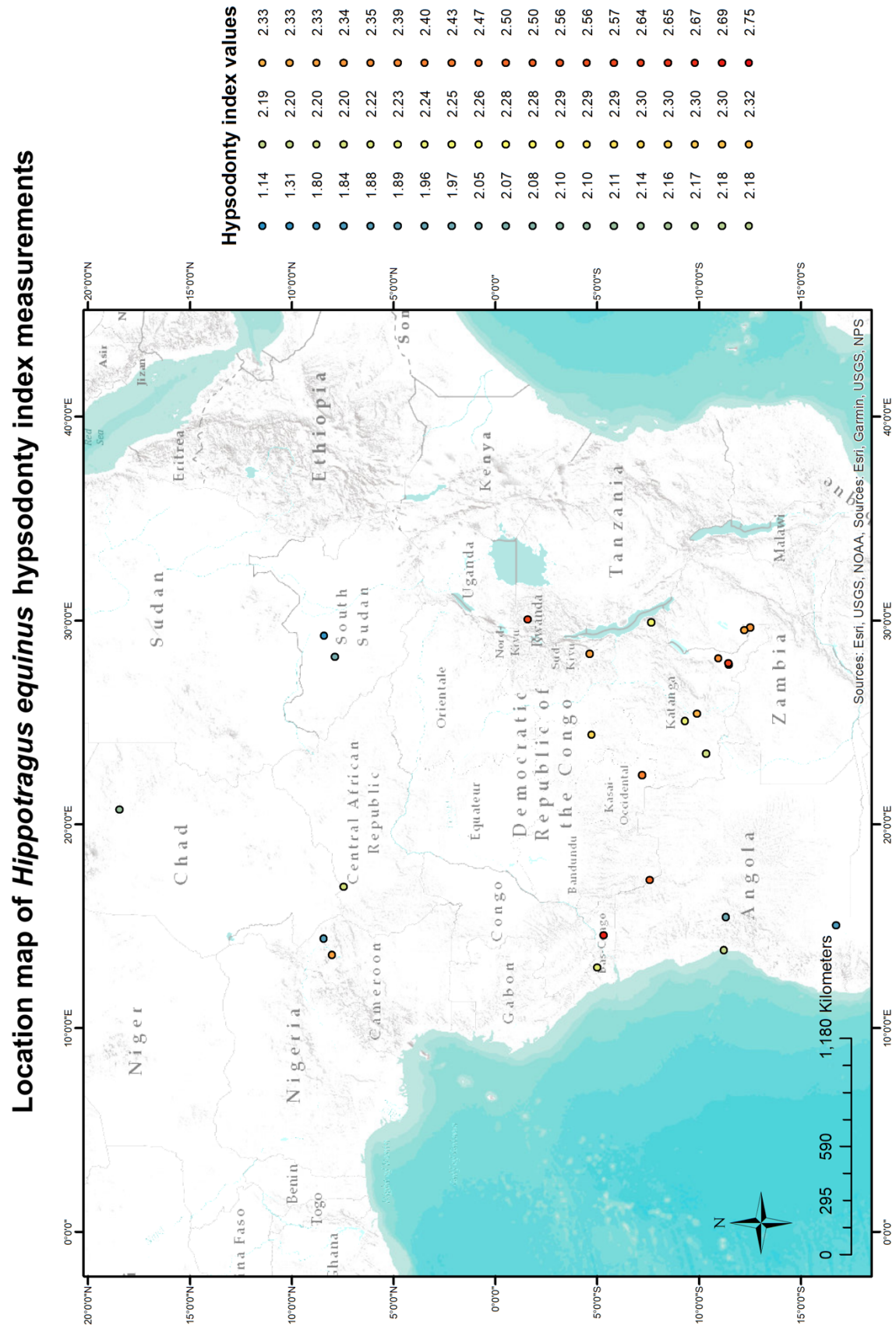

Figure 5.7: Location map of hypsodonty index measurements of *Hippotragus equinus*.

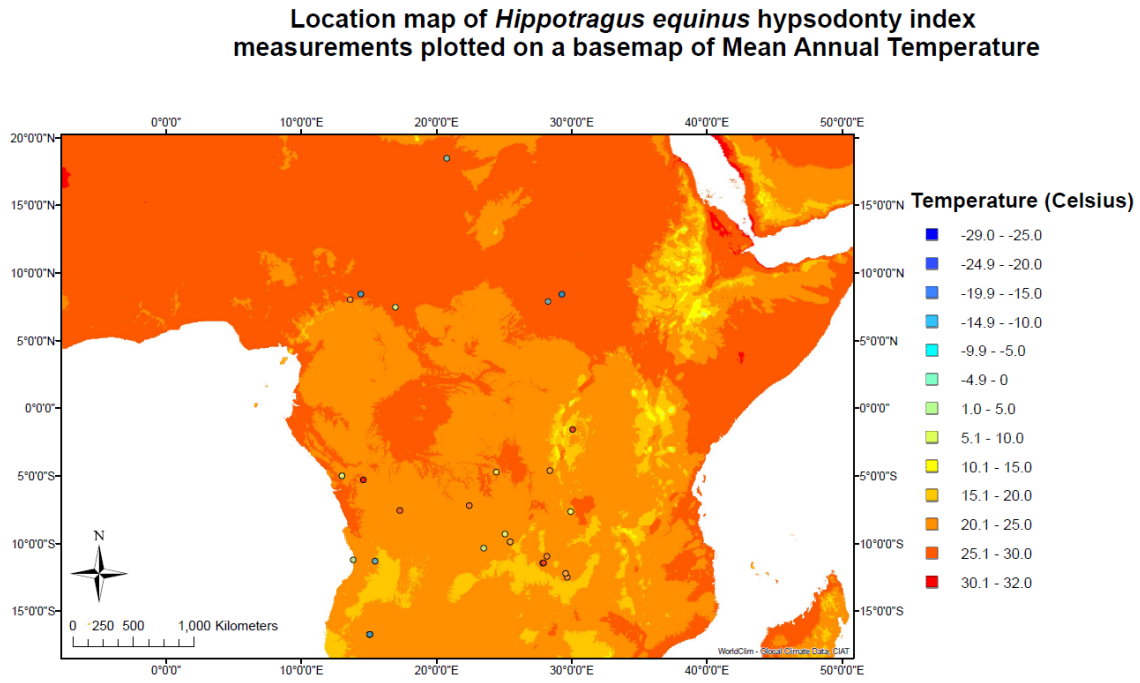

Figure 5.8: Location map of hypsodonty index measurements of *Hippotragus equinus* plotted on a basemap of mean annual temperature. See Figure 5.7 for legend for hypsodonty index measurements.

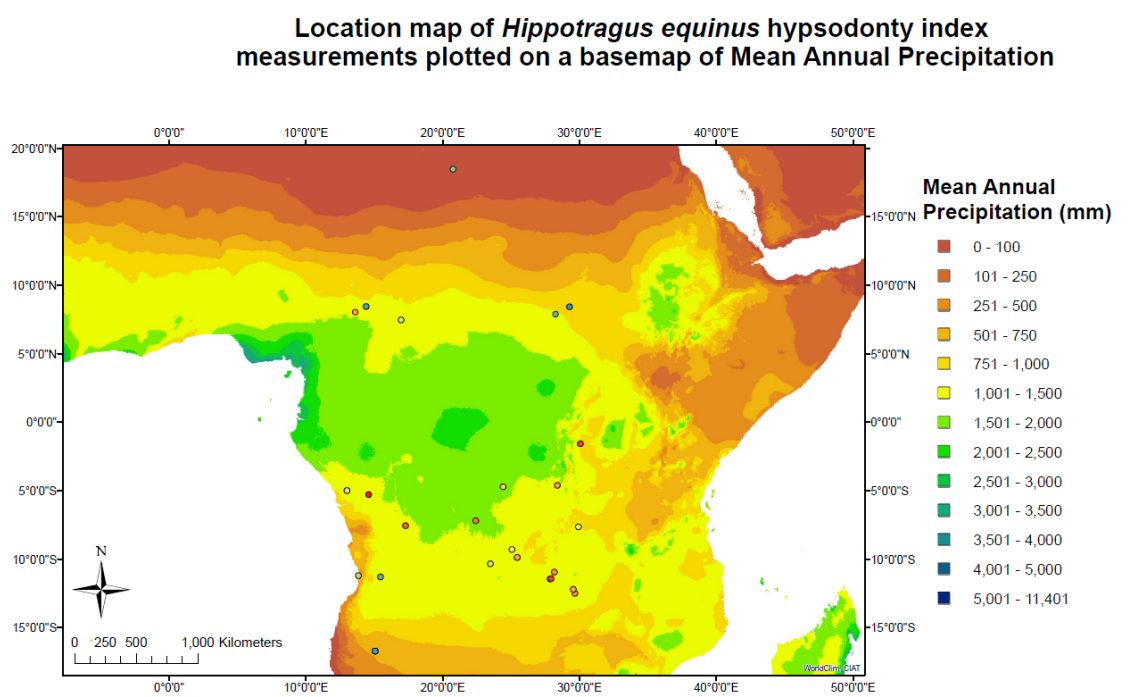

Figure 5.9: Location map of hypsodonty index measurements of *Hippotragus equinus* plotted on a basemap of mean annual precipitation. See Figure 5.7 for legend for hypsodonty index measurements.

5.2.2.4 Kobus ellipsiprymnus Ogilby, 1833

Hypsodonty index measurements for the waterbuck (*Kobus ellipsiprymnus*) are indicated by the Shapiro-Wilk test as not normally distributed, however this may be due to the sample size as the histogram for this taxon (see appendix) shows a normal distribution. The geographical distribution of the measured teeth also appears to show no patterns or clustering (see Figure 5.10). However, the range of values is particularly large, from a minimum hypsodonty index of 1.31 to a maximum of 4.05, over a three-fold difference. *K. ellipsiprymnus* has a diet that consists of around 75-90% grasses, on rare occasions including wetland grasses such as *Phragmites*. There is also a reported switch to dependence on long-life grasses and tree foliage during the dry season (Kassa *et al*., 2008). The species is highly dependent on water and lives in close proximity to water sources and hence has a sparse ecotone distribution (Nowak, 1999). The large range in hypsodonty index may be in part to differing local populations existing over long timescales in areas with longer or shorter dry seasons and thus adapting to consuming higher or lower levels of non-grass foods. Despite the large range, there do not appear to be any spatial differences and the measurements are closer to a normal distribution than the Shapiro-Wilk test indicates. More data for this species may indicate if there is a spatial component to the large range in hypsodonty index values here.

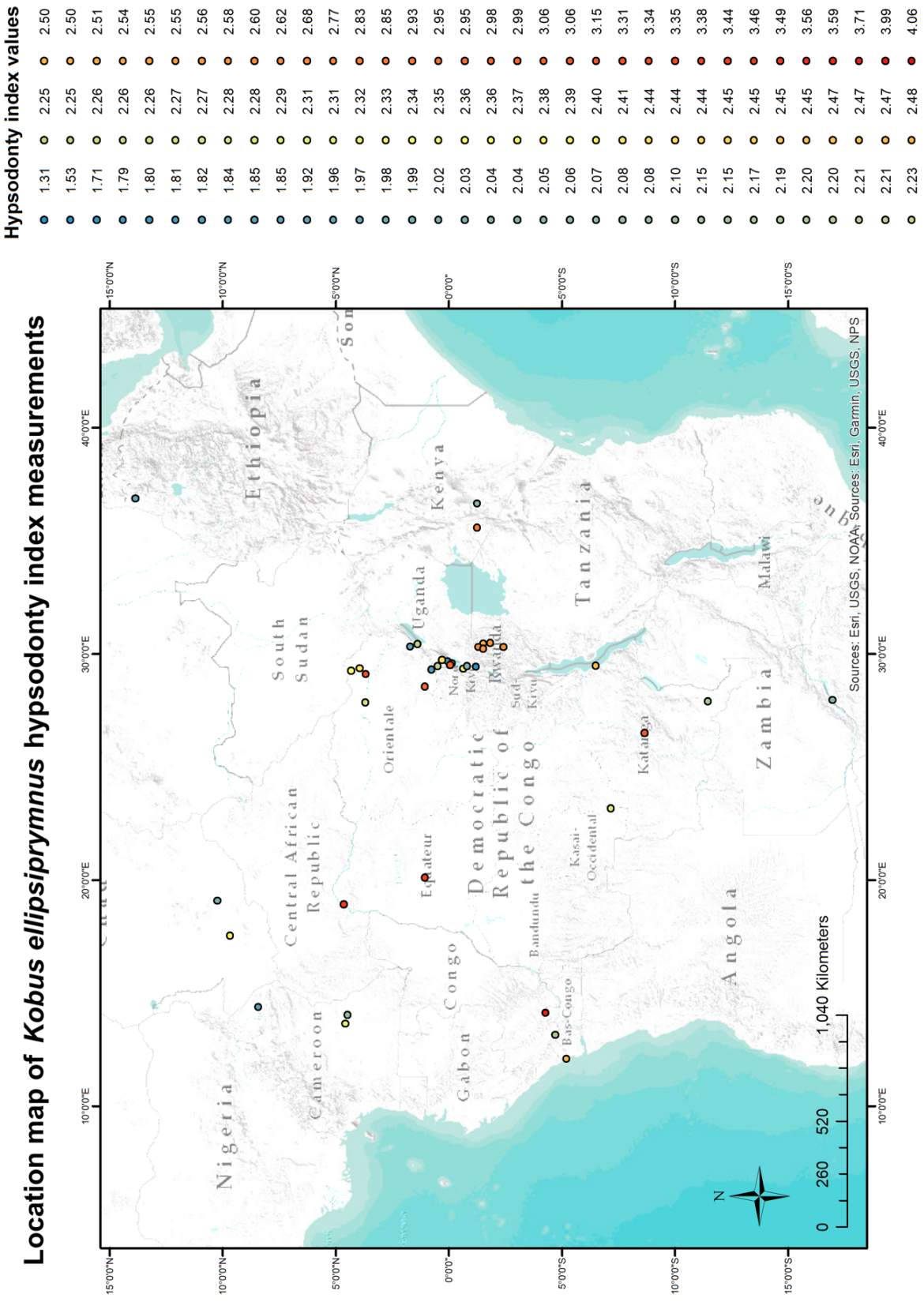

Figure 5.10: Location map of hypsodonty index measurements of *Kobus ellipsiprymnus*.

5.2.2.5 Ourebia ourebi Zimmermann, 1782

The Shapiro-Wilk test indicates that the measurements of hypsodonty index for the oribi (*Ourebia ourebi*) were not normally distributed. However, with a low sample size of 31 and a histogram that does not indicate anything other than one mode, it is unclear if the Shapiro-Wilk result is valid, especially if more hypsodonty index measurements were to be collected.

5.2.2.6 Syncerus caffer (Sparrman, 1779)

The bovid with the largest number of individual hypsodonty index measurements in this study is the African buffalo (*Syncerus caffer*). The Shaprio-Wilk test indicates that the data is not normally distributed, and this can equally be seen in the histogram (see appendix). There are a large number of individual measurements clustered around a lower mode of around 1.5 but there are a few but widespread number of measurements of a hypsodonty index of 3.0-5.0. This is a marked difference and although this second grouping may not be a mode in itself, it is interesting nonetheless. It is worthy to note that all the individuals were only identified to genus level, despite there being two sub-species *S. caffer caffer* (the Cape buffalo) and *S. caffer nanus* (the African forest buffalo), the latter being unsurprisingly present in more forested environments rather than savanna grasslands (Korte, 2008). However, as can be seen from the maps in Figures 5.11-13, it appears that both the lower and higher value for hypsodonty index are present in forested and savanna areas so it is unlikely that subspecific issues explain the differences.

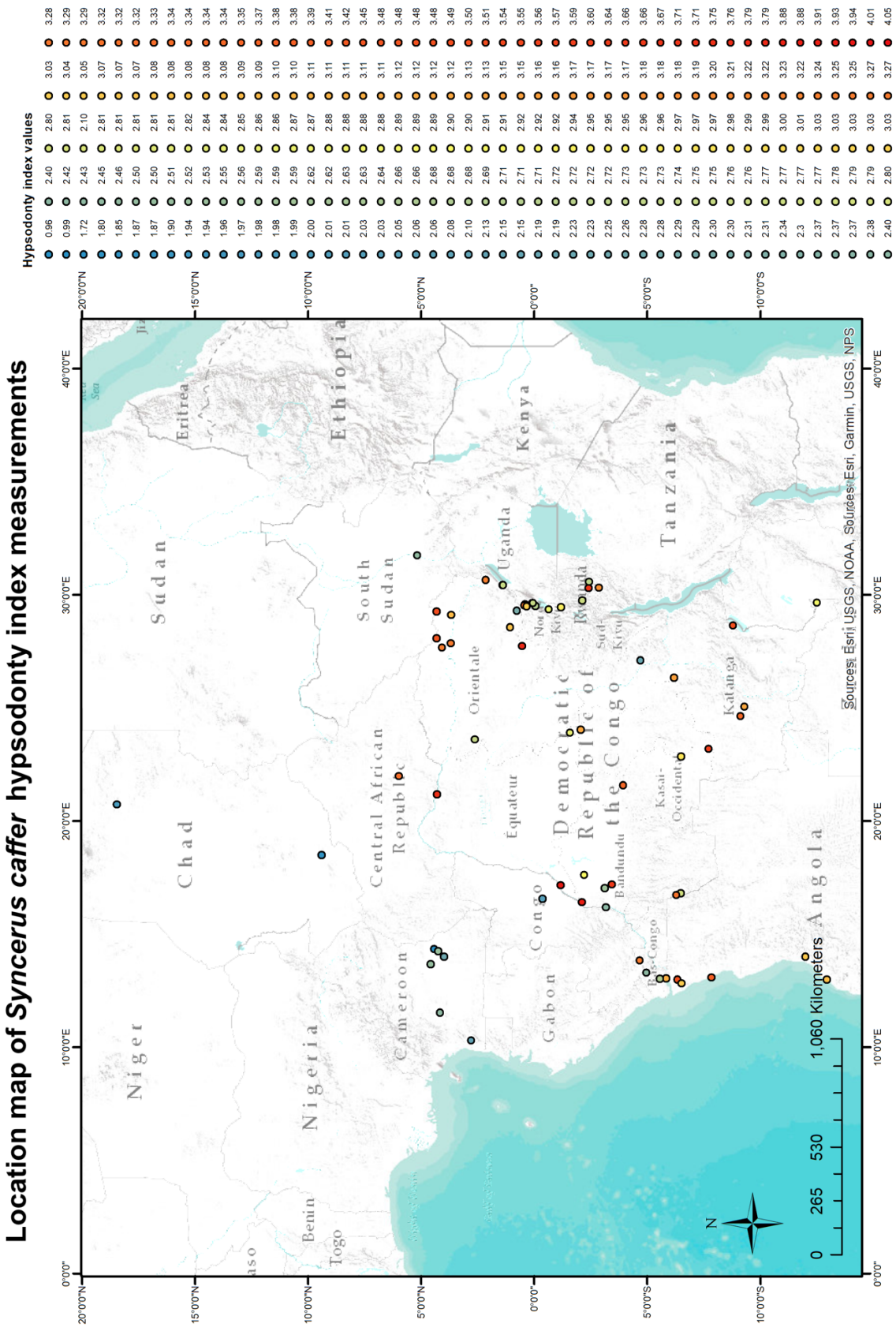

Figure 5.11: Location map of hypsodonty index measurements of *Syncerus caffer*.

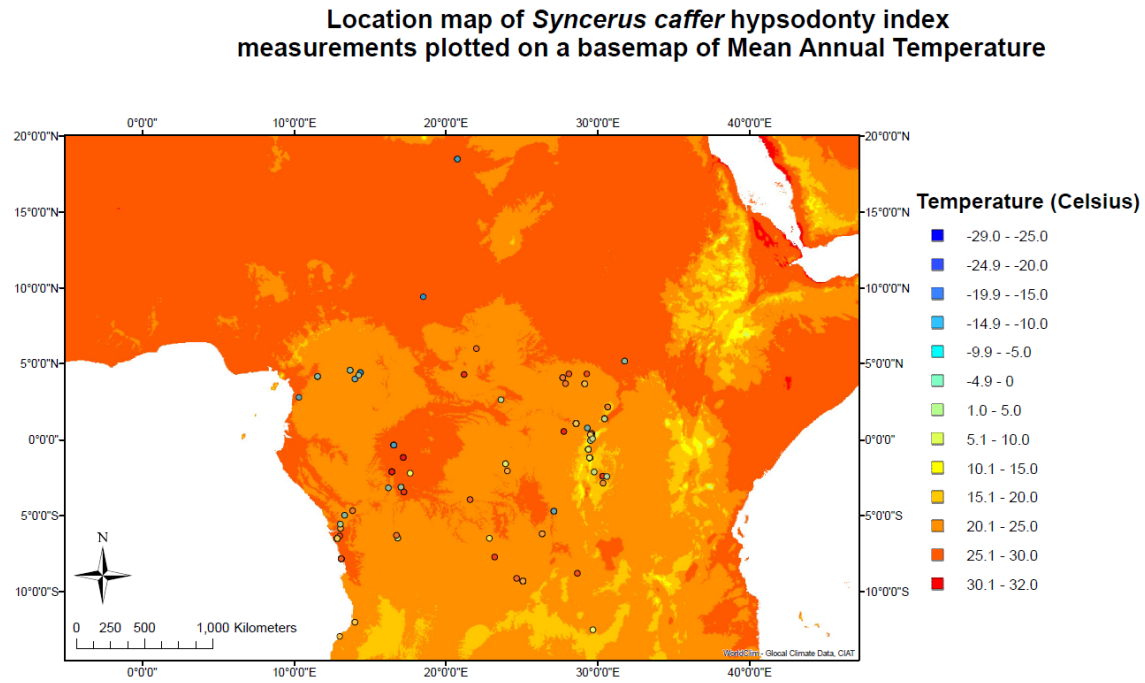

Figure 5.12: Location map of hypsodonty index measurements of *Syncerus caffer* plotted on a basemap of mean annual temperature. See Figure 5.11 for legend for hypsodonty index measurements.

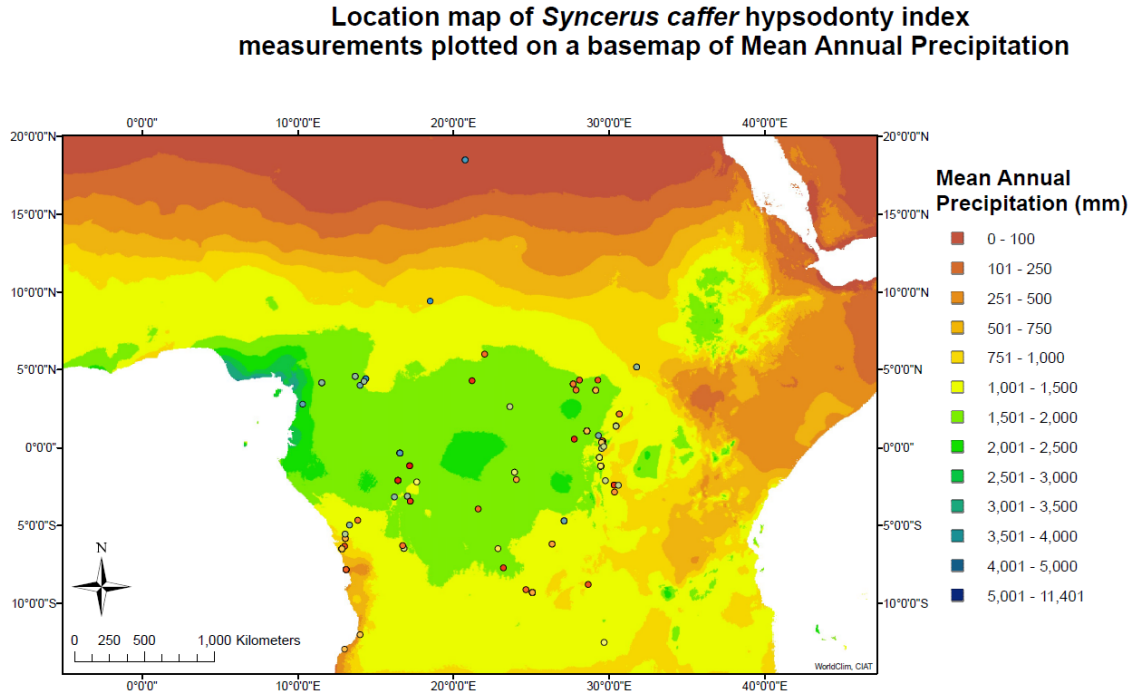

Figure 5.13: Location map of hypsodonty index measurements of *Syncerus caffer* plotted on a basemap of mean annual precipitation. See Figure 5.11 for legend for hypsodonty index measurements.

5.2.2.7 Tragelaphus scriptus (Pallas, 1766)

The hypsodonty index values for the harnessed bushbuck (*Tragelaphus scriptus*) consisted of 176 individual measurements, a comparatively high number of samples. The Shapiro-Wilk test indicated that the distribution was not normal but the histogram suggests normality of the dataset. The location map (see Figure 5.14) shows that there does not appear to be any spatial clustering of any potential populations with higher or lower levels of hypsodonty. The harnessed bushbuck is present in wooded savannas, forest-savanna mosaics, some rainforest (although not deep in the Congo basin), in montane forests and semi-arid lowlands (Furstenburg, 2010), encompassing a wide range of climatic and environmental regimes, although dietary analysis of faecal matter suggests the species is predominantly a browser (MacLeod *et al.*, 1996). With this wide distribution across many ecotones, it may be expected that some clustered areas of differing levels of hypsodonty may exist although it is difficult to assess as the detailed ecology of this species is very poorly understood (Wronski *et al*., 2006).

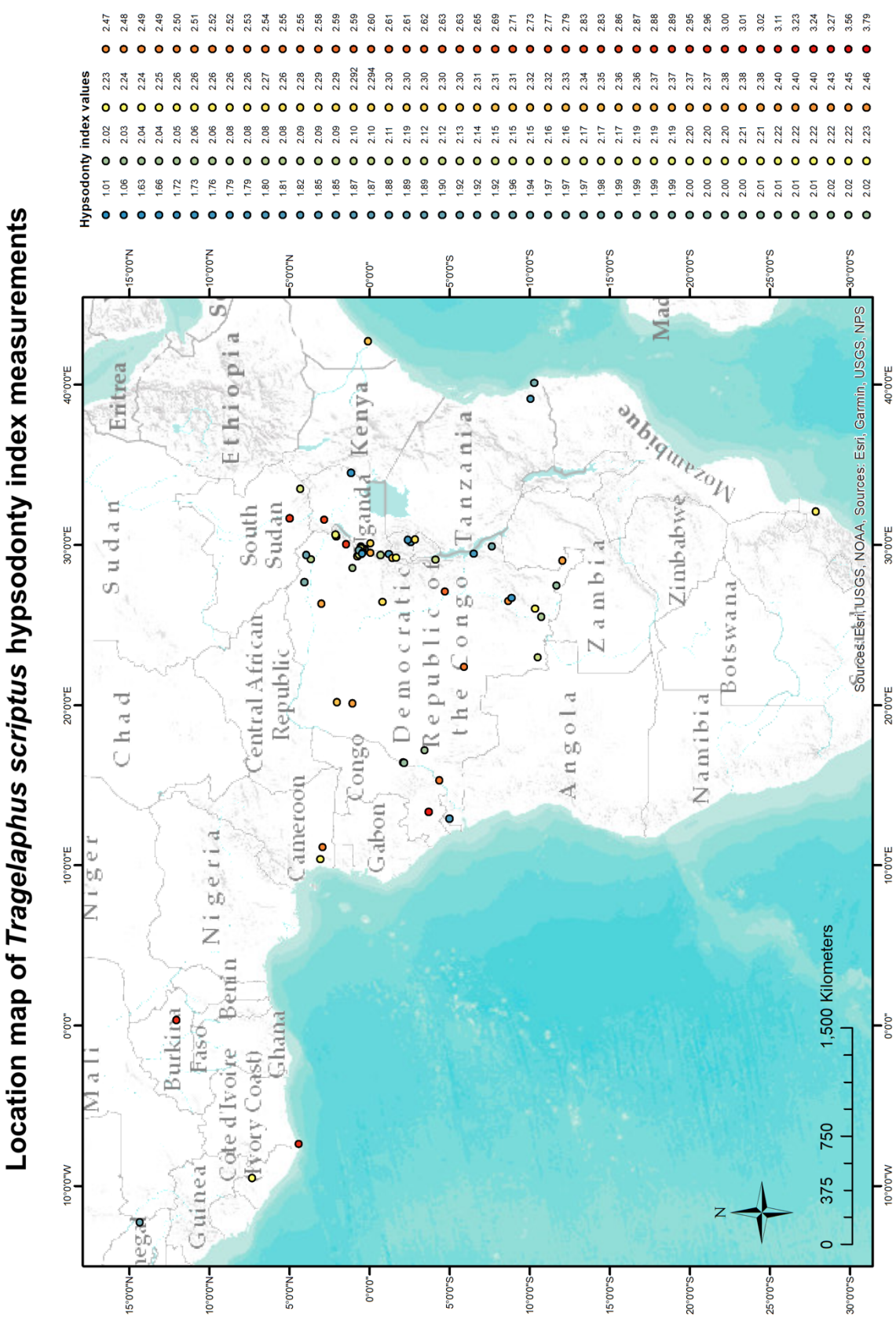

Figure 5.14: Location map of hypsodonty index measurements of *Tragelaphus scriptus*.

5.2.3 Cervidae

The second largest number of hypsodonty measurements on a family level was for Cervidae. Three taxa had very large sample sizes: *Alces alces* (*n*=129), *Capreolus capreolus* (*n*=507) and *Cervus elaphus* (*n*=279). Across all the cervids, the minimum of 0.880 and a maximum of 2.47 represents a smaller range of values than in the bovids, and with a lower mean hypsodonty index. This reflects the diets of cervids, which are more focussed on mixed-feeding and browsing compared to grazing (Parker, 2003), which may be expected to lead to increased hypsodonty (Janis, 1988). The narrower range also reflects the fact that cervid taxa have more similar diets to one another (Parker, 2003) rather than the differing diets found within the Bovidae.

The majority of cervid taxa studied here were shown to have normal distributions. However, many of the cervid taxa that were measured in this study have very low sample sizes. Of those that showed a non-normal distribution, only *Rangifer tarandus* (Linneaus, 1758) had a sample size above 25 (36 measurements) and this taxon is further considered below.

5.2.3.1 Rangifer tarandus (Linneaus, 1758)

The hypsodonty index measurements for reindeer (*Rangifer tarandus*) were shown by the Shapiro-Wilk test to be not normally distributed. However, the histogram does not agree with this (see appendix). The sample size is relatively low, with only 36 samples but to investigate any spatial differences in hypsodonty index it is appropriate to plot these values on a location map (see Figure 5.15). The 36 individual measurements are from only four locations in the Arctic, in northern Scandinavia and Svalbard. The points all very closely spaced (the points plot on top of each other at the map scale used in Figure 5.15; only 4 points are visible out of the total of 36) so it is impossible to see the variation in detail on this map alone. Interestingly, there are two individual measurements (left and right teeth from specimen number NHM1998.395) from Bear Island, in between Svalbard and mainland Norway that show a hypsodonty index of 1.8 and 1.9, the highest in the sample. The flora on Bear Island is very restricted, with reports of only moss, liverworts and lichens present, no trees and an open landscape (Engelskjøn, 1987). As reindeer on the island are feeding on lichens, close to ground level in an open environment, it may be that soil and dust particles (as suggested by Janis, 1988) and the influence of permafrost and frost cover (Engelskjøn, 1987) have led to this population increasing their level of hypsodonty. However, this island is small and remote, and it is likely that the individual reindeer from Bear Island was introduced from another population somewhere else by the Norwegians who established a weather monitoring station on the island as well as a small mining settlement in the 1920s. This introduction

is not documented but is likely as the main purpose of Engelskjøn's work was to investigate potential for grazing reindeer. This may mean that the individuals may not be naturally adapted to the environment at this location and may exhibit hypsodonty levels not related to their present locality (if any relationship at all).

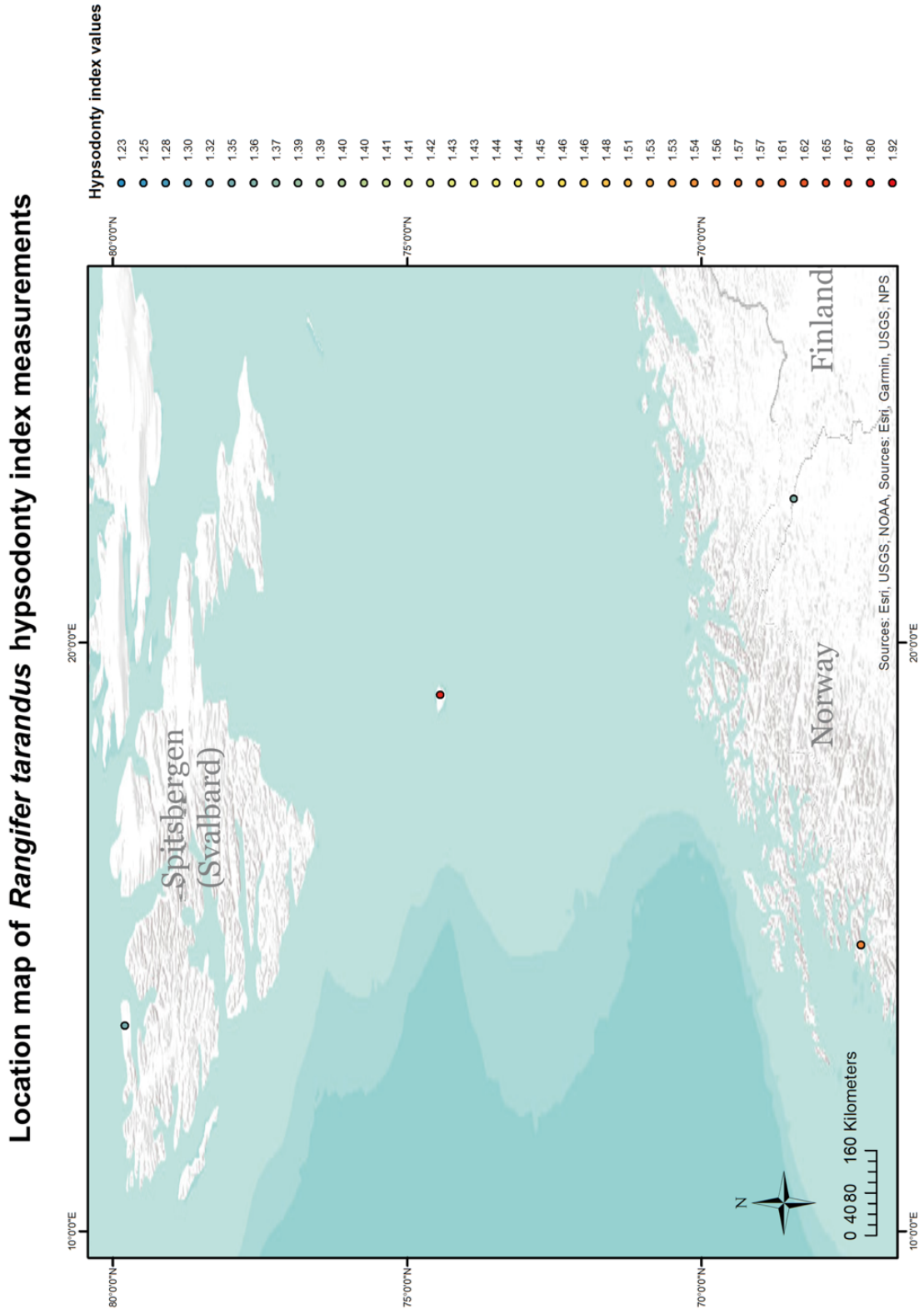

Figure 5.15: Location map of hypsodonty index measurements of *Rangifer tarandus*. Map inset shows the location within northern Europe.

5.2.4 Moschidae

The Siberian musk deer (*Moschus moschiferus* Linnaeus, 1758) was the sole taxon measured from the Moschidae family. The sample size was low (*n*=16) so any true intraspecific variation cannot be reliably assessed here, however the data collected appears to be normally distributed.

5.2.5 Suidae

Nine taxa were measured from the Suidae family, although wild boar (*Sus scrofa* Linnaeus, 1758) was the only taxon that had a sufficiently large enough sample for intraspecific variation to be assessed. The Shapiro-Wilk test and the histogram indicate that the data are normally distributed, and the variation is equally spread about the mean, suggesting low variation within *Sus scrofa*. As a highly versatile omnivore, the species consumes plant and animal matter (Graves, 1984), so as expected, the mean hypsodonty index is relatively low (the lowest hypsodonty index in the whole modern dataset is a wild boar specimen) compared to the rest of the taxa in the ungulate group such as grazers who generally exhibit higher levels of hypsodonty (Janis, 1984).

5.2.6 Tayassuidae

The range of hypsodonty index values for the Tayassuidae family is relatively low compared to that seen in the bovids. This is perhaps due to the similar diets of the peccaries, which are omnivorous like the suids discussed above. The sample sizes for each taxon are very low so, although one taxon (*Tayassu tajacu* (Linnaeus, 1758)) is suggested to have a non-normal distribution from the Shapio-Wilk test, the low sample size means that accurate assessments of intraspecific variation cannot be undertaken for this family.

5.2.7 Tragulidae

The range of hypsodonty index values is very similar to that seen in the Tayassuidae, again, quite low compared to the bovids. The sample size for *Hyemoschus aquaticus* Ogilby, 1841 (n=10) and *Tragulus javanicus* (Osbeck, 1765) (n=4) is quite low so intraspecific variation in these taxa cannot be robustly assessed although the Shapiro-Wilk test indicates a normal distribution. There are 36 measurements only attributed to genus level of *Tragulus* Brisson, 1762 so it is inappropriate to make an assessment of intraspecific variation, although the range across *Tragulus* is comparable to that of the other Tragulidae and the Shapiro-Wilk test indicates normality and therefore variation is not siginifcant in the majority of the Tragulidae although it is necessary to resolve the specimens to species level to be more certain.

5.3 Utility of hypsodonty index as a climatic predictor

As can be seen in section 4.2.1, the hypsodonty index measurements were modified into six different datasets to investigate the relationship between hypsodonty index and climate. Establishing the strongest correlations would then guide approaches to data collection and analysis with any application to fossil material.

5.3.1 Different strengths of correlations with climate between the different datasets

The correlation matrices revealed that there are indeed differences between the different forms of the data, not only in the strength of correlations but also in the degree to which climatic variables are correlated. Even with the most modified datasets, where mean hypsodonty index was calculated for each locality, the number of datapoints remained high at *n*=947, resulting in statistically significant correlations at the 95% confidence level for almost all tested pairs of variables (see section 4.2.2.5). It can therefore be stated with some confidence that the testing process is sufficiently robust but as discussed above, regarding intraspecific variation (see section 5.1), there are some data gaps in certain taxa and some taxa such as *Syncerus caffe*r, *Cervus elaphus* and *Capreolus capreolus* vastly outnumber many other taxa where sample sizes are too low to adequately assess intraspecific variation. However, when all taxa are combined, there is a distribution close to normal, with no empty bin-widths in the histogram (see Figure 4.6). Combining the dataset across all taxa was deemed appropriate as the relationship between hypsodonty index and climatic variables has been suggested to be a global phenomenon across all ungulates (Janis, 1988; Eronen *et al*., 2010a).

The dataset that has the strongest correlations with climatic variables is the mean average hypsodonty index per locality (see Figure 4.6). This was to be expected, as the relationship between hypsodonty index and precipitation found by Eronen *et al*. (2010a), for example, is shown to be at a community level. However, as discussed in Chapter 2, Eronen *et al*. (2010a) artificially created communities at ecoregion level, which in some cases extended across large spatial areas and their associated environmental gradients. Through examination of the nature of the environmental gradients, it is suggested that the ecoregion scale is too large to be appropriate for investigating relationships between a morphological characteristic and climate. As outlined in Chapter 3, the methodological approach of this study narrows and focuses the spatial scale (or ‘community’) down to locality level of individual tooth measurements. Not only does organising the hypsodonty index data in this way show the strongest correlations with climate, it is also methodologically the most rigorous.

Removing the migratory species did not have any effect on strengthening the correlation, in fact, this weakened it. This approach was not tested in the previous research by Eronen and colleagues, but it was appropriate to test, since migratory species will be moving across potentially large spatial areas and also across some environmental and climatic gradients that would potentially add noise to the dataset. However, removing the migrant taxa decreased the strength of correlations. Additionally, removal of the migratory taxa caused the strongest climatic correlates to change slightly, with the strength of the relationship with precipitation of the driest month increasing. In contrast, with the full dataset (migrants included), the strongest correlates are all temperature components of the climate. This would suggest that the migrant taxa will move to track precipitation during the driest period of the year, as seen from many biological migration studies of ungulates (Ogutu *et al*., 2008). The decrease in the correlation strength when migrants are removed is also expected if there is a significant component of environmental (and hence climate tracking) inherent within the ungulate communities included in this study. This result suggests that there is a real ability of mammal communities to (at least partially) track changing environmental conditions and that it is not appropriate to exclude migrant taxa from the dataset and analysis. Hence, the decision was taken to focus analysis on the mean hypsodonty index per locality dataset.

5.3.2 Correlations with the different climate variables

The section will discuss some of the individual relationships between the mean hypsodonty index per locality dataset and the climatic variables. First, it will address the strongest correlations, followed by a discussion of those variables that do not seem to have any effect on mean hypsodonty index, and finally examine the possible reasons and mechanisms behind these results.

5.3.2.1 Discussion of the strongest correlating climate variables

Mean hypsodonty index has a moderate positive correlation with isothermality (bio3; R=0.48). Isothermality “quantifies how large the day-to-night temperatures oscillate relative to the summer-to-winter (annual) oscillations” (O’Donnell and Ignizio, 2012, p. 5). When examining Figure 4.21A, there is a large amount of scatter on the plot with some clustering in the bottom left of the plot (lower hypsodonty index and lower isothermality), whereas above isothermality values of 30%, the scatter becomes very large. This suggests that communities with lower mean hypsodonty index are living in areas where the diurnal difference in temperature is much smaller than the difference between summer and winter mean temperatures, which is most locations outside of the tropics.

The second strongest correlation is with mean temperature of the coldest quarter. Figure 4.21B shows a small cluster of datapoints around a 0°C mean temperature of the coldest quarter and mean hypsodonty index values at this point on the graph are clustered around 1.5, a relatively low level of hypsodonty. However, at locations where the mean temperature of the coldest quarter is above 15-20°C, there is a large range of mean hypsodonty index values, from the lowest levels of hypsodonty to the highest. The ecosytems present at these high mean temperatures of the coldest quarter range from semi-arid grasslands to rainforests , whereas locations where the mean temperature of the coldest quarter is around 0°C supports a lower range of ecosystems, although this temperature range includes both environments such as the Andean peaks and southern Scandinavia and the north European plains that stretch to the Baltic Sea (from data exploration from Olson *et al*., 2001), very different ecosystems with different floral taxa, although the range of different types of plants may be equally restrictive (i.e. more homogenous flora, rather than mosaic; e.g. De Knegt *et al*., 2008). This may explain the lower range of mean hypsodonty index values at these localities.

Temperature seasonality, almost a mirror image of mean temperature of the coldest quarter, may be controlled largely by the winter rather than summer temperatures as the similarity between temperature seasonality and 'winter' mean temperature is more visible than with mean temperature of the warmest quarter ('summer'). However, it is impossible to determine whether changes in temperature seasonality are due to summer or winter changes due to the way temperature seasonality is calculated across the year (O'Donnell and Ignizio, 2012). It can be seen that the two variables themselves have a strong positive correlation between them of 0.89. Unsurprisingly, the correlations with hypsodonty index are the same strength although acting in different directions (positive vs. negative). When examining the data points, there is a very large amount of scatter, especially at the left-hand side of Figure 4.21C. In locations where temperature seasonality is low, the range of hypsodonty values is very large, whereas in localities with higher temperature seasonality, there is a lower mean hypsodonty index. A possible explanation may be that taxa with lower levels of hypsodonty are present at locations regardless of temperature seasonality, perhaps because these taxa are more flexible as mixed feeders, whereas those with higher levels of hypsodonty appear to be present in localities with lower temperature seasonality. As temperature seasonality is strongly correlated with mean temperature of the coldest quarter, and a similar scatter pattern is also present there (see Figure 4.21B), it is perhaps mean temperature of the coldest quarter that is more important to consider (see discussion above).

Mean diurnal temperature range has a positive correlation with mean hypsodonty index (R=0.47), although when looking at the scatter plot (see Figure 4.21D) the datapoints

are very dispersed away from the line of best fit with no apparent clear relationship. The correlation calculated may be a factor of the large sample size. There is a slight cluster of datapoints around a mean diurnal temperature range of around 7-8°C and a mean hypsodonty index of around 1.5. The regions with this level of diurnal temperature range are much of the world outside the sub-tropical desert belts. Interestingly, it might be hypothesised that the mean hypsodonty index for localities with this low mean diurnal temperature range should be wider in range, since much of the world does not have a very high diurnal temperature range. As the main driving mechanism between ungulate hypsodonty and the environment is suggested to be vegetation (both vegetation in the diet and climatic control of vegetation type [Janis, 1984; Fortelius and Janis, 2011]), and there is a limited link between diurnal temperature ranges and vegetation development, it is unclear whether this correlation has an ecological mechanism underpinning it or whether it appears by chance. The strength of 0.47 and the high scatter of the datapoints suggests that there is no real relationship.

5.3.2.2 Discussion of the weakest and non-correlating climate variables

In contrast to the view in the literature that mean annual precipitation correlates with mean hypsodonty index (e.g. Eronen *et al*., 2010a; Liu *et al*., 2012), it has been demonstrated here that mean annual precipitation has no correlation with mean hypsodonty index per location. The *p*-value of 0.68 shows that the *R* value of 0.013 is not statistically significant. Figure 4.22A shows a large amount of scatter and it is clear from visual inspection that no relationship exists between the two variables. It appears that the relationship is not present in solely ungulate taxa, perhaps because the vegetation-hypsodonty-climate link has a large number of possible variables that cannot be easily accounted for in this type of modelling. The regression models created in the past (Eronen *et al*., 2010a; Liu *et al*., 2012; Žliobaitė *et al*., 2016; Oksanen *et al*., 2019) added other dental traits (e.g. loph count) to improve correlation with mean annual precipitation. Unfortunately, this is deemed here to be futile when focussing only on ungulate taxa as many of these dental traits (which were not added to models as continuous variables, but instead as discrete categorical variable) are the same for a large number of ungulate taxa. For example, in the case of loph count, a majority of ungulates have two lophs. As there is not an ecometric approach here, this inclusion would not improve correlation or model fit in the case of this study. The same approach was carried out in the previous studies mentioned for mean annual temperature, for which a correlation of 0.45 is apparent in this dataset, but as discussed above, the scatter revealed by plotting the temperature variables against hypsodonty is very problematic,

perhaps suggesting that there is no clear mechanistic link between temperature and hypsodonty.

There are three other variables that show no correlation with hypsodonty index and these are all precipitation components. Particularly for precipitation of the coldest quarter, there are a large number of points plotting on the scatter plot in vertical lines (see Figure 4.22B), showing that for localities with very low precipitation in their coldest quarter, the mean hypsodonty index values cover almost the full range that was measured in the dataset.

Aridity index was also investigated as a potential correlation with hypsodonty index, as suggested in the literature (Fortelius *et al*., 2002; Eronen *et al*., 2010a). It is clear that aridity index includes both a component of precipitation (the mean annual preicipitation) but also a component of temperature (potential evapotranspiration). The correlation between mean hypsodonty index and the calculated aridity index values is weakly negative (R=-0.29) but the plot has a large degree of scatter and very few points plot within the 95% confidence interval of the line of best fit. It appears that there is no real correlation between aridity index and mean hypsodonty index at the localities in this dataset.

5.3.2.3 Implications of the regression modelling

The choice of the variables that were included in the attempt at regression modelling is outlined in section 4.2.4. As there is one dependent variable sought (hypsodonty index) from a number of independent variables (climate), multiple linear regression was first attempted. Mean diurnal temperature range, annual temperature range and precipitation seasonality were chosen as the variables for the model as they showed the highest correlation (albeit rather weak R values) and were not redundant after checking for autocorrelations of the climate variables. The three variables together explained only 36% of the variation in mean hypsodonty index. The scatter in all the correlation plots is so large and the biological variation so noisy, that it appears that none of the climatic variables can accurately predict mean hypsodonty index, either alone (the strongest correlating variable used in the regression (mean diurnal temperature range) only explained 23% of the variation) or in combination.

5.4 Summary and potential approach for application to Late Pleistocene fossils

From the analysis of correlations between mean hypsodonty index and the nineteen different climate variables, it can be seen that there is little evidence of a strong relationship between hypsodonty and climate. The prior assumption that the relationship existed on a global scale, regardless of taxa, means that when all taxa are included, the scatter in every mean hypsodonty index-climate variable pair is very large, and the dataset is inclusive of all the noisy biological variation present across the ungulate group. There are, however, still some interesting patterns that can be observed. In particular, the key idea in the literature, that precipitation and aridity are controlling hypsodonty (e.g. Damuth *et al.*, 2002; Janis *et al.*, 2004, Eronen *et al.*, 2010a), does not seem to be upheld by the data in this study. Temperature components of climate have more of a correlation with mean hypsodonty index but the mechanisms behind this are unclear. The large amount of scatter also suggests that the relationships observed may not be ecologically real but, instead, a factor of the large sample size. Even restricting the study to ungulates still reveals the inherent data noise problems of variations across 148 taxa with very different ecologies. The effect of many climatic variables in combination is also adding more factors and possible mechanisms than cannot easily be disentangled through this method. Multiple regression with these datasets has not led to a robust model that has any predictive power and regrettably, no new model for easy application to fossil assemblages can be generated as a result. The fossil sites and material used in this study nevertheless still have a very useful role to play, as the large amount of environmental proxy data available can provide some additional tests of those mechanisms and climatic variables that may have a link to hypsodonty index. This is explored in the following chapters.

CHAPTER 6
Results – hypsodonty in Late Pleistocene communities

This chapter presents the results of the investigation of hypsodonty index at seven localities across the Mediterranean with fossil material that dates to the Late Pleistocene. The site selection criteria for these sites is outlined in Chapter 3. The results will be presented for each site, covering the material studied, the taphonomy and condition of the remains, a description of specimens suitable for measurement in each unit or layer and the measurements of hypsodonty index.

6.1 Abric Romaní (Capellades, Spain)

6.1.1 Materials, condition and taphonomy

All available M_3s were inspected to see if they were suitable for measurement in this study. Out of the five ungulate taxa present at the site (Rosell *et al*., 2012), only two taxa yielded suitable teeth for measurement: one specimen of *Bos* sp. and fourteen specimens of *Equus* sp. Measureable specimens of ungulates were only available from levels A, B, E, I, J (a and b), L and M, whereas layers C, D, F, G, H and K yielded no appropriate specimens, despite there being at least one ungulate represented in each level (see Table 3.2).

Of the available M_3s, a large proportion of teeth were broken in a manner that precluded measurement, with many specimens fractured diagonally across the tooth. From those specimens measured in this study, many had worn or broken roots or sediment adhering to the surface but this did not prevent accurate measurement of crown height or width. 28 M_3s from ungulate taxa were available, all but one of these were isolated teeth with the remaining one *in situ* in a broken piece of mandible (specimen number AR 1993 N43 No 1). Fifteen of these were suitable for measurement and are presented in Table 6.1 below. In addition to this, twelve teeth were broken across the crown with the lower part of the crown and roots missing and two more were too worn to be measured.

6.1.2 Measurements of individual specimens

Measurements were taken from the suitable specimens and the data are presented below in Table 6.1.

Table 6.1: Table showing the individual hypsodonty index measurements of suitable M_3 specimens from Abric Romaní. The Level, Quad and Number shown per specimen relate to the site-specific cataloguing system used.

Year of excavation	Level	Quad	Number	Taxon	Hypsodonty Index
Unknown	A	M44	11	*Bos* sp.	4.81
Unknown	B	Unknown	42	*Equus* sp.	3.30
Unknown	B	Unknown	39	*Equus* sp.	4.26
1985	E	P58	182	*Equus* sp.	3.27
1991	I	P49	12	*Equus* sp.	3.90
1991	I	J49	12	*Equus* sp.	4.56
1991	I	N49	7	*Equus* sp.	5.30
1995	Ja	J63	4	*Equus* sp.	2.40
1994	Ja	K59	60	*Equus* sp.	4.64
1993	Ja	L58	44	*Equus* sp.	3.77
1993	Ja	P47	3	*Equus* sp.	4.64
1992	Ja	M58	7	*Equus* sp.	4.30
1995	Jb	M54	130	*Equus* sp.	4.17
1997	L	K56	4	*Equus* sp.	4.14
2002	M	L52	1	*Equus* sp.	3.63

6.1.3 Mean hypsodonty index per level

For each level, the mean hypsodonty index was calculated and this is presented below in Table 6.2. For most levels the number of hypsodonty index measurements were very low, in most cases only a single tooth yielded measurements. For levels with three or more measurements a standard deviation is also presented.

Table 6.2: Mean hypsodonty index per level at Abric Romaní. Ages for each level are from Gabucio *et al*. (2014), *N* indicates the number of specimens measured per level.

Level	Age (ka)	*N*	Mean Hypsodonty Index	Standard deviation
A	39	1	4.81	
B	43.8	2	3.78	
E	45	1	4.26	
I	48	3	4.59	0.676
Ja	49.3	5	3.95	0.935
Jb	50.4	1	4.56	
L	51.8	1	5.30	
M	54.5	1	2.40	

Changes in mean hypsodonty index measurements through the sequence are shown in Figure 6.1. Based on these results, it is clear that the mean hypsodonty index has changed through the sequence, increasing from 2.404 in level M (c. 54.5 ka) to 5.304 in level L (c. 51.8 ka). Following this maximum mean value, there is fluctuation through levels Jb to B. However, the majority of these levels have a very low number of measurements in order to calculate the mean and, as can be seen by the overlapping error bars of levels Ja and I, the values may not be statistically distinct. This means that mean hypsodonty index throughout the sequence has not significantly changed, except perhaps from level M to level L, although the data as they stand cannot confidently support this. Also, the measurements are very limited in terms of taxa, with all measurements from Equus sp. except for a sole Bos sp. tooth that was measured in Level A. This lack of diversity in the taxa that were measured may in some way explain the possible lack of change in mean hypsodonty that is seen through the Abric Romaní sequence.

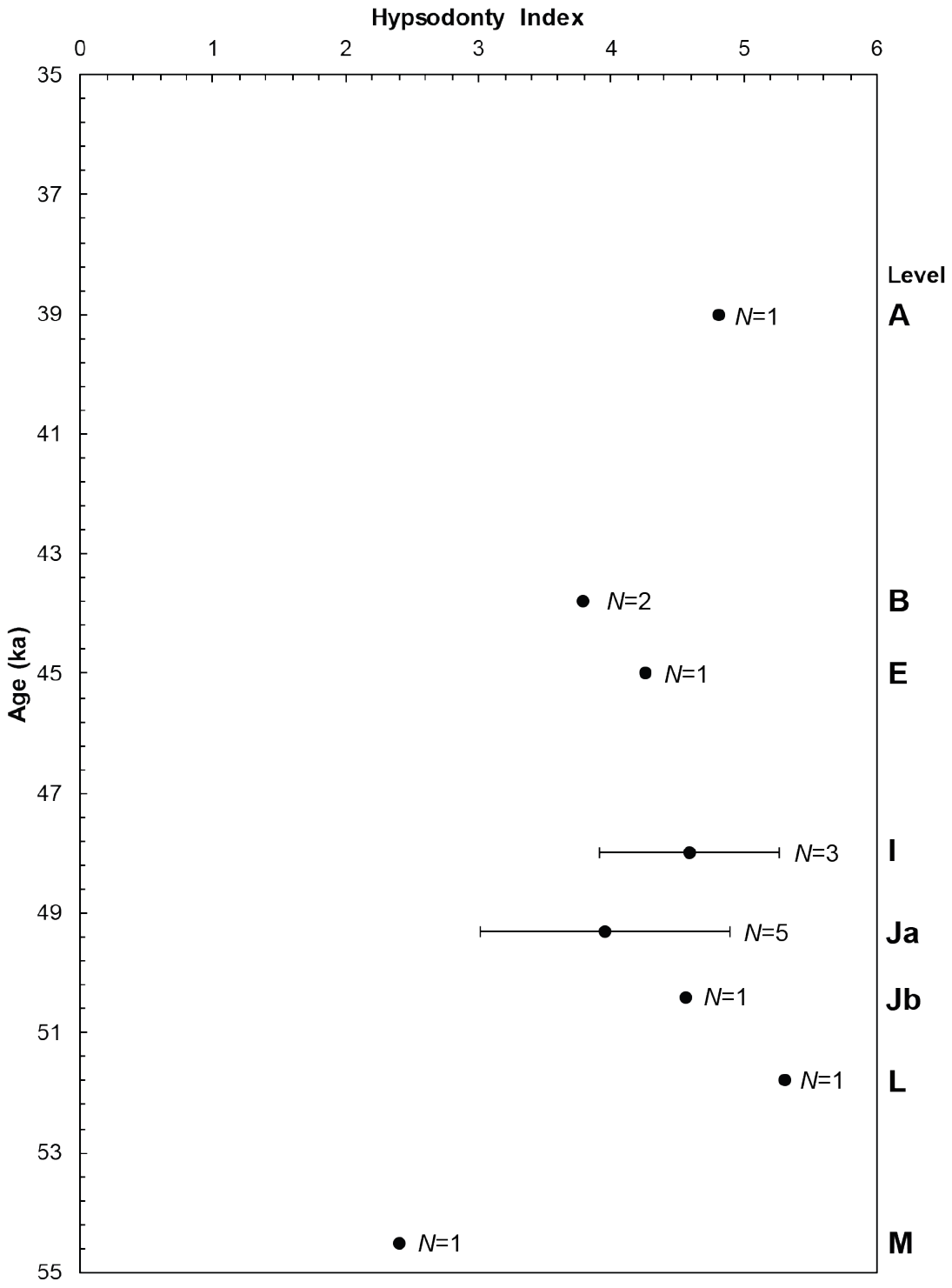

Figure 6.1: Changes in mean hypsodonty index per level at Abric Romaní. The error bars indicate the standard deviation of the mean. For the points without errors bars the number of measurements was too low to calculate a mean and associated standard deviation (see Table 6.2). *N* refers to the sample size for each level.

6.2 Teixoneres (Moià, Spain)

6.2.1 Materials, condition and taphonomy

57 ungulate M_3s were available for study, 21 of which were suitable for measurement for hypsodonty index (see section 6.2.2). 36 specimens were unsuitable, 24 of which were broken with parts of the crown missing, five were too worn, three were juvenile teeth, three had large amounts of sediment adhering to the surface and one tooth was set in resin and therefore could not be measured. Only Units II and III yielded suitable specimens for use in this study with Unit II only yielding three suitable teeth, each from different ungulate families. Unit III yielded suitable teeth from a more diverse range of taxa (see Table 6.3).

6.2.2 Measurements of individual specimens

Measurements were taken from the suitable specimens and the data are presented below in Table 6.3.

Table 6.3: Table showing the individual hypsodonty index measurements of suitable M_3 specimens from Teixoneres. The Unit, Sub-level, Square and Number shown per specimen relate to the site-specific cataloguing system used.

Year of Excavation	Unit	Sub-level	Square	Number	Taxon	Hypsodonty Index
2006	II	a	L13	47	*Sus scrofa*	0.71
2007	II	a	W20	61	*Cervus elaphus*	2.53
2007	II	a	K15	35	*Equus hydruntinus*	2.57
2012	III	b	L07	167	*Cervus elaphus*	2.08
2016	III	b	L10	9	*Capreolus capreolus*	1.12
2016	III	b	N10	291	*Cervus elaphus*	2.17
2016	III	b	L10	267	*Equus* sp.	4.00
2016	III	b	O10	272	*Equus ferus*	2.71
2016	III	b	N10	618	*Equus* sp.	3.25
2013	III	b	K11	49	*Capreolus capreolus*	1.54
2010	III	b	M15	19	*Cervus elaphus*	1.67
2011	III	b	L11	344	*Cervus elaphus*	1.94
2011	III	b	M11	37	*Bos primigenius*	2.00
2011	III	b	N08	36	*Capreolus capreolus*	1.23
2011	III	b	O10	263	*Capra* sp.	3.64
2015	III	b	M10	179	*Cervus elaphus*	1.62
2010	III		J15	80	*Bos primigenius*	2.00
2009	III		K14	53	*Capreolus capreolus*	2.23

2010	III	L12	127	*Cervus elaphus*	1.68
2010	III	J13	55	*Cervus elaphus*	1.39
2010	III	L13	135	*Cervus elaphus*	1.92

6.2.3 Mean hypsodonty index per unit

For each unit, the mean hypsodonty index was calculated and this is presented below in Table 6.4. The measurements are plotted on the chronology from Talamo *et al*. (2016) and are shown in Figure 6.2.

Table 6.4: Mean hypsodonty index per unit at Teixoneres. Ages for each level are from Talamo *et al*. (2016), *N* indicates the number of specimens measured per unit.

Unit	Age (cal yr BP)	*N*	Mean Hypsodonty Index	Standard deviation
II	44,210-33,060	3	1.94	1.07
III	>51,000-44,210	18	2.12	0.80

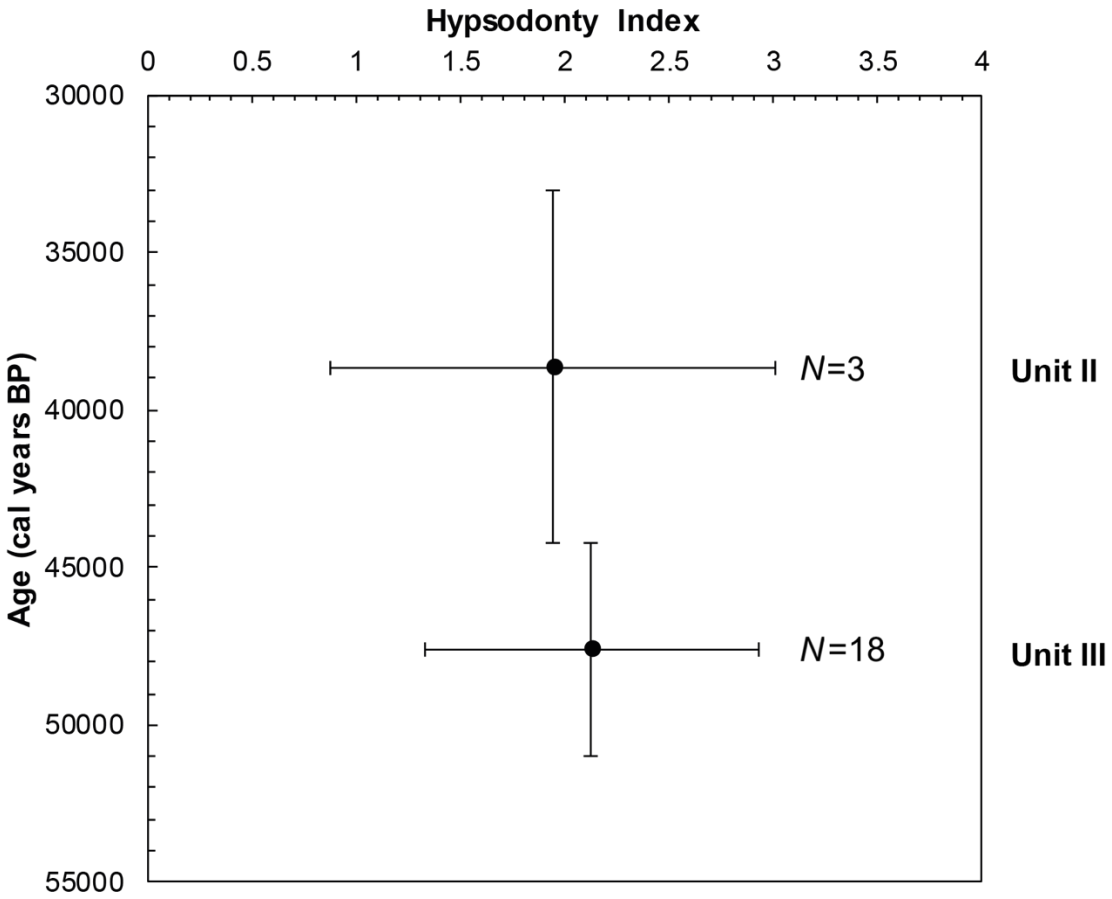

Figure 6.2: Changes in mean hypsodonty index per unit at Teixoneres. The horizontal error bars indicate the standard deviation of the mean hypsodonty index and the vertical error bars indicate the age range on the dates given for each unit (chronology from Talamo *et al*. (2016)). *N* refers to the sample size for each level.

From Table 6.4 and Figure 6.2 above, it can be seen that in both units III and II the mean hypsodonty index is around 2.0, with only a very slight decrease in the mean through time, however the horizontal error bars clearly overlap, suggesting no statistically significant difference, indicating no change in hypsodonty index between Unit III and Unit II.

6.3 Le Portel-Ouest (Ariège, France)

6.3.1 Materials, condition and taphonomy

From the Portel-Ouest collection at CERP, 44 M_3s were suitable for measurement. Specimens were largely in good condition with the majority of those measured being in excellent condition, and another three being broken with pieces missing, another fragmented but could be refitted, and one obscured by cave sediment stuck to the surface. Additionally, there were three M_3s in-situ in fragments of mandible. All of these specimens were suitable for measurement.

6.3.2 Measurements of individual specimens

Table 6.5 below presents the hypsodonty index for each specimen measured from Portel-Ouest.

Table 6.5: Table showing the individual hypsodonty index measurements of suitable M_3 specimens from Portel-Ouest. The number shown per specimen relates to the site-specific cataloguing system used.

Specimen Number	Level	Taxon	Hypsodonty Index
3456	B	*Cervus elaphus*	1.54
3460	B	*Cervus elaphus*	1.36
33730	B1	*Bos* sp.	3.40
3268	B1A	*Bos* sp.	3.57
DA1	C/D	*Bos* sp.	4.97
1253	D	*Bos* sp.	3.51
2144	D	*Bos* sp.	3.16
1118R	F	*Rangifer tarandus*	1.52
2167	F1	*Bos* sp.	2.87
2168	F1	*Bos* sp.	2.14
2046	F1	*Bos* sp.	4.06
2041	F1	*Bos* sp.	3.18
2874	F1	*Equus* sp.	3.85
2154	F2	*Bos* sp.	2.04
3119	F2	*Bos* sp.	3.34
2158	F2	*Bos* sp.	1.89

DA2	F2	*Capra* sp.	5.59
2039	F2	*Bos* sp.	2.55
3153	F2	*Cervus elaphus*	2.66
1215	F2	*Rangifer tarandus*	1.85
1221	F2	*Rangifer tarandus*	1.76
1216	F2	*Rangifer tarandus*	2.36
1219	F2	*Rangifer tarandus*	1.56
1214	F2	*Rangifer tarandus*	1.32
1205	F2	*Rangifer tarandus*	1.80
1202	F2	*Rangifer tarandus*	1.68
1201	F2	*Rangifer tarandus*	1.74
1196	F2	*Rangifer tarandus*	1.83
1344	F2	*Rangifer tarandus*	2.30
2834	F2	*Equus* sp.	4.07
2849	F2	*Equus* sp.	4.28
2868	F2	*Equus* sp.	2.79
2832	F2	*Equus* sp.	4.56
2852	F2	*Equus* sp.	3.97
2829	F2	*Equus* sp.	4.22
2847	F2	*Equus* sp.	4.95
1217	F2	*Rangifer tarandus*	1.99
1231	F3	*Rangifer tarandus*	1.89
1232	F3	*Rangifer tarandus*	2.04
1152	F3	*Rangifer tarandus*	1.65
1334	G	*Rangifer tarandus*	1.47
DA3	"Mousterian"	*Capra* sp.	4.77
DA4	"Mousterian"	*Capra* sp.	5.44
DA5	"Mousterian"	*Capra* sp.	5.19

6.3.3 Mean hypsodonty index per level

In accordance with the available chronological and sedimentological information in the literature (summarised in Vézian, 2014), mean hypsodonty index was calculated for each bed, combining some of the sub-levels of the site. Chronological control on the site is poor with only one date of 38.4 ± 6 ka for bed F (F2 and F3 combined). Changes throughout the sequence are shown visually against depth in Figure 6.3.

Table 6.6: Table showing the mean hypsodonty index measurements per level and their associated depth in the Portel-Ouest sequence.

Level	Depth Top	Depth Bottom	*N*	Mean Hypsodonty Index	Standard Deviation
B	0.11	1.01	4	2.47	1.02
C/D	1.66	1.66	1	4.97	
D	1.66	2.06	2	3.34	
F	2.31	3.13	33	2.77	1.14
G	3.13	3.28	1	1.47	

Mean hypsodonty index appears to increase through the sequence from bed G through to the boundary of beds D and C but this may be a factor of low sample numbers. With regards to the beds with adequate sample numbers (beds F and B) the errors (standard deviation) are large and the error bars overlap indicating that the mean hypsodonty index between these two layers cannot be statistically shown to be different, despite the differences in mean. The high peak at the boundary of beds D and C is a single measurement which may be anomalous. The same could be said for the other beds where no error bars are presented, this is due to the sample number being too low to calculate the standard deviation.

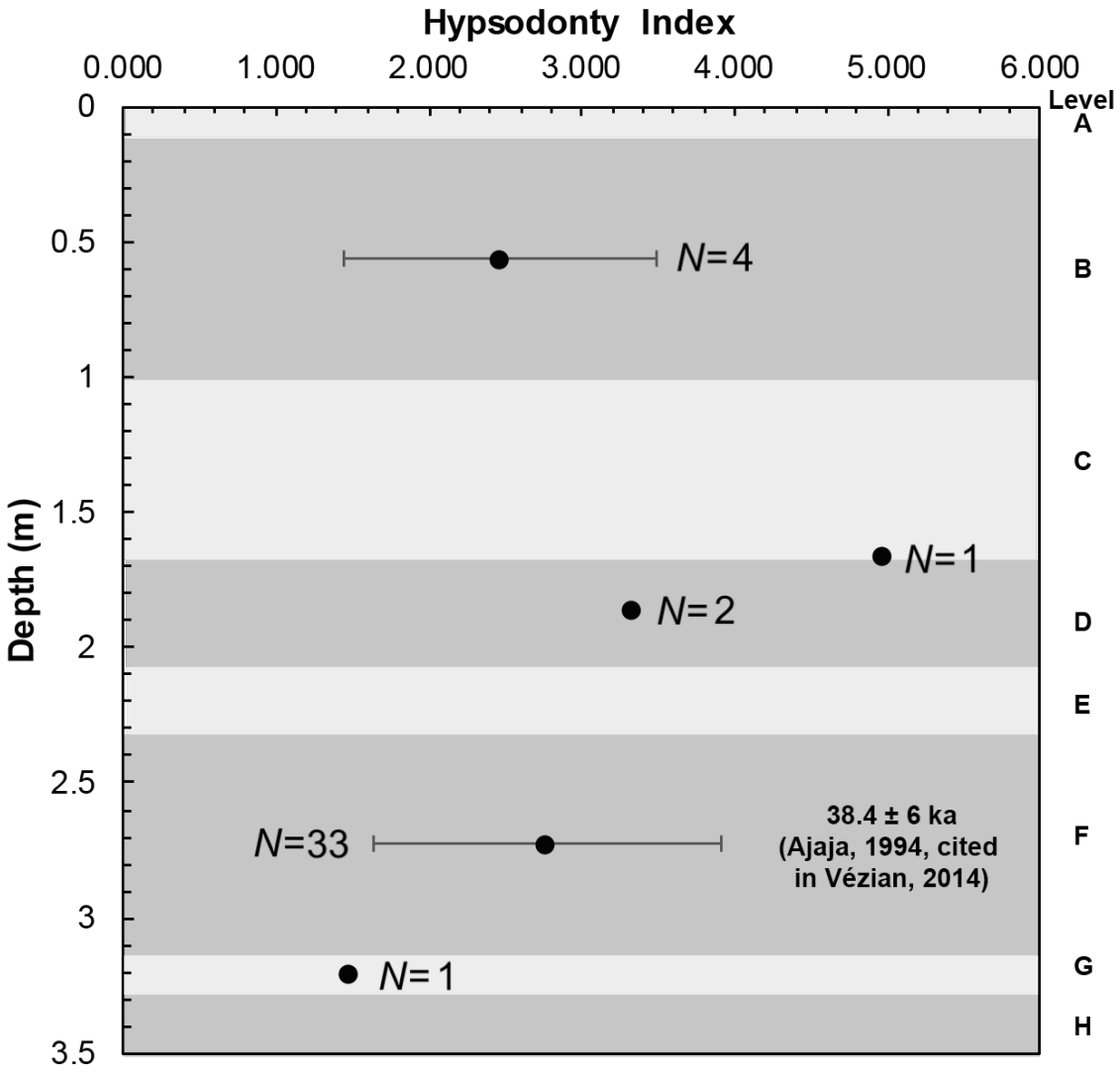

Figure 6.3: Mean hypsodonty index per level at Portel-Ouest, plotted against depth. Absolute date for Level F is indicated (from Ajaja, 1994, cited in Vézian, 2014). Error bars indicate standard deviation (see Table 6.6). *N* refers to the sample size for each level.

6.4 Grotta del Romito (Calabria, Italy)

6.4.1 Materials, condition and taphonomy

79 M_3s were available for study, 56 of which were suitable for measurement in this study. Out of the 23 unsuitable for measurement, fourteen had crowns that were too worn, eight were too broken and one was juvenile and not fully formed. Out of the 56 suitable specimens, twenty were from young adults, thirteen were *in situ* within fragments of mandible and one tooth had sediment adhering to the surface.

6.4.2 Measurements of individual specimens

Table 6.7 shows the hypsodonty index for each suitable specimen from Grotta del Romito.

Table 6.7: Table showing the hypsodonty index measurements of the suitable specimens from Grotta del Romito. The specimen numbers, strata and sub-section information relates the site-specific cataloguing system used.

Specimen Number	Stratum	Sub-section	Taxon	Hypsodonty Index
271	C	C	*Capra ibex*	3.02
177	C	C	*Cervus elaphus*	1.86
404	C	C1	*Capra ibex*	3.71
458	C	C1	*Cervus elaphus*	1.78
576	C	C1	*Sus scrofa*	0.74
929	C	C2	*Capra ibex*	4.76
673	C	C2	*Rupicapra rupicapra*	3.48
921	C	C2	*Sus scrofa*	0.77
1066	C	C3	*Capra ibex*	3.98
1245	C	C3	*Sus scrofa*	0.71
1062	C	C3	*Sus scrofa*	0.97
2943	C	C3	*Capra ibex*	5.03
2888	C	C3	*Capra ibex*	4.67
3044	C	C3	*Capra ibex*	3.54
743	C	D2	*Capra ibex*	4.64
1604	D	D	*Sus scrofa*	1.11
2937	D	D10	*Rupicapra rupicapra*	3.88
3178	D	D11	*Sus scrofa*	0.74
3421	D	D12	*Rupicapra rupicapra*	3.73
3528	D	D12	*Sus scrofa*	0.94
3499	D	D12	*Capreolus capreolus*	1.44
3575	D	D12	*Sus scrofa*	0.91

3696	D	D13	*Capreolus capreolus*	1.37
2163	D	D14	*Capra ibex*	4.58
2028	D	D17	*Capra ibex*	4.27
1870	D	D18	*Rupicapra rupicapra*	3.76
1896	D	D19	*Capra ibex*	4.86
7249	D	D19	*Rupicapra rupicapra*	4.27
1922	D	D19	*Capra ibex*	4.10
8104	D	D23	*Sus scrofa*	0.73
1693	D	D25	*Rupicapra rupicapra*	3.79
1672	D	D26	*Cervus elaphus*	2.08
6526	D	D26	*Capra* sp.	3.64
6572	D	D27	*Rupicapra rupicapra*	3.59
1564	D	D28	*Rupicapra rupicapra*	4.23
1389	D	D29A	*Capra ibex*	4.41
8060	D	D32	*Cervus elaphus*	2.73
1143	D	D33	*Capra ibex*	4.49
1152	D	D33	*Capra ibex*	4.53
2221	D	D5B	*Rupicapra rupicapra*	3.72
2512	D	D8	*Capreolus capreolus*	1.40
2687	D	D9	*Sus scrofa*	0.99
1631	D		*Rupicapra rupicapra*	4.32
918	E	E1	*Capra ibex*	4.72
443	E	E12	*Capra ibex*	4.66
423	E	E13	*Cervus elaphus*	1.64
412	E	E15	*Capra ibex*	3.64
837	E	E4	*Capra ibex*	3.93
824	E	E4	*Capra ibex*	3.59
756	E	E5	*Capra ibex*	4.45
709	E	E7	*Capra ibex*	4.16
655	E	E8	*Capra ibex*	4.19
3535	E	Ebase	*Capra ibex*	3.36
394	F	F3	*Capra ibex*	4.89
4682	G	G3	*Cervus elaphus*	3.35
254	H	H4	*Capra ibex*	5.06

6.4.3 Mean hypsodonty index per level

To increase sample size, specimens from the different sub-strata within a single stratum were combined. Mean hypsodonty index was calculated per stratum and is presented below in Table 6.8 and visually in Figure 6.4. Ages are taken from the results of the age model published in Blockley *et al*. (2018) with the youngest and oldest ages available for sub-strata within a given stratum.

Table 6.8: Table showing the mean hypsodonty index values for each stratum at Grotta del Romito. Ages are calculated from Blockley *et al*. (2018).

Stratum	Top age (cal yr BP)	Middle age (cal yr BP)	Bottom age (cal yr BP)	*N*	Mean Hypsodonty Index	Standard Deviation
C	12805	13048	13291	14	2.91	1.57
D	13274	14682	16090	28	3.02	1.45
E	16375	18054	19733	10	3.83	0.85
F	20696	21728	22760	1	4.88	
G	22910	23281.5	23653	1	3.35	
H	23653	24283	24913	1	5.06	

The mean hypsodonty index per stratum varies throughout the sequence, with a high value in stratum H, oscillating to a lower value in stratum G and back to a higher value in stratum F. However, these three strata yielded only one suitable specimen for measurement. When looking at the mean hypsodonty index values for strata C, D and E, the standard deviation for each is quite large, and hence the error bars all overlap. The mean values between each stratum are not statistically significantly different between these parts of the sequence.

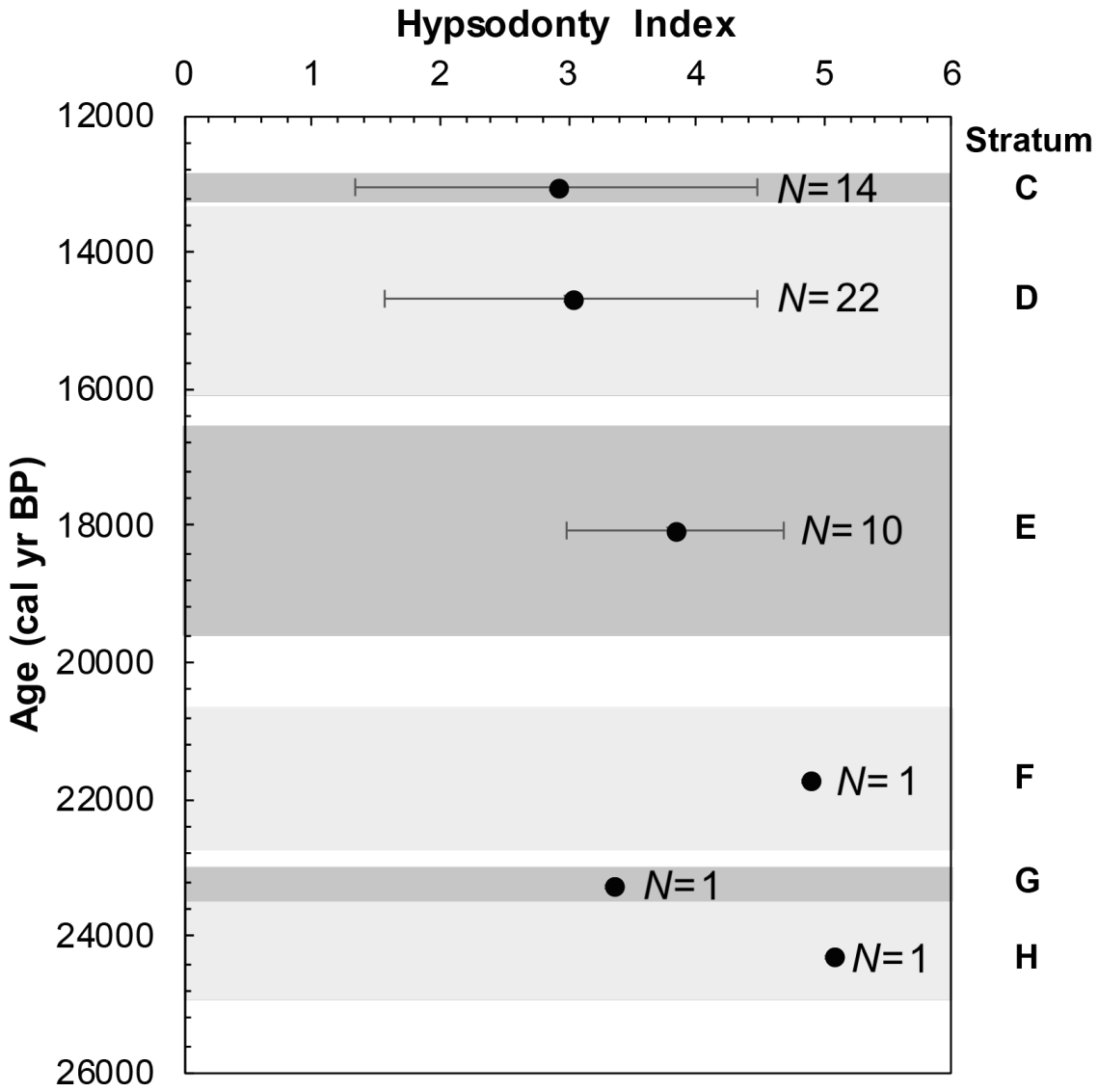

Figure 6.4: Mean hypsodonty index values plotted against age for Grotta del Romito. The ages are calculated from Blockley *et al*. (2018). The error bars represent the standard deviation. Points without error bars have a sample size too low to allow calculation of the standard deviation. *N* refers to the sample size for each level.

6.5 Tabun (Mount Carmel, Israel)

6.5.1 Materials, condition and taphonomy

200 ungulate M_3s were available for study, 117 of which were suitable for measurement (see section 6.5.2) and 83 of which were unsuitable. Of these unsuitable teeth, the majority were too worn (51), twenty were too broken to allow measurements, six were cemented in cave breccia, two were juvenile, one was partially destroyed for stable isotope sampling and three were unstratified.

6.5.2 Measurements of individual specimens

Table 6.9 shows all the hypsodonty index measurements for the 117 suitable teeth. The majority of these are from Level B (94; 80% of the suitable teeth), with 10 teeth from Level Ea (8.5% of the suitable teeth) whilst some of the other levels only yielded a handful of teeth each.

Table 6.9: Table showing the hypsodonty index measurements of the suitable specimens from Tabun. The specimen numbers, and level information relates the site-specific cataloguing system used.

Specimen Number	Level	Taxon	Hypsodonty Index
NHMUK PV M 16173	B	*Dama* sp.	1.10
NHMUK PV M 85751	B	*Bos* sp.	4.31
NHMUK PV M 85742	B	*Bos* sp.	4.89
NHMUK PV M 51768	B	*Capreolus capreolus*	4.07
NHMUK PV M 51770	B	*Capreolus capreolus*	3.88
NHMUK PV M 51769	B	*Capreolus capreolus*	4.46
NHMUK PV M 85691	B	*Cervus elaphus*	1.48
NHMUK PV M 86367	B	*Dama dama*	1.86
NHMUK PV M 86357	B	*Dama dama*	1.60
NHMUK PV M 86369	B	*Dama dama*	1.56
NHMUK PV M 86353	B	*Dama dama*	1.28
NHMUK PV M 86356	B	*Dama dama*	1.41
NHMUK PV M 86389	B	*Dama dama*	2.14
NHMUK PV M 86388	B	*Dama dama*	1.84
NHMUK PV M 86392	B	*Dama dama*	1.99
NHMUK PV M 86393	B	*Dama dama*	1.86
NHMUK PV M 86397	B	*Dama dama*	2.28
NHMUK PV M 86396	B	*Dama dama*	2.23
NHMUK PV M 86390	B	*Dama dama*	2.06
NHMUK PV M 86394	B	*Dama dama*	1.94

NHMUK PV M 86391	B	*Dama dama*	2.06
NHMUK PV M 86399	B	*Dama dama*	1.87
NHMUK PV M 86395	B	*Dama dama*	1.97
NHMUK PV M 86398	B	*Dama dama*	2.00
NHMUK PV M 86368	B	*Dama dama*	1.71
NHMUK PV M 86326	B	*Dama dama*	1.97
NHMUK PV M 86358	B	*Dama dama*	1.86
NHMUK PV M 86366	B	*Dama dama*	2.01
NHMUK PV M 86364	B	*Dama dama*	1.80
NHMUK PV M 86363	B	*Dama dama*	1.63
NHMUK PV M 86360	B	*Dama dama*	1.98
NHMUK PV M 86384	B	*Dama dama*	1.99
NHMUK PV M 86380	B	*Dama dama*	1.78
NHMUK PV M 86379	B	*Dama dama*	1.86
NHMUK PV M 86372	B	*Dama dama*	2.17
NHMUK PV M 86371	B	*Dama dama*	1.70
NHMUK PV M 86370	B	*Dama dama*	2.01
NHMUK PV M 86373	B	*Dama dama*	2.13
NHMUK PV M 86378	B	*Dama dama*	2.07
NHMUK PV M 86377	B	*Dama dama*	1.66
NHMUK PV M 86322	B	*Dama dama*	1.57
NHMUK PV M 86324	B	*Dama dama*	1.42
NHMUK PV M 86345	B	*Dama dama*	2.01
NHMUK PV M 86347	B	*Dama dama*	1.56
NHMUK PV M 86346	B	*Dama dama*	1.67
NHMUK PV M 86344	B	*Dama dama*	1.83
NHMUK PV M 86340	B	*Dama dama*	1.98
NHMUK PV M 86146	B	*Dama dama*	1.88
NHMUK PV M 86179	B	*Dama dama*	2.11
NHMUK PV M 86177	B	*Dama dama*	1.29
NHMUK PV M 86183	B	*Dama dama*	1.82
NHMUK PV M 86181	B	*Dama dama*	1.91
NHMUK PV M 86182	B	*Dama dama*	1.72
NHMUK PV M 86184	B	*Dama dama*	1.67
NHMUK PV M 86214	B	*Dama dama*	1.92
NHMUK PV M 86215	B	*Dama dama*	1.94
NHMUK PV M 86216	B	*Dama dama*	1.79

NHMUK PV M 86218	B	*Dama dama*	1.83
NHMUK PV M 86217	B	*Dama dama*	2.07
NHMUK PV M 86219	B	*Dama dama*	1.99
NHMUK PV M 86220	B	*Dama dama*	2.13
NHMUK PV M 86207	B	*Dama dama*	1.49
NHMUK PV M 86209	B	*Dama dama*	1.59
NHMUK PV M 86211	B	*Dama dama*	1.32
NHMUK PV M 86212	B	*Dama dama*	2.11
NHMUK PV M 86213	B	*Dama dama*	1.70
NHMUK PV M 86223	B	*Dama dama*	1.67
NHMUK PV M 86237	B	*Dama dama*	2.13
NHMUK PV M 86226	B	*Dama dama*	1.77
NHMUK PV M 86227	B	*Dama dama*	1.71
NHMUK PV M 86228	B	*Dama dama*	1.75
NHMUK PV M 86231	B	*Dama dama*	1.88
NHMUK PV M 86233	B	*Dama dama*	1.89
NHMUK PV M 86234	B	*Dama dama*	1.75
NHMUK PV M 86235	B	*Dama dama*	2.14
NHMUK PV M 86239	B	*Dama dama*	2.06
NHMUK PV M 86240	B	*Dama dama*	1.92
NHMUK PV M 86242	B	*Dama dama*	1.79
NHMUK PV M 86243	B	*Dama dama*	1.92
NHMUK PV M 86244	B	*Dama dama*	1.99
NHMUK PV M 86238	B	*Dama dama*	1.90
NHMUK PV M 86241	B	*Dama dama*	1.65
NHMUK PV M 86194	B	*Dama dama*	1.64
NHMUK PV M 86193	B	*Dama dama*	1.66
NHMUK PV M 87379	B	*Gazella* sp.	3.27
NHMUK PV M 87377	B	*Gazella* sp.	2.85
NHMUK PV M 87381	B	*Gazella* sp.	2.69
NHMUK PV M 87376	B	*Gazella* sp.	3.17
NHMUK PV M 87375	B	*Gazella* sp.	3.21
NHMUK PV M 87390	B	*Gazella* sp.	3.19
NHMUK PV M 87399	B	*Gazella* sp.	3.18
NHMUK PV M 87398	B	*Gazella* sp.	3.33
NHMUK PV M 87397	B	*Gazella* sp.	3.13
NHMUK PV M 51779	B	*Gazella* sp.	3.26

NHMUK PV M 87571	C	*Bos primigenius*	3.85
NHMUK PV M 87563	C	*Bos primigenius*	3.62
NHMUK PV M 51790	C	*Gazella* sp.	3.73
NHMUK PV M 51798	D	*Gazella* sp.	3.51
NHMUK PV M 88380	D-E	*Gazella* sp.	3.78
NHMUK PV M 88366	D-E	*Bos primigenius*	5.36
NHMUK PV M 88514	Ea	*Dama dama*	1.77
NHMUK PV M 51803	Ea	*Gazella* sp.	2.89
NHMUK PV M 51805	Ea	*Gazella* sp.	3.37
NHMUK PV M 88513	Ea	*Dama dama*	1.68
NHMUK PV M 88509	Ea	*Dama dama*	1.59
NHMUK PV M 88451	Ea	*Dama dama*	1.73
NHMUK PV M 88491	Ea	*Dama dama*	1.96
NHMUK PV M 88493	Ea	*Dama dama*	2.09
NHMUK PV M 88895	Ea	*Cervus elaphus*	1.92
NHMUK PV M 88832	Ea	*Gazella* sp.	2.53
NHMUK PV M 88542	Eb	*Equus* sp.	4.70
NHMUK PV M 88543	Eb	*Equus* sp.	3.63
NHMUK PV M 89064	Eb	*Cervus elaphus*	1.69
NHMUK PV M 89096	Eb	*Bos* sp.	3.54
NHMUK PV M 89097	Eb	*Bos* sp.	3.40
NHMUK PV M 89318	Ed	*Dama dama*	1.85
NHMUK PV M 89310	Ed	*Dama dama*	1.76

6.5.3 Mean hypsodonty index values per level

Table 6.10 shows the mean hypsodonty index per level at Tabun. As noted above, the distribution of suitable teeth is not even across levels with the majority coming from level B. The data are visually presented against the chronology in Figure 6.5.

Table 6.10: Table showing the mean hypsodonty index per level at Tabun. Ages are taken from Mercier and Valladas (2003) except the values denoted * where the date is from Grün and Stringer (2000) and the date denoted ** which is arbitrary calculated as halfway between the dates for levels D and Ea.

Level	Age negative uncertainty (ka)	Age (ka)	Age positive uncertainty (ka)	*N*	Mean Hypsodonty Index	Standard Deviation
B	18*	104*	33*	94	2.10	0.70
C	16	165	16	3	3.73	0.10
D	21	196	21	1	3.51	
D-E	**	231**	**	2	4.57	

Ea	22	267	22	10	2.15	0.56
Eb	31	324	31	5	3.39	0.97
Ed	27	302	27	2	1.81	

As Level Ed is stratigraphically lower than level Eb, this is taken here as the lowest level for which there are hypsodonty index data available, despite the dating indicating a younger age then level Eb. The age uncertainties (represented by the vertical error bars on Figure 6.5) for Ed and Eb are overlapping anyway, and the uncertainty for Ed also overlaps with Ea, potentially meaning that the calculated age for all of level E could be the same. For level Ed, the hypsodonty index is low at 1.81 but this a mean of only two values so the low value may be a factor of sample size. Curiously, this does not overlap with the standard deviation of the hypsodonty index in level Eb, centred much higher at a mean of 3.39, however the spread around the mean is quite large and overlaps with the mean hypsodonty index error in level Ea above, despite the Ea's mean being 2.15. The apparent oscillation through level E may therefore be real or a factor of the data, small sample size and overlapping errors. The highest mean hypsodonty index is at the D-E boundary, but again this is an average of only two hypsodonty index values. Through levels D and C, there is a return to values similar to those in level Eb but sample size is low. Level B has the most data and the mean hypsodonty index of 2.10 would indicate a decrease in level B from the preceding levels but taking the standard deviation into account, this overlaps with levels Ea and Eb and may indicate little change through the sequence.

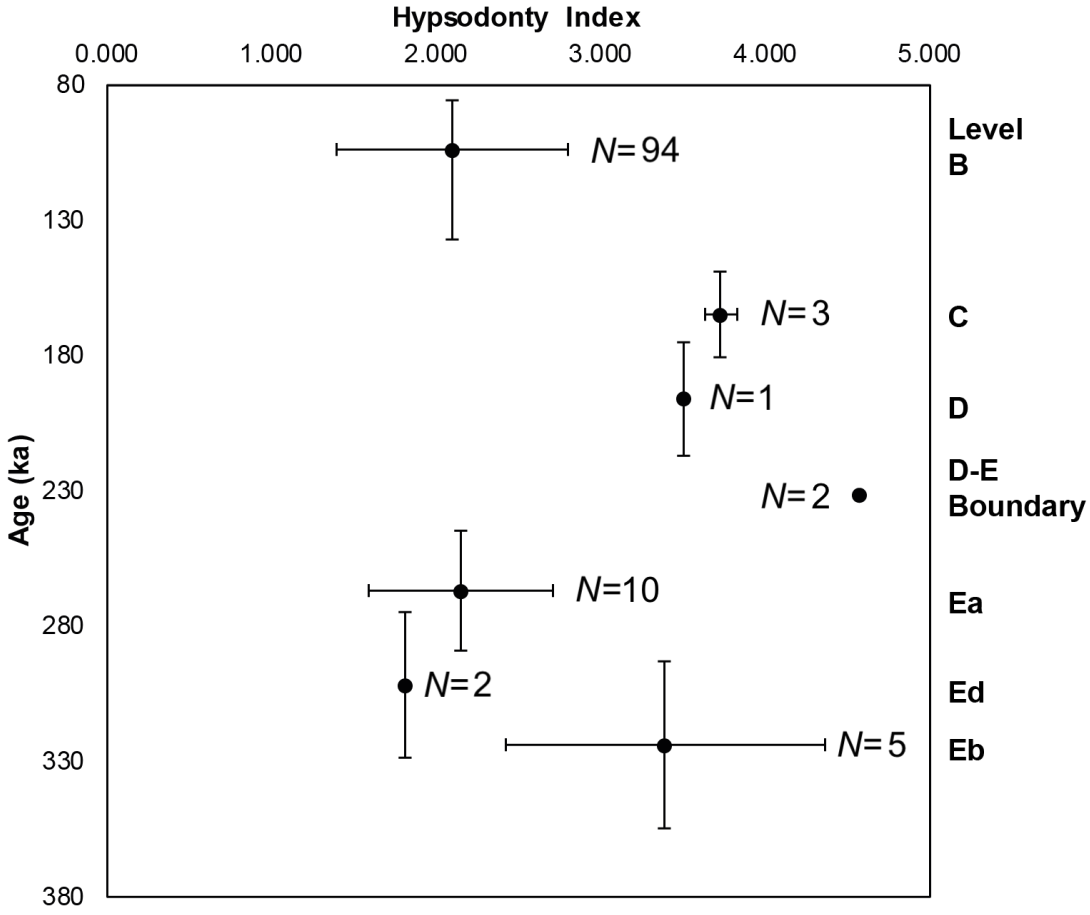

Figure 6.5: Plot of mean hypsodonty index per level against age for the Tabun sequence. Levels are labelled on the side. Note the reversal of the levels Eb and Ed. This is due to the dates for level Ed being younger than the date for Eb. *N* refers to the sample size for each level.

6.6 Qafzeh (Mount Precipice, Israel)

6.6.1 Materials, condition and taphonomy

74 M_3s were available for measurement, 27 of which were suitable, and 47 unsuitable. Out of these unsuitable teeth there were 24 that were too worn, 22 were broken or fragmented and one was unable to be measured as it was cemented with cave material.

6.6.2 Measurements of individual specimens

Table 6.11 presents the hypsodonty index measurements of the individual specimens that were suitable for measurement from Qafzeh.

Table 6.11: Table showing the hypsodonty index measurements of the suitable specimens from Qafzeh. The specimen numbers, and level information relates the site-specific cataloguing system used.

Specimen Number	Level	Taxon	Hypsodonty Index
DA1	2	*Dama* sp.	1.66
14	C-4	*Gazella gazella*	3.63
3100	C-5	*Gazella gazella*	3.37
1672	C-6	*Bos* sp.	2.15
1630	C-6	*Bos* sp.	3.69
1639	C-7	*Gazella* sp.	2.99
1691	C-7	*Gazella* sp.	3.19
1646	C-8	*Dama* cf. *mesopotamica*	1.73
3046	F-6	*Capra* sp.	4.22
2093	X	*Bos* sp.	3.44
2091	X	*Bos* sp.	3.19
864	XI	*Capra* sp.	3.25
932	XI	*Cervus elaphus*	2.09
3043	XII	*Cervus elaphus*	1.73
911	XII	*Capra* sp.	4.24
740	XIII	*Sus* cf. *gadarensis*	0.78
465	XIII	*Capra* sp.	3.89
890	XIII	*Gazella gazella*	3.07
Qafzeh 67?	XIV	*Dicerorhinus (= Stephanorhinus) hemitoechus*	1.62
432	XV	*Cervus elaphus*	2.13
493	XV	*Dama* sp.	1.94
473	XV	*Capra* sp.	4.29
461	XV	*Sus* cf. *gadarensis*	0.75
485	XVB	*Dama* sp.	1.12

320	XVI	*Capra* sp.	4.14
322	XVI	*Cervus elaphus*	1.94
433	XVI	*Cervus elaphus*	1.64

6.6.3 Mean hypsodonty index per level

Mean hypsodonty index was calculated per level and these are shown in Table 6.12 but also visually in Figure 6.6 below.

Table 6.12: Table showing the mean hypsodonty index per level at Qafzeh.

Level	*N*	Mean Hypsodonty Index	Standard Deviation
2	1	1.66	
C-4	1	3.63	
C-5	1	3.37	
C-6	2	2.92	
C-7	2	3.09	
C-8	1	1.73	
F-6	1	4.22	
X	2	3.32	
XI	2	2.67	
XII	2	2.99	
XIII	3	2.58	1.32
XIV	1	1.62	
XV	4	2.28	1.27
XVB	1	1.12	
XVI	3	2.57	1.12

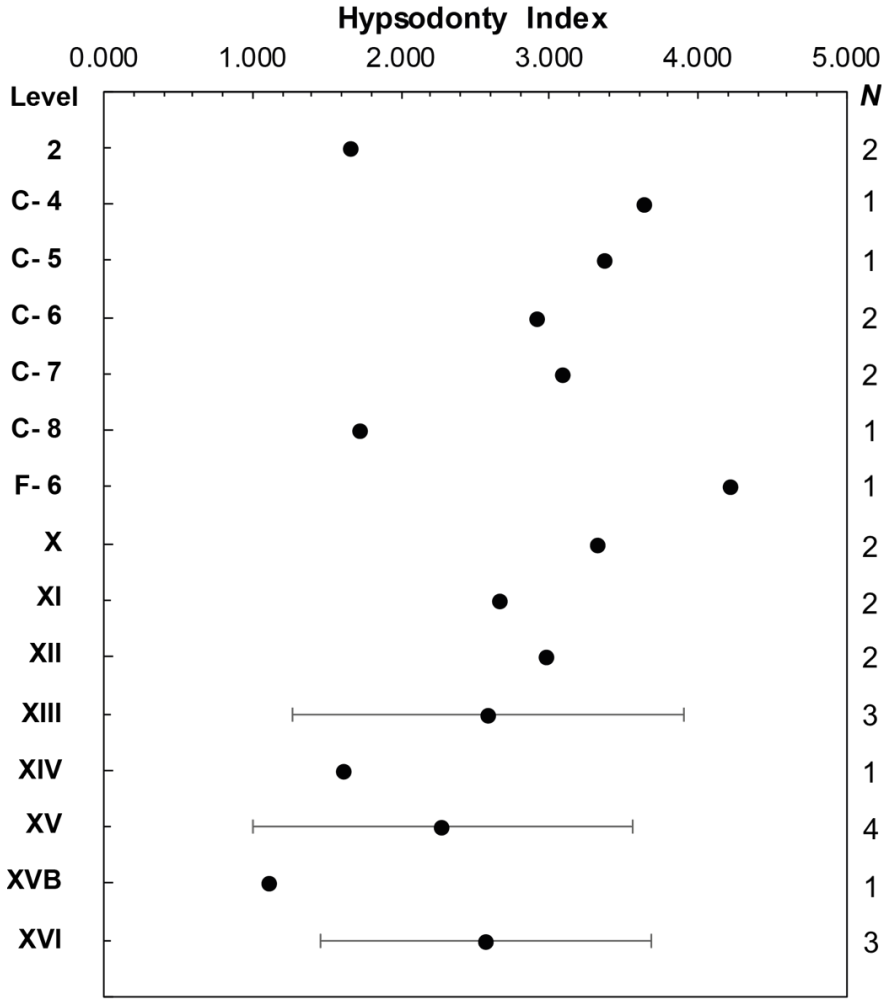

Figure 6.6: Mean hypsodonty index measurements per level at Qafzeh plotted per level rather than against age. Error bars represent the standard deviation where it was possible to calculate. *N* refers to the sample size for each level.

Unfortunately, the only teeth suitable for measurement at Qafzeh were from levels above those with good chronological control. Therefore Figure 6.6 shows the mean hypsodonty index measurements per level in stratigraphic order rather than against age so the vertical spacing between data points does not reflect age or actual position in the sequence. The majority of levels have very few teeth and therefore no standard deviation is calculated. For levels XVI, XV and XIII, where there are more data, it can be seen that the standard deviation is large, and they all overlap with each other. Taking just the means and including the upper levels with limited data, it could be argued that the mean hypsodonty index increases up the sequence to a high of 4.22 in level F-6 and then decreases again but this is only tentative as the upper levels are very data poor.

6.7 Haua Fteah (Cyrenaica, Libya)

6.7.1 Materials, condition and taphonomy

56 M_3s were available for measurement, twelve of which were suitable for measurement and these data are presented in section 6.7.2. 44 were unsuitable, of which, 25 were too worn and nineteen were broken and fragmented, several of which were destroyed through stable isotope sampling.

6.7.2 Measurements of individual specimens

Table 6.13 shows the hypsodonty index values for all of the suitable specimens from Haua Fteah. As can be seen from the table, a number of specimens are poorly provenanced and cannot be definitively attributed to a particular layer. Measurements were collected but subsequent analysis on mean hypsodonty index per level does not include these unprovenanced specimens.

Table 6.13: Table showing the individual hypsodonty index for specimens from Haua Fteah. Specimen number, box and excavation/spit number refers to the sit-specific cataloguing system used in these excavations and the curation of the material.

Specimen number	Box	McBurney Excavation/Spit Number	Layer	Taxon	Hypsodonty Index
HR23	HFT90.00-5X	55/17	XII, XIV, XV	*Ammotragus lervia*	4.27
HR30	HFT90.00-5X	55/17	Unknown	*Ammotragus lervia*	3.94
HR200	HFT117.04	55/08 and 9	VIII	*Ammotragus lervia*	4.10
HR59	HFT117.04	55/08 and 9	VIII	*Ammotragus lervia*	4.12
HR41	HFT61.01	52/06	X	*Bos primigenius*	3.36
DA1	HFT50.05	55/12	X	*Ammotragus lervia*	3.95
HR54	HFT41.08	52/3	VI, VIII	*Ammotragus lervia*	4.22
None	HFT93.02	52/09	XII, XIII, XIV	*Ammotragus lervia*	4.47
None	HFT112.03	51/04	VI, VIII, X	*Ammotragus lervia*	3.78
HR77	HFT111.05	-	VI, VII, IX, X	*Ammotragus lervia*	4.02
None	HFT114.05	52	Unknown	*Gazella* sp.	4.82
None	HFT94.01	55/04	VI	*Ammotragus lervia*	4.31

6.7.3 Mean hypsodonty index per layer

Table 6.14 shows the mean hypsodonty index per level using the teeth from Table 6.13 for which it is clear on which level they were collected from. Unfortunately, this leaves only three layers for which data are available and the sample size is very low. From this

data, it can be tentatively stated that the mean hypsodonty index increases from level X to a higher level of hypsodonty in layers VIII and VI but the sample size is too low to be confident.

Table 6.14: Table showing the mean hypsodonty index per layer at Haua Fteah for the layers which provenance of specimens is certain.

Level	*N*	Mean Hypsodonty Index
VI	1	4.31
VIII	2	4.11
X	2	3.66

6.8 Summary

This chapter has presented the hypsodonty index results for each fossil site, both describing the full set of measurements, and the mean values for different stratigraphic units or levels as appropriate. These Late Pleistocene hypsodonty index results will be discussed in the next chapter, but a detailed site-by-site and regional discussion can be found in Appendix 2.

CHAPTER 7
Discussion and synthesis – hypsodonty index as a climatic proxy: past and present

This chapter provides a synthesis of the understanding of the hypsodonty-climate relationship, as investigated through this thesis. First, the climatic signals that may be present in the mean hypsodonty index at the Late Pleistocene study sites are briefly discussed. The main framework of this discussion is based on highlighting issues and key themes that future researchers need to be aware of when investigating hypsodonty index as a palaeoclimate and palaeoenvironmental proxy. More detailed site-by-site discussions of the site results outlined in Chapter 6 are provided in Appendix 2 and cover:

- Detailed discussions of the nature and quality of the hypsodonty index data collected from fossil specimens at each site
- Comparison of hypsodonty index changes through time with site-specific proxy data (as presented in Chapter 3)
- A discussion of hypsodonty index in the three Mediterranean regions on a longitudinal gradient from west to east, providing cross-site, regional and inter-regional comparisons useful in analysing whether any climatic or environmental signals can be seen on larger spatial and temporal scales beyond individual site contexts

Second, following a summary of current understanding of hypsodonty index and proxy data, the overall nature of the hypsodonty-climate relationship is debated in light of both this and previously published studies. Both sections highlight the complexities of this relationship and evaluate the main factors that require the established methodology to be challenged. Finally, suggestions regarding future approaches in the hypsodonty-climate field are discussed.

7.1 Challenges of using hypsodonty index as a climatic predictor in the Late Pleistocene

7.1.1 Introduction

This section brings together the evidence from the fossil localities covering the Late Pleistocene indicating no significant change in hypsodonty index between any sampled

horizons or levels at any of the seven Late Pleistocene sites studied. Each site presented a number of similar problems that fall into four main areas: poor preservation, problems of sample sizes, taxon bias and issues of chronology and temporal resolution. These are discussed below.

7.1.2 Poor preservation

Whilst the preservation of teeth in fossil assemblages is generally relatively high compared to other elements, poor preservation of fossil material affects the results by reducing the potential number of teeth suitable for measurement. General taphonomic alterations are common, most often fractured or fragmented crowns and broken or absent cusps, so accurate measurement of crown height and width is not always possible. This issue, together with large numbers of teeth from elderly individuals which are too worn (see Chapter 3 for definitions), reduced the number of M_3s that were suitable for measurement. At sites such as Teixoneres and Grotta del Romito, there were also many M_3s that were fractured diagonally due to the breakage of mandibles for marrow extraction by human occupants of the sites. Often, the state of preservation of a specimen is almost never recorded in available databases so a researcher cannot pre-select suitable specimens with adequate levels of preservation, leading to extensive searching and sorting through fossil material in order to ascertain suitability.

7.1.3 Sample size issues

Whilst poor preservation can reduce sample size within a single horizon at a fossil site, this also has consequences when looking at the site as a whole. Often the sample size in a single horizon can be less than five specimens, and on some occasions the sample size can be limited to a single specimen. In these cases, the sample size is too small to be statistically significant. Thus, it is common practice to combine samples from adjacent horizons in order to increase sample sizes. This is done through examination of palaeoenvironmental proxy data or archaeological data contemporaneous with the deposition of the fossils in these layers so that the amalgamation of horizons is appropriate. However, it is common that certain horizons cannot be appropriately combined, leaving many horizons with statistically insignificant sample sizes. This can mean that the hypsodonty index data of certain horizons in a fossil sequence are of little or no value.

7.1.4 Taxon bias

One significant problem that arises in the approach used in this study is one of taxon bias. The taxa present in the mammalian assemblage within a particular geological bed and the taxa present in the hypsodonty index dataset are not always the same. Therefore, the mean hypsodonty index at any one point in the sequence may not be

representative of the fossil community during the deposition of the bed in question. Consequently, changes seen (or not seen) in the hypsodonty index may be entirely dependent on the nature of the available data and entirely independent of climate or environment.

Table 7.1 illustrates this problem and provides some additional discussion points. Taking Abric Romaní first, it can be clearly seen that the taxa represented in the hypsodonty index study are restricted to a single taxon per level. Furthermore, it is worth noting that in all levels except Level A, this taxon is *Equus* sp. Horses have much higher crowned teeth than many of the other taxa represented in the assemblage as reported by Rosell *et al*. (2012). This is an example of where the mean hypsodonty index (and associated standard deviation) of any sample is strongly influenced by one specimen of a high-crowned (or low-crowned) taxon.

Table 7.1: Table showing the taxa present at the sites of Abric Romaní and Teixoneres in comparison to the taxa present in the hypsodonty index data from this study. *N* = number of specimens.

Abric Romaní					Teixoneres				
Level	*N*	Age (ka)	Taxa in assemblage (Rosell *et al.*, 2012)	Taxa in hypsodonty index data	Unit	*N*	Age (cal years BP)	Taxa in assemblage (Álvarez-Lao *et al.*, 2017)	Taxa in hypsodonty index data
A	1	39	*Equus ferus* *Cervus elaphus* *Bos primigenius* *Rupicapra rupicapra*	*Bos* sp.				*Cervus elaphus* *Capreolus capreolus* Bovini cf. *Bos primigenius* *Rupicapra pyrenaica*	*Cervus elaphus*
					II	3	44,210 – 33,060	*Capra pyrenaica* *Sus scrofa* *Equus ferus* *Equus hydruntinus* *Equus* sp. *Coelodonta antiquitatis*	*Equus hydruntinus* *Sus scrofa*
B	2	43.8	*Equus ferus* *Cervus elaphus* *Rupicapra rupicapra*	*Equus* sp.					
E	1	45	Proboscidea *Equus ferus* *Cervus elaphus* *Bos primigenius* *Rupicapra rupicapra*	*Equus* sp					
I	3	48	*Equus ferus* *Cervus elaphus* *Bos primigenius*	*Equus* sp				*Cervus elaphus* *Capreolus capreolus* Bovini cf. *Bos primigenius* *Rupicapra pyrenaica* *Capra pyrenaica* *Sus scrofa* *Equus ferus* *Equus hydruntinus* *Equus* sp. *Coelodonta antiquitatis* *Mammuthus primigenius*	*Cervus elaphus* *Capreolus capreolus* *Equus ferus* *Equus* sp. *Bos primigenius* *Capra* sp.
Ja	5	49.3	*Stephanorhinus hemitoechus* *Equus ferus* *Cervus elaphus* *Bos primigenius* *Rupicapra rupicapra*	*Equus* sp	III	18	>51,000 – 44,210		
Jb	1	50.4	*Stephanorhinus hemitoechus* *Equus ferus* *Cervus elaphus* *Bos primigenius* *Rupicapra rupicapra*	*Equus* sp					
L	1	51.8	*Equus ferus* *Cervus elaphus* *Bos primigenius*	*Equus* sp					
M	1	54.5	*Equus ferus* *Cervus elaphus* *Bos primigenius*	*Equus* sp					

7.1.5 Chronological resolution

Amalgamating samples can preclude correlations of hypsodonty index with better resolved palaeoenvironmental proxy data of higher resolution, which then prevents testing for the presence of abrupt environmental shifts in the hypsodonty index data. When the standard deviation of the mean hypsodonty index of each sample is considered, along with associated dating uncertainties, there is a lot of overlap and no statistically significant change can be elucidated from any of the sites. The summary diagram below (Figure 7.1) shows these challenges visually.

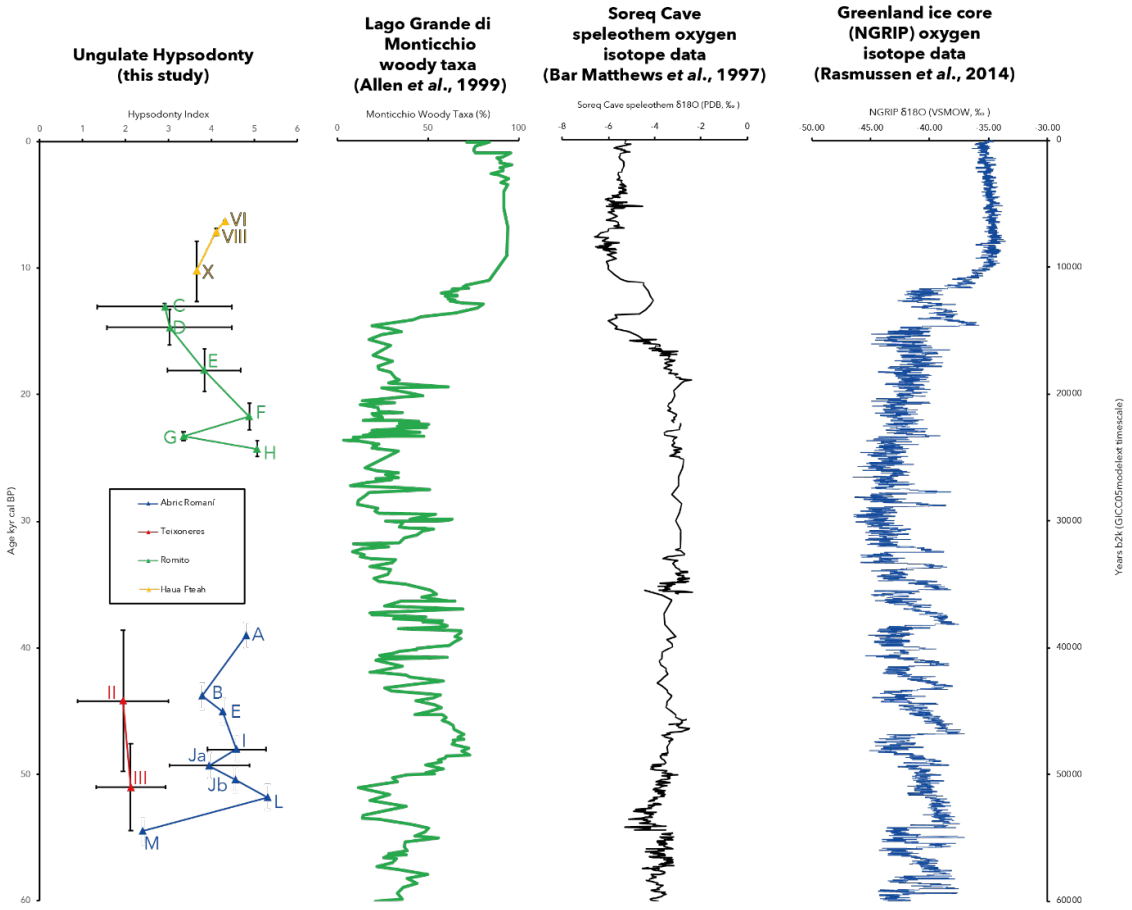

Figure 7.1: Summary diagram showing (from left to right) the hypsodonty index of Abric Romaní, Teixoneres, Grotta del Romito and Haua Fteah with site-specific horizon labels coloured corresponding to the legend (inset), the woody taxa from the pollen spectra from Lago Grande di Monticchio (green line; data from Allen *et al*., 1999), oxygen isotope data from the Soreq Cave speleothem record, Israel (black line; data from Bar-Matthews *et al*., 1997) and the oxygen isotope record from NGRIP (blue line; data from NGRIP Members, 2004 and Rasmussen *et al*., 2014).

7.2 Hypsodonty index as a climatic predictor in present-day mammal communities

After exploring the limitations and challenges of the Late Pleistocene application, it is only appropriate now to return to the modern context, since it can be assumed through uniformitarian principles that the same relationships and mechanisms operate in both the past and at the present day. As Chapter 5 concluded, the relationship between hypsodonty and climatic variables is complex and no clear single climate variable (or combination) appears to explain global variations in hypsodonty index of ungulates today. Investigations with fossils and palaeoclimate data in this study have revealed significant challenges in the approach, ultimately forcing a return to the original crux of the relationship between hypsodonty and climate. It is therefore now appropriate to re-ask the following questions: (1) is the per species mean hypsodonty index appropriate to use, and on what spatial and temporal scales?, (2) are ecometric approaches suitable and robust enough to be applied to Quaternary timescales?, and (3) what really explains variations in hypsodonty index?

7.2.1 Mechanisms and factors at play in the hypsodonty-climate relationship

Per species mean hypsodonty alone was reported by Liu *et al*. (2012) as not useful for predicting climate. The present study therefore explored hypsodonty and climate in the opposite way, similar to a species-distribution modelling approach, by avoiding explaining climate from hypsodonty or other ecometric traits and instead trying to explain hypsodonty variations from climatic variables. This, in part, was to avoid any approach that involves fitting a regression model where more and more ecometric traits are added to increase model fit (e.g. Liu *et al*., 2012; Oksanen *et al*., 2019). Under such processes, the mechanisms underlying the apparent relationships become extremely complex and unclear, especially as when using this method, any intraspecific variation is rarely considered. Regression models that incorporate several climatic variables to explain hypsodonty would lead to potential multiple climatic unknowns in a palaeoenvironmental reconstruction context. This would not have been useful, and therefore emphasis was placed on finding a single environmental variable that explained global variation in the mean hypsodonty index of modern ungulate communities. As the original primary goal of this study was to simplify the quantification of palaeoprecipitation (or some other palaeoclimatic variable) of Late Pleistocene fossil sites, where, typically, fossil dental remains are abundant and well-preserved, there was significant emphasis on using hypsodonty index alone. These data could be rapidly collected and potentially provide quantifiable palaeoclimate data in lieu of other time and resource intensive methods such

as stable isotope geochemical analysis of tooth enamel, bone collagen or molluscan shell carbonate.

According to the approach taken in the modern study, there is not a single environmental variable that robustly explains hypsodonty index as measured and calculated in this study. This is despite the global ungulate hypsodonty-climate correlation tests including up to thousands of datapoints and the correlations being statistically significant. The literature already stressed the complex factors that are involved, including the role of exogenous dust and grit (Damuth and Janis, 2011). This may be a missing component in the approach taken in this study but modern global data on dust and grit is not available at the same spatial scale and resolution as the modelled climatic data from Fick and Hijmans (2017). This factor would also be another unknown in a paleoenvironmental context, where proxy data for dust and grit is often absent, especially in fossil sites where sedimentation is not continuous.

The testing of intraspecific variation revealed that the majority of taxa do not show any significant levels of variation. In any case, where a specific taxon's hypsodonty index measurements are not from a normal distribution, these are, more often than not, explained by factors relating to sample size and the nature of the data collected. These results support the idea that hypsodonty, at least in ungulates, can be considered not to vary significantly between individuals. Thus, per species mean hypsodonty could be a valid approach in certain circumstances since it apparently does not mask as much variation as assumed at the beginning of this research.

7.3 Suggestions for future approaches

One of the main outcomes of this project is the large dataset of well-provenanced ungulate hypsodonty index measurements and an improved understanding of intraspecific variation of hypsodonty. The analyses tentatively support the notion of per species mean hypsodonty as defined by Janis (1988), whose work on diet and niche could be furthered using the dataset from this study, particularly focussing on specific regions for which there is a lot of data (e.g. Africa and Europe, for which there are potential regional differences in the relationships between hypsodonty index and diet and/or climate). Significant work could be carried out on the taxa with large sample sizes such as *Cervus elaphus* (which has a wide distribution with respect to climate), *Capreolus capreolus* and *Syncerus caffer*. Although this research reveals that intraspecific variation is insignificant, a different focus on niche partitioning and herbivore competition could be attempted to see if the large sample size from the present study is

able to pick out different diets as Janis (1988) suggested. Additional data could be collected for all taxa, or for individual taxa subjected to more in-depth analysis.

Some of the ecometric work produced by researchers based at the University of Helsinki includes all herbivorous mammals, including primates. As primates are very rare in Quaternary fossil assemblages, and there is also poor understanding of mechanisms between the more frugivorous diet of many primates and climate, they were not included in the modern study in this thesis. The approach based on ungulates could be applied to primates and a larger dataset could be built up to investigate not only the hypsodonty-climate relationship but equally, intraspecific variation. Additional research could be undertaken to investigate whether median ungulate hypsodonty index correlates with climate. Furthermore, hypsodonty is not restricted to large mammals. Small mammals, especially rodents, exhibit hypsodonty; they have been subject to study in the literature (e.g. Williams, 2001) and their teeth are often very abundant in fossil sites. A dataset collected from well-provenanced museum collections could further explore the potential of small mammal teeth as a climate indicator, although the condition of hypselodonty (ever-growing teeth) would have to be considered and the methodology adjusted to account for this. Collecting the ungulate data was very time consuming but the dataset is very valuable. Any additional data would be extremely relevant as herbivorous mammal communities include more than just ungulates, despite Quaternary assemblages often being dominated by them.

Finally, there could be more data collected on ungulates, to fill in spatial gaps in the data. As hypsodonty-climate relationships are envisaged to be global, an attempt was made in this study to collect as many hypsodonty index measurements as possible, from a wide spatial area. Coverage of Eurasia and Africa is good, but there are still many gaps both geographically (see the distribution map (Figure 3.1)) and in the datapoints of correlation plots (see section 4.2). This is especially notable for the Americas, which potentially hide part of the hypsodonty-climate story. The details of herbivore evolution in the New World are hotly debated, especially through the lens of coevolution of North American grasslands and horses through the Miocene (e.g. Janis *et al*., 2004; Stromberg *et al*., 2006, 2013), and the 'grit not grass' argument (see Mendoza and Palmqvist; 2007; Jardine *et al*., 2012). The role of exogenous dust is one that needs to be addressed further, but in the absence of global datasets on dust and grit at feeding level and a lack of global data on soil minerals such as quartz, this is an avenue that as yet cannot be fully explored. Adding a soil, dust or grit component to hypsodonty-climate models would be extremely important in further enhancing our understanding of the modern relationship, but in a palaeoenvironmental context, this may simply add another unknown.

In a Quaternary context, the challenges are numerous, and are largely the same as those faced in any palaeontological study. Some challenges will be difficult to overcome such as the fundamental numbers of lower third molars in an assemblage. It has been suggested that expanding the methodology to include second molars (e.g. Janis, 1988), and even upper molars would increase sample size, but these teeth would have to be investigated in the modern context in as much detail as the lower third molars have been in this study in order to ensure consistency and replicability. It may be necessary in future to further test the minimum number of specimens required to deliver a repeatable mean per taxon (in modern and fossil contexts), which may help determine whether results are of value. It would be extremely fortunate to find a Quaternary assemblage that provides hypsodonty index data mirroring the taxa in the assemblage at each time interval, and which also had proxy data available for the exact same temporal units or resolution. Since the results so far for Late Pleistocene sites have been site-specific, it would require testing on a large number of sites before any patterns or signals can be elucidated.

CHAPTER 8
Conclusions

The aim of this thesis is to assess the relationship between hypsodonty of modern ungulates and climate, in an attempt to improve upon existing models in a way that is appropriate for subsequent application to Quaternary fossil material, especially that from the Late Pleistocene. Intraspecific variation was investigated in an attempt to validate the assumption that per-species hypsodonty ordination values are appropriate. Late Pleistocene fossils from seven sites were measured for hypsodonty index and the values through each sequence were compared to pre-existing proxy data in an attempt to elucidate any climatic signals in the mean hypsodonty of Late Pleistocene ungulate communities.

This thesis has been the first study to undertake large-scale data collection of actual measurements of ungulate hypsodonty on a global scale, following a systematic approach using measurements from the third lower molar exclusively. There is now a database of 3,788 measurements of ungulate hypsodonty index from 148 different ungulate taxa from 950 unique localities. Intraspecific variation was investigated for these 148 different ungulate taxa and the results indicate that intraspecific variation is not significant, and those taxa that had hypsodonty index measurements that were not normally distributed could mostly be explained by the nature of the data itself.

This thesis is the first to attempt to correlate actual measurements of hypsodonty index of ungulates with climatic variables, departing from the ecometric approach in an effort to simplify the methodology to be more applicable to reconstructing palaeoclimate on timescales of abrupt climate change. The results indicate that there are no clear strong correlations with either temperature or precipitation components of climate, but that a minor signal of temperature, rather than precipitation, is captured by hypsodonty index. This is at least the case on a global scale using the dataset from this study. Unfortunately, these findings mean that a more robust model of the relationship could not be created and applied to fossils to provide quantitative estimates of precipitation in the Late Pleistocene. The main conclusion from the modern study is that the relationship between climate, diet and hypsodonty is very complex and that biological interactions, competition, niche partitioning and exogenous dust and grit are all key factors. The likelihood of reliably accounting for all of these, especially on a global level, is slim and leaves significant challenges to address when not using an ecometric approach.

This thesis has investigated the utility of hypsodonty index as a climate signal on Late Pleistocene timescales. However, there are very site-specific issues such as specimen preservation, presence of teeth, wear and taphonomic biases that reduce sample size. There is clear evidence that taxa present in hypsodonty index measurements may not be representative of the true community that is present, and that presence-absence of the taxa must always be considered in interpretations of the mean community hypsodonty index. Chronological challenges as well as mismatching resolutions of proxy data has hindered the elucidation of climate signals in the hypsodonty data. Opportunities to overcome this are few and far between for most Quaternary fossil sites, and it may be suggested that this method is not robust and inappropriate for this type of fossil material on these timescales. From this it may be suggested that the agreement achieved in the literature between hypsodonty and climate in the past is limited to a certain spatial and temporal scale and there is limited merit in attempting to apply this adaptation of the method to short, discrete time intervals such as the Late Pleistocene.

References

Allen, J.R.M., Brandt, U., Brauer, A., Hubberten, H.-W. Huntley, B., Keller, J., Kraml, M., Mackensen, A., Mingram, J., Negendank, J.F.W., Nowaczyk, N.R., Oberhänsli, H., Watts, W.A., Wulf, S. and Zolitschka, B. (1999) 'Rapid environmental changes in southern Europe during the last glacial period', *Nature*, **400**, 470-743.

Álvarez-Lao, D.J., Rivals, F., Sánchez-Hernández, C., Blasco, R. and Rosell, J. (2017) 'Ungulates from Teixoneres Cave (Moià, Barcelona, Spain): Presence of cold-adapted elements in NE Iberia during the MIS 3', *Palaeogeography, Palaeoeclimatology, Palaeoecology*, **466**, 287-302.

Ambrose, S.H. (2018) *Calibrating the Chronology of Late Pleistocene Modern Human Dispersals, Climate Change and Archaeology with Geochemical Isochrons*. Poster presented at Paleoanthropology Society 2018 Meeting, Austin, Texas, USA. Available at: http://www.paleoanthro.org/media/meetings/files/Ambrose_2018.pdf, [Accessed on: 04/07/2018].

Anon. (2018) 'The Cave of Kedumim', Available at: http://amudanan.co.il/w/P44234, Accessed on: 03/07/2018].

Armitage, S.J., Bristow, C.S. and Drake, N.A. (2015) 'West African monsoon dynamics inferred from abrupt fluctuations of Lake Mega-Chad', *Proceedings of the National Academy of Sciences*, **112**, 8543-8548.

Arsenault, R. and Owen-Smith, N. (2002) 'Facilitation versus competition in grazing herbivore assemblages', *OIKOS*, **97**, 3, 313-318.

Bar-Yosef, O. and Belfer-Cohen, A. (2004) 'The Qafzeh Upper Paleolithic Assemblages: 70 Years Later', *Eurasian Prehistory*, **2**, 1, 145-180.

Bar-Yosef, O. and Vandermeersch, B. (1981) 'Notes concerning the possible age of the Mousterian layers in Qafzeh cave', In: Cauvin, J. and Sanlaville, P. (Eds.) *Préhistoire du Levant*, Centre national de la recherche scientifique, Paris, 281-285.

Bar-Yosef, O. and Vandermeersch, B. (1993) 'Modern Humans in the Levant', *Scientific American*, **268**, 94-99.

Bar-Yosef Mayer, D.E., Vandermeersch, B., Bar-Yosef, O. (2009) 'Shells and ochre in Middle Paleolithic Qafzeh Cave, Israel: indications for modern behaviour', *Journal of Human Evolution*, **56**, 307-314.

Barker, G., Hunt, C. and Reynolds, T. (2007) 'The Haua Fteah, Cyrenaica (Northeast Libya): renewed investigations of the cave and its landscape, 2007', *Libyan Studies*, **38**, 93-114.

Barker, G., Basell, L., Brooks, I., Burn, L., Cartwright, C., Cole, F., Davison, J., Farr, L., Hamilton, R., Hunt, C., Inglis, R., Jacobs, Z., Leitch, V., Morales, J., Morley, I., Morley, M., Pawley, S., Pryor, A., Rabett, R., Reynolds, T., Roberts, R., Simpson, D., Stimpson, C., Touati, M., der Veen, M. (2008) 'The Cyrenaican Prehistory Project 2008: the second season of investigations of the Haua Fteah cave and its landscape, and further results from the 2007 fieldwork', *Libyan Studies*, **39**, 175-222.

Barker, G., Antoniadou, A., Barton, H., Brooks, I., Candy, I., Drake, N., Farr, L., Hill, E., Hunt, C., Ibrahim, A.A., Inglis, R., Jones, S., Morales, J., Rabett, R., Reynolds, T., Simpson, D., Twati, M. and White, K. (2009) 'The Cyrenaican Prehistory Project 2009: the third season of investigations of the Haua Fteah cave and its landscape, and further results from the 2007-2008 fieldwork', *Libyan Studies*, **40**, 1-41.

Barker, G., Antoniadou, A., Armitage, S., Brooks, I., Candy, I., Connell, K., Douka, K., Drake, N., Farr, L., Hill, E., Hunt, C., Inglis, R., Jones, S., Lane, C., Lucarini, G., Meneely, J., Morales, J., Mutri, G., Prendergast, A., Rabett, R., Reade, H., Reynolds, T., Russell, N., Simpson, D., Smith, B., Stimpson, C., Twati, M. and White, K. (2010) 'The Cyrenaican Prehistory Project 2010: the fourth season of investigations of the Haua Fteah cave and its landscape, and further results from the 2007-2009 fieldwork', *Libyan Studies*, **41**, 36-88.

Barker, G., Bennett, P., Farr, L., Hill, E., Hunt, C., Lucarini, G., Morales, J., Mutri, G., Prendergast, A., Pryor, A., Rabett, R., Reynolds, T. and Twati, M. (2012) 'The Cyrenaican Prehistory Project 2012: the fifth season of investigations of the Haua Fteah cave', *Libyan Studies*, **43**, 115-136.

Bezzobs, T. and Sanson, G. (1997) 'The effects of plant and tooth structure on intake and digestibility in two small mammalian herbivores', *Physiological Zoology*, **70**, 338-351.

Bergqvist, L.P. (2003) 'The Role Of Teeth In Mammal History', *Brazilian Journal of Oral Sciences*, **2**, 6, 249-257.

Bertini Vacca, B. (2012) 'The hunting of large mammals in the upper Palaeolithic of southern Italy: A diachronic case study from Grotta del Romito', *Quaternary International*, **252**, 155-164.

Beyer, W.N., Connor, E.E. and Gerould, S. (1994) 'Estimates of soil ingestion by wildlife', *Journal of Wildlife Management*, **58**, 375-382.

Bischoff, J.L., Julià, R., Mora, R. (1988) 'Uranium-series dating of the Mousterian occupation at Abric Romaní, Spain', *Nature*, **332**, 68-70.

Blásquez, M.C. and Pleguezuelos, J.M. (2002) '*Malpolon monspessulanus*' In: Pleguezuelos, J.M., Márquez, M. and Lizana, M. (Eds.), *Atlas y libro rojo de los Añbios y Reptiles de España*, Dirección General de Conservación de la Naturaleza-Asociación Herpetologica Española, Madrid, 284-286.

Blockley, S., Pellegrini, M., Colonese, A.C., Lo Vetro, D., Albert, P.G., Brauer, A., Di Giuseppe, Z., Evans, A., Harding, P., Lee-Thorp, J., Lincoln, P., Martini, F., Pollard, M., Smith, V., and Donahue, R. (2018) 'Dating human occupation and adaptation in the southern European last glacial refuge: The chronostratigraphy of Grotta del Romito (Italy)', *Quaternary Science Reviews*, **184**, 5-25.

Bolker, B.M. (2015) 'Linear and generalized linear mixed models', In: Fox, G.A., Negrete-Yankelevich, S. and Sosa, V.J. (Eds.) *Ecological Statistics: Contemporary Theory and Application*, Oxford University Press, Oxford.

Brauer, A., Allen, J.R.M., Mingram, J., Dulski, P., Wulf, S. and Huntley, B. (2007) 'Evidence for last interglacial chronology and environmental change from Southern Europe', *Proceedings of the National Academy of Sciences of the United States of America (PNAS)*, **104**, 2, 450-455.

Briggs, J.M., Knapp, A.K. and Collins, S.L. (2008) 'Steppes and prairies', In: Jørgensen, S.E. and Fath, B.D. (Eds.) *Encyclopedia of Ecology*, Academic Press, Cambridge, MA, USA, 3373-3382.

Bronk Ramsey, C. (2008) 'Radiocarbon dating: revolutions in understanding', *Archaeometry*, **50**, 2, 249-275.

Buckley, D. and Alcobendas, M. (2002) '*Salamandra salamandra*' In: Pleguezuelos, J.M., Márquez, M. and Lizana, M. (Eds.), *Atlas y libro rojo de los Añbios y Reptiles de España*, Dirección General de Conservación de la Naturaleza-Asociación Herpetologica Española, Madrid, 55-57.

Bugalho, M.N. and Milne, J.A. (2003) 'The composition of the diet of red deer (*Cervus elaphus*) in a Mediterranean environment: a case of summer nutritional constraint?', *Forest Ecology and Management*, **181**, 23-29.

Burjachs, F. and Julià, R. (1994) 'Abrupt climatic changes during the last glaciation based on pollen analysis of the Abric Romaní, Catalonia, Spain', *Quaternary Research*, **42**, 308-315.

Burjachs, F. and Julià, R. (1996) 'Palaeoenvironmental evolution during the Middle-Upper Palaeolithic transition in the NE of the Iberian Peninsula', In: Carbonell, E. and Vaquero, M. (Eds.) *The Last Neanderthals/The First Anatomically Modern Humans. Cultural Change and Human Evolution: Crisis at 40 ka BP*, Igualada, Barcelona, Spain, 377-383.

Burjachs, F., López-García, J.M., Alluė, E., Hughes-Alexandre, B., Rivals, F., Bennàsar, M. and Expósito, I. (2012) 'Palaeoecology of Neanderthals during Dansgaard-Oeschger cycles in northeastern Iberia (Abric Romaní): From regional to global scale', *Quaternary International*, **247**, 26-37.

Butler, P.M. (2000) 'The evolution of tooth shape and tooth function in primates' In: Teaford, M.F., Smith, M.M., Ferguson, M.W.J., (Eds.) *Development, function and evolution of teeth*, Cambridge University Press, Cambridge, 201-11.

Carbonell, E., (Ed.) (2008) *High Resolution Archaeology and Neanderthal Behavior: Time and Space in Level J of Abric Romaní (Capellades, Spain)'*, Springer, Amsterdam.

Carbonell, E., Cebrià, A., Allué, E., Cáceres, I., Castro, Z., Díaz, R., Esteban, M., Ollé, A., Pastó, I., Rodríguez Álvarez, X.P., Rosell, J., Sala, R., Vallverdú, J., Vaquero, M. and Vergés, J.M. (1996) 'Behavioural and organisational complexity in the Middle Palaeolithic from Abric Romaní', In: Carbonell, E. and Vaquero, M. (Eds.) *The Last Neanderthals/The First Anatomically Modern Humans. Cultural Change and Human Evolution: Crisis at 40 ka BP*, Igualada, Barcelona, Spain, 385-434.

Chatterjee, S. and Hadi, A.S. (2015) *Regression Analysis by Example*, Wiley, Hoboken, United States.

Colonese, A.C., Zanchetta, G., Fallick, A.E., Martini, F., Manganelli, G. and Lo Vetro, D. (2007) 'Stable isotope composition if Lateglacial land snail shells from Grotta del Romito (Southern Italy): palaeoclimatic implications', *Palaeogeography, Palaeoclimatology, Palaeoecology*, **254**, 550-560.

Craig, O.E., Biazzo, M., Colonese, A.C., Di Giuseppe, Z., Martinez-Labarga, C., Lo Vetro, D., Lelli, R., Martini, F. and Rickards, O. (2010) 'Stable isotope analysis of Late Upper Palaeolithic human and faunal remains from Grotta del Romito (Cosenza), Italy', **37**, 10, 2504-2512.

Dam van, J.A. and Utescher, T. (2016) 'Plant- and micromammal based paleoprecipitation proxies: Comparing results of the Coexistence and Climate-Diversity Approach', *Palaeogeography, Palaeoclimatology, Palaeoecology*, **443**, 18-33.

Damuth, J., Fortelius, M., Andrews, P., Badgely, C., Hadly, E.A., Hixson, S., Janis, C., Madden, R.H., Reed, K., Smith, F.A., Theodor, J., Van Dam, J.A., Van Valkenburgh, B. and Werdelin, L. (2002) 'Reconstructing mean annual precipitation based on mammalian dental morphology and local species richness', *Journal of Vertebrate Palaeontology*, **22** (conference abstract supplement), 48A.

Damuth, J. and Janis, C.M. (2011) 'On the relationship between hypsodonty and feeding ecology in ungulate mammals, and its utility in palaeoecology', *Biological Reviews*, **86**, 733- 758.

De Knegt, H.J., Groen, T.A., Van De Vijver, C.A.D.M., Prins, H.H.T. and Langevelde (2008) ' Herbivores as architects of savannas: inducing and modifying spatial vegetation patterning', *OIKOS*, **117**, 4, 543-554.

Douka, K., Jacobs, Z., Lane, C., Grün, R., Farr, L., Hunt, C., Inglis, R.H., Reynolds, T., Alber, P., Aubert, M., Cullen, V., Hill, E., Kinsley, L., Roberts, R.G., Tomlinson, E.I., Wulf, S. and Barker, G. (2014) 'The chronostratigraphy of the Haua Fteah cave (Cyrenaica, northeast Libya)', *Journal of Human Evolution*, **66**, 39-63.

Dudley, J.P. (1998) 'Reports of carnivory by the common hippo *Hippopotamus amphibius*', *South African Journal of Wildlife Research*, **28**, 2, 58-59.

Dumont, E.R. (1995) 'Enamel Thickness and Dietary Adaptation among Extant Primates and Chiroptera*, Journal of Mammalogy*, **76**, 4, 1127-1136.

Engelskjøn, T. (1987) 'Eco-geographical relations of the Bjornoya vascular flora, Svalbard', *Polar Research*, **5**, 1, 79-127.

Erickson, K.L. (2014) 'Prairie grass phytolith hardness and the evolution of ungulate hypsodonty', *Historical Biology*, **26**, 737-744.

Eronen, J.T. (2006) 'Eurasian Neogene large herbivorous mammals and climate', *Acta Zoologica Fennica*, **216**, 1-72.

Eronen, J.T., Puolamäki, K., Liu, L., Lintulaakso, K., Damuth, J., Janis, C. and Fortelius, M. (2010a) Precipitation and large herbivorous mammals I: estimates from present-day communities, *Evolutionary Ecology Research*, **12**, 217-233.

Eronen, J.T., Puolamäki, K., Liu, L., Lintulaakso, K., Damuth, J., Janis, C. and Fortelius, M. (2010b) 'Precipitation and large herbivorous mammals II: application to fossil data', *Evolutionary Ecology Research*, **12**, 235–248.

Estes, R. (1991) *The Behavior Guide to African Mammals: Including Hoofed Mammals, Carnivores, Primates*, University of California Press, London.

Estes, R. (1993) *The Safari Companion: A Guide to Watching African Animals*, Chelsea Green Publishing, Vermont, USA.

Evans, A.R. and Pineda-Munoz, S. (2018) 'Inferring Mammal Dietary Ecology from Dental Morphology', In: Croft, D.A., Su, D.F. and Simpson, S.W. (Eds.) *Methods in Paleoecology: Reconstructing Cenozoic Terrestrial Environments and Ecological Communities*, Springer, Cham, Switzerland, 37-51.

Faith, J.T., Du, A. and Rowan, J. (2019) 'Addressing the effects of sampling on ecometric-based paleoenvironmental reconstructions', *Palaeogeography, Palaeoclimatology, Palaeoecology*, **528**, 175-185.

Farr, L., Lane, R., Abdulazeez, F., Bennett, P., Holman, J., Marasi, A., Prendergast, A., Al-Zweyi, M. and Barker, G. (2014) 'The Cyrenaican Prehistory Project 2013: the seventh season of excavations of the Haua Fteah cave', *Libyan Studies*, **45**, 163-173.

Farrand, W.R. (1979) 'Chronology and Palaeoenvironment of Levantine Prehistoric Sites as Seen from Sediment Studies', *Journal of Archaeological Science*, **6**, 369-392.

Fedriani, J.M., Delibes, M., Ferreras, P. and Roman, J. (2002) 'Local and landscape habitat determinants of water vole distribution in a patchy Mediterranean environment', *Ecoscience*, **9,** 12-19.

Fernández-Lazo, M.C., Rivals, F. and Rosell, J. (2010) 'Intra-site changes in seasonality and their consequences on the faunal assemblages of Abric Romaní (Middle Palaeolithic, Spain)', *Quaternaire*, **21**, 2, 255-263.

Fernández-Laso, M.C., Chacón, M.G., García-Antón, M.D., Rivals, F. (2011) 'Territorial mobility Neanderthals groups: a case study from level M of Abric Romaní (Capellades, Barcelona, Spain)' In: Conard, N.J., Richter, J (Eds.) *Neanderthal Lifeways, Subsistence and Technology: One Hundred Fifty Years of Neanderthal Study*, Springer, Dordrecht, pp. 187-202.

Fick, S.E. and Hijmans, R.J. (2017) 'WorldClim 2: new 1-km spatial resolution climate surfaces for global land areas', *International Journal of Climatology*, **37**, 12, 4302-4315.

Fletcher, W.J., Sánchez-Goñi, M.F., Allen, J.R.M., Cheddadi, R., Combourieu-Nebout, N., Huntley, B., Lawson, I., Londeix, L., Magri, D., Margari, V., Müller, U.C., Naughton, F., Novenko, E., Roucoux, K., Tzedakis, P.C. (2010) 'Millennial-scale variability during the last glacial in vegetation records from Europe', *Quaternary Science Reviews*, **29**, 21-22, 2839-2864.

Frumkin, A., Ford, D.C., Schwarcz, H.P. (2000) 'Paleoclimate and vegetation of the last glacial cycles in Jerusalem from a speleothem record', *Global Biogeochemical Cycles*, **14**, 3, 863-870.

Frumkin, A., Bar-Yosef, O. and Schwarcz, H.P. (2011) 'Possible paleohydrologic and paleoclimatic effects on hominin migration and occupation of the Levantine Middle Paleolithic', *Journal of Human Evolution*, **60**, 437-451.

Frumkin, A., and Comay, O. (2019) 'The last glacial cycle of the southern Levant: Paleoenvironment and chronology of modern humans', To be published in *Journal of Human Evolution* [in press]. Available at: https://www.sciencedirect.com/science/article/pii/S0047248419300156#bib111, [Accessed on 26/6/19].

Ford. C. (2019) 'Understanding Q-Q plots', Available at: < https://data.library.virginia.edu/understanding-q-q-plots/>, Accessed on: 18/06/2019.

Fortelius, M. (1985) 'Ungulate cheek teeth: developmental, functional, and evolutionary interrelations' [online], *Acta Zoologica Fennica*, Available at: <http://ci.nii.ac.jp/naid/10009969860/>.

Fortelius, M., Bibi, F., Tang, H., Žliobaitė, I., Eronen, J.T. and Kaya, F. (2019) 'The painting on the wall: what's the matter with dental ecometrics?', *Nature Ecology &*

Evolution, Available at: < https://natureecoevocommunity.nature.com/users/207009-mikael-fortelius/posts/45791-the-painting-on-the-wall-what-s-the-matter-with-dental-ecometrics> [Accessed on 26th June 2019].

Fortelius, M., Eronen, J., Jernvall, J., Liu, L., Pushkina, D., Rinne, J, Tesakov, A., Vislobokova, I., Zhang, Z. and Zhou, L. (2002) 'Fossil mammals resolve regional patterns of Eurasian climate change over 20 million years', *Evolutionary Ecology Research*, **4**, 1005-1016.

Fortelius, M., Eronen, J.T., Kaya, F., Tang, H., Raia, P. and Puolamäki, K. (2014) 'Evolution of Neogene Mammals in Eurasia: Environmental Forcing and Biotic Interactions', *Annual Review of Earth and Planetary Sciences*, **42**, 579-604.

Fortelius, M., Eronen, J., Liu, l., Pushkina, D., Tesakov, A., Vislobokova, I and Zhang, Z. (2006) 'Late Miocene and Pliocene large land mammals and climatic changes in Eurasia', *Palaeogeography, Palaeoclimatology, Palaeoecology*, **238**, 1-4, 219-227.

Fortelius, M. and Solounias, N. (2000) 'Functional charaterization of ungulate molars using the abrasion-attrition wear gradient: a new method for reconstructing paleodiets', *American Museum Novitates*, **3301**, 1-76.

Furstenburg, D. (2010) *Focus on the Bushbuck (Tragelaphus scriptus)*, GeoWild Consult, Heidelberg, South Africa.

Gabucio, M.J., Cáceres, I., Rivals, F., Bargalló, A., Rosell, J., Saladié, P., Vallverdú, J., Vaquero, M., Carbonell, E., 2018. Unraveling a Neanderthal palimpsest from a zooarcheological and taphonomic perspective, *Archaeological and Anthropological Sciences* **10,** 1, 197-222.

Gabucio, M.J., Cáceres, I., Rosell, J., Saladié, P. and Vallverdú, J. (2014) 'From small bone fragments to Neanderthal activity areas: The case of Level O of the Abric Romaní (Capellades, Barcelona, Spain)', *Quaternary International*, **330**, 36-51.

Gaillard, J.- M., Hebblewhite, M., Loison, A., Fuller, M., Powell, R., Basille, M., Van Moorter, B. (2010) 'Habitat-performance relationships: finding the right metric at a given scale', *Proceedings of the Royal Society B: Biological Sciences*, **365**, 1150, 2255-2265.

Galbrun, E. and Miettinen, P. (2017) *Redescription Mining*, Springer, New York.

Galbrun, E., Tang, H., Fortelius, M. and Žliobaitė, I. (2018) 'Computational biomes: The ecometrics of large mammal teeth', *Palaeontologia Electronica*, **21**, 1.3A, 1-31.

Gardeisen, A. (1997) 'La grotte Ouest du Portel, Ariège, France: Restes fauniques et strategies de chasse dans le Pléistocène supérieur pyrénéen', *British Archaeological Report International Series*, **S673**, 352.

Gardeisen, A. (1999) 'Middle Palaeolithic Subsistence in the West Cave of "Le Portel" (Pyrénées, France), *Journal of Archaeological Science*, **26**, 1145-1158.

Garrod, D.A. and Bate, D.M.A. (1937) *The Stone Age of Mount Carmel—I. Excavations at the Wadi-el-Mughara*, Clarendon, Oxford.

Gebert, C. and Verheyden-Tixier, H. (2001) 'Variations of diet composition of Red Deer (*Cervus elaphus* L.) in Europe', *Mammal Review*, **31**, 189-201.

Ghinassi, M., Colonese, A.C., De Giuseppe, Z., Govoni, L., Lo Vetro, D., Malavasi, G., Martini, F., Ricciardi, S. and Sala, B. (2009) 'The Late Pleistocene clastic deposits in the

Romito Cavem southern Italy: a proxy record of environmental changes and human presence', *Journal of Quaternary Science*, **24**, 4, 383-398.

Giralt, S. and Julià, R. (1996) 'The sedimentary record of the Middle-Upper Palaeolithic transition in the Capellades area (NE Spain), In: Carbonell, E. and Vaquero, M. (Eds.) *The Last Neanderthals/The First Anatomically Modern Humans. Cultural Change and Human Evolution: Crisis at 40 ka BP*, Igualada, Barcelona, Spain, 365-376.

Graves, H.B. (1984) 'Behavior and ecology of wild and feral swine (*Sus scrofa*), *Journal of Animal Science*, **58**, 482-492.

Graziosi, P. (1962) 'Découverte de gravures rupestres de type paléolithique dans l'abri du Romito (Italie)', *L'Anthropologie*, **66**, 262-268.

Graziosi, P. (1971) 'Dernières découvertes de gravures paléolithiques dans la grotte du Romito en Calabre', In: Mélanges de préhistoire, d'archéocivilisation et d'ethnologie: offerts à André Varagnac, SevPen, Paris, 355-357.

Green, N. and Dodd, N.J. (1988) 'The uptake of radionuclides from inadvertent consumption of soil by grazing animals', *Science of the Total Environment*, **69**, 367-377.

Grey, J. and Harper, D.M. (2002) 'Using stable isotope analyses to identifty allochthonous inputes to Lake Naivasha mediated via the *Hippoptamus* gut', *Isotopes in Environmental and Health Studies*, **38**, 4, 245-250.

Grignolio, S., Rossi, I., Bassano, B., Parrini, F., and Apollonio, M. (2004) 'Seasonal variations of spatial behaviour in female Alpine ibex (*Capra ibex ibex*) in relation to climatic conditions and age', *Ethology, Ecology and Evolution*, 16, 255–264.

Gurevitch, J. and Nakagawa, S. (2015) 'Research synthesis methods in ecology', In: Fox, G.A., Negrete-Yankelevich, S. and Sosa, V.J. (Eds.) *Ecological Statistics: Contemporary Theory and Application*, Oxford University Press, Oxford, 201-228.

Haas, G. (1972) 'The microfauna of the Djebel Qafze Cave', *Paleovertebrata*, 5, 261-270.

Hallin, K.A., Shoeninger, M.J. and Schwarcz, H.P. (2012) 'Paleoclimate during Neanderthal and anatomically modern human occupation at Amud and Qafzeh, Israel: the stable isotope data', *Journal of Human Evolution*, 62, 59-73.

Hanley, T.A., Robbins, C.T., Hagermann, A.E. and McArthur, C. (1992) ' Predicting digestible protein and digestible dry-matter in tannin-containing forages consumed by ruminants', *Ecology*, **73**, 537-541.

Harvati, K., Röding, C., Bosman, A.M., Karakostis, F.A., Grün, R., Stringer, C., Karkanas, P., Thompson, N.C., Koutoulidis, V., Moulopoulos, L.A., Gorgoulis, V.G. and Kouloukoussa, M. (2019) 'Apidima Cave fossils provide earliest evidence of *Homo sapiens* in Eurasia, *Nature*, **571**, 500-504.

Healy, W.B. and Ludwig, T.G. (1965a) 'Ingestion of soil by sheep in New Zealand in realation to wear of the teeth', *Nature*, **208**, 806-807.

Healy, W.B. and Ludwig, T.G. (1965b) 'Wear of sheep's teeth I: The role of ingested soil', *New Zealand Journal of Agricultural Research*, **8**, 737-752.

Higham, T. (2011) 'European Middle and Upper Palaeolithic radiocarbon dates are often older than they look: problems with previous dates and some remedies', *Antiquity*, **85**, 327, 235-249.

Hijmans, R.J., Cameron, S.E., Parra, J.L., Jones, P.G. and Jarvis, A. (2005) 'Very high resolution interpolated climate surfaces for global land areas', *International Journal of Climatology*, **25**, 15, 1965-1978.

Hodge, E.J., Richards, D.A., Smart, P.L., Andreo, B., Hoffmann, D.L., Mattey, D.P. and González-Ramón (2008) 'Effective precipitation in southern Spain (~266 to 46 ka) based on a speleothem stable carbon isotope record', *Quaternary Research*, 69, 447-457.

Horowitz, A. (1979) *The Quaternary of Israel*, Academic Press, London.

Hunt, C., Davison, J., Inglis, R., Farr, L., Simpson, D., el-Rishi, H. and Barker, G. (2010) 'Site formation processes in caves: the Holocene sediments of the Haua Fteah, Cyrenaica, Libya', *Journal of Archaeological Science*, **37**, 1600-1611.

Inglis, R. (2012) *Human occupation and changing environemnts during the Middle to Later Stone Ages: soil micromorphology at the Haua Fteah, Libya*. PhD thesis, University of Cambridge.

Jackson, J. (1980) 'The annual diet of the Roe deer (*Capreolus capreolus*) in the New Forest, Hampshire, as determined by rumen content analysis', *Journal of the Zoological Society of London*, **192**, 71-83.

Jacobs, Z., Li, B., Farr, L., Hill, E., Hunt, C., Jones, S., Rabett, R., Reynolds, T., Roberts, R.G., Simpson, D. and Barker, G. (2017) 'The chronostratigraphy of the Haua Fteah cave (Cyrenaica, northeast Libya) – Optical dating of early human occupation during Marine Isotope Stages 4, 5 and 6', *Journal of Human Evolution*, **105**, 69-88.

Janis, C.M. (1984) 'The significance of fossil ungulate communities as indicators of vegetation structure and climate' In: Brenchley, P.J. (Ed.) *Fossils and Climate,* John Wiley and Sons, New York, 85-104.

Janis, C.M. (1988) 'An estimation of tooth volume and hypsodonty indices in ungulate mammals, and the correlation of these factors with dietary preferences', In: Russell, D.E., Santoro, J.-P. and Sigogneau-Russell, D. (Eds.) *Teeth revisited: Proceedings of the VIIth International Symposium on Dental Morphology, Paris, 1986*, Mémoires du Muséum national d'histoire naturelle, Paris, series C, Paris, France.

Janis, C.M. (1990) 'The correlation between diet and dental wear in herbivorous mammals, and its relationship to the determination of diets of extinct species' In: Boucot, A.J. (Ed.), *Evolutionary Paleobiology of Behavior and Coevolution*, Elsevier Press, New York, 241- 259.

Janis, C.M. (1995) 'Correlation between craniodental morphology and feeding behavior in ungulates: reciprocal illumination between living and fossil taxa' In: Thomason, J.J. (Ed.), *Functional Morphology in Vertebrate Paleontology*, Cambridge University Press, Cambridge, UK, 76-98.

Janis, C.M. and Fortelius, M. (1988) 'On the means whereby mammals achieve increased functional durability of their dentitions, with special relevance to limiting factors', *Biological Reviews*, **63**, 197-230.

Janis, C.M., Damuth, J. and Theodor, J.M. (2000) 'Miocene ungulates and terrestrial primary productivity: Where have all the browsers gone?', *Proceedings of the National Academy of Sciences,* **97,** 7899-7904.

Janis, C.M., Damuth, J. and Theodor, J.M. (2004) 'The species richness of Miocene browsers, and implications for habitat type and primary productivity in the North American grassland biome', *Palaeogreography, Palaeoclimatology and Palaeoecology*, **207**, 371-398.

Jardine, P.E., Janis, C.M., Sahney, S. and Benton, M.J. (2012) 'Grit not grass: Concordant patterns of early origin of hypsodonty in Great Plains ungulates and Glires', *Palaeogeography, Palaeoclimatology, Palaeoecology*, **365-366**, 1-10.

Jelinek, A., Farrand, W.R., Haas, G., Horowitz, A. and Goldberg, P. (1973) 'New excavations at the Tabun Cave (Mount Carmel Israel). Preliminary report', *Paléorient*, **1/2**, 151–183.

Jernvall, J. and Thesleff, I. (2012) 'Tooth shape formation and tooth renewal: evolving with the same signals', *Development*, **139**, 19, 3487–97.

Johnsen, S.J., Dahl-Jensen, D., Dansgaard, W. and Gundestrup N. (1995) 'Greenland palaeotemperatures derived from GRIP bore hole temperature and ice core isotope profiles', *Tellus B***, 47**, 5, 624-629.

Johnsen, S.J., Dahl-Jensen, D., Gundestrup, N., Steffensen, J.P., Clausen, H.B., Miller, H., Masson-Delmotte, V., Sveinbjörnsdottir, A.E., White, J. (2001) 'Oxygen isotope and palaeotemperature records from six Greenland ice-core stations: Camp Century, Dye-3, GRIP, GISP 2, Renland, NorthGRIP', *Journal of Quaternary Science*, **16**, 4, 299-307.

Jongen, M., Pereira, J.S., Aires, L.M.I., Pio, C.A. (2011) 'The effects of drought and timing of precipitation on the inter-annual variation in ecosystem-atmosphere exchange in a Mediterranean grassland', *Agricultural and Forest Meteorology*, **151**, 5, 595-606.

Kahlke, R,-D. and Kaiser, T.M. (2011) 'Generalism as a subsistence strategy: advantages and limitations of the highly flexible feeding traits of Pleistocene Stephanorhinus hundsheimensis (Rhinocerotidae, Mammalia)', *Quaternary Science Reviews*, **30**, 17-18, 2250-2261.

Kassa, B., Libois, R. and Sinsin, B. (2008) 'Diet and food preference of the waterbuck in the Pendjari National Park, Benin', *African Journal of Ecology*, **46**, 3, 303–10.

Kay, R.F. (1981) 'The nut crackers – a new theory of the adaptations of the Ramapithecidae', *American Journal of Physical Anthropology*, **55**, 141-151.

Kermack, K.A., Mussett, F. and Rigney, H.W. (1973) 'The lower jaw of Morganucodon' *Zoological Journal of the Linnean Society*, **53**, 87-175.

Kermack, K.A., Mussett, F. and Rigney, H.W. (1981) 'The skull of Morganucodon', *Zoological Journal of the Linnean Society*, **71**, 1-158.

Kirby, D.R. and Stuth, J.W. (1980) 'Soil ingestion rates of steers following brush management in central Texas', *Journal of Range Management*, **33**, 207-209.

Klein, R.G. and Scott, K. (1986) 'Re-analysis of faunal assemblages from the Haua Fteah and other late quaternary archaeological sites in Cyrenaican Libya', *Journal of Archaeological Science*, **13**, 6, 515-542.

Kohn, M.J. (2010) 'Carbon isotope compositions of terrestrial C3 plants as indicators of (paleo)ecology and (paleo)climate, *Proceedings of the National Academy of Sciences*, **107**, 46, 19691-19695.

Kojola, I., Helle, T., Huhta, E. and Niva, A. (1998) 'Foraging conditions, tooth wear and herbivore body reserves: a study of female reindeer', *Oecologica*, **117**, 26-30.

Korte, L.M. (2008) 'Variation of group size among African buffalo herds in a forest-savanna mosaic landscape', *Journal of Zoology*, **275**, 3, 229-236.

Kottek, M., Grieser, J., Beck, C. Rudolf, B. and Rubel, F. (2006) 'World Map of the Köppen-Geiger climate classification updated', *Meteorologische Zeitschrift*, **15**, 3, 259-263.

Krinner, G., Genthon, C. and Jouzel, J. (1997) 'GCM analysis of local influences on ice core δ signals', *Geophysical Research Letters*, **24**, 22, 2825-2828.

Kubo, M.O. and Yamada, E. (2014) 'The Inter-Relationship between Dietary and Environmental Properties and Tooth Wear: Comparisons of Mesowear, Molar Wear Rate, and Hypsodonty Index of Extant Sika Deer Populations', *PLoS One*, **9**, 3, 90745-90757.

Laca, E.A., Shipley, L.A. and Reid, E.D. (2001) 'Structural anti-quality characteristics of range and pasture plants', *Journal of Range Management*, **54**, 419-419.

Laerd Statistics (2018) 'Testing for Normality using SPSS Statistics', Available at: < https://statistics.laerd.com/spss-tutorials/testing-for-normality-using-spss-statistics.php>. Accessed on: 15/05/2019.

Lamprey, H.F. (1963) 'Ecological separation of the large mammal species in the Tarangire Game Reserve, Tanganyika', *African Journal of Ecology*, **1**, 1, 63-92.

Large Herbivore Network (2015) 'Factsheet: Persian Fallow Deer', Available at: <https://web.archive.org/web/20150905112236/http://www.lhnet.org/persian-fallow-deer/>, Accessed on: 17/06/2019.

Larsen, E., Sejrup, H.P., Johnsen, S.J. and Knudsen, K.L. (1995) 'Do Greenland Ice Cores Reflect NW European Interglacial Climate Variations?', *Quaternary Research*, **43**, 2, 125-132.

Lawing, A.M., Eronen, J.T., Blois, J.L., Graham, C.G. and Polly, P.D. (2016) 'Community functional trait composition at the continental scale: the effects of non-ecological processes', *Ecography*, **40**, 5, 651-663.

Lazuén, T. (2012) 'European Neanderthal stone hunting weapons reveal complex behaviour long before the appearance of modern humans', *Journal of Archaeological Science*, **39**, 7, 2304-2311.

Lem, R., Drake, N.A., Armitage, S.J., White, K.H., El-Hawat, A., and Salem, S.J. (2016) 'Termination of the African Humid Period: Insights from Wadi Shati, Libya', *Quaternary International*, **404**, B, 176.

Lintulaakso, K., Polly, P.D. and Eronen, J.T. (2019) 'Land mammals from eight functionally and climatically distinct faunas in North America but only one in Europe', *Journal of Biogeography*, **46**, 1, 185-195.

Lisiecki, L.E. and Raymo, M.E. (2005) 'A Pliocene-Pleistocene stack of 57 globally distributed benthic δ 18 O records', *Paleoceanography*, **20**, 1, 1-17.

Lister, A.M. and Stuart, A.J. (2019) 'The extinction of the giant deer *Megaloceros giganteus* (Blumenbach): New radiocarbon evidence', *Quaternary International*, **500**, 185-203.

Liu, L., Puolamäki, K., Eronen, J.T., Ataabadi, M.M., Hernesniemi, E. and Fortelius, M. (2012) 'Dental functional traits of mammals resolve productivity in terrestrial ecosystems past and present', *Proceedings of the Royal Society B*, **279**, 2793-2799.

López-García, J.M. (2008) *Evolución de la diversidad taxonómica de los micromamíferos en la Península Ibérica y cambios paleoambientales durante el Pleistoceno Superior*, Ph.D. Thesis, Universitat Rovira i Virgili, Spain.

López-García, J.M., Blain, H.-A., Burjachs, F., Ballesteros, A., Allué, E., Cuevas-Ruiz, G.E., Rivals, F., Blasco, R., Morales, J.I., Hidalgo, A.R., Carbonell, E., Serrat, D. and Rosell, J. (2012) 'A multidisciplinary approach to reconstructing the chronology and environment of southwestern European Neanderthals: the contribution of Teixoneres cave (Moià, Barcelona, Spain)', *Quaternary Science Reviews*, **43**, 33-44.

López-García, J.M., Sevilla, P., Cuenca-Bescós, G. (2009) 'New evidence for the greater noctule bat (Nyctalus lasiopterus) in the Late Pleistocene of Western Europe', *Comptes Rendus Palevol*, **8**, 551-558.

López-García, J.M. and Cuenca-Bescós, G. (2010) 'Évolution climatique durant le Pléistocène supérieur en Catalogne (Nord-est de l'Espagne) d'après de l'étude des micromammifères', *Quaternaire*, **21**, 3, 249-257.

López-García, J.M, Bero, C., Colamussi, V., Dalla Valle, C., Lo Vetro, D., Luzi, E., Malavasi, G., Martini, F. and Sala, B. (2014) 'Palaeoenvironmental and palaeoclimatic reconconstruction of the latest Pleistocene-Holocene sequence from Grotta del Romito (Calabria, southern Italy) using the small-mammal assemblages, *Palaeogeography, Palaeoclimatology, Palaeoecology*, **409**, 169-179.

Lucas, P.W., Omar, R., Al-Fadalah, K., Almusallam, A.S., Henry, A.G., Michael, S., Thai, L.A., Watzke, J., Strait, D.S. and Atkins, A.G. (2013) 'Mechanisms and causes of wear in tooth enamel: implications for hominin diets', *Journal of the Royal Society Interface,* **10**, 20120923.

Ludwig, T.G., Healy, W.B. and Cutress, T.W. (1968) 'Wear of sheep's teeth III: Seasonal variation in wear and ingested soil', *New Zealand Journal of Agricultural Research*, **9**, 157- 164.

Luzi, E., López-García, J.M., Blasco, R., Rivals, F. and Rosell, J. (2017) 'Variations in *Microtus arvalis* and *Microtus agrestis* (Arvicolinae, Rodentia) Dental Morphologies in an Archaeological Contect : the Case of Teixoneres Cave (Late Pleistocene, North-Eastern Iberia)', *Journal of Mammalian Evolution*, **24**, 4, 495-503.

MacFadden, B.J. (1992) *Fossil Horses: Systematics, Paleobiology and Evolution of the Family Equidae*, Cambridge University Press: Cambridge.

MacFadden, B.J. (2000) 'Cenozoic mammalian herbivores from the Americas: reconstructing ancient diets and terrestrial communities', *Annual Review of Ecology and Systematics*, **31**, 33-59.

Marrín-Arroyo, A.B. (2013) 'New Opportunities for Previously Excavated Sites: Paleoeconomy as a Human Evolutionary Indicator at Tabun Cave (Israel)' In: Clark, J.L. and Speth, J.D. (eds) *Zooarchaeology and Modern Human Origins: Human Hunting Behavior during the Later Pleistocene*', Springer, London, 59-76.

Marín, J., Saladié, P., Rodríguez-Hidalgo, A. and Carbonell, E. (2017) 'Ungulate carcass transport strategies at the Middle Palaeoolithic site of Abric Romaní (Capellades, Spain), *Comptes Rendus Palevol*, **16**, 103-121.

Marquet, J.-C., Vézian, R. and Gardeisen, A. (1998) 'Le Portel-Ouest: Associations fauniques et paléoenvironnements sur la frange septentrionnale des Pyrénées ariègeoises au Würm ancien', *Quaternaire*, **9**, 303-314.

Martin-Garcia, G. (2019) 'Oceanic Impact on European Climate Changes during the Quaternary', *Geosciences*, **9**, 119, 1-21.

Martini, F., Cilli, C., Colonese, A.C., Di Giuseppe, Z., Ghinassi, M., Govoni, L., Lo Vetro, D., Martino, G. and Ricciardi, S. (2007) 'L'Epigravettiano tra 15.000 e 10.000 anni da oggi nel basso versante tirrenico: casi studio dell'area calabro-campana', In: Martini, F. (Ed.), *L'Italia tra 15.000 e 10.000 anni fa. Cosmopolitismo e regionalita nel Tardoglaciale, vol. 18*, Atti della tavola rotonda, Florence, 157-207.

Martini, F. and Lo Vetro, D. (2005a) 'Grotta del Romito (Papasidero, Cosenza): recenti risultati degli scavi e degli studi', In: Ambrogio, B. and Tine, V. (Eds.), *Atti delle giornate di studio sulla Preistoria e Protostoria della Calabria: Scavi e Ricerche 2003,* Atti delle giornate di studio, Pellaro (RC), 5-15.

Martini, F. and Lo Vetro, D. (2005b) 'Il passaggio Gravettiano-Epigravettiano a Grotta del Romito (scavi 2003-2004). Prime osservazioni', In: Martini, F. (Ed.), *Askategi, miscellanea in memoria di Georges Lapace, Rivista di Scienze Preistoriche LV, supplemento 1*, Firenze, 151-175.

Martini, F. and Lo Vetro, D. (2007) 'Grotta del Romito (Papasidero, Prov. Di Cosenza)', *Rivista di Scienze Preistoriche*, **57**, 441-442.

Martini, F. and Lo Vetro, D. (Eds.) (2011) *Grotta del Romito a Papasidero: uomo, ambiente e cultura nel Paleolitico della Calabria: ricerche 1961-2011. Guide del Museo e Istituto fiorentino di Preistoria, Firenze*, Editoriale Progetto 2000, Cosenza, 43-53.

Martini, F., Lo Vetro, D. and Timpanelli, L. (2016) 'New insight on the Romito Shelter (Calabria): the lithic production of the mesolithic levels' In: Fontana, F., Visentin, D., Wierer, U. (Eds.), *Proceedings of the MesoLife Conference, Selva di Cadore, 11th-14th June 2014, Preistoria Alpina,* **48**, 233-238.

Massey, F.P., Ennos, A.R. and Hartley, S.E. (2006) 'Silica in grasses as a defence against insect herbivores: contrasting effects on folivores and a phloem feeder', *Journal of Animal* Ecology, **75**, 595– 603.

Massey, F.P., Ennos, A.R. and Hartley, S.E. (2007) 'Grasses and the resource availability hypothesis: the importance of silica-based defences', *Journal of Ecology*, **95**, 414– 424.

Masson-Delmotte, V., Jouzel, J., Landais, A., Stievenard, M., Johnsen, S.J., White, J.W.C., Werner, M.. Sveinbjörnsdottir, A. and Fuhrer, K. (2005) 'GRIP Deuterium Excess Reveals Rapid and Orbital-Scale Changes in Greenland Moisture Origin', *Science*, **309**, 5731, 118-121.

Matthew, W.D. (1926) 'The Evolution of The Horse: A Record and its Interpretation', *The Quarterly Review of Biology*, **1**, 2, 139-185.

McBurney, C.B.M. (1967) The Haua Fteah (Cyrenaica) and the Stone Age of the South-East Mediterranean, Cambridge University Press, Cambridge.

Mendoza, M. and Palmqvist, P. (2007) 'Hypsodonty in ungulates: an adaptation for grass consumption or for foraging in open habitat?', *Journal of Zoology*, **274**, 2, 134-142.

Merceron, G., Ramdarshan, A., Blondel, C., B, J.-R., Brunetier, N., Francisco, A, Gautier, D, Milhet, X, Novello, A. and Pret, D. (2016) 'Untangling the environmental from the dietary: dust does not matter', *Proceedings of the Royal Society B*, **283**, 1838-1846.

Mercier, N. and Valladas, H. (2003) 'Reassessment of TL ages estimates of burnt flints from the Paleolithic site of Tabun Vabe, Israel', *Journal of Human Evolution*, **45**, 401-409.

Moon, J., Lee, W.K., Song, C., Lee, S.G., Heo, S.B., Shvidenko, A., Kraxner, F., Lamchin, M., Lee, E.J., Zhu, Y., Kim, D., Cui, G. (2017) 'An introduction to mid-latitude ecotone: sustainability and environmental challenges', *Siberian Journal of Forest Science*, **6**, 41–53.

Moyer, C. (2003) The Organisation of Lithic Technology in the Middle and Early Upper Palaeolithic Industries at the Haua Fteah, Libya. Unpublished PhD thesis, University of Cambridge.

Müller, T. and Fagan, W.F. (2008) 'Search and navigation in dynamic environments – from individual behaviours to population distributions', *OIKOS*, **117**, 5, 654-664.

Mwasi, S.M., Heitkönig, I.M.A., Van Weiren, S.E. and Prins, H.H.T. (2017) 'Foraging behaviour of wild impala (*Aepyceros melampus*) and Burchell's zebra (*Equus burchelli*) in relation to sward height', *African Journal of Ecology*, **56**, 2, 334-341.

Neuville, R. (1951) 'Le Paléolithique et le Mésolithique du desert de Judée. La grotte de Djebel Qafzeh', *Archive de l'Institut de Paléontologie Humaine*, 179-185.

Nowak, R. M. (1999) *Walker's Mammals of the World (Volume 1)*, 6th edition, Johns Hopkins University Press, Baltimore, USA.

O'Donnell, M.S., and Ignizio, D.A. (2012) 'Bioclimatic predictors for supporting ecological applications in the conterminous United States', *U.S. Geological Survey Data Series 691*.

Ogutu, J.O., Piephi, H.-P., Dublin, H.T., Bhola, N., Reid, R.S. (2008) 'Rainfall influences on ungulate population abundance in the Mara-Serengi ecosystem', *Journal of Animal Ecology*, **77**, 4, 814-829.

Oksanen, O., Žliobaitė, I., Saarinen, J., Lawing, A.M. and Fortelius, M. (2019) 'A Humboldtian approach to life and climate of the geologic past : Estimating palaeotemperature from dental traits of mammalian communities', *Journal of Biogeography*, **46**, 8, 1760-1776.

Owen-Smith, N., Fryxell, J.M. and Merrill, E.H. (2010) 'Foraging theory upscaled: the behavioural ecology of herbivore movement', *Proceedings of the Royal Society B: Biological Sciences*, **365**, 1150, 2267-2278.

Pandolfi, L., Boscato, P., Crezzini, J., Gatta, M., Moroni, A., Rolfo, M. and Tagliacozzo, A. (2017) 'Late Pleistocene Last Occurrences of the narrow-nosed rhinoceros

Stephanorhinus hemitoechus (Mammalia, Perrisodactyla) in Italy', *Revisita Italiana di Paleontologica e Stratigrafia*, **123**, 2, 177-192.

Parker, K.L. (2003) 'Advances in the nutritional ecology of cervids at different scales', *Écoscience*, **10**, 4, 395-411.

Parker, K.L., Barboza, P.S. and Gillingham, M.P (2009) 'Nutrition integrates environmental response of ungulates', *Functional Ecology,* **23,** 1, 57-69.

Parrini, F., Grignolio, S., Luccarini, S., Bassano, B., and Apollonio, M. (2003) 'Spatial behaviour of adult male Alpine ibex *Capra ibex ibex* in the Gran Paradiso National Park, Italy', *Acta Theriologica*, **48**, 411–423.

Parrini, F., Cain, J.W. and Krausman, P.R. (2009) '*Capra ibex* (Artiodactyla : Bovidae)', *Mammalian Species*, **830**, 1-12.

Pedrotti, L. and Lovari, S. (1999) '*Rupicapra rupicapra'* In: Mitchell-Jones, A.J., Amori, G., Bogdanowicz, W., Kryštufek, B., Reijnders, P.J.H., Spitzenberger, F., Stubbe, M., Thissen, J.B.M., Vohralík, V. and Zima, J. (Eds.), *The Atlas of European Mammals*, Academic Press, London.

Pérez-Barbería, F.J. and Gordon, I.J. (1998) 'The influence of molar occlusal surface area on the voluntary intake, digestion, chewing behaviour and diet of red deer (*Cervus elaphus*), *Journal of Zoology*, **245**, 307-316.

Piperno, D.R. (2006) *Phytoliths: A Comprehensive Guide for Archaeologists and Paleoecologists*, Alta Mira Press: Oxford.

Pita, R., Mira, A. and Beja, P. (2014) '*Microtus cabrerae* (Rodentia: Cricetidae)' *Mammalian Species*, **46**, 912, 48-70

Prendergast, A.L., Stevens, R.E., O'Connell, T.C., Hilla, E.A., Hunt, C.O. and Barker, G.W. (2016) 'A late Pleistocene *refugium* in Mediterranean North Africa? Palaeoenvironmental reconstruction from stable isotope analyses of land snail shells (Haua Fteah, Libya)*, Quaternary Science Reviews*, **139**, 94-109.

Rabett, R., Farr, L., Hill, E., Hunt, C., Lane, R., Moseley, H., Stimpson C. and Barker, G. (2013) 'The Cyrenaican Prehistory Project 2012: the sixth season of excavations of the Haua Fteah cave', *Libyan Studies*, **44**, 113-125.

Rabinovich, R., Bar-Yosef, O., Vandermeersch, B. and Horowitz, L.K. (2004) 'Hominid-Carnivore interactions in the Paleolithic site of Qafzeh cave, Israel', *Revue de Paléobiologie*, **23**, 2, 627-637.

Rabinovich, R. and Tchernov, E. (1995) 'Chronological, Paleoecological and taphonomical aspects of the Middle Paleolithic site of Qafzeh, Israel', In: Buitenhuis, H. and Uerpmann, H.-P.(Eds) *Archaeozoology of the Near East II,* Backhuys Publishers, Leiden, 5-44.

Ramos, A., Pereira, M.A., Soares, A., Rosário do, L., Matos, P, Nunes, A., Branquinho, C. and Pinho, P. (2015) ' Seasonal patterns of Mediterranean evergreen woodlands (Montado) are explained by long-term precipitation', *Agriciultural and Forest Meterology*, **202**, 44-50.

Rasmussen, S.O., Andersen, K.K., Svensson, A.M., Steffensen, J.P., Vinther, B.M., Clausen, H.B., Siggaard-Andersen, M.L., Johnsen, S.J., Larsen, L.B., DahlJensen, D., Bigler, M., Rothlisberger, R., Fischer, H., Goto-Azuma, K., € Hansson, M.E. and Ruth,

U. (2006) 'A new Greenland ice core chronology for the last glacial termination', *Journal of Geophysical Research: Atmospheres*; **111**, 18-28.

Rasmussen, S.O., Bigler, M., Blockley, S.P., Blunier, T., Buchardt, S.L., Clausen, H.B., Cvijanovic, I., Dahl-Jensen, D., Johnsen, S.J., Fischer, H., Gkinis, V., Guillevic, M., Hoek, W.Z., Lowe, J.J., Pedro, J.B., Popp, T., Seierstad, I.K., Steffensen, J.P., Svensson, A.M., Vallelonga, P., Vinther, B.M., Walker, M.J.C., Wheatley, J.J. and Winstrup, M. (2014) 'A stratigraphic framework for abrupt climatic changes during the Last Glacial period based on three synchronized Greenland ice-core records: refining and extending the INTIMATE event stratigraphy', *Quaternary Science Reviews*, **106**, 14–28.

Reade, H., Stevens, R.E., O'Connell, T.C. and Barker, G. (2016) 'Pleistocene and Holocene herbivore diets and palaeoenvironments in the Gebel Akhdar (Libya): Implications for past human populations', *Palaeogeography, Palaeoclimatology, Palaeoecology*, **449**, 62-78.

Reade, H., O'Connell, T.C., Barker, G. and Stevens, R.E. (2018) 'Increased climate seasonality during the late glacial in the Gebel Akhdar, Libya', *Quaternary Science Reviews*, **192**, 225-235.

Reimer, P.J., Bard, E., Bayliss, A., Beck, J. W., Blackwell, P.G., Bronk Ramsey, C., Grootes, P.M., Guilderson, T.P., Hafliidason, H., Hajdas, I., Hatte, C., Heaton, T.J., Homann, D.L., Hogg, A.G.,Hughen, K. A., Kaiser, K.F., Kromer, B., Manning, S.W., Niu, M., Reimer, R.W., Richards, D.A., Scott, E.M., Southon, J.R., Staff, R.A., Turney, C.S.M., and van der Plicht, J. (2013) 'IntCal13 and Marine13 Radiocarbon Age Calibration Curves 0- 50,000 Years cal BP', *Radiocarbon*, **55**, 1869-1887.

Rensberger, J.M. (1973) 'Occlusion model for mastication and dental wear in herbivorous mammals', *Journal of Paleontology*, **47**, 515-528.

Rivals, F., Schulz, E and Kaiser, T.M. (2009) 'Late and middle Pleistocene ungulates dietary diversity in Western Europe indicate variations of Neanderthal paleoenvironments through time and space', *Quaternary Science Reviews*, **28**, 27-28, 3388-3400.

Rohling, E.J., Mayewski, P.A., Abu-Zied, R.H., Casford, J.S.L., Hayes, A. (2002) 'Holocene atmosphere-ocean interactions: records from Greenland and the Aegean Sea', *Climate Dynamics*, **18**, 587.-593.

Ronen, A. and Vandermeersch, B. (1972) 'The Upper Paleolithic sequence in the cave of Qafza (Israel), *Quaternaria*, **16**, 189-202.

Rosell, J., Blasco, R., Rivals, F., Gema Chacón, M., Arilla, M., Camrós, E., Rufà, A., Sánchez-Hernández, C., Picin, A., Andrés, M., Blain, H.-A, López-García, J.M., Iriarte, E. and Cebrià, A. (2017) 'A resilient landscape at Teixoneres Cave (MIS 3; Moià, Barcelona, Spain): The Neanderthals as disrupting agent', *Quaternary International*, **435**, 195-210.

Rosell, J., Cácers, I., Blaso, R., Bennàsar, M., Bravo, P., Campeny, G., Esteban-Nadal, M., Fernández Lazo, M.C., Gabucio, M.J., Huguet, R., Ibáñez, N., Martín, P., Rivals, F., Rodríguez-Hidalgo, A. and Saladié, P. (2012) 'A zooarchaeological contribution to establish occupational patterns at Level J of Abric Romaní (Barcelona, Spain)', *Quaternary International*, **247**, 69-84.

Sanson, G.D., Kerr, S.A. and Read J. (2017) 'Dietary exogenous and endogenous abrasives and tooth wear in African buffalo', *Biosurface and Biotribology*, **3**, 4, 211-223.

Sanson, G.D., Kerr, S.A. and Gross, K.A (2007) 'So silica phytoliths really wear mammalian teeth?', *Journal of Archaeological Science*, **34**, 526-531.

Schreve, D., (2007) 'Vertebrate Overview', In: Elias, S. (Ed.) *Encyclopedia of Quaternary Science*, Elsevier, Amsterdam, 3123-313

Schwarz, H.P., Grün, R., Vandermeersch, B., Bar-Yosef, O., Valladas, H., Tchernov, E. (1988) 'ESR dates for the hominid burial site of Qafzeh in Israel', *Journal of Human Evolution*, **17**, 733-737.

Semprebon, G.M. and Rivals, F., (2007) 'Was grass more prevalent in the pronghorn past? An assessment of the dietary adaptations of Miocene to recent Antilocapridae (Mammalia: Artiodactyla)', *Palaeogeography, Palaeoclimatology, Palaeoecology*, **253**, 332-347.

Semprebon, G.M., Rivals, F. and Janis, C. (2019) 'The Role of Grass vs. Exogenous Abrasives in the Paleodietary Patterns of North American Ungulates', *Frontiers in Ecology and Evolution*, **7**, 65, 1-23.

Shapiro, S.S. and Wilk, M.B. (1965) 'An analysis of variance test for normality (complete samples)', *Biometrika*, **52**, 3/4, 591-611.

Shea, J.J. (2008) 'Transition or turnovers? Clmiatically-forced extinctions of *Homo sapiens* and Neanderthals in the east Mediterranean Levant', *Quaternary Science Reviews*, **27**, 2253-2270.

Sheldon, N.D. and Tabor, N.J. (2009) 'Quantitative paleoenvironmental and paleoclimatic reconstruction using paleosols', *Earth-Science Reviews*, **95**, 1-52.

Shimelmitz, R., Kuhn, S.L., Jelinek, A.J., Ronen, A., Clark, A.E. and Weinstein-Evron, M. (2014) ''Fire at will': The emergence of habitual fire use 350,000 years ago', *Journal of Human Evolution*, **77**, 196-203.

Shea, J.J. and Bar-Yosef, O. (2005) 'Who Were The Skhul/Qafzeh People? An Archaeological Perspective on Eurasia's Oldest Modern Humans', *Journal of The Israel Prehistoric Society*, **35**, 451-468.

Siani, G., Magny, M., Paterne, M., Debret, M. and Fontugne, M. (2013) 'Paleohydrology reconstruction and Holocene climate variability in the South Adriatic Sea', *Climate of the Past*, **9**, 499-515.

Sneva, F.A., Mayland, H.F. and Vavra, M. (1983) 'Soil ingestion by ungulates grazing a sagebrush-bunchgrass range in eastern Oregon', *Oregon Agricultural Experiment Station Special Report (Oregon State University, Corvallis)*, **682**, 1-48.

Spinage, C. (1986) *Natural History of Antelopes*, Facts on File Publications, New York.

Stiner, M.C. (1994) *Honor Among Thieves: A Zooarchaeological Study of Neanderthal Ecology*, Princeton University Press, Princeton, NJ, USA.

Stocker, T.F., D. Qin, G.-K. Plattner, L.V. Alexander, S.K. Allen, N.L. Bindoff, F.-M. Bréon, J.A. Church, U. Cubasch, S. Emori, P. Forster, P. Friedlingstein, N. Gillett, J.M. Gregory, D.L. Hartmann, E. Jansen, B. Kirtman, R. Knutti, K. Krishna Kumar, P. Lemke, J. Marotzke, V. Masson-Delmotte, G.A. Meehl, I.I. Mokhov, S. Piao, V. Ramaswamy, D. Randall, M. Rhein, M. Rojas, C. Sabine, D. Shindell, L.D. Talley, D.G. Vaughan and Xie, S.-P. (2013) 'Technical Summary' In: *e*, Stocker, T.F., D. Qin, G.-K. Plattner, M. Tignor, S.K. Allen, J. Boschung, A. Nauels, Y. Xia, V. Bex and Midgley, P.M. (Eds.), *Climate*

Change 2013: The Physical Science Basis. Contribution of Working Group I to the Fifth Assessment Report of the Intergovernmental Panel on Climate Chang, Cambridge University Press, Cambridge, United Kingdom and New York, NY, USA.

Strickland, B.K., Hewitt, D.G., DeYoung, C.A. and Bingham, R.L. (2005) 'Digestible energy requirements for maintenance of body mass of white-tailed deer in southern Texas', *Journal of Mammalogy*, **86**, 1, 56-60.

Stringer, C.B. (1978) 'Some problems in Middle and Upper Pleistocene hominid relationships', In: Chivers, D.J, and Joysey, K.A. (Eds) *Recent Advances in Primatology*, Academic Press, London, 395-418.

Stringer, C.B. and Trinkaus, E. (1981) 'The Shanidar Neanderthal crania', In: Stringer, C.B. (Ed) *Aspects of Human Evolution*, Taylor and Francis, London, 129-165.

Strömberg, C.A.E. (2006) 'Evolution of hypsodonty in equids: testing a hypothesis of adaptation', *Paleobiology*, **32,** 2, 236-258.

Strömberg, C.A.E., Dunn, R.E., Madden, R.H., Kohn, M.J. and Carlini, A.A. (2013) 'Decoupling the spread of grasslands from the evolution of grazer-type herbivores in South America', *Nature Communications*, **4**, 1478-1486.

Talamo, S., Blasco, R., Rivals, F., Picin, A., Chacón, M.G., Iriarte, E., López-García, J.M., Blain, H.-A., Arilla, M., Rufà, A., Sánchez-Hernández, C., Andrés, M., Camarós, E., Ballesteros, A., Cebrià, A., Rosell, J. and Hublin, J.-J. (2016) 'The radiocarbon approach to Neanderthals in a carnivore den site: a well-defined chronology for Teixoneres Cave (Moià, Barcelona, Spain)', *Radiocarbon*, **58**, 2, 247-265.

Tchernov, E. (1981) 'The biostratigraphy of the middle east', In: Cauvin, J. and Sanlaville, P. (Eds.) *Préhistoire du Levant*, Centre national de la recherche scientifique, Paris, pp. 67-97.

Tchernov, E. (1991) 'The Middle Paleolithic mammalian sequence and its bearing on the origin of *Homo sapiens* in the southern Levant', In: Bar-Yosef, O. and Vandermeersch, B. (Eds) *Le Squelette Mousterien de Kebara 2*, *Cahiers de Paleoanthropologie*, Editions du CNRS, Paris, 77-88.

Teaford, M.F. and Walker, A. (1983) 'Dental microwear in adult and still-born guinea pigs (Cavia porcellus), *Archives of Oral Biology*, **28**, 1077-1081.

Teitelbaum, C.S., Fagan W.F., Fleming, C.H., Dressler, G., Calabrese, J.M., Leimgruber, P. and Müller, T. (2015) 'How far to go? Determinants of migration distance in land mammals', *Ecology Letters*, **18**, 6, 545-552.

Tellería, J.L., Santos, T. and Alcántara, M. (1991) 'Abundance and Food-Searching Intensity of Wood Mice (*Apodemus sylvaticus*) in Fragmented Forests', *Journal of Mammalogy*, **72,** 1, 183–187.

Tissoux, H. (2004) *Datations par Uranium-Thorium et par Résonance Paramagnétique Electronique de quelques gisements paléolithiques du Pléistocène supérieur de Catalogne (Espagne) et du Sud de la France*, PhD thesis, Muséum national d'Histoire naturelle, Paris, France.

Tissoux, H., Falguères, C., Bahain, J.-J., Rosell I Ardèvol, J., Carbonell, E. and Serrat, D. (2006) 'Datation par les series de l'Uranium des occupations moustériennes de la grotte de Teixoneres (Moia, Province de Barcelone, Espagne)', *Quaternaire*, **17**, 1, 27-33.

Tzedakis, P.C. (2005) 'Towards an understanding of the response of southern European vegetation to orbital and suborbital climate variability', *Quaternary Science Reviews*, **24**, 14-15, 1585-1599.

Ungar, P.S. (2015) 'Mammalian dental function and wear: a review', *Biosurface and Biotribology*, **1**, 25-41.

Ungar, P.S. and M'Kirera, F. (2003) 'A solution to the worn tooth conundrum in primate functional anatomy, *Proceedings of the National Academy of Sciences*, **100**, 3874-3877.

Valero-Garcés, B.L., González-Sampériz, P., Gil-Romera, G., Benito, B.M., Moreno, A., Oliva-Urcia, B., Aranbarri, J., García-Prieto, E., Frugone, M., Morellón, M., Arnold, L.J., Demuro, M., Hardiman, M., Blockley, S.P.E. and Lane, C.S. (A multi-dating approach to age-modelling long continental records: The 135 ka El Cañizar de Villarquemado sequence (NE Spain)', *Quaternary Geochronology*, **54**, 101006, 1-22.

Valladas, H., Reyss, J.L., Loron, J.L., Valladas, G., Bar-Yosef, O. and Vandermeersch, B. (1988) 'Thermoluminescence dating of Mousterian 'Proto-Cro-Magnon' remains from Israel and the origin of modern man', *Nature*, **331**, 614-616.

Vandermeersch, B. (1966) 'Nouvelles découvertes de restes humains dans les couches levalloiso-moustériennes du gisement de Qafzeh (Israël)', *Comptes rendus de l'Académie des Sciences*, **262**, 1434–1436.

Vandermeersch, B. (1969a) 'Découverte d'un objet en ocre avec traces d'utilisation dans le moustérien de Qafzeh (Israël)' *Bulletin de la Société Préhistorique Française*, **66**, 157–158.

Vandermeersch, B. (1969b) 'Les nouveaux squelettes moustériens découverts à Qafzeh (Israël) et leur signification', *Comptes rendus de l'Académie des Sciences*, **268**, 2562–2565.

Vandermeersch, B. (1970) 'Une sépulture moustérienne avec offrandes découverte dans la grotte de Qafzeh', *Comptes rendus de l'Académie des Sciences*, **268**, 298–301.

Vandermeersch, B. (1972) Récentes découvertes de squelettes humains à Qafzeh (Israël): essai d'interprétation. In: Bordes, F. (Ed.), *Origine de l'homme moderne*. UNESCO, Paris, pp. 49–54.

Vandermeersch, B. (1981) *Les hommes fossiles de Qafzeh (Israël)*, Centre national de la recherche scientifique, Paris.

Vetter, S. (2005) 'Rangelands at equilibrium and non-equilibrium: recent developments in the debate', *Journal of Arid Environments*, **62**, 2, 321-341.

Vézian, R. (2014) *Etude paléontologique des Bovinae et des Equidae de la grotte moustérienne du Portel-Ouest (Ariège, France). Cadres biostratigraphique, biochronologiqque et paleo-environnmental*, PhD thesis, Université de Perpignan Via Domitia, Perpignan, France.

Voelker, A.H.L. and workshop participants (2002) 'Global distribution of centennial-scale records for Marine Isotope Stage (MIS) 3: a database', *Quaternary Science Reviews*, **21**, 10, 1185-1212.

Walker, M., Johnsen, S., Rasmussen, S.O., Popp, T., Steffensen, J., Gibbard, P., Hoek, W., Lowe, J., Andrews, J., Björck, S., Cwynar, L.S., Hughen, K., Kershaw, P., Kromer, 53 B., Litt, T., Lowe, D.J., Nakagawa, T., Newnham, R. and Schwander, J. (2009)

'Formal definition and dating of the GSSP (Global Stratotype Section and Point) for the base of the Holocene using the Greenland NGRIP ice core, and selected auxiliary records', *Journal of Quaternary Science*, **24**, 1, 3–17.

Werner, M., Mikolajewicz, Heimann, M. and Hoffman, G. (2000) 'Borehole versus isotope temperatures on Greenland: Seasonality does matter', *Geophysical Research Letters*, **27**, 5, 723-726.

Whitlock, J.A. and Richman, J.M. (2013) 'Biology of tooth replacement in amniotes', *International Journal of Oral Science*, **5**, 66-70.

Williams, S.H. and Kay, R.F. (2001) 'A comparative test of adaptive explanations for hypsodonty in ungulates and rodents', *Journal of Mammalian Evolution*, **8**, 207-229.

Wronski, T., Tiedemann, R., Apio, A. and Plath, M. (2006) 'Cover, food, competitors and individual densities within bushbuck *Tragelaphus scriptus* female clan home ranges', *Acta Theriologica*, **51**, 3, 319-326.

Wuersch, P., Del Vedevo, S. and Koellreutter, B. (1986) 'Cell structure and starch nature as key determinants of the digestion rate of starch in legumes', *American Journal of Clinical Nutrition*, **43**, 25-29.

Žliobaitė, I., Rinne, J., Tóth, A.B., Mechenich, M., Liu, L., Behrensmeyer, A.K. and Fortelius, M. (2016) 'Herbivore teeth predict climatic limits in Kenyan ecosystems', *Proceedings of the National Academy of Sciences*, **113**, 4, 12751-12756.

Appendix 1

The data appendix for this thesis is presented in electronic format for download by the reader. There is a 'README' file that explains the contents of each of the data files.

This electronic appendix contains the following folders and files:

- **Folder:** Data

  Files:

  1_modern_hypsodonty.xlsx [This Excel workbook contains sheets of the datasets used in Chapter 4 and discussed in Chapter 5].

  2_intraspecific_summary_stats_shapiro_wilk.xlsx [This Excel workbook contains a sheet with the summary statistics and Shaprio Wilk tests for the investigation into intraspecific variation of hypsodonty].

  3_fossil_data.xlsx [This Excel workbook contains seven sheets of hypsodonty index measurements, one for each fossil site as discussed in Chapters 6 and 7 and Appendix 2.]

- **Folder:** Histograms and Q-Q plots

  Files:

  1_Intraspecific_variation_histograms.pdf [This pdf contains a histogram for each taxon in the modern dataset].

  2_Intraspecific_variation_QQ_plots.pdf [This pdf contains a Q-Q plot for each taxon in the modern dataset].

- **Folder:** Correlation plots

  Files:

  1_correlation_plots_bioclim_HI.pdf [This pdf contains correlation plots of hypsodonty index versus every bioclim variable, as well as bioclim variables against each other.

Appendix 2

A2.1 Introduction

This appendix presents detailed discussions that supplement the body of the main thesis. Firstly, section A2.2 discuss each fossil site in turn and then secondly, section A2.3 discusses regional comparisons of the fossil sites and their results.

A2.2 Discussion – hypsodonty index as an indicator of aridity in Late Pleistocene communities (site by site)

This section discusses the seven Late Pleistocene sites and the changes in hypsodonty index of the mammal communities at each site, with comparison to existing environmental proxy data available for each site. Overall, section A2.2 will bring together all of the sites and discuss the validity of hypsodonty index as a reliable indicator of past aridity in relation to environmental trends and changes seen in these other proxies.

A2.2.1 Abric Romaní (Capellades, Spain)

A2.2.1.1 Hypsodonty index data

It is pertinent to discuss the nature of the data collected from Abric Romaní before it is compared with site-specific environmental proxy data in order to assess the robustness and reliability of any inferences made. As mentioned in section 6.1.1 of the main thesis, there were a very limited number of teeth that were suitable for measurement and therefore the number of hypsodonty index measurements are low. There are another number of potential issues with the dataset including the yield of data from the different levels of the site. Nine out of the fifteen levels yielded suitable specimens but the large majority of the measurements were from level Ja. This level is one of the most important archaeological levels and this level alone has been subject to extensive multi-proxy investigation (see Carbonell, 2012; Rosell *et al*., 2012). The low sample size is largely due to the condition of the available M_3s, with 43% of those in the Abric Romaní collection at IPHES being broken, the majority diagonally across the crown of the tooth with the roots completely missing. This sharp breakage of the teeth may be as a result of marrow extraction from the mandible which would require breakage of the mandible, especially around the mandibular angle between the mandibular body and ramus which would have likely fractured the posterior molars including the M_3. Mandibular breakage by Neanderthals has been reported from level O of the site based on taphonomic and lithic evidence (Gabucio *et al*., 2018). This is strong evidence that the assemblage was accumulated by Neanderthals and that there may be a hunting bias to consider in the

assemblage when interpreting the results as the taxa represented in the assemblage may not capture the natural ungulate diversity in the community at this time.

Another issue with the hypsodonty index measurements from Abric Romaní is the low diversity of taxa represented in the measurements in this study compared to the taxa actually present at the site as revealed in palaeontological studies. Five ungulate taxa are present across the whole sequence (Rosell *et al*., 2012); however, in the present study, the measurements are almost all from *Equus* sp. with one sole measurement from a *Bos* sp. tooth. Ecometric data are highly dependent on the diversity of taxa present in a sample (Faith *et al*., 2019) and this will have undoubtedly affected the mean hypsodonty index that has been calculated, especially as equids are the most hypsodont ungulates. This will be important to consider in the following discussions.

Figure 6.1 in the main thesis shows the changes in mean hypsodonty index through the levels for which data was available for collection. At first glance, the mean hypsodonty index appears to change throughout the levels, particularly increasingly from the lowest in level M (c. 54.5 ka) to the highest in level L (c. 51.8 ka) with oscillations up through the sequence. However, this apparent change may not be due to the low sample levels, since within standard deviation, the values overlap (see levels Ja and I). What is curious is that the mean hypsodonty index value for level M (2.40) is 37% lower than level B which has the second lowest mean hypsodonty index of 3.78.The question remains as to whether this is significant or again, a fact of poor data? The data through the sequence will be discussed in the next section in relation to pre-existing environmental proxy data to assess whether any real change in mean hypsodonty index exists through the Abric Romaní sequence and if so, to explore the likely environmental driver(s) of this change.

A2.2.1.2 Comparison with palynological proxy data

Pollen data is available from Abric Romaní, the most detailed of which is the arboreal pollen record from Burjachs *et al*. (2012). This is presented below in Figure A2.1 alongside the hypsodonty index data from this study. Comparing the mean hypsodonty index measurements with the pollen, in order from oldest to youngest levels, will allow possible links between vegetation and hypsodonty through time to be examined. Beginning with the oldest level, M, the lowest of the mean hypsodonty index measurement coincides with a peak in arboreal pollen of around 20%. As hypsodonty is suggested to be an indicator of aridity in the literature, and from the modern study in Chapters 4 and 5, as well as the literature (e.g. Liu *et al*., 2012), hypsodonty has a potential link to temperature, a low level of hypsodonty may indicate a wetter, less arid environment, which may manifest in a more vegetated environment. The mean hypsodonty index of Level L above is apparently the highest in the sequence, but the

sample size is too low for this value to be considered reliable. However, this apparent maximum hypsodonty coincides with a slight dip in the arboreal pollen percentage (down to approximately 13%) between two peaks. Fewer trees on the landscape suggests a transition, albeit, short lived, to a more open landscape, more suited to taxa like *Equus*, which is heavily represented in the samples. In this case high hypsodonty may be associated with slightly more open landscapes near Abric Romaní and this notion is supported by the literature (e.g. Janis, 1988). However, the links suggested here a very tenuous and the evidence from these two lines of evidence is very far from conclusive. The sample size for hypsodonty index is far too low and the temporal resolution of the levels is low compared to the pollen data which is available at a much higher resolution. For example, level L, apparently coinciding with a small dip between two peaks in arboreal pollen, may not be exactly contemporaneous with the dip as the chronology gives only a mean age and the uncertainty may include several of the small peaks and troughs in the arboreal pollen curve.

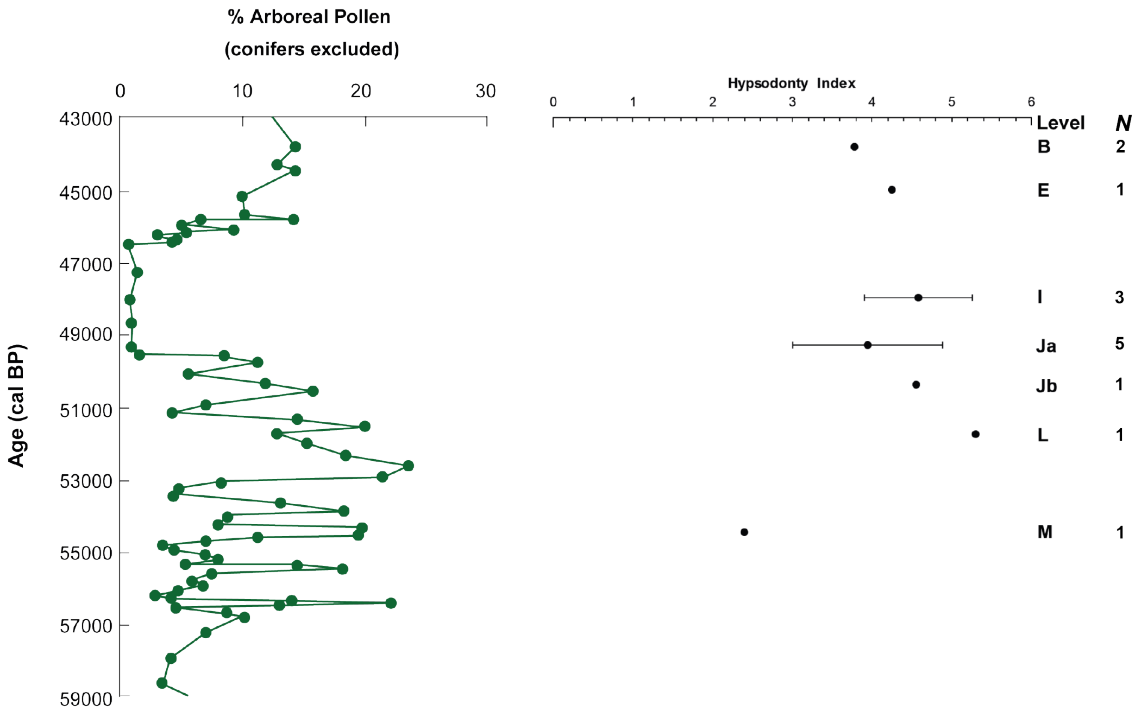

Figure A2.1: The arboreal pollen record from Abric Romaní (left, data from Burjachs *et al*., 2012) plotted alongside the mean hypsodonty index data (right, the level and the sample size (*N*) relating to each data point is labelled to the right). Both are plotted against the chronology from Gabucio *et al*. (2014). Mean hypsodonty index from level A is not shown as this is beyond the limit of the available arboreal pollen data.

From level L to Jb and then to Ja, the mean hypsodonty index decreases and this appears to match a downwards trend in arboreal pollen percentage during this time. Again, the caveats of differing temporal resolutions of the levels and the pollen sampling must be taken into consideration, as well as the small sample sizes for the hypsodonty index but there appears to be a downward trend in both. A decrease in mean hypsodonty is suggested to indicate an increase in moisture and a decrease in arboreal pollen

indicates a potentially more open landscape, whether that be open and dry or open and moist. From the arboreal pollen percentage alone, this cannot be determined but luckily there are proxy data from micromammals and herpetofauna that can provide additional information and this will be discussed in the next section.

After the decline in arboreal pollen discussed above (c. 53,000 – 49,500 cal years BP), there is a clear plateau in arboreal pollen percentage. For c. 2,500 cal years, the level remains at around 1-2%, indicating an almost treeless landscape around Abric Romaní. The palynological data show that this period is characterised by high abundance of *Artemisia*, Asteraceae and Poaceae, indicators of regional steppe vegetation. This event is coincident with Heinrich event 5 in the Northern Hemisphere. The hypsodonty index data through the levels corresponding to this time interval is limited to levels Ja and I, for which there is the most available data. The overlapping errors may mean that the mean community hypsodonty index did not change through these levels, which is consistent with a regional landscape where the vegetation is also not changing as a stable flora would unlikely warrant a response in the mammal community. On the other hand, the mean hypsodonty index does increase between level Ja and level I, which could indicate a response of the mammal community to changes in their environment. Based on the premise that higher mean hypsodonty index indicates higher levels of aridity this may mean a slightly drier environment during the deposition of level I. However, *Rupicapra rupicapra*, an indicator of rugged, rocky environments with preference for alpine meadows in summer and pine forests in winter (Pedrotti and Lovari, 1999), and *Stephanorhinus hemitoechus*, an indicator of open habitats rich in low-growing vegetation (Pandolfi *et al*., 2017), which are present in level Ja and disappear during level I before reappearing in level H. It is possible that Heinrich event 5 (which correlates with all three of levels Ja, I and H) had led to environmental deterioration as seen in the decrease in arboreal pollen to a plateau which persisted for approximately 3,000 years. However, as there are no hypsodonty index measurements from level H, it is impossible to suggest confidently that there is a response in the hypsodonty to Heinrich event 5. The fact that only *Equus* measurements are included in the mean hypsodonty index from levels Ja and I means that one cannot say anything regarding other taxa for certain but if the mean hypsodonty index of the horse community increased, this could reflect an environmental response. The increase in hypsodonty in level I at the same time as a virtual absence of trees may indicate that hypsodonty here is exhibiting a signal of either lower moisture availability and/or a decrease in temperature. It may be possible that slightly more hypsodont horses were better adapted to the environmental conditions (perhaps climatically-induced changes to coarser grasses or more dust or grit) and they were more successful that the less hypsodont horses and it is these successful more

hypsodont individuals that are represented in the data at this time interval. Unfortunately, it is difficult to resolve this further as there are no other proxies from the same time period in the sequence, and as seen in the literature and the modern study presented in Chapters 4 and 5, unresolved signals of both aridity and temperature may be carried in the mean hypsodonty index of the community.

Abric Romaní, Spain

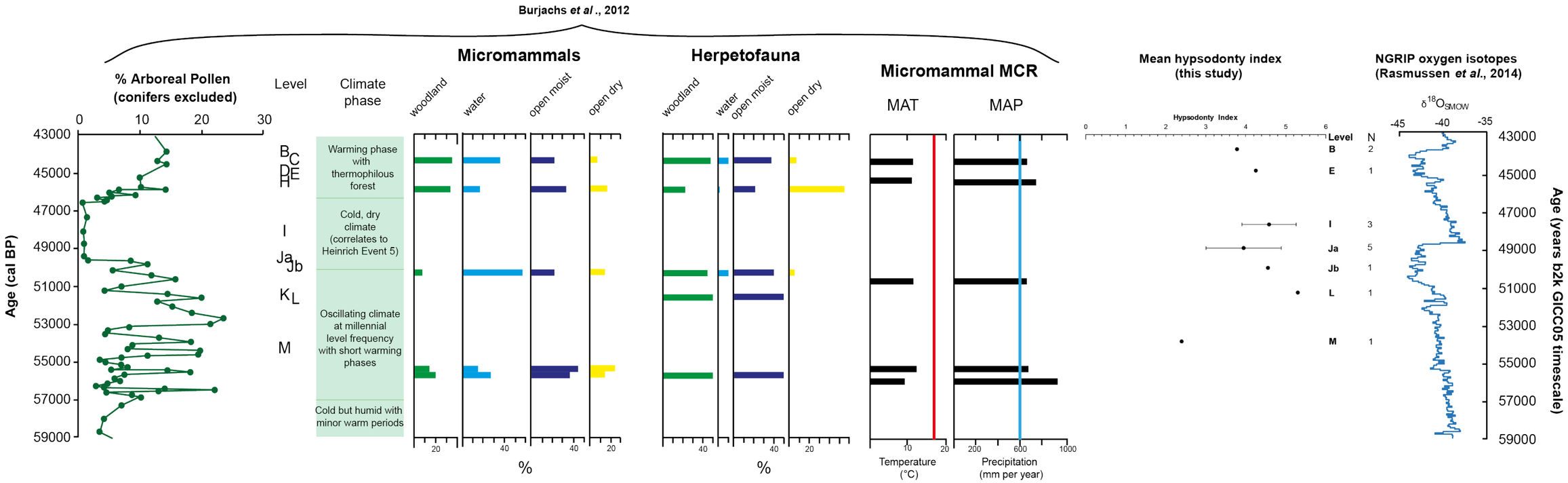

Figure A2.2: Composite diagram showing palaeoenvironmental proxy data from Burjachs *et al*. (2012) plotted on the chronology from Gabucio *et al*. (2014) alongside the hypsodonty index data from this study (level labels and sample size (*N*) are also shown) and the NGRIP data from Rasmussen *et al*. (2014). The diagram is partially adapted from Burjachs *et al*. (2012). Mean hypsodonty index from level A is not shown as this is beyond the limit of the available arboreal pollen data.

A2.2.1.3 Comparison with micromammal proxy data

Neither the hypsodonty index data from this study nor the micromammal data from Burjachs *et al*. (2012) cover all of the levels. There are no micromammal data from levels M and L; however, level Jb, for which there are some hypsodonty index data, has some micromammal data against which they can be compared. For this depositional period, around 50,000 cal years BP, the micromammal habitat preferences indicate the presence of water (~45% of the assemblage) with open moist indicators making up 20% of the assemblage, followed by open dry and then woodland indicators having the lowest representation. This indicates a permanent aquatic environment near to the site and what could be interpreted as a large proportion of moist open grassland, perhaps meadow. As the hypsodonty data in this study comprises only horses, it is therefore appropriate to focus on this type of grazing vegetation. Under such moist conditions, grasses would likely have been more supple and less abrasive as there is higher water uptake into the plant material and thus less need for the development of fibrous plant tissue to remain upright in times of water stress (Briggs *et al*., 2008). Dew and water present on the surface of vegetation would also remove abrasive dust and soil particles (Damuth and Janis, 2011). This would be more suitable for individual equids with lower levels of hypsodonty as the amount of tooth wear would be lower. At this time (level Jb) the mean hypsodonty index is 3.94, but with very little data, poor reliability and mismatching temporal resolutions between the micromammal data and the hypsodonty index data, it is not possible to discuss such mechanisms any further in the micromammal context alone. Again, for levels Ja and I, there are no micromammal data to compare with.

Interestingly (and notwithstanding the low number of datapoints), when examining the micromammal Mutual Climatic Range precipitation reconstructions of those samples that are *approximately* contemporaneous with the deposition of levels Jb and level B, it is apparent that the reconstructions are very similar (approximately 675 mm per year) and the mean hypsodonty index for Jb and B are also similar (3.95 and 3.78, respectively).

A2.2.1.4 Comparison with herpetofauna data

Herpetofaunal habitat preferences are available for five discrete points within the Abric Romaní sequence and are presented in Figure A2.2 above. Between c. 56,000 cal years BP and c. 52,000 cal years BP, there is little change in the habitat preferences of the herpetofauna, with an equal proportion of woodland and moist open environment indicators. For the lower sample, there are no hypsodonty index data that are contemporaneous. However, the hypsodonty data for level L can be compared with the c. 52,000 cal year BP herpetofauna sample. Curiously, the hypsodonty index between M and L drastically increases. Level L shows the highest hypsodonty index in the entire

sequence and potentially indicates higher aridity, although there are no reptiles appearing to indicate such aridity at this time. A marked change in herpetofauna is recorded in the sample at c. 46,000 cal years BP where the percentage of open dry taxa increases to more than 50%. There are no hypsodonty index data for this exact time but Level E, which dates to 45 ka, has a mean hypsodonty index of 4.26, very close to the 3.95 of level Jb where the percentage of open dry adapted herpetofauna is very low. This mismatch of similar mean hypsodonty index values but opposing herpetofauna ecological affinities may suggest that changes in hypsodonty index may not resolve the difference between open-dry and open-moist environments, the key component of which, of course, is differences in moisture availability and aridity. This contradicts the idea in the literature that hypsodonty carries a precipitation and aridity signal (Damuth *et al.*, 2002; Janis *et al.*, 2004, Eronen *et al.*, 2010a), but based on results from the modern study undertaken in this thesis, there is no clear climatic signal carried by hypsodonty index. Therefore, the inability to resolve aridity changes here is not surprising.

A2.2.1.5 Comparison to the NGRIP record

Burjachs *et al*. (2012) already report that a suggested expression of North Atlantic climate exists in their pollen spectra from Abric Romaní, through comparison with the NGRIP record. The stable isotope signal seen in the NGRIP record (along with other Greenland ice core records) is seen as a proxy for air temperature over Greenland (Johnsen *et al*., 1995, 2001; Rasmussen *et al*., 2014) as well as having minor components of other variables such as surface condensation conditions (Masson-Delmotte *et al*., 2005), changes in precipitation seasonality (Werner *et al*., 2000) and changes in moisture sources (Krinner *et al*., 1997; Masson-Delmotte *et al*., 2005). It is a matter of intense debate regarding the size of the spatial extent over which this climate signal expressed, and whether stable isotope changes in Greenland are representative of climate of the North Atlantic region as a whole (Larsen *et al*., 1995; Voelker *et* al., 2002). Over the past few decades, it has been proposed that climate events seen in proxy records in the Mediterranean have close correlates in the North Atlantic Region. Pollen spectra in lacustrine records across Europe show significant shifts in arboreal to non-arboreal vegetation and these changes are proposed as evidence of a direct response to North Atlantic regional climate changes (e.g. Allen, 1999; Tzedakis, 2005). Sea-surface temperature records of the coast of Greenland and from the Aegean Sea show similarities (Rohling *et al*., 2002) and Greenland events are also seen in the Adriatic Sea (Siani *et al*., 2013), further suggesting a regional link between climate events happening in Greenland, and the eastern Mediterranean. This regional link is supported further by isotope signals in speleothems in Israel that have also been attributed to Greenland events (Bar-Matthews *et al*., 1999, 2007). All of these records hint that the

changes seen in the Greenland ice core oxygen isotope records (i.e. temperature changes) are expressed across the North Atlantic to the Mediterranean and that there is a regional 'temperature' signal. However, it is difficult to say that changes in proxy records are reflecting temperature changes directly as the teleconnections between Greenland and the wider region (e.g. the Mediterranean) are complicated and include a number of atmospheric components such as the polar front and other European storm tracks (Martin-Garcia, 2019).

Of interest here is the observation that the trends seen in the oxygen isotope record from NGRIP (Rasmussen *et al*., 2014) may be reflected in the hypsodonty index data. To note, level M has a mean hypsodonty index of 2.40, which is 40% lower than the mean of the whole sequence, thereby suggesting that this value is anomalous and may be excluded. When following the downward trend from level L through level Jb and to level Ja, this closely mirrors the downward trend seen in the NGRIP oxygen isotope record between c. 52,000 and c. 49,000 years b2k (interpreted as a temperature decrease by Rasmussen *et al*. (2014)). Following this decrease in the oxygen isotope ratios, there is a reversal of the signal towards interstadial conditions, which peak around c. 48,500 years b2k. At c. 48,000 cal years BP in the hypsodonty index record, there is also a reversal in the trend, with the mean hypsodonty index increasing from 3.952 in level Ja to 4.587 in Level I. This 'peak' in the hypsodonty index record occurs c. 500 years later than ice core isotope peak at c. 48,500 years b2k. This may represent an offset if there is a linked response, or it may be that the temporal resolution and calculation of mean hypsodonty index across this time period makes this hypsodonty peak seem lagged compared with the NGRIP record. There is a similar trend between the two records between levels E and B (45,000-43,800 cal years BP) where there is a decrease in mean hypsodonty index and a decrease in the oxygen isotope ratios between 45,000 and 44,000 years b2k.

Mechanistically, it is difficult to suggest how hypsodonty index and temperature are linked, although the literature suggests that hypsodonty index can predict temperature (Liu *et al*., 2012; Žliobaitė *et al*., 2016). In the modern study (Chapters 4 and 5 in the main thesis), it is also shown that, despite being weak, the correlation between hypsodonty index and temperature-related climate variables, is stronger than with precipitation-related climate variables. The similarity of the trends seen through Abric Romaní sequence and the NGRIP record may indicate that this correlation existed in the past, either lagged or in synchrony, but the poor sample sizes mean that this is far from a conclusive assessment.

A2.2.1.6 Summary

The vegetation, micromammal and herpetofauna proxy data largely complement each other, following similar trends that are assumed to be climatically controlled. However, the hypsodonty index data do not appear to follow the same trends, which, as is apparent from the Abric Romaní data, that in this case there is limited support for the theory that hypsodonty index carries a climatic signal, especially one of aridity, although as discussed above, comparisons with the NGRIP record may hint at a temperature signal. However, the poor quality of the data collected must be taken into consideration here. One of the contributing factors to this is that the data from this study contain almost exclusively measurements from *Equus ferus*, a typically highly hypsodont taxon. Equids are suggested to be hypergrazers in the "present" (Semprebon *et al*., 2019). Small changes in dietary abrasiveness, which may or may not be climatically controlled, may therefore not have any effect on tooth wear. This evolution to a hypergrazer state may mean that small changes in dietary abrasiveness are buffered by the adaptation of equid hypsodonty. In the absence of other taxa that were not hypergrazers, small climatic or environmental effects on tooth wear may not be seen. What is notable, however, regarding the hypsodonty index data from Abric Romaní, is that there may be a temperature control, based on the similarity of trends in both the hypsodonty and NGRIP isotope data. This "wiggle-matched" relationship may not be causal and could be coincidental (as a factor of small sample size giving false trends) but this putative relationship can be tested at other fossil sites in this thesis. A summary assessment of hypsodonty index as a respondent to climatic and environmental change in the past is discussed in more detail in Chapter 7 in the main thesis.

A2.2.2 Teixoneres (Moià, Spain)

A2.2.2.1 Hypsodonty index data

Limited temporal resolution of the measured specimens has had a significant effect on the value of the results obtained from Teixoneres. Despite the site having a detailed and high resolution radiocarbon chronology (Talamo *et al*., 2016), which can be applied to the other proxies, the resolution of the large mammal data has generated two groupings: Unit II and Unit III. Sample size is also different between the two levels, with Unit II only yielding three measurements of hypsodonty index, compared to eighteen from Unit III. However, taxonomic diversity in the Teixoneres results is much higher than that seen at Abric Romaní. As shown in Chapter 6, the mean hypsodonty index data calculated for each unit have overlapping errors, statistically indicating no change throughout the sequence. Although the younger level has a sample size of three specimens, it has a large standard deviation. This is due to the presence of *Sus scrofa*, which is an omnivorous species (IUCN, 2008) and therefore not hypsodont. Wild boar have a less abrasive diet than grazers and have therefore not evolved wear-resistant crown types (Janis, 1984). The other two specimens measured in Unit II have almost identical hypsodonty index values but are from two taxa with differing typical diets. One is *Cervus elaphus*, which is a mixed feeder with varying dietary compositions of grass and sedges (Gebert and Verheyden-Tixier, 2001), but also takes herbs and browse (Bugalho and Milne, 2003). The other is the extinct European ass *Equus hydruntinus,* which is likely to have predominately been a grazer but, as is known from extant asses, may have consumed more browse, particularly when favoured grasses are poor quality or scarce (Estes, 1991). The fact that *E. hydruntinus* in this unit has a lower hypsodonty index that might be expected for an equid (albeit based on a single specimen) may indicate that favoured grazing material was not available.

In Unit III, there is a much higher number of taxa present in the dataset, although *Sus scrofa*, while present in the assemblage (Rosell *et al*., 2017), was not measured for hypsodonty index due to the absence of suitable teeth. This may cause the mean hypsodonty index of Unit III to be higher as a product of this sampling issue. There is a mixture of more hypsodont grazing taxa such as *Equus ferus* and *Capra* sp. and those that are mixed feeders with a higher component of browse in their diets such as *Cervus elaphus* (Gebert and Verheyden-Tixier, 2001; Bugalho and Milne, 2003) and *Capreolus capreolus* (Jackson, 1980). This explains the large error (standard deviation) in the mean hypsodonty index from this unit, which would have likely matched the dispersion of the data in Unit II if *Sus scrofa* measurements had been available for inclusion in the dataset for Unit III. Therefore, from this study it can be suggested that the hypsodonty index at

Teixoneres does not likely change from Unit III to Unit II, although more measurements from Unit II are necessary to be more definitive in this assessment.

A2.2.2.2 Comparison with the palynological data

Pollen data from López-García *et al*. (2012) suggest that Level III has an assemblage indicative of humid conditions and that Level II has vegetation more representative of dry conditions. Both Units II and III have open and woodland indicators in varying abundances. The hypsodonty index data appear to show no response to this proposed drying and cooling of the climate as seen in the pollen record.

A2.2.2.3 Comparison with the small vertebrate data

Addressing the micromammal proxy data first, the presence of the wood mouse *Apodemus sylvaticus* throughout the sequence indicates consistent woodland above 60% (López-García *et al*., 2012). The presence of *Cervus elaphus* in the hypsodonty index dataset in both units is concordant with this. Despite the consistent amount of woodland, the micromammal habitat associations nevertheless indicate change between Unit III and Unit II, similarly to that found in the pollen record. In Unit III, a more humid environment is indicated by more meadow and stream indicators in the vicinity, whereas Unit II (particularly subunit IIb) has indicators of an increase in dry meadows and rocky areas and a decrease in the number of streams in close proximity to the site. The herpetofaunal remains also indicate that open-dry habitats increased from the bottom of Unit III to the top of Unit III (López-García *et al*., 2012; Luzi *et al*., 2017). As hypsodonty index is hypothesised to be mechanistically linked to moisture availability, it is surprising that no significant evidence of change in the hypsodonty index between the units that would reflect the transition from a more humid environment to a drier one.

A2.2.2.4 Summary

The hypsodonty index data from Teixoneres shows no significant difference through the two main units of occupation (Units II and III), contrary to the trends seen in the pollen and small vertebrate data, which show a transition from warm and humid conditions in Unit III to cold and dry ones in Unit II. With a transition such as this, it might be expected that the hypsodonty would show at least some change. There are a number of issues with the data that must be considered here that may help explain this. First, there is a very small sample size for Unit II, and also for both units, there is a large dispersion in the data and overlapping errors, obscuring any change between units. Second, the nature of the occupations and thus the mode of accumulation of the palaeontological assemblages of Units II and III must also be considered. It is likely that in Unit II, there is only a seasonal snapshot recorded by the large mammal assemblage accumulated by

Neanderthals, as opposed to a full year average of climatic conditions recorded by the natural accumulations of small mammals and herpetofauna. Large mammals may not be present in the proximity of the site throughout the year and seasonal migrations away from the site may mean that the taxa that were hunted during the preferred season may not be representative of the colder and drier conditions suggested by the annual, rather than seasonal, small vertebrate signal.

The regional climatic context must also be taken into account as the Teixoneres sequence has accumulated over MIS 3, a time period characterised by rapid climatic oscillations. As the hypsodonty index data are only available at a resolution of the two units, it is impossible to attribute any hypsodonty changes to one or more of these oscillations. The signal is therefore averaged and muted, which may also explain why, at the unit resolution, there is no apparent significant change in hypsodonty at Teixoneres compared to the other proxies that provide palaeoenvironmental data at a higher resolution.

A2.2.3 Le Portel-Ouest (Ariège, France)

A2.2.3.1 Hypsodonty index data

The results from Le Portel-Ouest are more difficult to assess than the results from Abric Romaní or Teixoneres as the chronological control and temporal resolution are relatively poor for the palaeontological remains. Sub-beds were combined to increase sample size and coverage of the sequence when calculating mean hypsodonty index, therefore "beds" refer here to the chronological unit used, whereas the interpretation predominantly relies on depth within the sequence.

Many beds yielded very poor numbers of suitable specimens and therefore sample sizes are low for most beds. The exception is Bed F, which yielded 33 hypsodonty index measurements. This bed was the only one to include a wide variety of different taxa with diverse environmental preferences (*Rangifer tarandus*, *Bos* sp., *Cervus elaphus*, *Equus* sp. and *Capra* sp. are all present). This is in comparison to the other remaining beds, which contain more limited diversity in the hypsodonty index results. Bed B, for example, contains measurements from *Bos* sp. and *Cervus elaphus*, the results at the boundary of bed C and D and bed D itself contain only measurements from *Bos* sp. and Bed G contains only one measurement from *Rangifer tarandus*. This will undoubtedly skew the mean hypsodonty index as it can be seen that such low diversity is not a true representation of the fauna present when considering the list of taxa recovered from all beds (see Gardeisen, 1998).

The values of the means and their associated errors must also be discussed. The lowest mean hypsodonty index is for Bed G, with a sole specimen of *Rangifer tarandus* yielding a value of 1.47. *Rangifer tarandus* is a generalist herbivore and although it has a seasonally selective diet, it consumes forbs, sedges, grasses, shrubs and even lichen. There is no dominance of abrasive plants in the diet and thus has no need to adapt to resist wear by having more hypsodont teeth. This may explain why Bed G appears to have the lowest hypsodonty index at Portel-Ouest. However, the other taxa that are present in this bed, but which could not be measured for hypsodonty index, are more selective in their diets, with *Capra* and *Equus* typically more hypsodont as an adaptation to grazing behaviour. It can be assumed here, then, that bed G has an artificially low mean hypsodonty index. The opposite may be said for the value for the boundary of B/C, where a single *Bos* specimen provides the maximum mean hypsodonty index at Portel-Ouest. The palaeontological study by Gardeisen (1998) does not list *Bos* but instead lists *Bison* but either way, both taxa have much more graze in their diet and are morphologically adapted for this by having hypsodont cheek teeth. The presence of *Cervus elaphus* and *Rangifer tarandus* in beds C and D indicates that this high value at

the boundary is likely to be a factor of the small sample size and is therefore not representative of the true mean hypsodonty index of the ungulate community at this time. For the values in bed F and bed B where the error can be calculated, it can be seen that they overlap, indicating no statistically significant differences; this will be discussed further in comparison to environmental proxy data in the following section.

A2.2.3.2 Comparison to environmental proxy data

Gardeisen (1999, p. 1155) reports that bed G is an excellent representation of an "open arctic biotope, such as tundra", highlighted by the dominance of *Rangifer tarandus* in the assemblage over bison and horse. Therefore, it is no surprise that out of all the specimens, the only one suitable for measurement of hypsodonty index was from *Rangifer tarandus*. The sedimentological study reports bed G as having a stony fraction with karstic pebbles (Vézian, 2014), supporting the inference of a cold environment at this time. However, the presence of *Megaloceros giganteus* and *Cervus elaphus* indicate that woodland must have been present within close proximity, despite the predominantly open landscape. The relatively low levels of grazers such as *Equus caballus* (Gardeisen, 1998) suggests that the environment would have not been dominated by grasses, indicating a less arid environment. The presence of *Megaloceros giganteus* and *Cervus elaphus* also support the idea that a (partially) open environment existed but with an important component of more luscious herbs and shrubs instead of drier grasses, as these taxa are mixed-feeders rather than grazers (Gebert and Verheyden-Trixier. 2001; Lister and Stuart, 2019). This is also supported by the study of rodent remains at the site which, although they are predominantly cold-adapted, the presence of *Microtus oeconomus* (Pallas, 1776) indicates the existence of damp grassland during the deposition of bed G (Marquet *et al*., 1998). Although there is only one single hypsodonty index measurement for bed G, the low value, potentially indicating less aridity, does not appear discordant with the environmental reconstructions from other proxies, aside from the pollen data which suggest a drier environment through beds K to C (Renault-Miskovsky and Girard, 1998, cited in Vézian, 2014), although bed-by-bed palynological detail is not available.

Microtus oeconomus continues to be present in Bed F, although *Microtus agrestis* declines in abundance. Marquet *et al*. (1998) suggest that during the deposition of bed F, there would have been a dominance of open environments on the surrounding plateaux but the moisture levels in the environment increased to a level that allowed the development of a number of humid environments in valley bottoms, potentially caused by temperature inversions which trapped moisture in areas of confined topography, as is the case around the Portel caves. In comparison to Bed G, through Bed F, the

proportion of arctic-adapted and montane ungulates (reindeer, alpine ibex and chamois) decreases whilst the proportion of non-arctic faunal elements of horse, bison and *Megaloceros* increase. The mean hypsodonty index in Bed F increases compared to that of Bed G. If hypsodonty is more related to moisture availability, then a decrease in the mean hypsodonty index might be expected if the local environment were becoming more humid through the deposition of bed F. However, the decrease in the abundance of reindeer suggests that the environment may not be as cold during this time. The hypsodonty index data are only available for bed F as a whole, but it could be that the increase seen in the mean hypsodonty index between Beds G and F is not related to moisture availability but to a temperature increase. This may have also led to the development of open steppe type environment at higher altitudes which would continue support horse, bison and giant deer but no longer be as suitable to support reindeer, alpine ibex and chamois.

A potential increase in temperature between Beds G and F is plausible because a relationship is apparent, albeit a weak one, between hypsodonty index and temperature in the modern study (Chapters 4 and 5). Unfortunately, this cannot be assessed further as the chronological control is poor for the hypsodonty data. Marquet *et al*. (1998) conclude that beds G to F2 correspond with MIS 4, which itself is shows some climatic variability in the western Mediterranean (Hodge *et al*., 2008). However, the lower part of Bed F, has been dated to 38.4 ± 6 ka (Ajaja, 1994, cited in Vézian, 2014), placing it in MIS 3, which is particularly unstable in terms of its climate across Western Europe and the Mediterranean (e.g. Brauer *et al*., 2008; Rasmussen *et al*., 2014). It is therefore difficult to interpret the palaeoecology in the context of wider, more regional climate change, without being able to assign changes to any particular stadial or interstadial during these Marine Oxygen Isotope Stages.

In level B, there appears to be a mismatch between the environmental conditions indicated by the rodents and the ungulates. The marked presence of the European snow vole [*Chionomys nivalis* (Martins, 1842)] in the rodent assemblage shows a return to a cold environment. However, the ungulates show an increase in non-arctic and mosaic grassland faunal elements (Marquet *et al*., 1998), likely indicating that the environment is not deteriorating as the rodents might suggest. This contradiction is noted in the literature (Marquet *et al*., 1998), but it is highly likely that these apparently disharmonious faunal elements are coexisting due to the complex topographic nature of the site and likelihood of microclimates and refugial areas such as valley bottoms and on slopes with differing aspects. The mean hypsodonty index in bed B is almost exactly the same in mean value and error as that of bed F, which is discussed above as potentially reflecting higher temperatures rather than moisture change, despite the presence of the European

snow vole, which may have lived in some kind of refugium. Here, this may be the case too, although the sample size is much smaller and contains measurements from only two taxa: *Bos* sp. and *Cervus elaphus*. Humidity is suggested to be lower in Bed B than in Bed F according to the rodent proxy data, resulting in differing levels of humidity between the two beds, but similar mean hypsodonty index values. This does not definitively suggest that moisture availability is not related in hypsodonty index but that the ungulate community is not recording it through changes in mean hypsodonty. Of course, this assumes that the very few measurements in bed B carry the same weight as the more numerous measurements in the samples from the other beds at the site.

A2.2.4 Grotta del Romito (Calabria, Italy)

A2.2.4.1 Hypsodonty index data

Compared to Abric Romaní, Teixoneres and Portel-Ouest, Grotta del Romito yielded more specimens that were suitable for measurement for hypsodonty index. However, this number was not evenly distributed between the different strata, with strata F, G and H only yielding one suitable specimen each. The upper strata of C, D and E provided more measurements, with stratum D yielding the most measurements and hence, perhaps, a more reliable mean hypsodonty index value. Through comparison of the different proxies, it can be established whether the strata with fewer measurements are showing any palaeoenvironmental response, compared to those with more measurements.

As seen in the other sites, it is typical that the taxonomic diversity in the hypsodonty measurements is not always reflected in the taxonomic diversity of the mammalian assemblage at that time in the depositional sequence. Focussing on the different taxa measured for hypsodonty, in stratum H (23,653 – 24,913 cal years BP; Blockley *et al*., 2018), only a single measurement of *Capra ibex* is available. This is a hypsodont taxon, yielding a value of 5.06, the highest for the whole sequence. Following this, a decline in hypsodonty index is apparent to 3.348 in stratum G (22,910 – 23,653 cal years BP; Blockley *et al*., 2018), which, if hypsodonty is responding to an environmental forcing, could indicate rapid change. However, the nature of the data must be considered here.

The only measured specimen from stratum G was a tooth from *Cervus elaphus*, as discussed previously, a non-hypsodont taxon with a mixed diet indicating a (partially) open environment (Gebert and Verheyden-Trixier, 2001) but also known to be present in deciduous woodlands (Ahlen, 1965) and in coniferous forests (Catt and Staines, 1987). This taxon represents less than ten percent of the assemblage, whereas the higher-crowned *Capra* (which could not be measured) actually makes up over 60% of the assemblage (Bertini-Vacca, 2012) in this stratum. It is therefore clear that the apparent drop in hypsodonty index is a factor of the taxa that could be measured rather than reflecting a real palaeoenvironmental shift. However, for bed H, where *Capra ibex* has been measured, this species represents around 75% of the assemblage (Bertini-Vacca, 2012), suggesting greater likely fidelity of the mean hypsodonty index with prevailing conditions (although again, inferences from only one measurement is an issue).

There appears to be a reversal in the mean hypsodonty index from stratum G to F, with the value in stratum F (20,696 – 22,760 cal years BP; Blockley *et al*., 2018) increasing

to 4.89, almost returning to the maximum of 5.06 in stratum H. Again, this is only a single measurement of hypsodonty index from a *Capra ibex* individual. The proportion of *Capra ibex* in the assemblage in stratum F is still high, around 60% (Bertini-Vacca, 2012), as discussed above for stratum H, this may be a representative value for hypsodonty index but without more measurements, it will not be possible to assess except by making comparisons with other environmental proxies.

The upper levels yielded more specimens and dispersion of the data can be examined through the error which is expressed by the standard deviation of the mean hypsodonty index. In stratum E (16,375 – 18,054 cal years BP; Blockley *et al*., 2018), the mean has decreased to 3.83 but the standard deviation almost overlaps with the value from stratum G. However, the error does not overlap with that of stratum F, indicating a statistic difference between strata F and E. There are only ten measurements from stratum E but the nature of the data can provide some explanation behind the apparent decrease in values between strata, as well as assessing the error (dispersal). In stratum E, over 75% of the large mammal assemblage is *Capra ibex*, which supplied nine out of ten measurements (the one remaining measurement being from *Cervus elaphus*). The *Cervus elaphus* measurement of 1.64 contributes to the lower mean hypsodonty index for this level but the error is also interesting as the hypsodonty index values for the *Capra ibex* specimens in this stratum range from 3.36 to 4.72. This may mean that there is a mixture of different individuals adapted in different ways to tooth wear through their diets. *Capra ibex* are known to have alpine grasses composing over half of their diet, but also eat herbaceous plants and shrubs (Parrini *et al*., 2009). Range contractions are common through the different seasons with the winter range being up to 65-70% smaller than the summer range. Altitudinal changes also occur throughout the year, with males preferring higher elevations in summer (Parrini *et al*., 2003). These spatial changes throughout the year may have an influence on the type of plant material available as a result of rainfall differences between spatial areas. Female ibex are also known to have restricted ranges when compared to males (Grignolio *et al*., 2004); this may potentially have a restrictive effect on the type and amount of plant material consumed and therefore influence the range in hypsodonty index seen in this species, although the sex of isolated fossil teeth cannot be established.

Stratum D at Grotta del Romito has generated the most hypsodonty index measurements. These show a decrease in mean hypsodonty index from stratum E to D, however the errors overlap so statistically there is no change. The error itself is large, a product of the range of taxa present in the hypsodonty dataset for this stratum. There is a mixture of very low-crowned taxa such as *Sus scrofa*, low- to mid-crowned taxa such as *Capreolus capreolus* and *Cervus elaphus* and more high-crowned taxa such as *Capra*

ibex and *Rupicapra rupicapra*. Even though the errors in stratum D overlap with those in stratum E, the lower mean is anticipated because of the marked increase in the low-crowned *Sus scrofa* in stratum D, which increases from ~4% to ~30% of the assemblage (Bertini-Vacca, 2012). With regards to the hypsodonty index measurements from stratum D, 21.43% are from *Sus scrofa*, 32.43% from *Rupicapra rupicapra*, 10.71% from *Capreolus capreolus*, 28.57% from *Capra ibex* and 7.14% from *Cervus elaphus*. These are the five most represented taxa (Bertini-Vacca, 2012) and all of these are present in the hypsodonty index data for this stratum, although the proportions of these taxa in the hypsodonty data do not reflect their abundance overall. This may mean an overrepresentation of *Rupicapra rupicapra* in the hypsodonty data but dentally, this species is very similar to *Capra ibex* in crown height, and together, in this dataset and in the overall abundance, they make up 50% of the measurements/assemblage. The mean hypsodonty index for stratum D and its associated error are thus considered representative of the ungulate community at the time of deposition.

Stratum C also contains the same top five represented taxa, and the proportions of abundance remain largely unchanged with only a percent or two increase in *Sus scrofa* and *Cervus elaphus*, whereas the combined *Capra*/*Rupicapra* percentage drops slightly below 50% (Bertini-Vacca, 2012). It is therefore no surprise to see that the mean hypsodonty index drops only slightly, reflecting the abundance proportional changes between low and high crowned taxa. The error also is very similar and thus the two strata have mean hypsodonty index values that cannot be statistically distinguished from one other. This will be discussed further in the next section with comparison to the other environmental proxy data that is available from Grotta del Romito.

A2.2.4.2 Comparison to the molluscan isotope record and NGRIP

Unfortunately, the molluscan isotope record constructed by Colonese *et al*. (2007) only covers the period from c. 14,300 to c. 13,000 cal years BP when plotted on the most up to date chronology from Blockley *et al*. (2018). In relation to the hypsodonty data, this corresponds to strata D and C. It is likely that only the very top part of stratum D is covered by the isotopes but as the resolution of this study is limited to individual strata and includes the very top part of this stratum, it is appropriate to compare both D and C to the isotopes (both are plotted alongside each other in Figure A2.3).

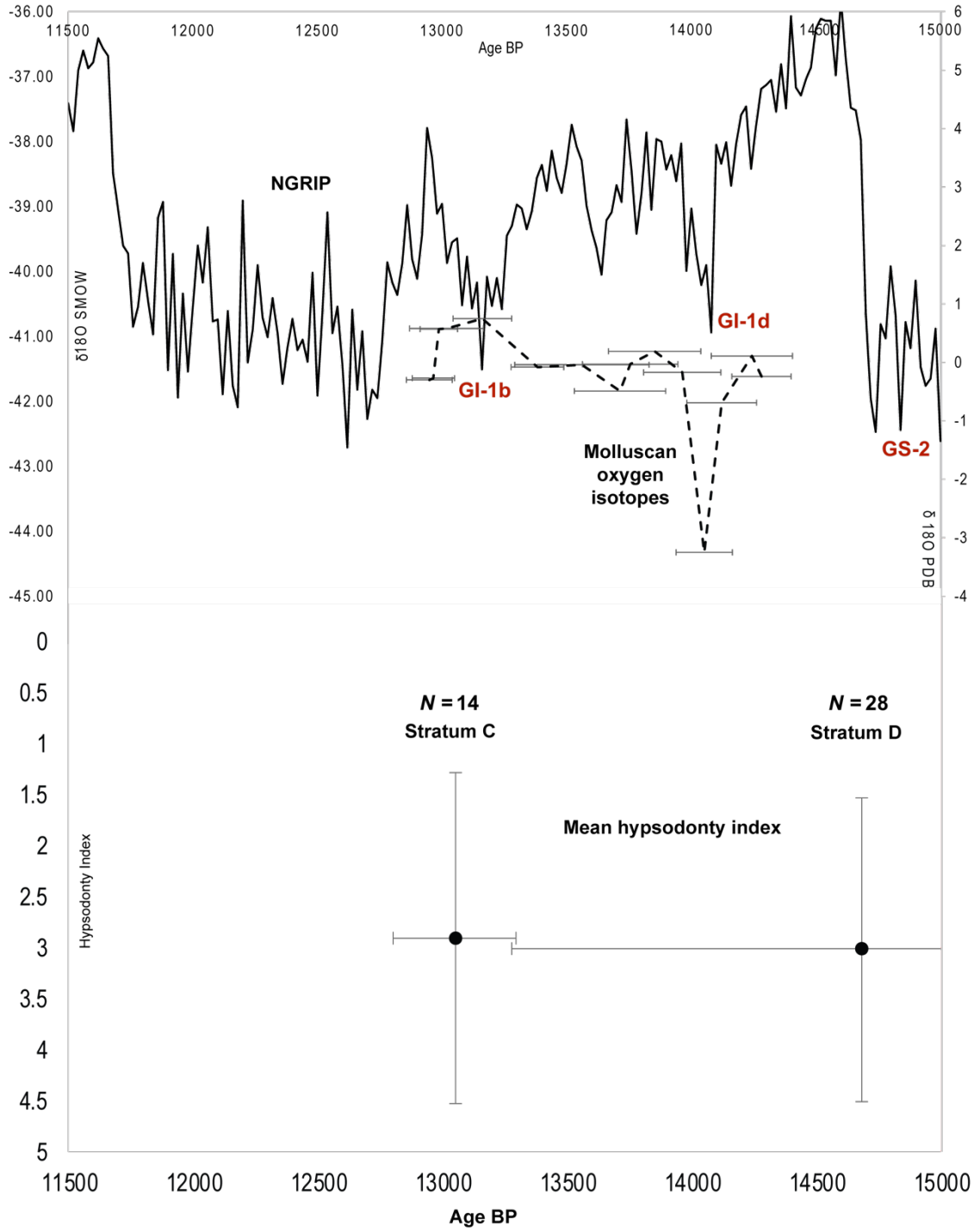

Figure A2.3: Composite figure modified from Blockley *et al*. (2018) showing the molluscan isotope record from Colonese *et al*. (2007) from Grotta del Romito plotted on the revised chronology with the horizontal error bars representing age uncertainty of the samples. NGRIP oxygen isotope record is also shown and events referred to in the text are labelled (see Rasmussen *et al*., 2014)Hypsodonty index data for strata C and D are shown, again with horizontal error bars representing age uncertainty and vertical error bars representing the standard deviation of the mean hypsodonty index values. Sample sizes (*N*) for these strata are also shown.

As can be seen above, the mean hypsodonty index from strata D and C does not significantly change and does not track the excursion seen in the molluscan oxygen isotope record, which is considered to be an expression of the GI-1d event in NGRIP (Blockley *et al*., 2018). Technically, as the hypsodonty index measurements are

amalgamated as samples per strata, the resolution is much coarser and the age uncertainties actually overlap slightly, although stratigraphically the two strata are clearly separate. Focussing on the mean age of each stratum and hypsodonty sample, stratum D may coincide with the end of GS-2 in NGRIP. Stratum C may coincide with the GI-1b event, both events around the -41.00 and -42.00 $\delta^{18}O$ SMOW values. As the mean hypsodonty index for both strata are also similar, this could indicate a link to regional air temperature which the $\delta^{18}O$ record is suggested to represent. However, a higher resolution hypsodonty index record would be needed to assess this fully, especially to investigate any response to the isotopic excursion that corresponds to the GI-1d event.

A2.2.4.3 Comparison with local to regional landscape evolution and NGRIP

Paleoenvironmental changes have been reconstructed using the small mammal remains and their associated habitat preferences. This reveals a significant shift to the dominance of woodland-adapted taxa after the Heinrich 1 event in Greenland. This response appears to be a regional event as the pollen record from Lago Grande di Monticchio also indicates a shift from steppe to woodland taxa (Brauer *et al*., 2007; Blockley *et al*., 2018). These are presented again in Figure A2.4 alongside hypsodonty index data collected from Grotta del Romito in this study and the NGRIP oxygen isotope record.

Examining the results from oldest to youngest, there is a oscillation between stratum H and F, since the mean hypsodonty index decreases from stratum H to stratum G and then returns to a similar value in stratum F. The small mammal proxy data do not cover the same time period as the deposition of stratum H, but changes in the hypsodonty index data are not reflected by the small mammals, which maintain the same percentages of dry, woodland and water-adapted taxa through the period c. 23,500 – 21,000 cal years BP (Blockley *et al.*, 2018). With regards to the large mammal fauna and its direct impact on the mean hypsodonty index, the abundance of *Cervus elaphus*, a woodland indicator, slowly decreases from stratum H to F, whilst *Rupicapra rupicapra*, an indicator of alpine meadow and rocky habitats, slowly increases (Bertini-Vacca, 2012). The effect of this abundance change in mean hypsodonty index cannot be reliably assessed as the three strata in question have mean hypsodonty index values only represented by one specimen and hence one taxon. Worthy of note is that the decrease in stratum G occurs around one hundred calibrated years after a small peak in mesic woody taxa percentage at Lago Grande di Monticchio, only 115km to the north and suggested to represented regional vegetation at this time (Brauer *et al*,, 2007). Indeed, based on our understanding of hypsodonty and vegetation, it might be expected that an increase in woodland and a corresponding decrease in more abrasive grasses might have had an effect on mean hypsodonty index. Unfortunately, in this case, stratum G is

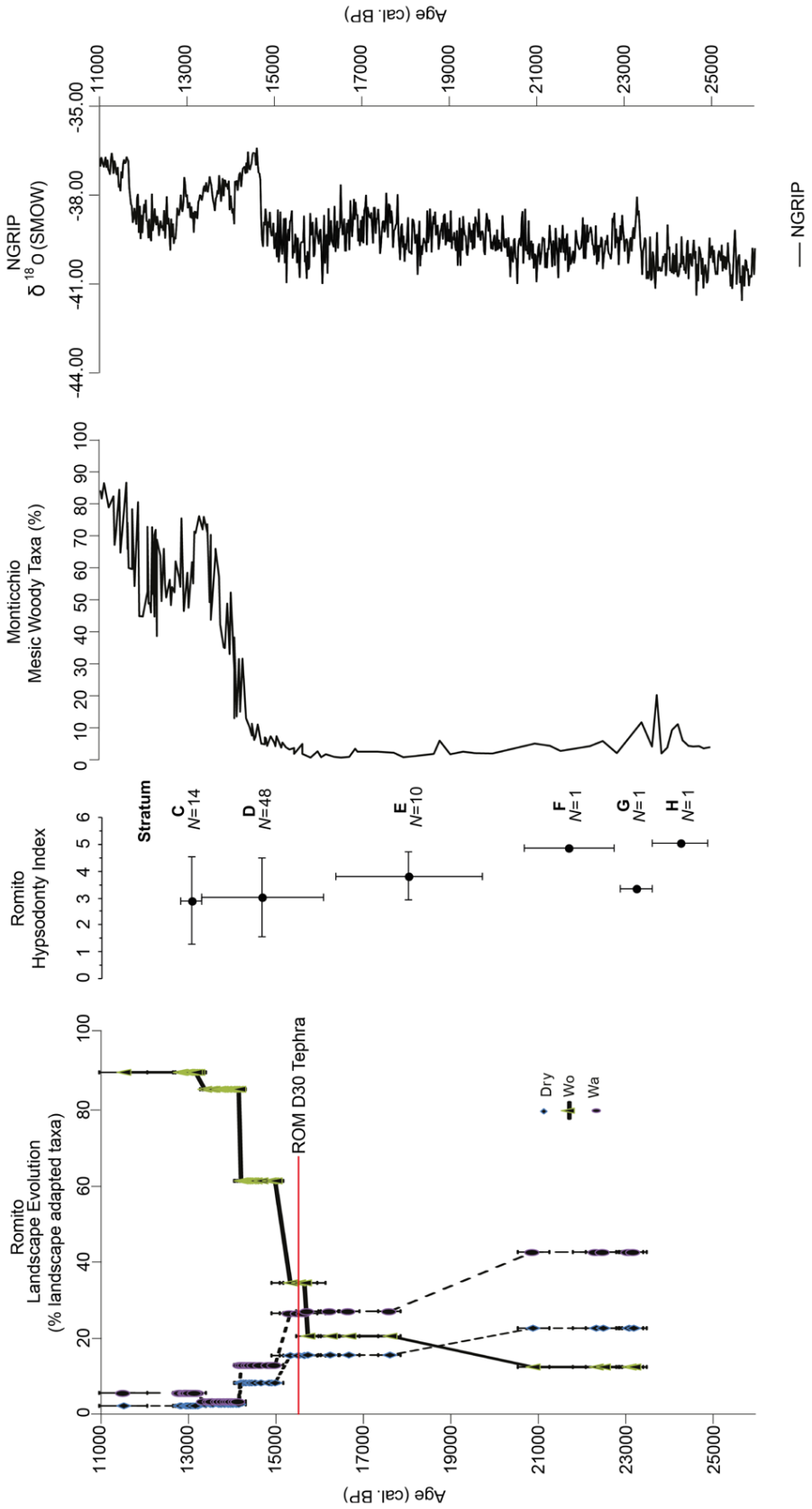

Figure A2.4: Composite figure, adapted from Blockley *et al*. (2018). Left to right: percentages of small mamma taxa with reference to their habitat preferences (Dry, Woodland (Wo), Water (Wa)) plotted on the revised Blockley *et a*l. (2018) chronology with the position of the ROM-D30 tephra also marked, original small mamma data from López-García *et al*. (2014), Grotta del Romito mean hypsodonty index (this study, strata labels and sample sizes (*N*) are also shown), percentage of mesic woody taxa in the pollen record from Lago Grande di Monticchio published by Brauer *et al*. (2007) and the NGRIP oxygen isotope cord (Rasmussen *et al*., 2006, 2014).

only represented by *Cervus elaphus*, compared to strata H and F which are only represented by *Capra ibex*. Between strata H and G the abundance of the taxa with the lowest levels of hypsodonty actually decreases (Bertini-Vacca, 2012). This should have the effect of increasing the mean level of hypsodonty between these levels. However, in this study this is not the case and this is likely attributed to the fact that values from single specimens are not representative of the community hypsodonty.

The errors can also be quantified for the other three strata for which mean hypsodonty values are available. The three mean hypsodonty index values are all overlapping, statistically indicating no change. With the regards to the means alone, there is a steady decrease from strata E to D and to C. The age uncertainties are also large, a result of combining the samples from different sub-strata to increase sample size. This hampers any comparisons with the higher resolution proxies but there the clear shift seen in the small mammal data is not reflected in mean hypsodonty index, although there is a slight decrease. As discussed in section A2.2.4.2, from E to D, there is a decrease in mean hypsodonty index, albeit slight, largely reflecting the abundance increase of the woodland indicator and lower crowned taxa of *Sus scrofa* and *Cervus elaphus*. It is highly likely that this is linked to woodland development close to Grotta del Romito, a result of climatically-driven regional forest expansion. The same trend is seen in the Greenland ice cores, where the excursion in the oxygen isotope curve represents the start of the Lateglacial in northwest Europe (Blockley *et al*., 2018). The mean hypsodonty index value for stratum C is not statistically different from the two preceding strata but the small mammal proxies from Grotta del Romito and the regional pollen record from Lago Grande di Monticchio show rapid change at this time (Blockley *et al*., 2018). There may potentially be a lag between the local and regional vegetation and small mammals and any changes in the large mammal community, since although periods of rapid change are suggested by these proxies, the large mammal community does not significantly change during this time. However, there is a marked increase in woodland indicators in the large mammal fauna between strata F/E and strata D/C (see Figure 3.22; Bertini-Vacca, 2012) but a response appears very muted (and statistically there is no change) in the hypsodonty index record. As with other sites, this is likely to be a product of poor sample size as a result of a limited number of suitable teeth. In the case of Grotta del Romito, this was largely due to the older age profile of the individual animals as many teeth were worn.

Regrettably, the temporal resolution of the hypsodonty index data at stratum level, alongside the poor yield of measurements of hypsodonty index, precludes further examination of the causal mechanisms between changes in mean hypsodonty index

local and regional environmental changes, and exploration of the potential for these to be climatically driven.

A2.2.5 Tabun (Mount Carmel, Israel)

A2.2.5.1 Hypsodonty index data

Of all of the Late Pleistocene sites examined in this study, Tabun yielded the most measurements, although of the 117 total measurements, 80% were from level B, the youngest level in the hypsodonty dataset. Going from the oldest to youngest deposits, level Ed (302 ± 27 ka; Mercier and Valladas, 2003) yielded only two measurements, both from *Dama* sp.. From level Ed to Eb, there is an increase in the mean hypsodonty index from 1.806 to 3.390. In level Eb, the measurements are taken from one specimen of the lower-crowned taxon *Cervus elaphus* and two each of higher-crowned taxa *Bos* sp. and *Equus* sp., which explains the increase observed in the mean. Mean hypsodonty index in level Ea decreases, due to the presence of six *Dama* sp. teeth which are low crowned. The marked increase in mean hypsodonty index at the D-E boundary is a result of no low crowned taxa being present in the measurements here, instead only *Bos* sp. and *Gazella* sp. are present. Here there are very few measurements so it is unclear whether this peak in the mean hypsodonty index is an artefact of the data or whether it is a real representation of the mammalian community at this time.

Bed D contains only one measurement from *Gazella* sp. but the hypsodonty index of this individual is very similar to that of the gazelle specimen at the D-E boundary, highlighting the impact that the presence of the higher crowned *Bos* sp. specimen has on the mean in the older bed. This also can be seen in Bed C where the *Gazella* sp. specimen hypsodonty index is again similar to that of other gazelles in the previous two samples, but the mean hypsodonty index is increased by the presence two measurements of the even higher-crowned *Bos primigenius*. The mean hypsodonty index values for beds C, D and Ea all overlap each other when the standard deviations are considered, so there are no significant differences between these levels. The only significant deviation from these levels of mean hypsodonty index would be at the D-E boundary but this may reflect the limitations of the data. This will be further discussed in the next section in relation to available environmental proxy data.

Level B, with its relatively high sample size of 94 measurements, is regarded as the best available dataset. 77 of these measurements (81.9%) are *Dama* sp. specimens, which is representative of the assemblage as a whole, since 78.5% of the number of individual specimens (NISP) in Tabun B were attributed to *Dama mesopotamica*. The attribution of the isolated teeth to *Dama* sp. is likely to be overly cautious here, rather than uncertainty, as the size clearly indicates fallow deer. The dominance of such a lower crowned taxon undoubtedly contributes to a lower mean hypsodonty. This increase in *Dama mesopotamica* was interpreted by Bate (1937) as a result of a changing climate. This

taxon inhabits open woodland, but also riparian forest thickets (Large Herbivore Network, 2015) and therefore this dramatic increase from 0.5% of the assemblage in Tabun C to 65-66% of the assemblage in Tabun B (Garrod and Bate, 1937) may indicate a rapid expansion of open woodland environments in close proximity to the site, but also riparian forest, both of which would indicate increasing moisture availability in the locality. The mean hypsodonty index for level B does have a significant error as shown on Figure 6.5 but this does not overlap with the hypsodonty data from levels C and D. Therefore, it may be possible to say something more substantial about links between mean hypsodonty index and climate between these two levels. It will also be interesting to compare proxy data in level B to those in level E as in both of these levels the hypsodonty data overlap and statistically indicate no differences and therefore little change throughout the sequence. This will be discussed further below.

The temporal resolution of the hypsodonty index data must also be discussed here. The age uncertainties for levels Ed, Eb and Ea all overlap so inferences can only be made here for level E as a whole. The same can be said for levels D and C as the age uncertainties also overlap. This does not cause too much of an issue when comparing to the pollen data, as similar zonation is present in this data. However, stratigraphic provenance of the specimens is clear. It is also clear that the timespan for some of the dating uncertainties are quite large. For example, level B could date from 84 ka to 137 ka (Grün and Stringer, 2000), which covers the end of MIS 6 through MIS 5e-a (Lisiecki and Raymo, 2006). This encompasses the Last Interglacial and a number of other climatic oscillations within the early last cold stage, so by having a temporal resolution only of “level B”, the signal in the hypsodonty index data will be an average and potentially masking any ‘real’ climatic signal that may be present in the data.

A2.2.5.2 Comparison to pollen data

A description of the flora at Tabun was first published by Horowitz (1979) and the sequence is split into two zones. The first zone comprises levels G, F and E and consists of low percentages of arboreal pollen (less than 10%). In addition, a more open environment is indicated by the presence of grass and sedges and high levels of Chenopodiaceae, a common inhabitant of warm and dry temperate areas, but is also a halophyte. These beds are interpreted as “very dry, interpluvial conditions” (Horowitz, 1979, p.253); the locality was affected by higher sea levels and the immediate vicinity became a coastal plain with sand dunes. The pollen from levels D and C, with a much higher percentage of arboreal taxa (between 30-50%), suggests that the environment around Mount Carmel shifted to oak and pine woodland and represents “pluvial conditions” (Horowitz, 1979, p.253).

The standard deviations of all of the mean hypsodonty values from level E overlap with the data-poor values from levels D and C, suggesting no statistically significant change in mean hypsodonty index between level E and the upper levels of D and C, therefore not reflecting the changes seen in the pollen sequence. However, differing trends may been seen in the mean hypsodonty index values themselves. If hypsodonty index has a relation to moisture availability, it would be expected that mean hypsodonty index would decrease under pluvial conditions, but instead the mean hypsodonty index increases, particularly from level Ea to levels D and C. The lower mean hypsodonty index seen in level B, as discussed above, likely indicates woodland development through the high representation of the open woodland adapted, and also the abundance of low-crowned, *Dama mesopotamica*. Again¸ however, the errors overlap with the values seen in level E, and as the pollen indicates, the lower and upper parts of the sequence have a differing floral and thus climatic signal, but the hypsodonty index data show no differences.

A2.2.6 Qafzeh (Mount Precipice, Israel)

A2.2.6.1 Hypsodonty index data

Qafzeh has been an important but contentious site in the study of human occupation of the Levant. Briefly recapping from Chapter 3 of the main thesis, the site consists of occupation layers inside the cave, on the terrace outside of the cave and also in the corridor between the two. Correlation of the occupation layers is extremely complex, and the chronology is poorly constrained with dates on only the lower part of the sequence (layers XVII to XXIV) and different dating methods have produced conflicting dates. Recent work suggests that the lower part of the Mousterian levels correlates to MIS 5e (Ambrose *et al.*, 2018; Frumkin and Comay, 2019). Rabinovich and Tchernov (1995) suggest that this part of the sequence should be correlated with the upper part of Tabun level D. However, these levels did not yield any hypsodonty index data, and thus the results reported in this study are limited to the upper levels of the Mousterian section and some overlying deposits about which reporting is poor. For example, this study did not find reporting on Level C and F and their subdivisions in the literature so correlation with the currently published stratigraphic framework is not possible. Therefore, as the results are chronologically unconstrained, they are presented in stratigraphical order.

Beginning with the oldest level for which data are available, level XVI, there were only three specimens measured giving a mean hypsodonty index of 2.57. The error is large as the sample includes two teeth of the lower-crowned taxon *Cervus elaphus* and one of the higher-crowned *Capra* sp. The mean hypsodonty index drastically decreases to 1.12 in the next available level (level XVB) but this is only represented by a single measurement of *Dama* sp. which is a low-crowned taxon. Without further data for this level, it cannot be said whether this dramatic decrease represents a real shift in the mean hypsodonty index. Problems correlating with the better understood stratigraphic system of Rabinovich *et al*. (2004) prevents an assessment of whether this low value is representative of the community or not.

Following the sequence up, the next level, XV, has four measurements from a wide range of taxa in terms of tooth morphology. Very low-crowned *Sus* cf. *gadarensis* is present in the dataset alongside the low-crowned *Dama* sp. and *Cervus elaphus* but also the higher-crowned *Capra*. The presence of these different taxa would indicate that both woodland and more open meadow/rocky grassland environments are present. A similar situation would be present in the oldest level, level XVI, as discussed above. The hypsodonty index values, both the mean and the error are very similar between level XVI and XV and it is likely that the hypsodonty index of the mammal community is responding to the same forcing factors.

The next level, XIV, has only a single measurement giving a mean hypsodonty index of 1.62, again indicating a decrease from 2.28 in the preceding level, although the datapoint here is only a single specimen of *Stephanorhinus hemitoechus*, a generalist mixed feeder of both grass and browse (Kahlke and Kaiser, 2011). This explains the lower hypsodonty value and also highlights that, although the value itself may not be representative of the mammal community at this time, the inference is that a mosaic environment of woodland and open landscapes persists here as it did in level XVI and XV. However, in XVB we are only seeing *Dama* sp. giving a false indication that woodland predominates. Following on from this, in level XIII again, a similar mean (and error) to XVI and XV is observed. This is suggesting that there is no change up to this point in the sequence, as again XIII contains both woodland (*Sus* cf. *gadarensis*) and more open landscape (*Capra* sp. and *Gazella gazella*) taxa.

Further up the sequence, the remaining levels in the upper part of the Mousterian (Levels XII-X) have very low sample sizes. Taking the values as they appear, the hypsodonty index seems to trend upwards, with level X containing measurements of two *Bos* sp. teeth. Without the ability to compare accurately to the species abundances as these are not published, it cannot be determined whether these values are representative of the community. Regardless of this fact, the values for levels XII-X are within the error range of the lower levels and thus it may be said that there is little or no change in mean hypsodonty index throughout the whole upper part of the Mousterian levels for which data are available.

For the remainder of the sequence, the stratigraphic location of the levels is poorly known and thus age and potential correlations with other proxy studies are impossible. An increase in hypsodonty index is seen from level X to level “F-6” but the date of these horizons is unknown. The rate of change of the hypsodonty index for the remainder of the levels cannot be assessed and it would thus be inappropriate to make climatic or environmental inferences from it. The levels have very few datapoints for each one, and the oscillations may be a factor of the sample size and selective taxa availability in the data collection. What is interesting is that again, all the data points (aside from F-6 which is interestingly the maximum hypsodonty index value at Qafzeh), lie within the errors of the lowest levels of the Mousterian, again meaning that potentially there is little to no change in mean hypsodonty index through the sequence at Qafzeh.

A2.2.6.2 Comparison to proxy data

Unfortunately, the poor understanding of the position of the hypsodonty index data within the chronological framework of Qafzeh prevents clear comparisons with other proxy data. As discussed above, the hypsodonty index itself is perhaps only revealing the same

information as the palaeontological assemblages have already done in the past, that there is a mosaic of landscapes in proximity to the cave (Rabinovich *et al*., 2004). This is also concordant with the isotopic study by Hallin *et al*. (2012), which suggests several different habitats in proximity to the site. These authors also show that there is no significant difference in isotopic ratios between the Middle and Upper Palaeolithic levels, and generally, the climate was dry and the environment mostly open. It is uncertain where the hypsodonty data from this study fits chronologically, but if there were no differences across the whole of MIS 5d-a, the hypsodonty data would support this, although conflicting speleothem evidence of Levantine climate stability/instability with evidence for both humidity (Frumkin *et al*., 2000) and aridity (Frumkin *et al*., 2011) complicates the story. Nevertheless, a great deal more data is needed to confirm this inference, which, in the absence of the possibilities of improved hypsodonty index data from Qafzeh, will have to remain tentative.

A2.2.7 Haua Fteah (Cyrenaica, Libya)

A2.2.7.1 Hypsodonty index data

The site of Haua Fteah had only twelve teeth suitable for measurement of hypsodonty index as provenance within the sequence is not accurate for all specimens. Many specimens were labelled with multiple levels, some of which were not adjacent and thus potentially could represent a significant period of deposition. Inferences made from these specimens would be spurious at best, and they are hence ignored in further assessment. Only measurements from specimens where stratigraphic provenance is certain are assessed in this study. This reduced the dataset size to only five teeth from three levels, meaning sample size was too low in each level for the calculation and assessment of errors.

In stratigraphic order, the hypsodonty index data indicates an increase through the sequence from level X, to level VIII and to level VI. In level X, the measurements are from one *Bos primigenius* tooth and one *Ammotragus lervia* tooth, whereas levels VIII and VI contain one measurement each from *Ammotragus lervia*. Using the dates published by Douka *et al*. (2014), level X has a proposed age of 12.3-9.3 ka, level VIII has a proposed age of 7.4-6.9 ka and VI a proposed age of 6.4-6.2ka. *Ammotragus lervia* is known to tolerate arid rocky grassland environments and does not require fresh drinking water if water can be obtained from its diet. *Bos primigenius,* on the other hand, does have a requirement for water and its presence in level X may indicate more moisture availability, although the presence of *Ammotragus lervia* indicates some arid and rocky habitats in close proximity. The disappearance of *Bos primigenius* upwards through the sequence may represent a change in environmental conditions, and therefore the hypsodonty index values increasing may reflect a loss of moisture availability. Alternatively, the results may be a factor of small sample size and therefore unrepresentative of changes in environmental or climatic conditions during the deposition of these layers.

A2.2.7.2 Comparisons to environmental proxy data

As discussed above, the layers for which data are available are suggested by the age model from Douka *et al*. (2014) to date from 12.9-6.2 ka. This period covers the end of the Last Glacial-Interglacial Transition and early Holocene which elsewhere incorporates major environmental shifts (e.g. in north west Europe as recorded in NGRIP; Rasmussen *et al*., 2014). In addition, of more local and regional importance, is that this period for which there is hypsodonty index data also coincides with the African Humid Period of ca 12 – 5 ka (Costa *et al*., 2014), where northern Africa was subject to increased precipitation due to a northwards movement of the tropical rainbelt (Gasse, 2000).

Through much of the occupation at Haua Fteah, the palaeoenvironmental conditions remained remarkably constant (Reade *et al*., 2016), although two arid phases at c.8.0 ka and c. 7.3 ka are suggested from the molluscan isotope studies (Prendergast *et al*., 2016).

Level VIII has an age that coincides with the later aridity increase indicated by the isotope signal in molluscan shell carbonate. Mean hypsodonty index does increase at this time, potentially indicating an aridity signal, although with two measurements for this sample, this is inconclusive.

Oxygen isotope values on herbivore tooth enamel oxygen have been published for the three levels for which hypsodonty data are available (Reade *et al*., 2018). These are plotted alongside hypsodonty index on Figure A2.5 below.

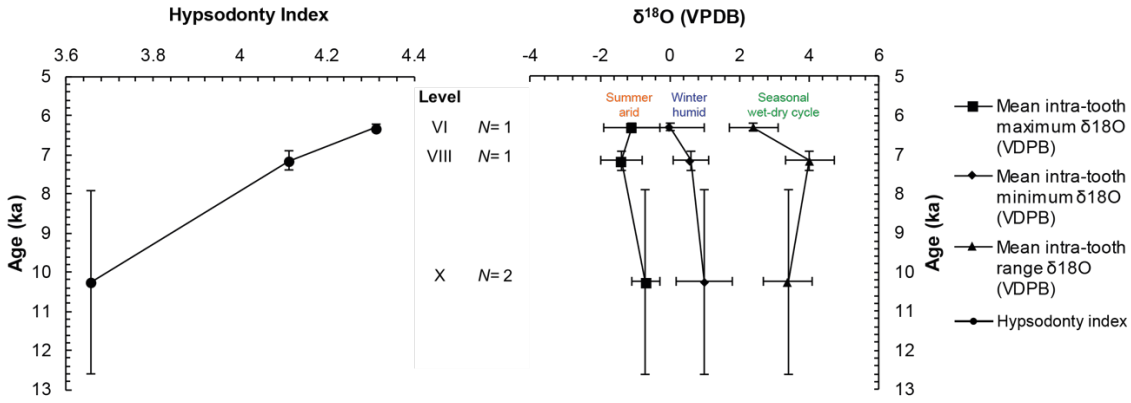

Figure A2.5: Hypsodonty index data from Haua Fteah, left, plotted against herbivore tooth enamel oxygen isotope data from the same levels from Reade *et al*. (2018), right. Sample sizes (*N*) are also shown.

As seen in Figure A2.5, the increase in hypsodonty index is not picking out the changes indicated by the oxygen isotopes, namely the seasonality peak in Level VIII.

Concerning the African Humid Period there is an interesting comparison to make between the Haua Fteah hypsodonty index record and the lake level of Lake Mega Chad, seen as a proxy for moisture availability and the African monsoon (Armitage *et al*., 2015). Figure A2.6 shows that the increase in hypsodonty index happens during the high lake level stand(s) reconstructed for Lake Mega Chad. The lake level dramatically decreases at the end of the African Humid Period, suggesting rapid aridification, however evidence from the Fezzan region of Libya, much more proximal to Haua Fteah than Lake Mega Chad, shows aridification began around 7.6 ka (Lem *et al*., 2016), very close in timing to the increase in hypsodonty index. This may indicate that the hypsodonty index at Haua Fteah has an aridity component. As the record from Lake Mega Chad is seen as a reflection of north African moisture availability during this time (Armitage *et al*., 2015), it could be expected that the hypsodonty index at Haua Fteah would show the same trend,

with stability through this time, however the lack in number of measurements of hypsodonty index prevents robust inferences being made.

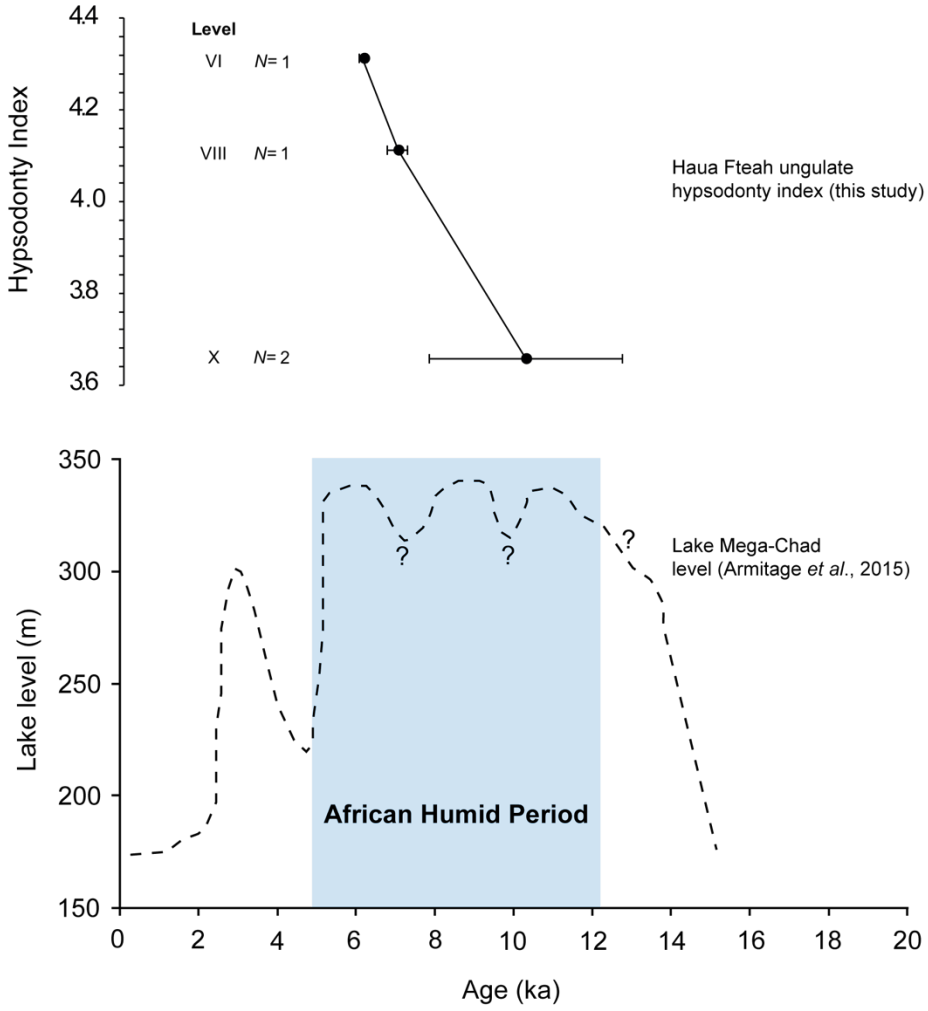

Figure A2.6: Top: Haua Fteah hypsodonty index data (this study; level labels and sample size (*N*) is shown). Below: Lake level of Lake Mega-Chad, data from Armitage *et al*. (2015). The African Humid Period is shown in blue.

A2.2.8 Summary

Section A2.2 has discussed each site in detail, comparing changes in the mean community hypsodonty with contemporaneous proxy information at each site. There may be potential that the mean community hypsodonty index is picking out changes recorded in other proxy data, but low sample sizes mean conclusions are tentative. This is especially the case when taxa present in the hypsodont index measurements are not always representative of the fossil community. Comparisons to other local and regional proxies are complicated by mismatching resolutions and undersampled parts of sequences, meaning that often proxies are available for strata with no suitable lower third molars.

A2.3 Hypsodonty index as a climatic predictor in the Late Pleistocene (regional comparisons)

A2.3.1 Introduction

This section brings together all of the Late Pleistocene study sites that were presented above in section A2.2. The approach here is to discuss the three regions of the Mediterranean on a longitudinal gradient from west to east. This approach has been taken due to the geographical proximity of certain sites, their ages and also the nature of the results and data obtained from the seven separate studies. Although each site has previously been discussed on its own and compared to any available proxy data, these cross-site, regional and interregional comparisons are essential in order to analyse thoroughly whether hypsodonty index shows any climatic or environmental signal.

A2.3.2 Western Mediterranean (55.0 to 30.0 ka BP)

Abric Romaní (Spain), Teixoneres (Spain) and Portel-Ouest (France) are all located in the western Mediterranean (see Figure 3.7 in the main thesis) and have overlapping ages, as confirmed by their independent chronologies (Talamo *et al*., 2016; Marín *et* al., 2017). The sites also lie in relatively close proximity to one other, with Abric Romaní and Teixoneres being approximately 50 km away from each other and Portel-Ouest located about 150 km to the north of the two Spanish sites. This allows for some interesting comparison of contemporaneous hypsodonty index changes within the same region at sites that were subject to the same dominant regional climatic regime. Furthermore, the role of the Pyrenees can also be discussed as this mountain range separates the French and Spanish sites.

A2.3.2.1 Comparison between Abric Romaní and Teixoneres

The rock shelter of Abric Romaní and the karstic cave system of Teixoneres have both been occupied by Neanderthals (Talamo *et al*., 2016; Marín *et* al., 2017), however, certain periods at Teixoneres are interrupted by periods of carnivore denning (Talamo *et al*., 2016). The agents of accumulation must be considered when assessing the nature of the large mammal assemblages found at each site, as well as the nature of the hypsodonty index data that has been collected and analysed in the present study.

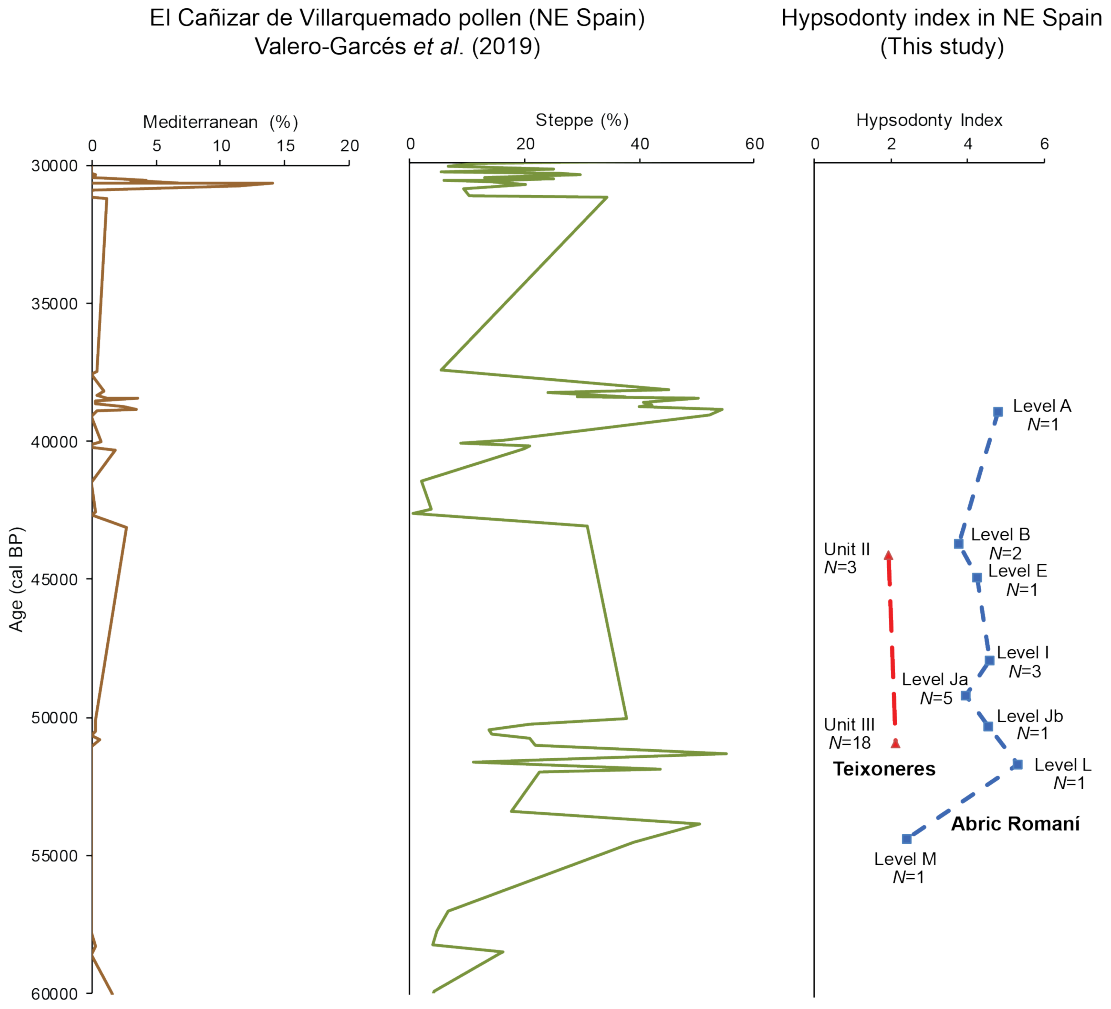

Figure A2.7: Diagram showing changes in percentage of pollen associated with Mediterranean and Steppe environments from the site of El Cañizar de Villarquemado in northeast Spain (data from Valero-Garcés *et al*. (2019) alongside the hypsodonty index data from Abric Romaní and Teixoneres (site-specific level labels are shown alongside sample sizes (*N*)).

The hypsodonty index values through the sequence at Abric Romaní show little change after an initial increase, although sample size is extremely low. The hypsodonty index values at Teixoneres also show little change, where the two units show no statistically significant difference in hypsodonty index. In contrast, proxy data from both sites show substantial environmental transitions over this period (see Burjachs *et al*., 2012; López-García *et al*., 2012) and it might therefore have been expected that if any climatic or environmental response is preserved within the mean hypsodonty index, this would be reflected in the measurements taken. This is especially true as mammalian herbivore communities respond well to changes in the main interface between climate and teeth, which is suggested to be the local vegetation (Janis, 1988; Damuth and Janis, 2011). Looking at a more regional picture, the hypsodonty index changes at the two sites can be compared with the pollen record from El Cañizar de Villarquemado (see Figure A2.7).

Here it can be see than the hypsodonty index data from Teixoneres does not seem to match the vegetation changes at El Cañizar de Villarquemado (pollen study by Valero-Garcés *et al*., 2019) as the Teixoneres hypsodonty index values overlap in error (see Figure 6.2). On the other hand, the hypsodonty index data from Abric Romaní appears to follow the same increase, steady decline and increase again in steppe pollen between c. 54 ka cal BP and 39 ka cal BP. This may indicate a link between steppe vegetation type and hypsodonty index. As steppe vegetation increases this may indicate increases in semi-arid climate, but at El Cañizar de Villarquemado, steppe pollen change is coupled inversely with Mediterranean pollen change. The key difference between Mediterranean and steppe biomes is temperature as the former is hot and semi-arid whilst the latter is cold and semi-arid. Considering this regional vegetation change and the hypsodonty index changes at Abric Romaní, it may be that there is indeed a temperature component of hypsodonty as hinted at by the results of the modern study (see Chapters 4 and 5 of the main thesis) and the literature (Liu *et al*., 2012; Žliobaitė *et al.*, 2016).

The fact that the hypsodonty index at the two Spanish sites does not change as might be expected based on *local* proxy data, begs the question as to whether the herbivore communities respond to environmental or climatic change in a different way to the rest of the ecological community. Alternatively, are the hypsodonty index data affected by other factors in play, beyond the biological? Both biology and the nature of the data itself must be considered here to make any valid interpretations. As seen in the individual site discussions previously, the nature of the data is important and the data cannot be considered without considering biological and ecological processes. The taxa present in the mammalian assemblage within a particular geological bed and the taxa present in the hypsodonty index dataset are not always the same, and therefore the mean hypsodonty index at any one point in the sequence may not be representative of the fossil community during the deposition of the bed in question. Therefore, changes seen (or not seen) in the hypsodonty index may be entirely dependent on the nature of the data and entirely independent of climate or environment.

Table A2.1 below illustrates this problem and also provides some additional discussion points. Taking Abric Romaní first, it can be clearly seen that the taxa represented in the hypsodonty index study are restricted to a single taxon per level. Furthermore, it is worth noting that in all levels except Level A, this taxon is *Equus* sp. Horses have much higher crowned teeth than many of the other taxa represented in the assemblage as reported by Rosell *et al*. (2012). However, looking back at the results (Figure 6.1 in the main thesis), it is clear that although the entire sequence comprises a series of measurements of hypsodonty index of horse teeth, there is much more variation than might be expected, especially since intraspecific variation in hypsodonty has been assumed not to be

significant (Chapter 5 of the main thesis). This may indicate that despite its reported status as a hypergrazer (MacFadden, 2000) it may mean that its dentition is not as resistant to small (potentially climatically induced) changes in abrasiveness of the diet. Could this variation through the sequence, within one taxon, contain a signal of an external climatic control? The composition of the mammal community changes through time, which might indicate environmental differences but even across levels where the faunal community remains the same, there are differences in hypsodonty index and vice-versa. It may therefore be concluded that changes in the faunal community (possibly environmentally driven) have no visible effect on hypsodonty of horse over the timescales at these sites and no climate signal is preserved.

Table A2.1: Table showing the taxa present at the sites of Abric Romaní and Teixoneres in comparison to the taxa present in the hypsodonty index data from this study.:

Abric Romaní					Teixoneres				
Level	*N*	Age (ka)	Taxa in assemblage (Rosell *et al.*, 2012)	Taxa in hypsodonty index data	Unit	*N*	Age (cal years BP)	Taxa in assemblage (Àlvarez-Lao *et al.*, 2017)	Taxa in hypsodonty index data
A	1	39	*Equus ferus* *Cervus elaphus* *Bos primigenius* *Rupicapra rupicapra*	*Bos* sp.				*Cervus elaphus* *Capreolus capreolus* Bovini cf. *Bos primigenius* *Rupicapra pyrenaica*	
B	2	43.8	*Equus ferus* *Cervus elaphus* *Rupicapra rupicapra*	*Equus* sp.	II	3	44,210 – 33,060	*Capra pyrenaica* *Sus scrofa* *Equus ferus* *Equus hydruntinus* *Equus* sp. *Coelodonta antiquitatis*	*Cervus elaphus* *Equus hydruntinus* *Sus scrofa*
E	1	45	Proboscidea *Equus ferus* *Cervus elaphus* *Bos primigenius* *Rupicapra rupicapra*	*Equus* sp					
I	3	48	*Equus ferus* *Cervus elaphus* *Bos primigenius*	*Equus* sp				*Cervus elaphus* *Capreolus capreolus* Bovini cf. *Bos primigenius*	
Ja	5	49.3	*Stephanorhinus hemitoechus* *Equus ferus* *Cervus elaphus* *Bos primigenius* *Rupicapra rupicapra*	*Equus* sp	III	18	>51,000 – 44,210	*Rupicapra pyrenaica* *Capra pyrenaica* *Sus scrofa* *Equus ferus* *Equus hydruntinus* *Equus* sp. *Coelodonta antiquitatis* *Mammuthus primigenius*	*Cervus elaphus* *Capreolus capreolus* *Equus ferus* *Equus* sp. *Bos primigenius* *Capra* sp.
Jb	1	50.4	*Stephanorhinus hemitoechus* *Equus ferus* *Cervus elaphus* *Bos primigenius* *Rupicapra rupicapra*	*Equus* sp					
L	1	51.8	*Equus ferus* *Cervus elaphus* *Bos primigenius*	*Equus* sp					
M	1	54.5	*Equus ferus* *Cervus elaphus* *Bos primigenius*	*Equus* sp					

Nevertheless, the taxa present in the hypsodonty index data for Portel Ouest (at least for Bed F) contain representatives of the more mesodont (e.g. *Cervus elaphus* and *Rangifer tarandus*) and the more hypsodont (*Bos* sp. and *Capra* sp.). *Equus* is not represented in the dataset, despite its presence in all levels within Bed F. As a highly hypsodont taxon, its absence may slightly skew the mean hypsodonty index of Bed F towards a lower end. Further negative skew also likely caused by the high number of *Rangifer tarandus* hypsodonty index measurements within the combined Bed F. The other beds for which there are data are not well-dated and those younger than Bed F stretch beyond the timeframe recorded in Abric Romaní and Teixoneres and will not be mentioned further here.

A2.3.2.2 Summary

When trying to compare the three sites at this time period (c. 38 ka) using only the hypsodonty index data, the approach is clearly not robust. The mean hypsodonty index from Abric Romaní is artificially high, the data from Teixoneres is of low temporal resolution, and the hypsodonty index values from Portel Ouest are potentially artificially low. In this respect, the presence-absence of just the taxa themselves provides better palaeoenvironmental information than hypsodonty index alone when approached using the methodology of this study.

A2.3.3 Central Mediterranean (33.0 – 27.3 ka cal BP to 11.3 ka cal BP)

Grotta del Romito is the youngest of the sites considered in this study, dated to 33.0 – 27.3 ka cal BP to 11.3 ka cal BP (Blockley *et al*., 2018) and is located in the central Mediterranean (see figure 3.7). Unfortunately, access to other sites within the central Mediterranean region spanning this time period was not possible during the present study, thereby precluding comparisons of hypsodonty index changes and climatic signals. However, this site is the most well-resolved in this study in terms of chronology and high-resolution environmental proxies recording an abrupt environmental shift, so it was treated as a test case to investigate the potential climatic or environmental signals hidden in the mean hypsodonty index of ungulate communities.

Haua Fteah, on Libya's Mediterranean coast, lies at the eastern fringes of what may be considered the central Mediterranean. It is considered here because the site yielded some hypsodonty index data from the period 12.9 – 6.2 ka BP, which overlaps with Grotta del Romito. However, the time periods for which there are hypsodonty index measurements at both sites do not overlap as the youngest level for which there is hypsodonty index data from Grotta del Romito is Level C, which pre-dates 12.9 ka. In n ideal scenario it would be possible to compare two sites on the European and African

sides of the Mediterranean, but this is not possible here due to the availability and nature of the fossil material and the data yielded from them.

Grotta del Romito is the youngest of the sites considered in this study, dated to 33.0 – 27.3 ka cal BP to 11.3 ka cal BP (Blockley *et al*., 2018) and is located in the central Mediterranean (see figure 3.7). Unfortunately, access to other sites within the central Mediterranean region spanning this time period was not possible during the present study, thereby precluding comparisons of hypsodonty index changes and climatic signals. However, this site is the most well-resolved in this study in terms of chronology and high-resolution environmental proxies recording an abrupt environmental shift, so it was treated as a test case to investigate the potential climatic or environmental signals hidden in the mean hypsodonty index of ungulate communities.

Haua Fteah, on Libya's Mediterranean coast, lies at the eastern fringes of what may be considered the central Mediterranean. It is considered here because the site yielded some hypsodonty index data from the period 12.9 – 6.2 ka BP, which overlaps with Grotta del Romito. However, the time periods for which there are hypsodonty index measurements at both sites do not overlap as the youngest level for which there is hypsodonty index data from Grotta del Romito is Level C, which pre-dates 12.9 ka. In n ideal scenario it would be possible to compare two sites on the European and African sides of the Mediterranean, but this is not possible here due to the availability and nature of the fossil material and the data yielded from them.

A2.3.4 Eastern Mediterranean

A2.3.4.1 Comparison between Tabun and Qafzeh Caves

As discussed above in section A2.2, it is unfortunate that the chronologies for the hypsodonty index data for both Tabun and Qafzeh caves are poorly resolved. Tabun, as currently understood, was deposited from c. 320 ka at the base (Mercier and Valladas, 2003) to c.104 ka at the top (Grün and Stringer, 2000), and fortunately hypsodonty index data are available for seven out of the ten levels described by Garrod (see Figure 3.24 and 3.25 in the main thesis for the stratigraphy). At Qafzeh, most of the hypsodonty index data comes from parts of the sequence that is younger than c. 95 ka (the youngest date published is for Layer XV (Schwarcz *et al*., 1988), which is conversely the oldest level for which hypsodonty index data was available. Therefore, even though the two sites themselves have mammalian assemblages suggested to have been deposited at the same time (due to the presence of a 'Tabun C-D fauna' (Farrand, 1979), there are no hypsodonty index data from the potentially contemporaneous deposits at Qafzeh, sadly precluding comparison of firstly, the mean hypsodonty index of the ungulate communities at two very proximal sites, and secondly, investigating any climatic signals as neither site

alone has yielded any robust possibilities of teasing out a climatic signal because of largely overlapping errors and poor sample sizes.

As discussed above in section A2.2, it is unfortunate that the chronologies for the hypsodonty index data for both Tabun and Qafzeh caves are poorly resolved. Tabun, as currently understood, was deposited from c. 320 ka at the base (Mercier and Valladas, 2003) to c.104 ka at the top (Grün and Stringer, 2000), and fortunately hypsodonty index data are available for seven out of the ten levels described by Garrod (see Figure 3.24 and 3.25 in the main thesis for the stratigraphy). At Qafzeh, most of the hypsodonty index data comes from parts of the sequence that is younger than c. 95 ka (the youngest date published is for Layer XV (Schwarcz *et al*., 1988), which is conversely the oldest level for which hypsodonty index data was available. Therefore, even though the two sites themselves have mammalian assemblages suggested to have been deposited at the same time (due to the presence of a 'Tabun C-D fauna' (Farrand, 1979), there are no hypsodonty index data from the potentially contemporaneous deposits at Qafzeh, sadly precluding comparison of firstly, the mean hypsodonty index of the ungulate communities at two very proximal sites, and secondly, investigating any climatic signals as neither site alone has yielded any robust possibilities of teasing out a climatic signal because of largely overlapping errors and poor sample sizes.

A2.3.4.2 Haua Fteah

As discussed in section A2.2.7, hypsodonty index changes at Haua Fteah do not appear to be tracking climatic and environmental changes picked out in proxy data. The site itself has accumulated deposits since approximately MIS 5e (Jacobs et al., 2017) until at least the mid-Holocene (Douka et al., 2014). Unfortunately, the material available for study and the nature of the specimens themselves means that hypsodonty index data are only available for three out of more than 30 archaeological layers. These three layers span 12.9 – 6.2 ka, not overlapping with any of the data obtained from Tabun and Qafzeh, meaning that comparisons are not possible.

A2.3.5 Summary of hypsodonty index and climate on Late Pleistocene timescales

The original aim of studying the seven Late Pleistocene sites considered in this thesis was to use hypsodonty index to quantify past precipitation. After testing the modern relationship between hypsodonty and climatic variables, it became clear that there was no simple correlative link between hypsodonty index and the climatic variables of temperature and precipitation, the latter of which is difficult to reconstruct in the past from the records available (Guiot *et al*., 2009) The approach taken with the Late Pleistocene material therefore became less about quantification and more about investigation of a

climatic signal that might be more easily elucidated in the context of palaeoclimatic and palaeoenvironmental proxy data. The question to be answered became one regarding abrupt climatic change: i.e. can any signal be discerned in the changes in mean hypsodonty index across environmental transitions on abrupt timescales? And if so, what might be the environmental and biological mechanisms controlling this? Finally, if explanations can be suggested on a site-specific basis, how far can this be extended to enable regional comparisons?

Figure A2.8 is a summary diagram showing the hypsodonty index data for the four well-dated sites of Abric Romaní, Teixoneres, Grotta del Romito and Haua Fteah and three regional palaeoclimate records for the Mediterranean and northwest Europe – this is also presented in Chapter 7 of the main thesis. Any relationships across all of the data may be visible when set out in this manner and this is appropriate as this part of the study aimed to investigate whether any climatic signal seen in proxy data can also be seen in the hypsodonty index data. The comparison between Abric Romaní and the El Cañizar de Villarquemado has already been highlighted in section A2.3.2.1 above, but there is also a similar comparison that can be made to the woody taxa pollen record from Lago Grande di Monticchio which shows a decrease at c. 52 ka cal BP and an increase at c. 50-49 ka cal BP, which suggests a more open environment being replaced by a less open environment.

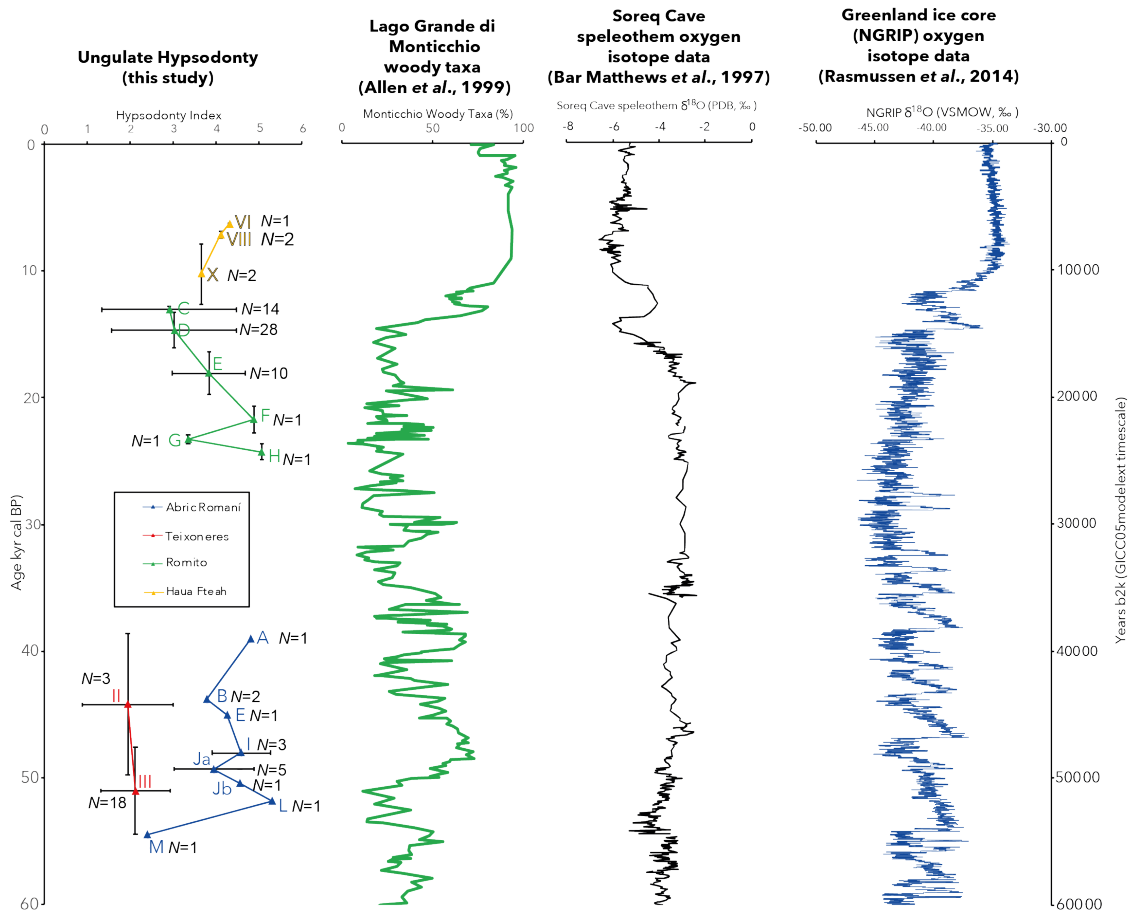

Figure A2.8: Summary diagram showing (from left to right) the hypsodonty index of Abric Romaní, Teixoneres, Grotta del Romito and Haua Fteah, the woody taxa from the pollen spectra from Lago Grande di Monticchio (green line; data from Allen *et al*., 1999), oxygen isotope data from the Soreq Cave speleothem record, Israel (black line; data from Bar-Matthews *et al*., 1997) and the oxygen isotope record from NGRIP (blue line; data from NGRIP Members, 2004 and Rasmussen *et al*., 2014).

The Abric Romaní hypsodonty index record has a 'peak' that may correlate with the lower levels of woody vegetation, meaning a more hypsodont community where there is a more open environment. This may be a drier or cooler open environment. There is a decrease in hypsodonty index at Abric Romaní that slightly precedes the increase in woody taxa, which may suggest a link between hypsodonty and the openness of a landscape. This is consistent with the conclusions made by Janis (1988, 2004). It must be noted that the hypsodonty index values for Abric Romaní have very low sample sizes so the commentary here is far from conclusive. As discussed in section A2.3.2.1 the Teixoneres data shows very little change during this time. The hypsodonty index data from Grotta del Romito and Haua Fteah do not appear to follow the trends seen in the regional proxy data presented here. In section A2.2 it was clear that any apparent links between hyspdonty and proxy data are very site-specific and here we see that the regional picture is less than clear or conclusive. Furthermore, much of the quality of the data (hypsodonty and other proxies) are also site-specific and must be considered in more detail before making any suggestions regarding climatic signals in the hypsodonty data.

To be able to see changes in hypsodonty index on the timescales of interest, and to elucidate possible signals through proxy comparison, there is a requirement for hypsodonty index data to be available at high and comparable resolution to that obtained for other proxy analyses. Site-selection is obviously important for this, and although some sites in this study have high-resolution chronologies, for example Abric Romaní, Teixoneres, Grotta del Romito and Haua Fteah, some are unfortunately less well-resolved such as Portel Ouest, Tabun and Qafzeh.

However, having good chronological control is not the only factor that would enable one to answer the questions posed in the previous paragraph. The nature and availability of the actual fossil material itself is key. Sample sizes for all sites are small when looking at individual teeth for hypsodonty index measurements. The methodology requires exclusively third lower molars, often the largest and most robust teeth, but also no guarantee of a high yield within an assemblage. The teeth must be adult, unworn or just in wear, and the entire crown must be present and able to be measured accurately. Late Pleistocene mammalian fossils can be accumulated in a number of ways, and agents of accumulation are key. For sites that are accumulated by hominin activity, there will be bias in the assemblage, with prey species highly represented. This has been suggested not to be an issue in terms of representation of the natural mammalian community if deposition is over a long enough period of time to override this bias (Davis, 1982), however this seems a subjective viewpoint and bias must always be considered. However, different accumulating agents can mean a significant impact on sample size through a number of ways: (1) carnivore selection can bias in favour of young individuals where the lower third molar has not yet erupted, (2) hominin hunting of old individuals with teeth that are too worn, (3) hominins extracting marrow from the mandible which often results in tooth breakage (Stiner, 1994). Of course, young and old individuals can be present in more naturally accumulated assemblages, and teeth can be taphonomically altered, further reducing the sample size of measurements.

Sample size can also differ greatly throughout a sequence, meaning that the mean hypsodonty index that is calculated for some levels may have more measurements behind them than for other levels. This can affect interpretations throughout a sequence, and when relying on pre-existing chronologies, the ability to analyse changes effectively in hypsodonty index can be crucially impacted. For example, with Qafzeh, most measurements that were able to be obtained came from levels above the part of the sequence that is relatively chronologically well-constrained. The data collection from Qafzeh did not yield useful results to answer the questions above, despite meeting the selection criteria for having good chronological control. Having data from un-dated levels is only one problem though, as having very small samples sizes per bed may mean that

assemblages may need to be combined in some sites. This is an issue at Teixoneres where the two sublevels in each of Unit II and III were combined as sample sizes within the individual levels were so small. This causes an issue when trying to look for climatic signals as the proxy data is still spilt by sublevel, and is especially problematic when other proxies identify environmental transitions within the sublevels themselves. This mismatch of resolutions and overlapping age errors precludes useful comparisons between mean hypsodonty index and the other proxies. On the contrary, without combining levels to increase sample sizes, any inferences from the comparisons with proxy data would not be robust, even when all the data are available at the same temporal resolutions.

One of the main outcomes of testing the method on Late Pleistocene sites is further highlighting of the importance of taxon representation. This is key in assessing the validity of the approach taken in this study, of trying to calculate mean hypsodonty index of fossil communities from hypsodonty index measurements taken on single teeth. This is in comparison to the per species mean hypsodonty approach that is inherently based on presence absence and is the current state of play in the literature. As a more detailed discussion in Chapter 7 of the main thesis, only a brief summary will be given here in the context of the Late Pleistocene application in this study. It is worth highlighting here the case of Grotta del Romito as taxon representation is a key consideration when interpreting the hypsodonty index changes. As seen in Chapter 3 of the main thesis and above in section A2.2.4, at Grotta del Romito, there is a significant environmental shift from a more open landscape to woodland (Blockley *et al*., 2018), and this is reflected more regionally in Italy (see Brauer *et al*., 2007). This coincides with a marked shift in hypsodonty index, however, this is interpreted as merely a factor of the taxa present in the hypsodonty index data at that level in the sequence. If the taxa in the hypsodonty index data and the assemblage overall at that level had been the same as before, or at least very close to the true assemblage, then the marked decrease in hypsodonty index might be faithfully reflecting the abrupt shift to woodland as seen in the other proxies. However, this is not the case and is a clear indication that caution must be applied when using the methodology of this study. This begs the question that if mean hypsodonty index calculated from actual tooth measurements is beset with such problems, is the presence-absence per species mean hypsodonty index method any more appropriate to use? This is discussed further in Chapter 7 of the main thesis, in the context of the modern hypsodonty-climate relationship.